# Identification and activity of bacteria consuming key intermediates of carbon and sulfur cycling in coastal sands

Dissertation
Zur Erlangung des Grades eines
Doktors der Naturwissenschaften
- Dr. rer. nat. -

Dem Fachbereich Biologie/Chemie
der Universität Bremen

vorgelegt von

**Stefan Dyksma**

Bremen, März 2016

Die vorliegende Arbeit wurde in der Zeit von Oktober 2012 bis Februar 2016 in der Abteilung für Molekulare Ökologie am Max-Planck-Institut für Marine Mikrobiologie in Bremen angefertigt.

1. Gutachter: Prof. Dr. Rudolf Amann
2. Gutachter: Prof. Dr. Ulrich Fischer

Tag des Promotionskolloquiums: 08.04.2016

## Abstract

Coastal and shelf sediments are hot spots for carbon remineralization and also for carbon fixation. Here, a large fraction of organic carbon is mineralized under anoxic conditions by microorganisms via fermentation or respiration of fermentation products such as molecular hydrogen ($H_2$) and acetate. Reduced inorganic metabolites released during these anaerobic processes and inorganic carbon are used by light-independent chemolithoautotrophs for so-called secondary production. However, still little is known about the *in situ* relevant organisms and how they contribute to key processes like chemoautotrophy as well as $H_2$ and acetate turnover.

To understand how inorganic carbon at sediment surfaces is turned over we surveyed the diversity of candidate bacterial chemolithoautotrophs in 13 tidal and sublittoral sediments and identified ubiquitous core groups of *Gammaproteobacteria* mainly affiliating with sulfur-oxidizing bacteria. In a novel methodological approach we quantified dark carbon fixation by scintillography of specific microbial populations extracted and flow-sorted from sediments that were short term incubated with $^{14}$C-bicarbonate. Here, we show that uncultured *Gammaproteobacteria* dominate dark carbon fixation in coastal sediments and three distinct gammaproteobacterial clades made up more than half of dark carbon fixation in a tidal sediment. Meta- and single cell genomics along with metatranscriptomics provided evidence for a largely sulfur-based carbon fixation. These chemolithoautotrophic gammaproteobacterial clades also accounted for a substantial fraction of the microbial community in 1,000 to 2,000 year old subsurface sediments, suggesting that burial of chemolithoautotrophic bacteria could possibly be a yet-unrecognized mechanism of carbon sequestration.

Microbial scavenging of $H_2$ is an essential process in anoxic carbon mineralization, because only low $H_2$ levels make $H_2$-forming fermentation thermodynamically feasible. In a sediment metagenome we identified a high diversity of genes encoding the [NiFe] uptake hydrogenases of numerous yet-uncultured, potentially $H_2$-oxidizing bacteria. Metatranscriptomics together with incubation experiments suggested uncultured *Desulfobacteraceae*, in particular the sulfate-reducing Sva0081-clade, as important $H_2$ oxidizers in anoxic sediments. On the contrary, *Gammaproteobacteria* and *Flavobacteria* encoding $O_2$-tolerant hydrogenases are possibly involved in $H_2$ oxidation in oxic sediments.

In a third study, we quantified the relative contribution of single bacterial populations to total acetate assimilation. Here, we showed that acetate was assimilated by physiologically and phylogenetically distinct bacterial groups such as *Gammaproteobacteria*, sulfate-reducing *Desulfobacteraceae* and *Desulfobulbaceae* as well as likely lithoheterotrophic sulfur-oxidizing *Roseobacter*-clade bacteria. We identified uncultured *Gammaproteobacteria* as a major

contributor to acetate assimilation under oxic and anoxic conditions accounting for 31-62% of the total acetate assimilation.

In summary, this thesis contributes to our understanding how distinct bacterial populations turn over key metabolites of organic carbon degradation in marine sediments. The quantification of uptake of $^{14}C$-labeleld model compounds by defined populations is a major step forward in the identification of key organisms in element cycling in marine sediments.

# Zusammenfassung

Küsten- und Schelfsedimente sind höchst aktive Systeme für die Remineralisierung von organischem Kohlenstoff und auch für die Kohlenstoffdioxidfixierung. In diesem größtenteils anoxischen Habitat bauen Mikroorganismen den organischen Kohlenstoff durch Fermentation ab, oder nutzen Fermentationsprodukte wie molekularen Wasserstoff ($H_2$) und Acetat als Substrate für die Energiegewinnung. Reduzierte Verbindungen wie Sulfid werden bei diesen anaeroben Prozessen abgegeben. Diese werden von Licht-unabhängigen chemoautotrophen Mikroorgansimen für die sogenannte Sekundärproduktion genutzt wobei Kohlenstoffdioxid fixiert wird. Jedoch sind die relevanten Organismen größtenteils noch nicht identifiziert und es ist wenig bekannt wie diese zu zentralen Prozessen wie Chemoautotrophie sowie $H_2$- und Acetat-Umsatz beitragen.

Um zu verstehen, wie anorganischer Kohlenstoff in Oberflächensedimenten umgesetzt wird, haben wir die Diversität potentieller chemolithoautotropher Bakterien in 13 tidalen und sublittoralen Sedimenten untersucht. Dabei wurden Gruppen von Gammaproteobakterien in allen Sedimenten identifiziert, die mit schwefeloxidierenden Bakterien verwandt sind. In einem neuartigen methodologischen Ansatz haben wir die Kohlenstoffdioxidfixierung für spezifische mikrobielle Populationen quantifiziert. Dafür wurden Bakterien nach der Inkubation mit $^{14}$C-Bikarbonat und Identifizierung mittels Fluoreszenz *in situ* Hybridisierung (FISH) durchflusszytometrisch aus den Sedimentproben sortiert und deren Substrataufnahme gemessen. Wir zeigen dass Gammaproteobakterien, im speziellen drei weit verbreitete Untergruppen, den Großteil der bakteriellen chemoautotrophen Kohlenstoffdioxidfixierung ausmachten. Metagenomik zusammen mit Metatranskriptomik zeigten größtenteils Schwefel-basierte Kohlenstofffixierung. Die Gruppen chemolithoautotropher Gammaproteobakterien machten auch in 1000-2000 Jahre altem Sediment in 5 m Tiefe noch einen wesentlichen Bestandteil der mikrobiellen Gemeinschaft aus, was auf eine bislang unerkannte Weise der Kohlenstoffsequestrierung hindeutet.

Der Abbau von $H_2$ ist ein unerlässlicher Prozess in anoxischen Habitaten wie in marinen Sedimenten, da die $H_2$ Konzentrationen auf niedrigen Level gehalten werden müssen, um Fermentation thermodynamisch möglich zu machen, was für den anaeroben Abbau von organischem Material eine zentrale Rolle spielt. In einem Metagenom identifizierten wir eine hohe Diversität von bislang unbekannten potentiellen $H_2$-Oxidierern. Metatranskriptomik in Kombination mit Sedimentinkubationen mit $H_2$ deuteten darauf hin, dass Sulfatreduzierer aus der Familie der *Desulfobacteraceae*, im Besonderen die Sva0081 Gruppe, wichtige $H_2$-Oxidierer in anoxischen Sedimenten sind. Gammaproteobakterien und Flavobakterien spielen hingegen für die $H_2$ Oxidation in oxischen Sedimenten eine Rolle.

In einer dritten Studie wurde die Assimilation von Acetat für phylogenetisch identifizierte bakterielle Populationen in marinem Sediment quantifiziert. Acetat wurde von physiologisch und phylogenetisch unterschiedlichen Gruppen assimiliert wie *Gammaproteobacteria*, sulfatreduzierende *Desulfobacteraceae* und *Desulfobulbaceae* sowie von wahrscheinlich lithoheterotrophen Schwefeloxidierern der *Roseobacter* Gruppe. Gammaproteobakterien trugen 31-62% zu der gesamten Assimilation von $^{14}$C-Acetat durch Bakterien bei und machten hier somit einen Großteil aus.

Diese Arbeit trägt wesentlich zum Verständnis bei wie Metaboliten aus dem Abbau von organischem Kohlenstoff in marinen Sedimenten von bestimmten Gruppen von Bakterien umgesetzt werden. Die hier vorgestellte Methode zur exakten Quantifizierung der Aufnahme von $^{14}$C-Kohlenstoff durch phylogenetisch identifizierte Bakterien ist ein wichtiges neues Werkzeug zur Identifizierung von Schlüssel-Organismen in Stoffkreisläufen mariner Sedimente.

# List of abbreviations

| | |
|---|---|
| APS | adenosine 5'-phosphosulfate reductase |
| ATP | adenosine triphosphate |
| CARD | catalyzed reporter deposition |
| CBB | Calvin-Benson-Bassham cycle |
| DIC | dissolved inorganic carbon |
| FACS | fluorescence-activated cell sorting |
| FISH | fluorescence *in situ* hybridization |
| GSB | green sulfur bacteria |
| HISH | halogen *in situ* hybridization |
| LSU | large subunit |
| MAR | microautoradiography |
| NAD | nicotinamide adenine dinucleotide |
| NADP | nicotinamide adenine dinucleotide phosphate |
| PHA | polyhydroxyalkanoate |
| PLFA | phospholipid fatty acid |
| PSB | purple sulfur bacteria |
| RCB | *Roseobacter*-clade bacteria |
| rDSR | reverse dissimilatory sulfite reductase |
| rRNA | ribosomal ribonucleic acid |
| rTCA | reductive tricarboxylic acid |
| SIMS | secondary ion mass spectrometry |
| SIP | stable isotope probing |
| SOB | sulfur-oxidizing bacteria |
| SRB | sulfate-reducing bacteria |
| SRM | sulfate-reducing microorganisms |
| SSr | *Siboglinidae*-symbiont related |
| SSU | small subunit |
| TCC | total cell count |
| TOF | time of flight |

# 1.) Introduction

## 1.1) The marine carbon cycle

The oceans are an immense reservoir for carbon. Falkowski *et al.* (2000) estimated the amount of stored carbon in the ocean at about 38,400 Gt, the majority of it (approximately 90%) as carbonate. Dissolved inorganic carbon (DIC), composed of carbon dioxide ($CO_2$), bicarbonate ($HCO_3^-$) and carbonate ($CO_3^{2-}$), plays a major role in the marine carbon cycle. The ocean contains 50 times more DIC than the atmosphere and the annual oceanic uptake was estimated at about 93 Gt C $y^{-1}$ while 90 Gt C $y^{-1}$ are released to the atmosphere (Suttle, 2005; Falkowski and Raven, 2013). Primary producers that are capable to fix inorganic carbon in the ocean are largely microbial, whereas macroalgae and vascular plants are only locally important (Walsh, 1997). Microorganisms fix $CO_2$ either by photosynthesis in the surface ocean or independent of light (chemosynthesis) at hydrothermal vents. The marine primary production has been estimated at about 48.5-54 Gt C, which is comparable to terrestrial primary production (Field *et al.*, 1998; Dunne *et al.*, 2007). A large fraction of the carbon fixed in surface waters is cycled by the microbial loop (Azam *et al.*, 1983). Phytoplankton biomass becomes dissolved organic matter by diverse processes such as excretion of substances, bacterial interactions or viral lysis (Azam and Malfatti, 2007). Most of the dissolved organic matter is subsequently respired to $CO_2$ by heterotrophic bacteria which in turn is available for primary producers (Azam and Malfatti, 2007). A fraction is channelled into the classical marine food chain (Azam and Malfatti, 2007) and only a small proportion of about 0.2-0.79 Gt C is exported to the seafloor and buried in sediments (Duarte *et al.*, 2005; Burdige, 2007; Dunne *et al.*, 2007). Up to 20-33% of the total marine primary production occurs in coastal and shelf areas (0-200 m) (Wollast, 1991; Hedges *et al.*, 1997). Here, also benthic cyanobacteria and diatoms contribute to total primary production (Middelburg *et al.*, 2000; Gattuso *et al.*, 2006; Evrard *et al.*, 2010) The fraction of organic matter that reaches the seafloor is largely dependent on the depth of the overlying water (Wenzhöfer and Glud, 2002; Jørgensen and Boetius, 2007). In coastal and shelf areas up to 50% of the primary production can reach the sediment surface (Jørgensen, 1982; Wollast, 1991; Canfield, 1993). Consequently, the productivity in surface ocean waters determines microbial respiration rates in the underlying sediments (Wenzhöfer and Glud, 2002).

### 1.1.1) Chemolithoautotrophy in marine environments

Dark carbon fixation in the ocean and in sediments can be considered as secondary production (Middelburg, 2011) as the energy is derived from the degradation of organic matter. Heterotrophs cannot use all energy from the organic matter. Some is shunted into reduced metabolites such as ammonium and sulfide. These reduced compounds are used

by chemoautotrophic bacteria and archaea to fuel dark carbon fixation (Howarth, 1984). Although chemoautotrophy in the ocean account for approximately only 1% of the carbon fixed by photosynthesis (Field *et al.*, 1998; Dunne *et al.*, 2007; Middelburg, 2011) it is similar to the amount of organic carbon that is buried in sediments (Duarte *et al.*, 2005; Burdige, 2007) and therefore a substantial part of the marine carbon cycle.

Chemolithoautotrophic microorganisms in marine sediments fix up to 370 Tg C/yr (Figure 1), accounting for nearly half of the total oceanic dark carbon fixation (Middelburg, 2011). Of these 370 Tg C/yr, 175 is fixed in shallow near-shore sediments. Here, reduced sulfur compounds were suggested to be the major energy source while nitrification is quantitatively less important (Middelburg, 2011; Boschker *et al*., 2014). Approximately half of the oceanic dark carbon fixation occurs by nitrifiers in the water column (Middelburg, 2011; Figure 1). Furthermore, chemolithoautotrophy by diverse *Gammaproteobacteria*, *Deltaproteobacteria* and *Thaumarchaeota* appears to be important in the oxygenated water column below the epipelagic (Reinthaler *et al.*, 2010; Swan *et al.*, 2011).

The key players of autotrophic carbon and sulfur cycling in OMZs and hydrothermal vents, such as *Epsilonproteobacteria* and the gammaproteobacterial SUP05-clade, have been extensively studied (Lavik *et al.*, 2009; Canfield *et al.*, 2010; Reinthaler *et al.*, 2010; Swan *et al.*, 2011; Grote *et al.*, 2012; Anantharaman *et al.*, 2013; Mattes *et al.*, 2013). In contrast, previous studies of benthic autotrophic sulfur oxidizers mostly focused on large, conspicuous sulfur bacteria such as *Beggiatoa*, which are widely distributed but occur in high abundances only in few habitats (Salman *et al.*, 2013; Ruff *et al.*, 2015). In support of a largely sulfur based chemoautotrophy in marine sediments, several groups of sulfur-oxidizing *Gammaproteobacteria* which are indeed chemoautotrophs were recently identified in coastal sediments (Lenk *et al.*, 2011; Boschker *et al.*, 2014; Vasquez-Cardenas *et al.*, 2015) but their environmental importance is still unexplored.

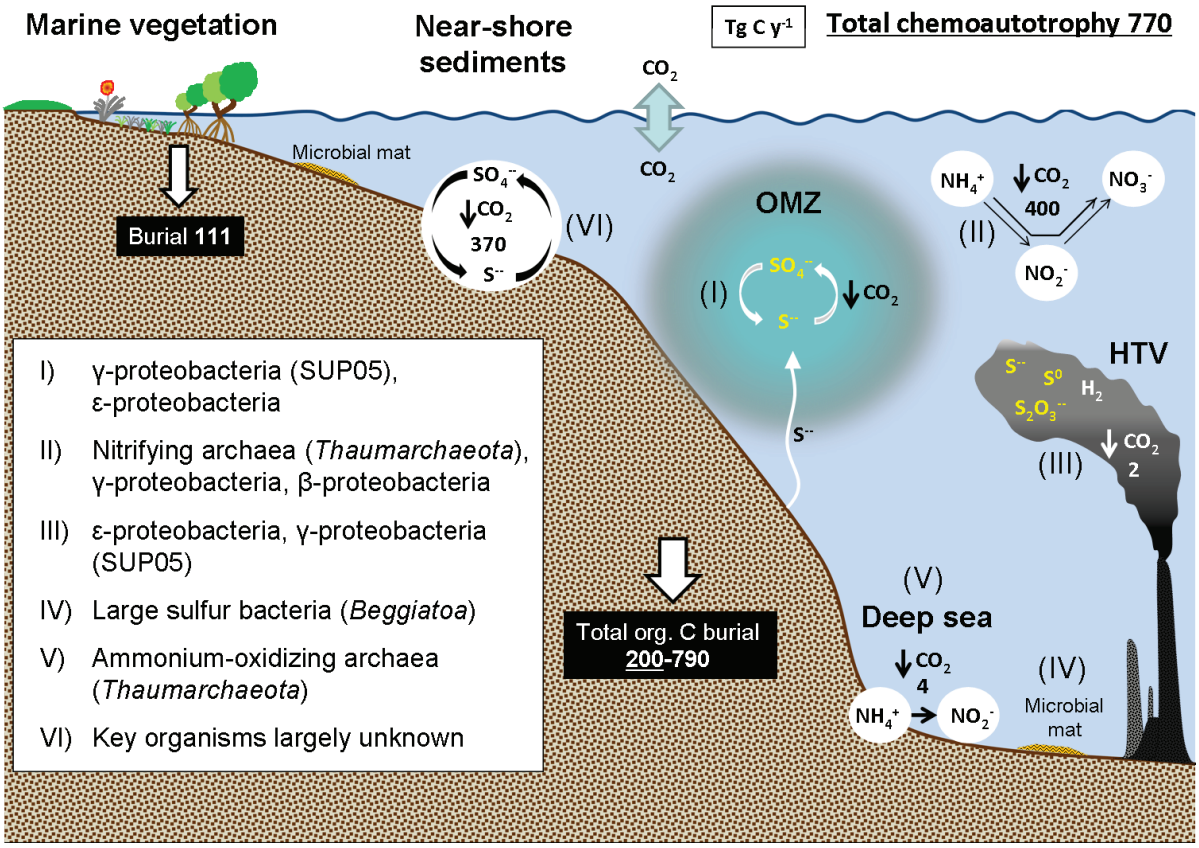


**Figure 1.** Dark carbon fixation in the ocean and the involved microbial key players. OMZ, oxygen minimum zone. HTV, hydrothermal vent. For details see text. Based on data presented in Duarte *et al.* (2007) and Middelburg (2011).

### 1.1.2) The organic carbon cycle in marine sediments

The organic carbon cycle can be subdivided into a biological and a geological part (Tissot and Welte, 2012). Commonly, primary production of organic matter is the first step and it ends in the decay of biomass into $CO_2$ with turnover times of days to tens of years (Rullkötter, 2006). The geological carbon cycle starts with the burial of organic matter and continues with the formation of gas, crude oil and coal or metamorphic forms of carbon, which finally may be reoxidized to $CO_2$. The carbon reservoir of the geological cycle is several orders of magnitude higher than that of the biological cycle with turnover times of millions of years (Rullkötter, 2006). The burial of organic matter is therefore an important process for long-term carbon sequestration and storage as it eventually leads to net removal of $CO_2$ from the atmosphere (Burdige, 2007).

Biogenic organic matter is sensitive to oxidative degradation either chemically or biologically mediated (Rullkötter, 2006) and the concentration of oxygen in particular at the water/sediment interface was suggested as a major factor determining the amount of organic matter that is finally buried in sediments (Demaison and Moore, 1980). During the biotic degradation of organic matter in marine sediments microbes use the easily degradable compounds first, leaving poorly-degradable (refractory) material. This is reflected by the

decrease of reactivity of organic matter with increasing sediment depth (Middelburg, 1989; Hedges and Keil, 1995; Dauwe *et al.*, 1999). Organic matter preservation is the absence of mineralization (Burdige, 2007) and the burial rate is regulated by the efficiency of microbial-driven diagenesis (Archer and Maier-Reimer, 1994).

Marine coastal sediments are global hot spots of carbon remineralization and burial (Hedges and Keil, 1995). The organic matter that reaches the sediment in particular in coastal and shelf sediments is mainly derived from marine primary production and from the input of terrestrial organic matter. Preservation of organic matter is strongly dependent on local environmental conditions and the extent of mineralization in the surface layers of the sediment can vary between 30 and 85% (Jørgensen, 1996; Whelan and Farrington, 2013). In current models of oceanic carbon cycling, the sequestration of microbially altered organic matter is the major mechanism of carbon preservation in sediments (Parkes *et al.*, 1993; Burdige, 2007). However, the burial of microorganisms and their persistence the subsurface might be a yet unrecognized mechanism of carbon sequestration in marine sediments.

### 1.1.3) Microbial degradation of organic matter in marine sediments

Dissolved organic matter (DOM) is the quantitatively most important part of dead organic material (detritus) in aquatic environments and can account for more than 95% of total organic matter in the ocean's water column (Canfield *et al*., 2005). The composition of DOM is still poorly understood and less than 20% of DOM has been classified into major biochemical classes such as carbohydrates, lipids and amino acids (Burdige, 2002). The total organic carbon (TOC) content in marine sediments ranges from 2.5 mg C per gram dry sediment ($g_{dw}$) in the open ocean to approximately 100-fold higher amounts (up to 200 mg C $g_{dw}^{-1}$) in coastal sediments (Premuzic *et al.*, 1982; Romankevich, 2013). Coastal and shelf sediments account for only a small area of the ocean but the majority of global ocean microbial respiration occurs in coastal and shelf sediments (Jørgensen and Kasten, 2006). Chemotrophic microorganisms use the energy gained during dissimilatory metabolism to fuel carbon assimilation. The energy gained from a redox-reaction depends, among others, on the difference in redox potentials of electron donor and electron acceptor. Strictly based on thermodynamics, respiration of oxygen is the most favourable process for organic carbon mineralization (Canfield *et al.*, 2005a). The free energy gain correlate with the distribution of electron accepting processes over sediment depth (Froelich *et al.*, 1979; Jørgensen, 1982; Jørgensen, 1983; Canfield *et al.*, 1993). In the uppermost sediment layer organic matter is mineralized by oxic respiration usually followed by denitrification, manganese and iron reduction, sulfate reduction and finally by methanogenesis (Jørgensen, 1983, Canfield *et al*., 1993) (Figure 2). Sulfate reduction was suggested as the most important electron accepting

process in marine sediments accounting for up to 50% of the mineralization (Jørgensen, 1982).

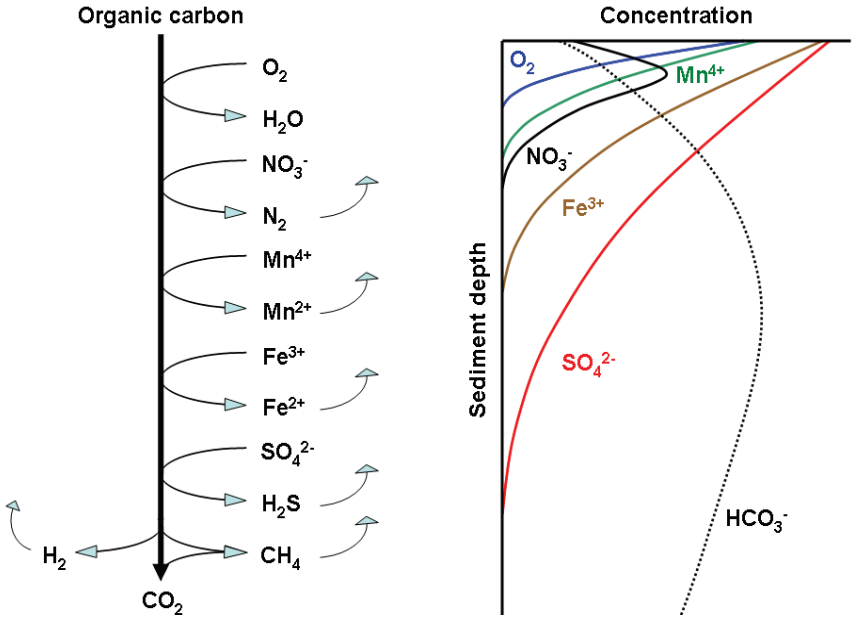


**Figure 2.** Sequence of electron accepting processes during the degradation of organic matter in sediments (a) and an idealized vertical distribution of electron acceptors (arbitrary scale) in a typical marine sediment (b). Modified from Jorgensen *et al*. (1983) (a). Adapted from Canfield *et al*. (2005b) (b).

However, factors such as substrate/product concentration, pH and temperature strongly affect the energetics of these reactions and may favour one process over the other (Canfield *et al*., 2005b; Jørgensen, 2000). Besides these respiratory processes, organic carbon can be degraded by fermentation where organic matter acts as both the electron acceptor and the electron donor. The following is a brief summary how organic matter is mineralized in sediments:

Microbial degradation of organic matter starts with the depolymerization of macromolecular material. Microbes release extracellular enzymes or use enzymes associated to the outer membrane or cell wall to initially hydrolyze particulate polymers to smaller molecules such as sugars, amino acids, long chain fatty acids and nucleic acids (Figure 3). During the sequence of mineralization depolymerization is generally the rate-limiting step (Arnosti, 2004). Aerobic microorganisms use a wide range of the smaller molecules released by hydrolysis and can mineralize these compounds completely to $CO_2$. However, the oxic zone in shelf sediments is only millimetres to centimetres thick (Jørgensen, 1982; Jørgensen and Boetius, 2007). Thus, fermentation and anaerobic respiration take over in the sequence of organic matter mineralization. Nitrifying bacteria are still capable of using a versatile range of organic substances and can oxidize these completely to $CO_2$. But deeper in the sediment the energy

yield of microbial redox reactions becomes smaller. Sulfate reducing bacteria on the other hand largely depend on rather simple molecules (Jørgensen, 2000). Fermenting microorganisms provide these fermentation products such as volatile fatty acids including formate, acetate, propionate, butyrate as well as molecular hydrogen and alcohols. However, acetate can be also excreted during aerobic growth (Majewski and Domach, 1990; Farmer and Liao, 1997). Acetate among other organic acids is a common substrate for sulfate reducing bacteria (Laanbroek and Pfennig, 1981; Thauer and Postgate, 1982). Some sulfate reducing bacteria are capable of oxidizing organic compounds to $CO_2$ (complete oxidizers) whereas others are incapable of such complete oxidation (incomplete oxidizers) and excrete acetate as a product (Widdel and Bak, 1992). In addition, several *Gammaproteobacteria* and heterotrophic sulfur-oxidizing members of the marine *Roseobacter*-clade utilize acetate as carbon source (Kuenen and Veldkamp, 1973; Hagen and Nelson, 1996; Otte *et al.*, 1999; Nielsen *et al.*, 2000; Schulz and Beer, 2002; Sorokin, 2003; Sorokin *et al.*, 2005). Methanogenesis is usually the final process in the degradation of organic matter and becomes important when sulfate is depleted. Methanogens can only use very few substrates, primarily molecular hydrogen, $CO_2$ and acetate. Overall, molecular hydrogen, acetate and $CO_2$ are at the heart of organic matter mineralization.

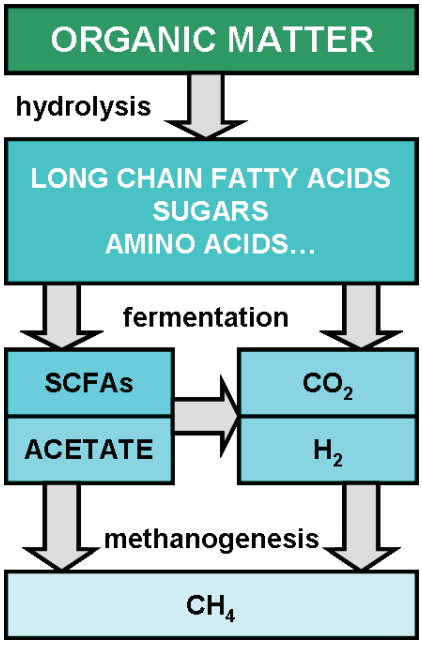


**Figure 3.** Sequence of organic matter mineralization in sediments. SCFA, short chain fatty acid. After Fenchel and Jørgensen (1977).

## 1.2) The marine sulfur cycle

The ocean waters and sediments are a major reservoir of sulfur on Earth. Sulfur compounds can have a broad range of oxidation states ranging from -2 (e.g. sulfide) to +6 (e.g. sulfate). This allows sulfur compounds to be used by microorganisms as both electron donors and acceptors depending on environmental conditions. Thereby the sulfur cycle is closely linked to other element cycles such as nitrogen, phosphorous, iron and in particular carbon. Sulfate, the most stable form of sulfur, is the second most abundant anion in today's ocean with concentrations of approximately 28 mM. Besides sulfate, sulfur is present in the ocean in many inorganic forms such as sulfide, elemental sulfur ($S^0$), thiosulfate and sulfite as well as organic sulfur compounds such as dimethyl sulfide or dimethylsulfoniopropionate (Ivanov, 1971; Andreae and Raemdonck, 1983; Taylor *et al.*, 1999; Zopfi *et al.*, 2004; Jansen *et al.*, 2009). All living organisms assimilate sulfur, where it is mainly present as constituent of proteins. But energy-yielding dissimilatory sulfur metabolism is essential for sulfur cycling in the ocean (Figure 4).

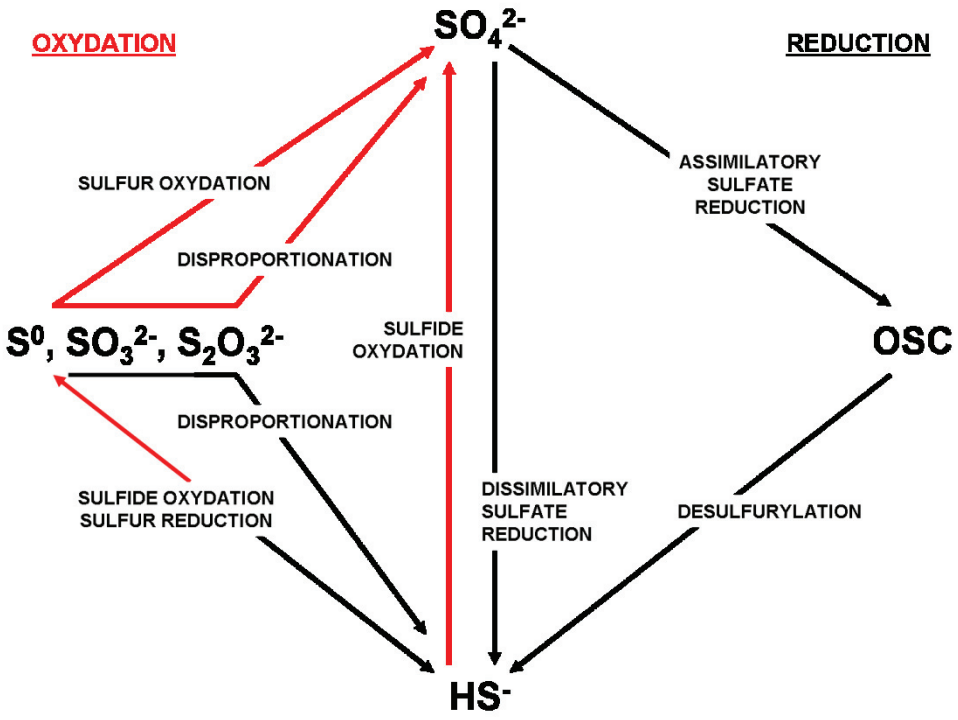


**Figure 4.** A simplified scheme of the biotic and abiotic sulfur cycle. Oxidative reactions are shown in red and reductive reactions are shown in black. OSC, organic sulfur compounds. Modified from Brüser *et al*. (2000).

In marine sediments dissimilatory sulfate reduction accounts for up to 50% of organic matter remineralization (Jørgensen, 1982) and thereby forms the fundament of biotic sulfur cycling (Rabus *et al.*, 2013). During this process sulfate-reducing bacteria and archaea produce large amounts of sulfide. A fraction of the produced sulfide is precipitated and retained in the

sediment as iron sulfide or pyrite, while the remaining can be either chemically or biologically reoxidized (Jørgensen, 1982; Howarth, 1984). The sulfide concentration typically increases with sediment depth (Zopfi *et al.*, 2004) and 80-99% of the sulfide is reoxidized to sulfate at the sediment surface (Jørgensen, 1977a; Howarth, 1984). Different sulfur intermediates are produced during microbial sulfur oxidation which can be further oxidized to sulfate, reduced or disproportionated (Figure 4). Disproportionation can be considered as inorganic fermentation where parts of the sulfur species are concurrently oxidized and reduced. Usually $S^0$ accumulates to higher concentrations in sediments than other intermediates such as polysulfide, thiosulfate, tetrathionate, sulfite (Zopfi *et al*., 2004).

### 1.2.1) Dissimilatory sulfur-metabolizing bacteria and archaea in marine sediments

The microbial reduction of inorganic sulfur significantly contributes to sulfur cycling and represents the counterpart of microbial sulfur oxidation (Rabus *et al.*, 2013). Among others, sulfate, $S^0$ and further reduced sulfur species can be used by bacteria and archaea as electron acceptor for anaerobic respiration (dissimilatory sulfate or sulfur reduction). Sulfur and sulfate reducers are distributed among various phylogenetic lineages (Figure 5). The only known sulfate-reducing archaea so far are found in the genera *Archaeoglobus* and *Caldivirga* whereas sulfur-reducing archaea include several orders (e.g. *Desulfurococcales*, *Thermococcales*, *Thermoproteales*, and *Sulfolobales*) (Muyzer and Stams, 2008; Rabus *et al.*, 2013; and references therein). On the other hand, several bacteria and archaea gain energy from the oxidation of reduced sulfur compounds. Likewise, sulfur oxidizers are physiologically and phylogenetically diverse. Archaeal sulfur-oxidizers are found in the order *Sulfolobales* (Segerer *et al.*, 1985; Huber and Prangishvili, 2006). The following section will focus on sulfur-oxidizing bacteria (SOB) and sulfate-reducing bacteria (SRB) as these groups were subject of this thesis.

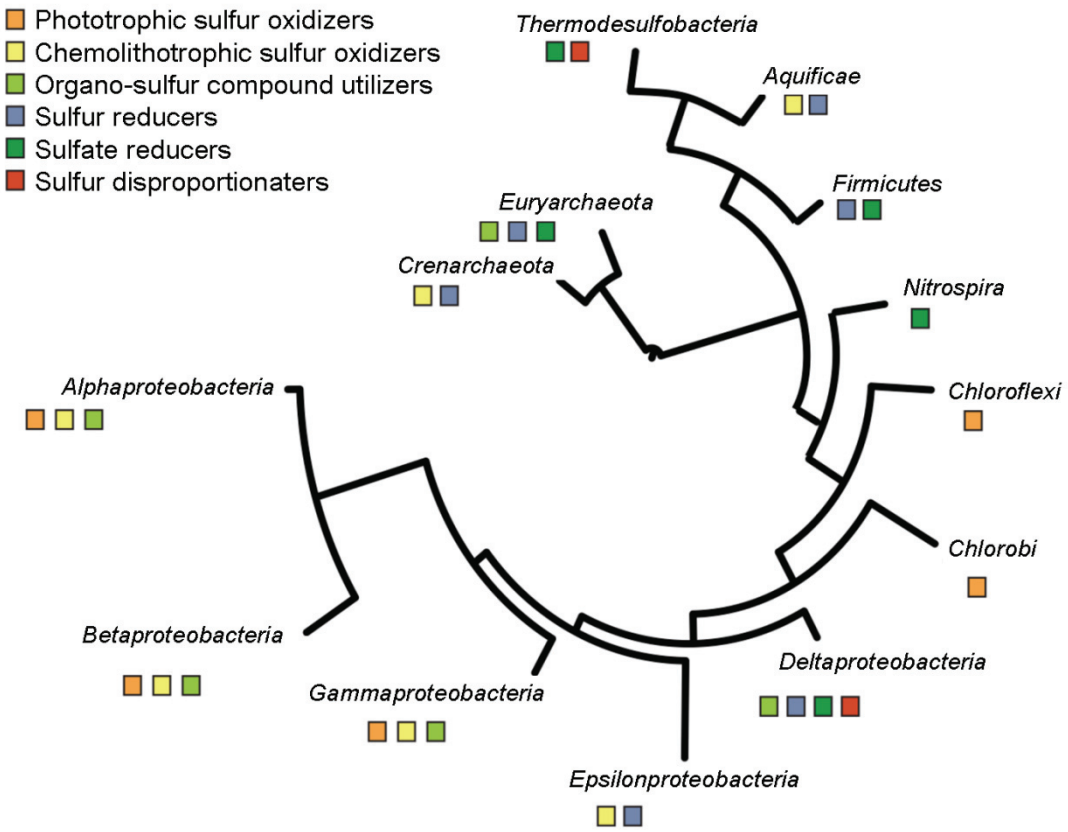


**Figure 5.** Schematic phylogenetic tree depicting the diversity of sulfur-metabolizing microorganisms among major phylogenetic lineages. Modified after Sievert *et al*. (2007). Figure adapted from Pjevac (2014)

*Sulfur-oxidizing bacteria*

Chemotrophic sulfur-oxidizing microorganisms fix inorganic carbon or assimilate organic carbon using energy gained from the oxidation of reduced sulfur species whereas phototrophic sulfur oxidizers use light as energy source and reduced sulfur compounds as electron donor for anoxygenic photosynthesis. The most prominent phototrophic sulfur oxidizers are the strictly anaerobic green sulfur bacteria (GSB) of the phylum *Chlorobi* and the gammaproteobacterial purple sulfur bacteria (PSB). GSB are restricted to very narrow zones in aquatic habitats and sediments as they require both light and reduced sulfur species for growth and they have relatively little metabolic flexibility (Bergstein *et al.*, 1979; Steinmetz and Fischer, 1982; Brune, 1989; Heising *et al.*, 1999; Overmann, 2006; Frigaard and Dahl, 2008). On the contrary, PSB are capable of using various electron donors for anoxygenic photosynthesis such as sulfide, elemental sulfur, thiosulfate, tetrathionate, polysulfides, sulfite, $H_2$ or ferrous iron (Steudel *et al.*, 1990; Sasikala and Ramana, 1997; Dahl, 2008). Some PSB can also live chemolithoautotrophically or chemoorganoheterotrophically in the dark (Imhoff, 2006; Frigaard and Dahl, 2008). Their

versatile metabolism allow the PSB to inhabit a broader niche than the GSB (Imhoff and Trüper, 1977; Bryantseva *et al.*, 1999; Oren, 2002; Overmann, 2008; Sorokin, 2008).

Most chemotrophic SOB belong to the alpha, beta, gamma and epsilon classes within the *Proteobacteria* (Figure 7; Friedrich *et al.*, 2005; Sievert *et al.*, 2007). In particular in marine environments, other chemolithotrophic sulfur oxidizers such as the archaeal *Sulfolobales* and the thermophilic *Aquificae* are rare (Huber and Stetter, 1991; Burggraf *et al.*, 1992; Huber *et al.*, 1992; Reysenbach and Cady, 2001). Furthermore, betaproteobacterial sulfur oxidizers are more common in freshwater habitats than in marine environments (Glöckner *et al.*, 1999).

Among the *Alphaproteobacteria*, the *Roseobacter*-clade (RCB) plays an important role in the oxidation of climate relevant dimethyl sulfide (DMS) which originate from dimethylsulfoniopropionate released by marine photoautotrophs (González *et al.*, 1999; González *et al.*, 2003; Zubkov *et al.*, 2002; Vila *et al.*, 2004; Howard *et al.*, 2008). RCB are ubiquitous in the ocean and abundant members of the bacterioplankton. Generally, RCB have a heterotrophic lifestyle with metabolically versatile capabilities such as anoxygenic phototrophy and oxidation of inorganic or organic sulfur compounds (Sorokin, 1995; González *et al.*, 1999; Howard *et al.*, 2006; Sass *et al.*, 2010; Curson *et al.*, 2011). The *Roseobacter*-clade was also found in high cell abundance in coastal sediment contributing up to 10% to the bacterial community, thereby outnumbering pelagic RCB by three orders of magnitude (Lenk *et al.*, 2012). In addition, members of the globally abundant alphaproteobacterial SAR11 clade can metabolize organo-sulfur compounds (González and Moran, 1997; González *et al.*, 1999; Buchan *et al.*, 2005; Howard *et al.*, 2006; Curson *et al.*, 2011).

Gammaproteobacterial sulfur oxidizers are physiologically highly versatile. Besides phototrophic sulfur oxidizers, the class *Gammaproteobacteria* harbour facultative and obligate chemolithoautotrophic SOB. Various gammaproteobacterial SOB are capable to use other inorganic and also organic compounds as electron donor or energy source (Sorokin, 2003; Petersen *et al.*, 2011; Anantharaman *et al.*, 2013; Hansen and Perner, 2015). Some representatives were also found in endo- or ectosymbiotic association with marine invertebrates (Dubilier *et al.*, 2008; Kleiner *et al.*, 2012; Petersen et al., 2012). Among the best studied sulfur-oxidizing *Gammaproteobacteria* are the large conspicuous *Beggiatoa*, *Thioploca* and *Thiomargarita* (Jørgensen, 1977; Fossing *et al.*, 1995; Schulz *et al.*, 1996; Schulz *et al.*, 1999; Schulz and Jørgensen, 2001; Schulz and Schulz, 2005). Furthermore, the ecophysiology and genetic composition of key players of sulfur cycling in OMZs and hydrothermal vents, such as the gammaproteobacterial SUP05-clade, have been extensively studied (Lavik *et al.*, 2009; Canfield *et al.*, 2010; Reinthaler *et al.*, 2010; Swan *et al.*, 2011; Grote *et al.*, 2012; Anantharaman *et al.*, 2013; Mattes *et al.*, 2013; Hawley *et al.*, 2014). In

the past decades, small and unicellular chemolithoautotrophic sulfur-oxidizing *Gammaproteobacteria* were repeatedly isolated from marine sediments (Kuenen and Veldkamp, 1972; Brinkhoff *et al.*, 1999; Park *et al.*, 2011) but these organisms do not seem to be the key players *in situ*. Culture-independent studies have shown that uncultured *Gammaproteobacteria* distantly related to cultured sulfur oxidizers, in particular to symbionts of marine invertebrates were abundant in sediments (Musat *et al.*, 2006; Lenk *et al.*, 2011; Boschker *et al.*, 2014; Vasquez-Cardenas *et al.*, 2015), while large sulfur bacteria such as *Beggiatoa* occur only patchily (Salman *et al.*, 2013; Ruff *et al.*, 2015).

Chemolithoautotrophic sulfur-oxidizing *Epsilonproteobacteria* represent a substantial fraction of the microbial community at hydrothermal vents (Nakagawa *et al.*, 2005; Takai *et al.*, 2006; Sievert *et al.*, 2008; Roalkvam *et al.*, 2011; Schauer *et al.*, 2011). Furthermore, members of the *Sulfurimonas*/*Sulfurovum* group are involved in $S^0$ oxidation at sediment surfaces (Pjevac *et al.*, 2014). In addition to the gammaproteobacterial SUP05-clade, members of the *Epsilonproteobacteria* were also abundant in oxygen-depleted pelagic environments (Campbell *et al.*, 2006; Grote *et al.*, 2007; Lavik *et al.*, 2009; Grote *et al.*, 2012). The well characterized chemolithoautotrophic sulfur oxidizers *Arcobacter sulfidophilus* and *Sulfurimonas denitrificans* have been isolated from coastal sediments (Hoor, 1975; Wirsen *et al.*, 2002). Nevertheless, in coastal sandy sediments only low relative abundance of sulfur-oxidizing *Epsilonproteobacteria* have been reported (Llobet-Brossa *et al.*, 1998; Lenk *et al.*, 2011).

*Sulfate-reducing bacteria*

Dissimilatory sulfate reduction is the defining trait of sulfate-reducing bacteria (SRB) and among anaerobic respirations in marine environments, the reduction of sulfate is most important (Rabus *et al.*, 2013; Rabus *et al.*, 2015). As end product of dissimilatory sulfate reduction SRB release substantial amounts of sulfide, which is corrosive and toxic already at micromolar concentrations. Several SRB have been isolated from marine sediments, of which a large fraction belong to the families *Desulfobacteraceae* and *Desulfovibrionaceae* within the class of *Deltaproteobacteria* (Widdel and Pfennig, 1981; Devereux *et al.*, 1989; Widdel and Bak, 1992; Rabus *et al.*, 2013). However, SRB are phylogenetically diverse and have versatile lifestyles with broad metabolic capabilities such as long-distance electron transport (cable bacteria) (Nielsen *et al.*, 2010; Pfeffer *et al.*, 2012) animal symbiosis (Woyke *et al.*, 2006; Kleiner *et al.*, 2012) or syntrophic associations. SRB use various organic molecules as carbon and energy source or can even grow lithoautotrophically (Rabus *et al.*, 2013; and references therein). The SRB known to date belong to the bacterial phyla *Proteobacteria*, *Fimicutes*, *Thermodesulfobacteria* and *Nitrospirae* (Figure 7) and were found besides marine environments in aquatic and terrestrial habitats as well as in the human gut

and animal microbiomes (Rabus *et al.*, 2015). Using cultivation-dependent and cultivation-independent approaches it has been shown that particularly members of the *Desulfosarcina/Desulfococcus* cluster within the *Desulfobacteraceae* dominate SRB communities in coastal-, shelf-, mangrove- and deep sea sediments (LlobetBrossa *et al.*, 2002; Dhillon *et al.*, 2003; Mußmann *et al.*, 2005; Gittel *et al.*, 2008; Leloup *et al.*, 2009; Varon-Lopez *et al.*, 2014). Given their abundance and their metabolic potential to completely oxidize organic compounds to $CO_2$, members of the *Desulfobacteraceae* were suggested to be the key players in carbon- and sulfur-cycling in organic rich marine sediments (Rabus *et al.*, 2015). On the other hand, incomplete-oxidizing SRB are incapable of such complete oxidation as these organisms lack the metabolic pathway to oxidize acetyl-CoA to $CO_2$ (Widdel and Bak, 1992). However, some incomplete-oxidizing SRB such as *Desulfobulbaceae* are capable of using acetate together with $CO_2$ as carbon source when additional energy sources such as $H_2$ are present (Kuever, 2014; Rabus *et al*., 2015). Disproportionating *Desulfobulbaceae* are also possible key players in anoxic $S^0$ consumption at the sea floor (Pjevac *et al.*, 2014).

### 1.2.2) Pathways of microbial sulfur oxidation and carbon fixation

The different microbial sulfur oxidation pathways have been extensively reviewed (Dahl *et al.*, 2001; Friedrich *et al.*, 2005; Mohapatra *et al.*, 2008; Frigaard and Dahl, 2008). The following section is a brief overview of enzymes involved in the oxidation of reduced sulfur compounds (see also Figure 6).

Among the best studied are the thiosulfate-oxidizing multi-enzyme system (SOX) for oxidation of thiosulfate or sulfite to elemental sulfur or sulfate and the reverse dissimilatory sulfite reductase complex (rDSR) for oxidation of sulfide/$S^0$ to sulfite (Figure 6). In addition, sulfide can be oxidized to elemental sulfur mediated by sulfide:quinine oxidoreductase (SQR) or flavocytochrome *c* sulfide dehydrogenase (FccAB). The adenosine 5'-phosphosulfate reductase (APS) and ATP sulfurylase (SAT) mediate the oxidation of sulfite to sulfate. Among others, the sulfite oxidoreductase (SorAB) or sulfite dehydrogenase (SoeABC) can also catalyze this final oxidation step.

Uncultured sulfur-oxidizing bacteria have been studied in the past by comparative sequence analysis of functional marker genes encoding the characteristic enzyme. Therefore, genes encoding subunits of the reverse dissimilatory sulfite reductase (*dsrAB*), of the adenosine-5'-phosphosulfate reductase (*aprA*) and of the thiosulfate-oxidizing multi-enzyme complex (*soxB*) have been used to target the diversity of marine benthic sulfur oxidizers (Petri *et al.*, 2001; Meyer and Kuever, 2007; Lenk *et al.*, 2011; Lenk *et al.*, 2012; Pjevac, 2014; Thomas *et al.*, 2014).

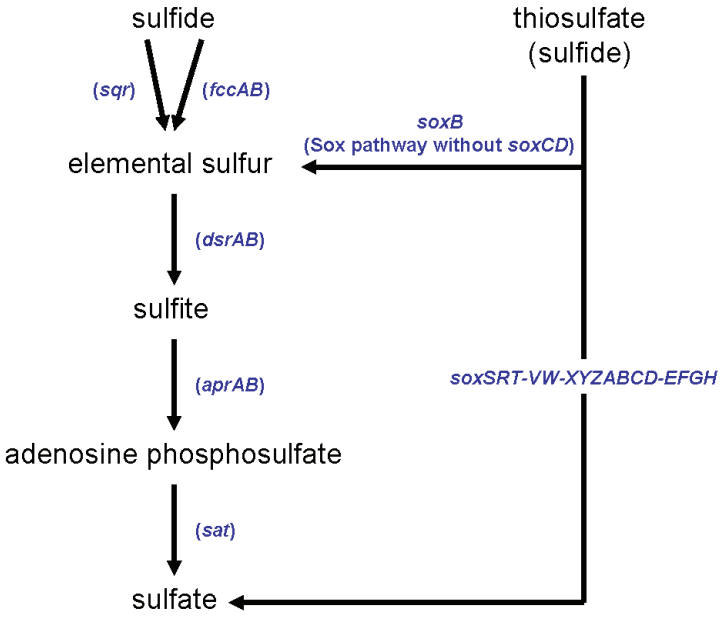


**Figure 6**. A simplified scheme of sulfur oxidation pathways. Adapted from Anantharaman *et al*. (2013) and modified after Frigaard and Dahl (2009).

Autotrophs fix inorganic carbon and thereby providing organic carbon to heterotrophs. This makes the balance between autotrophy and heterotrophy a key factor regulating $CO_2$ and $O_2$ concentrations in the atmosphere (Hügler and Sievert, 2011a). Currently, there are six pathways known for $CO_2$ fixation: the Calvin-Benson-Bassham (CBB) cycle (Bassham and Calvin, 1960), the reductive tricarboxylic acid (rTCA) cycle (Buchanan and Arnon, 1990), the reductive acetyl-CoA (Ljungdahl and Wood, 1969), the 3-hydroxypropionate (3-HP) cycle (Holo, 1989; Zarzycki *et al.*, 2009), the 3-hydroxypropionate/4-hydroxybutyrate (3-HP/4HB) cycle (Kandler and Stetter, 1981; Berg *et al.*, 2007) and the dicarboxylate/4-hydroxybutyrate (DC/4-HB) cycle (Huber *et al.*, 2008). Although the importance of the so-called alternative carbon fixation pathways is nowadays well known, the CBB cycle, which is the carbon fixation pathway used for oxygenic photosynthesis, is the most significant one (Field *et al.*, 1998; Falkowski *et al.*, 2000; Raven, 2009).

Bacteria use the CBB-, rTCA- and 3-HP cycle as well as the reductive acetyl-CoA pathway for carbon fixation. Some archaea also use the reductive acetyl-CoA for carbon fixation but the 3-HP/4HB- and DC/4-HB cycle have been exclusively identified in archaea so far (Hügler and Sievert, 2011). Carbon fixation pathways that harbour oxygen-tolerant enzymes and are used by aerobic organisms (CBB-, 3-HP- and 3-HP/4HB cycle) require more energy in form of ATP for synthesizing a three-carbon unit compared to pathways using oxygen-sensitive enzymes which are used by anaerobic or microaerophilic microorganisms (reductive acetyl-CoA pathway, rTCA- and DC/4-HB cycle) (Mccollom and Amend, 2005; Berg *et al.*, 2010; Berg, 2011; Fuchs, 2011).

In marine environments the CBB cycle is used by *Cyanobacteria*, photo- or chemoautotrophic *Alpha*-, *Beta*-, *Gamma*- and *Deltaproteobacteria* as well as some *Firmicutes* and *Chloroflexi* (Ivanovsky *et al.*, 1999; Caldwell *et al.*, 2007; Hügler and Sievert, 2011; Swan *et al.*, 2011). A genetic determinant for the CBB cycle is the *cbbM*/*cbbL* gene encoding the characteristic ribulose 1,5-bisphosphate carboxylase/oxygenase enzyme (RuBisCO), which catalyzes the initial carboxylation of ribulose 1,5-bisphosphate (Quayle *et al.*, 1954). The rTCA cycle is used by diverse groups of anaerobic and micoaerophilic bacteria. In particular, sulfur-oxidizing *Epsilonproteobacteria* use this carbon fixation pathway (Hügler *et al.*, 2005; Hügler *et al.*, 2007; Sievert *et al.*, 2008; Nakagawa and Takai, 2008). The gammaproteobacterial symbiont of *Riftia pachyptila* uses the rTCA cycle in addition to the CBB cycle (Markert *et al.*, 2007). A characteristic enzyme of this pathway is the ATP citrate lyase (ACL) that catalyzes the ATP-dependent cleavage of citrate (Wahlund and Tabita, 1997; Hügler *et al.*, 2005; Hügler *et al.*, 2007; Lücker *et al.*, 2010). The ACL is encoded by the *aclAB* genes. Further alternative carbon fixation pathways of significance in marine environments, in particular sediments, are the reductive acetyl-CoA pathway and the 3-HP/4-HB cycle. The latter is found in archaeal sulfur oxidizers and ammonia-oxdidizing archaea (Berg *et al.*, 2007; Könneke *et al.*, 2014). The reductive acetyl-CoA pathway is present in autotrophic sulfate-reducing bacteria and archaea as well as methanogenic archaea (Jansen *et al.*, 1984; Zeikus *et al.*, 1985; Schauder *et al.*, 1988; Fuchs, 1994; Vornolt *et al.*, 1995; Strous *et al.*, 2006)

## 1.3) Hydrogen-producing and -consuming processes

Molecular hydrogen ($H_2$) is a central intermediate in organic matter mineralization (Fenchel and Jørgensen, 1977; Hoehler *et al.*, 1998) and is widespread in the environment. Microorganisms release and oxidize $H_2$ during various processes (Figure 7). $H_2$ is an electron donor and a source of energy for diverse functional groups of microorganisms such as sulfate reducers, sulfur oxidizers, acetogens, methanogens and anoxygenic phototrophs and the potential to metabolize $H_2$ is common among diverse *Bacteria* and *Archaea* (Schwartz *et al.*, 2013). Moreover, $H_2$ is a primary thermodynamic control on most redox reactions (Hoehler *et al.*, 1998). Depending on the *in situ* concentration, $H_2$ supports different respiratory processes and affect the thermodynamics of fermentation processes (Hoehler *et al.*, 1998; Canfield *et al.*, 2005a).

Fermentation is the major source of $H_2$ in the biosphere (Schwartz *et al.*, 2013). In anaerobic food chains fermentation processes are an integral part of organic carbon remineralization (Schmitz *et al.*, 2006). In marine sediments the oxic layer varies from a few millimetres in coastal areas to several decimetres in deep sea sediments (Murray and Grundmanis, 1980; Revsbech *et al.*, 1980; Wenzhöfer and Glud, 2002). Couple of centimetres below the surface, shelf sediments are usually anoxic. Here, obligate and facultative fermenters release excess reducing equivalents in form of $H_2$. The production and oxidation of $H_2$ are closely coupled so that the produced $H_2$ does not accumulate and is generally kept at low concentrations (5-30 nM) (Novelli *et al.*, 1987; Novelli *et al.*, 1988; Michener *et al.*, 1988). Microbial fermentation processes become endergonic if $H_2$ would accumulate. It has been shown that fermentation of butyrate and propionate was inhibited by $H_2$ concentrations of 100 and 20 nM, respectively (Schwartz *et al.*, 2013).

An additional source of biologically produced $H_2$ in marine environments is nitrogen fixation. Here, $H_2$ is not produced by a specific $H_2$-transforming enzyme (hydrogenase) but rather evolved as by-product from nitrogenase activity (Schubert and Evans, 1976). Cyanobacteria are among the most widespread diazotrophs and in surface waters they can release significant amounts of $H_2$ to the environment. At sediment surfaces nitrogen fixation by cyanobacterial mats has been suggested as alternative source of $H_2$ (Hoehler *et al.*, 2001).

A minor source of $H_2$ is anaerobic carbon monoxide oxidation by carboxidotrophs (Schwartz *et al.*, 2013). The anoxygenic phototrophic bacterium *Rhodospirillum rubum* and some thermophilic *Firmicutes* are well described to perform this process (Fox *et al.*, 1996a; Fox *et al.*, 1996b; Sokolova *et al.*, 2001; Sokolova *et al.*, 2002; Sokolova *et al.*, 2004; Slepova *et al.*, 2006). In marine environments anaerobic CO oxidation is of unknown significance.

Apart from biologically mediated $H_2$ production $H_2$ can be produced photochemically possibly from chomophoric dissolved organic matter (Punshon and Moore, 2008). This process of $H_2$ production in the absence of biology may be an important source of $H_2$ in ocean and lake

surface waters (Punshon and Moore, 2008). $H_2$ may also be produced anaerobically along with formation of pyrite from ferrous sulfide and hydrogen sulfide (Wächtershäuser, 1988; Drobner *et al.*, 1990).

More than a century ago Kasserer (1906) described aerobic $H_2$ oxidizing bacteria that performed the "knallgas" reaction to gain energy for growth:

$$H_2 + ½O_2 \rightarrow H_2O \qquad (\Delta G^0 \text{ -210 kJ mol}^{-1})$$

The first isolated knallgas bacteria were facultative $H_2$ oxidizers that prefer organic acids and sugars or grow mixotrophically (Aragno and Schlegel, 1992). Much later the first obligate hydrogenotroph was isolated from marine environments (Nishihara *et al.*, 1991). Recently it has been shown that $H_2$ can be an important energy source also for chemoautotrophs at hydrothermal vents. Free living and symbiotic sulfur-oxidizing bacteria (SOB) of the gammaproteobacterial SUP05 clade as well as *Thiomicrospira* possess the metabolic flexibility to use $H_2$ as an alternative energy source besides reduced sulfur compounds with oxygen or nitrate as electron acceptor to fuel dark carbon fixation (Petersen *et al.*, 2011; Anantharaman *et al.*, 2013; Hansen and Perner, 2015).

In contrast to oxygenic phototrophs their anoxygenic counterparts use reduced molecules such as $H_2$ or reduced sulfur compounds as electron donor but not $H_2O$ (Roelofsen, 1934; Drews and Imhoff, 1991). Therefore, anoxygenic phototrophs do not produce oxygen. The marine bacterium *Thiocapsa roseopersicina* strain BBS has been shown to produce $H_2$ during fermentative growth in the dark and oxidize $H_2$ during anoxygenic photosythesis or aerobic chemolithotrophic growth in the dark (Ákos T. Kovács *et al.*, 2005; K.L. Kovács *et al.*, 2005; Rákhely *et al.*, 2007; Maróti *et al.*, 2010).

Further $H_2$ scavenging processes are dehalorespiration (Scholz-Muramatsu *et al.*, 1995), acetogenesis (Diekert and Wohlfarth, 1994), fumarate respiration (Dubini *et al.*, 2002) and Fe(III) reduction (Figure 7). The latter has been suggested as one of the earliest form of respiration (Vargas *et al.*, 1998; Kashefi and Lovley, 2000).

Methanogenesis and the reduction of sulfur compounds are the major $H_2$ consuming processes in the biosphere (Schwartz *et al.*, 2013), in particular in marine environments. Many sulfate reducing bacteria and archaea possess the metabolic potential to oxidize $H_2$. They grow either lithoautotrophically on $H_2$ and $CO_2$ or mixotrophically on $H_2$ together with organic compounds (Rabus *et al.*, 2015). Up to nine different hydrogenases were identified in the genome of the SRB *Syntrophobacter fumaroxidans* suggesting a versatile $H_2$ metabolizing potential (Bok *et al.*, 2002; Plugge *et al.*, 2012). Some sulfate reducing bacteria are capable to efficiently reoxidize $H_2$ produced during fermentation, thus no $H_2$ is released to the environment (Tsuji and Yagi, 1980). In surface sediments, so far sulfate reduction is suggested to be the quantitatively dominant $H_2$ consuming process, whereas in sulfate-depleted sediments SRB rather form $H_2$ and methanogenesis becomes the major $H_2$

consuming process (Winfrey and Zeikus, 1977; Oremland and Taylor, 1978; Oremland and Polcin, 1982).

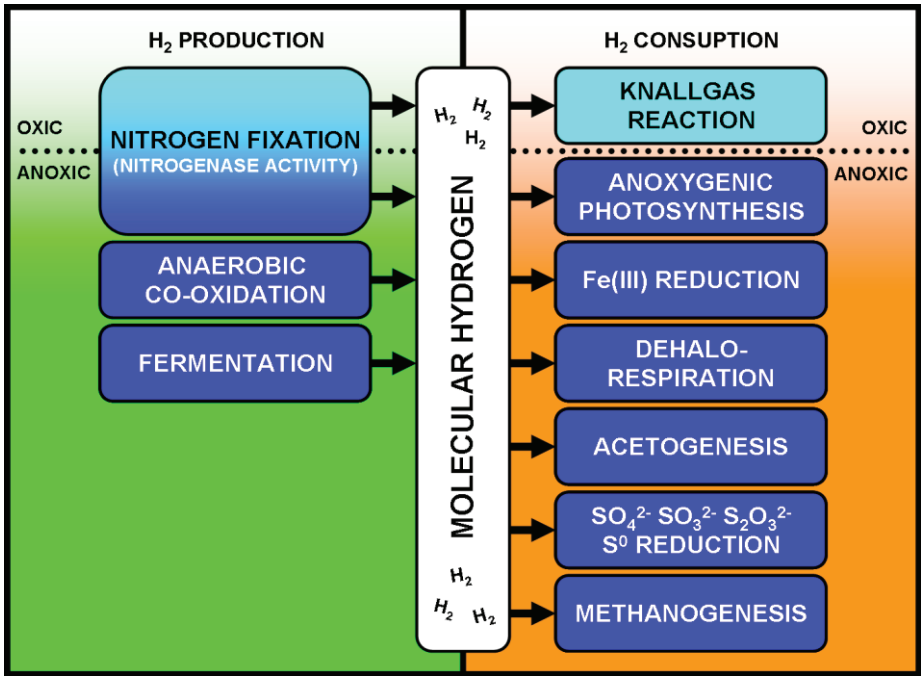


**Figure 7.** Overview of major biologically mediated $H_2$-producing and -consuming processes in the environment.

### 1.3.1) Classification of $H_2$-producing and -consuming enzymes

Hydrogenases ($H_2$ases) are metalloenzymes that catalyze the reversible cleavage of molecular hydrogen to protons and electrons:

$$H_2 \leftrightarrow 2H^+ + 2e^-$$

$H_2$ases can be divided into three major groups with a phylogenetically independent origin (Schwartz *et al.*, 2013): [NiFe]-$H_2$ases (including [NiFeSe]-$H_2$ases), [FeFe]-$H_2$ases and [Fe]-$H_2$ases. The first detailed classification scheme for $H_2$ases was presented and later on revised by Vignais and coworkers (Vignais *et al.*, 2001; Vignais and Billoud, 2007). Recently, an expanded $H_2$ase classification scheme (Figure 8) was introduced by Greening *et al.* (2015), which includes the prediction of biological functions.

[NiFe]-$H_2$ases can be subdivided into four groups of which each group contains several subclasses. Group 1 contains membrane-associated energy transducing enzymes that liberate electrons for respiration. Group 1 [NiFe]-$H_2$ases are heterodimeric enzymes composed of a large subunit that carries the catalytic site and a small subunit that contains three iron-sulfur clusters for electron transport (Volbeda *et al.*, 1995; Higuchi *et al.*, 1997). This group mainly consist of oxygen sensitive enzymes but also harbours oxygen-tolerant subclasses (1d and 1h, Figure 8). Diverse bacteria and archarea possess group 1 [NiFe]-$H_2$ases linking $H_2$ oxidation to processes such as sulfate-, nitrate-, oxygen respiration and

iron reduction. Some of these enzymes may function bidirectional and can also work in the direction of $H_2$ production (1c and 1e; Lukey *et al.*, 2010; Greening *et al.*, 2015). Group 2 contains cytoplasmic oxygen tolerant uptake $H_2$ases (2a), $H_2$-sensing enzymes that regulate $H_2$ase expression (2b) and $H_2$ases of unknown function (2c and 2d). Group 2a is mainly distributed among cyanobacteria (Schwartz *et al.*, 2013) but also found in nitrifying bacteria capable to use $H_2$ as alternative energy source during aerobic growth (Koch *et al.*, 2014). Group 3 [NiFe]-$H_2$ases were multimeric enzymes composed of several subunits. These bidirectional enzymes were soluble in the cytoplasm and interact with cofactors such as $F_{420}$, NAD or NADP. Group 4 contains membrane bound multisubunit energy converting $H_2$ases. The best studied example represents the $H_2$-evolving hydrogenase-3 (4a) from *E. coli* (McDowall *et al.*, 2014) that produces $H_2$ during mixed acid fermentation. Except of group 2, which is exclusively distributed among bacteria, all groups of [NiFe]-$H_2$ases have been identified in both bacteria and achaea.

[FeFe]-$H_2$ases are mainly $H_2$-evolving enzymes but also contain putatively $H_2$-sensory enzymes and $H_2$ases of unknown function. Fermentative production is a well described function of this structurally heterogeneous group which contains mono-, di-, tri- and tetrameric enzymes. Accordingly, Greening *et al.* (2015) proposed a subdivision of [FeFe]-$H_2$ases into six subtypes.

The third group, [Fe]-$H_2$ases are 5,10-methenyltetrahydromethanopterin reducing (Hmd) enzymes. This highly conserved group of $H_2$-activating $H_2$ases was so far only identified in methanogenic archaea. For further details about the expanded hydrogenase classification scheme see Greening *et al.* (2015).

$H_2$ase-encoding genes form operons with structures specific for each group and subclass. Besides the $H_2$ase genes most of these operons encode genes for proteins involed in maturation of the $H_2$ase precursor to an active enzyme and regulatory genes. For further details about the genetic organisation of $H_2$ase operons see Schwarz *et al.* (2013).

Evidence is accumulating that $H_2$-cycling has a central function in the energy transfer in diverse ecosystems. However, a comprehensive dataset on $H_2$ases and the corresponding microorganisms in marine sediments is still lacking. Moreover, $H_2$-cycling in marine surface sediments has hardly been studied on the molecular level so far and still little is known about the diversity and activity of *in situ* relevant $H_2$-metabolizing microorganisms.

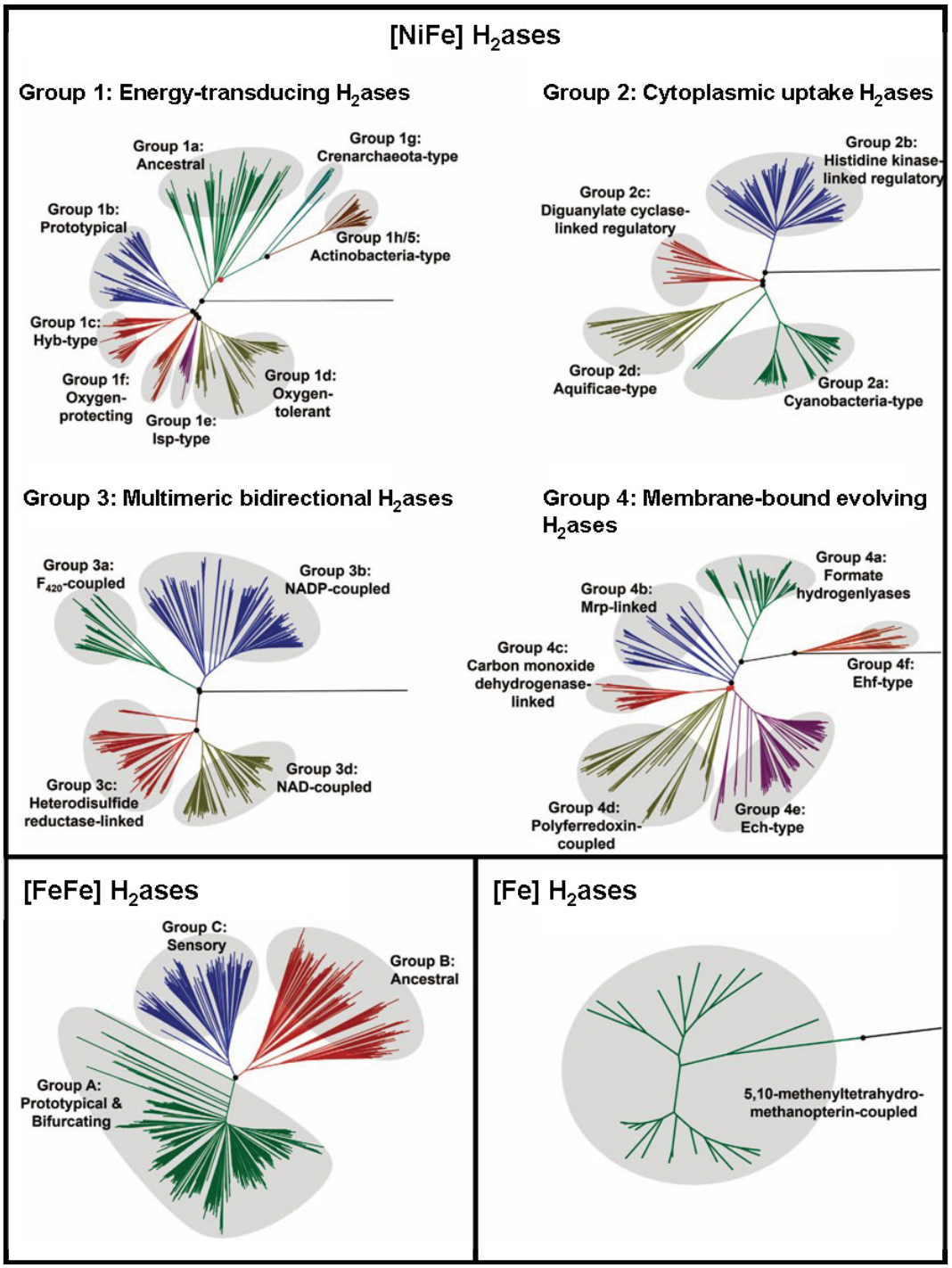


**Figure 8.** Classification and phylogeny of $H_2$ producing and consuming enzymes. Neighbour-joining trees showing the phylogenetic relationship of the $H_2$ase groups and subgroups. Black circles, bootstrap support >75%. Red circles, bootstrap support <75%. Modified from Greening *et al.* (2015).

## 1.4) Cultivation-independent molecular approaches to study microbial communities

Isolation of pure cultures is essential to study the physiology of microorganisms. However, to date, a great majority of microorganisms resist cultivation (Alain and Querellou, 2009; Vartoukian *et al.*, 2010; Stewart, 2012). To overcome this limitation and to study microbes in their natural environment several molecular tools have been developed.

The 16S rRNA gene but also functional genes have been widely used as phylogenetic marker to study the diversity of microbial communities. The full cycle rRNA approach is a cultivation-independent tool that allows the identification and *in situ* quantification of microbes in the environment (Amann *et al.*, 1995). After nucleic acid extraction the 16S rRNA gene is amplified and either cloned and sequenced or directly sequenced using next generation sequencing technologies. The diversity is explored by comparative gene analysis and nucleic acid probes can be designed for fluorescence *in situ* hybridization (FISH). To complete the cycle, FISH allows the visualization and quantification of microbes within complex microbial communities.

Meta-omics approaches such as metagenomics and metatranscriptomics rely on the extraction of bulk nucleic acids from an assemblage of microorganisms followed by direct sequencing without amplification of a particular gene (Riesenfeld *et al.*, 2004; Leininger *et al.*, 2006). Metagenomics allows in-depth analysis of the diversity and metabolic potential of microbial communities and combined with metatranscriptomics it can provide information which metabolic pathways are active. This produces large amounts of data and for the computational reconstruction comprehensive bioinformatic analysis such as assembly, gene prediction, binning and taxonomic classification are necessary.

Single-cell genomics require whole genome amplification from a single target cell to recover enough nucleic acid sufficient for sequencing without the need of isolation of a pure culture. Therefore, single cells can be separated from complex assemblages using fluorescence activated cell sorting (FACS) followed by multiple displacement amplification (MDA) for random primed genome amplification (Lasken, 2007). This workflow has been used to study the genetic potential of marine microbes from various habitats (Woyke *et al.*, 2009; Swan *et al.*, 2011; Lloyd *et al.*, 2013; Kashtan *et al.*, 2014). Metagenomics may not allow the taxonomic assignment of all the sequence data to a particular phylogenetic clade. In particular, in environments that harbour a high microbial diversity such as sediments assembly and binning of sequence data can be difficult. Single-cell genomics may overcome these limitations.

### 1.4.1) Methods to study the activity of uncultured microbes

Linking the identity of uncultured microorganisms with their metabolic potential to use a specific substrate is essential to understand the role of particular phylogenetic groups within complex microbial communities. Isotope-labeling using either stable isotopes or radioisotopes is a great tool for microbial ecologists to study the ecophysiology of uncultured microbial populations in the environment (Wagner, 2009). The following is a brief introduction of some isotope-labeling methods and their application in sediments.

Stable isotope probing (SIP) was developed to trace the incorporation of stable isotopes (e.g. $^{13}C$, $^{15}N$) into cellular biomarkers such as nucleic acids (DNA-SIP, RNA-SIP) or phospholipid-derived fatty acids (PLFA-SIP). Active populations of the microbial community incorporate the heavier isotopes into cell components. Boschker *et al.* (1998) introduced PLFA-SIP to identify SRB responsible for $^{13}C$-acetate oxidation in estuarine and brackish sediments by their specific phospholipid fatty acids. Webster *et al*. (2006) used PLFA-SIP with $^{13}C$-labeled acetate, glucose and pyruvate to study the function of a sulfate reducing microbial community in marine sediments.

In contrast, DNA- and RNA-SIP was established for a phylogenetic identification of the active population that incorporates a specific substrate (Radajewski *et al.*, 2000; Manefield *et al.*, 2002). Both, DNA- and RNA-SIP have been widely applied in sediments to track the incorporation of common substrates such as acetate into the microbial community. Uncultured *Desulfobacteraceae*, *Firmicutes* and *Crenarchaeota* were reported to assimilate acetate in anoxic sulfate-reducing marine sediments (Boschker *et al*., 1998; Webster *et al*., 2006; Webster *et al.*, 2010; Seyler *et al.*, 2014; Na *et al.*, 2015). On the contrary, diverse *Gammaproteobacteria* like *Alteromonadales*, *Oceanospirillales* and *Acidithiobacillales* as well as epsilonproteobacterial *Arcobacter* were identified by RNA-SIP as acetate oxidizers using oxygen, nitrate and manganese oxide as electron acceptor (Vandieken *et al.*, 2012; Vandieken and Thamdrup, 2013). MacGregor *et al*. (2006) combined SIP with magnetic bead capture of hybridized 16S rRNA (Mag-SIP) to study the incorporation of acetate, propionate, glucose and amino acids into microbes of a marine sediment. Mag-SIP was further used to identify sulfate-reducing *Deltaproteobacteria* utilizing propionate and glucose in a coastal sediment (Miyatake *et al.*, 2009). DNA-SIP experiments require high substrate concentrations and extended incubation time, as multiple cell reproduction cycles are needed. Consequently, *in situ* conditions cannot be simulated. Community shifts during the incubation and cross-feeding are well known biases of DNA-SIP experiments (Dumont and Murrell, 2005). Furthermore, DNA- and RNA-SIP would miss microbes that assimilate a substrate but did not channel the isotopes into nucleic acids and generally SIP does not allow an exact quantification of substrate assimilation.

The combination of fluorescence *in situ* hybridization and microautoradiography (MAR-FISH) requires much shorter incubation times than DNA-SIP (Lee *et al.*, 1999). This approach allows observing and visualizing the incorporation of substrates labeled with radioisotopes at single-cell level within complex microbial communities. The incubated sample is exposed to an autoradiography emulsion after FISH. The incorporated radioisotopes lead to the precipitation of silver grains in the emulsion around the cells that assimilated the labeled substrate. MAR-FISH has been also used for semi-quantitative analysis of specific substrate metabolism, as the number of silver grains formed during exposure correlates with radioactivity (Nielsen *et al.*, 2003). In marine sediments MAR-FISH was recently used to identify uncultured potential sulfur-oxidizing chemoautotrophic *Gammaproteobacteria* (Lenk *et al*., 2011).

A rather new single-cell approach is the application of nanoscale secondary ion mass spectometry (nanoSIMS) for microbial ecology. NanoSIMS analyses the surface composition (stable- or radioactive isotope content) of single microbial cells at a spatial resolution of 50 nm. Compared to MAR the senstivity of nanoSIMS in cellular $^{14}C$ detection is 1000 x higher (Kuypers and Jørgensen, 2007). In combination with halogen *in situ* hybridization (HISH-SIMS) this approach has been used to link phylogenetic identification and quantification of metabolic activities of mixed populations of phototrophic bacteria (Behrens *et al.*, 2008; Musat *et al.*, 2008). NanoSIMS combined with FISH has been used to identify metabolic active cells in deep subseafloor sediments (Morono *et al.*, 2011) and to track nitrogen fixation and carbon assimilation at single cell level in microbial consortia or electrogenic cable bacteria from marine sediments (Dekas and Orphan, 2011; Dekas *et al.*, 2014; Vasquez-Cardenas *et al.*, 2015). Major drawbacks of nanoSIMS applications are a low sample-throughput and time-consuming sample preparation and data processing.

Flow cytometry (FCM) is a fast and reliable technique that originates from clinical diagnostic and medical research. FCM allows a high sample-throughput and nowadays it has broad applications in microbiology and marine science (Ibrahim and Engh, 2007; Wang *et al.*, 2010). Flow cytometric cell sorting together with radio-labeling has been used in the past to measure the assimilation of radioactive substrates into individual populations of marine bacterioplankton (Zubkov *et al.*, 2004; Zubkov *et al.*, 2007; Jost *et al.*, 2008). The basic principle of FCM (Figure 9) is as follows: a heterogeneous mixture of particles and cells in suspension (sample) is injected into a larger, surrounding column of sheath fluid. Under laminar flow condition the sample becomes hydrodynamically focused. Particles and cells singly pass one or multiple light sources and optical characteristics such as light scatter or fluorescence are collected by an array of photo-detectors simultaneously. The detected light scatter and fluorescence signals correlate with morphology and particle size as well as intracellular composition. In combination with nucleic acid or protein staining techniques

different populations of the microbial community can be distinguished by flow cytometry based on their DNA or protein content. The identified populations can subsequently separated by fluorescence activated cell sorting (FACS). However, unspecific DNA- or protein-stain does not allow a phylogenetic identification.

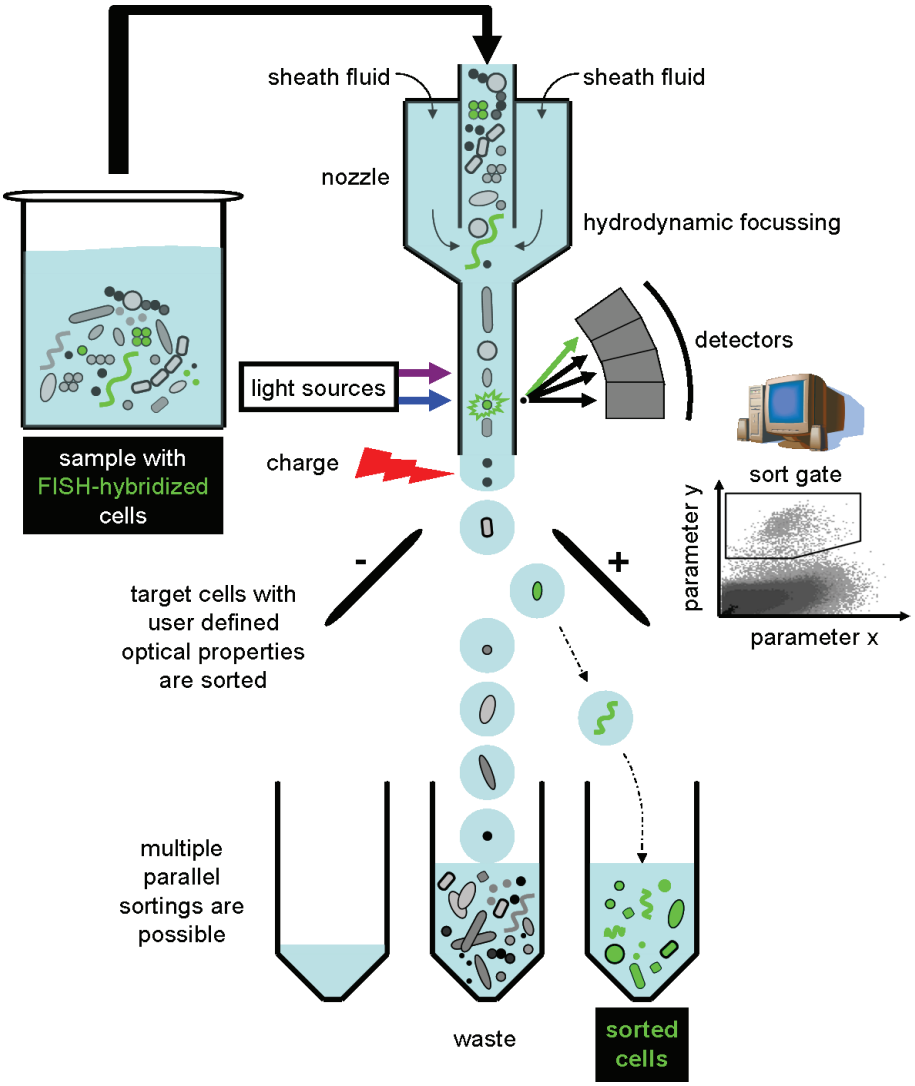


**Figure 9.** A simplified scheme for the basic principle of fluorescence-activated cell sorting using a jet-in-air flow cytometer. The example shows a mixture of cells hybridized with a specific FISH probe. Here, probe fluorescence is the defined optical parameter for cell sorting. Charged droplets containing cells with user defined optical properties are deflected by an electric field and thereby separated. Flow sorting with a jet-in-air flow cytometer allows sorting of multiple parallel fractions with different optical parameters.

## 2.) Objectives of my thesis

The overarching goals of the research presented in my thesis were the identification of microorganisms involved in the turnover of central products/intermediates of organic matter remineralization such as $CO_2$, $H_2$ and acetate in marine coastal sediments. Beyond the identification of organisms driving these processes and the investigation of their metabolic potential a major focus of this study was to quantify the contribution of microbial populations to specific carbon turnover processes. The specific objectives were:

(**3.1**) First, I asked the question: Are there ubiquitous groups of chemolithoautotrophs in coastal sediments and what energy sources they use? Recently, novel groups of chemolithoautotrophic sulfur-oxidizing *Gammaproteobacteria* were identified in a coastal sediment (Lenk *et al.*, 2011) but it is still unknown if there are cosmopolitan key players in marine sediments like the SUP05 group found in pelagic systems worldwide. 16S rRNA tag sequencing together with meta- and single cell genomics as well as metatranscriptomics should be used to shed light on these largely unresolved questions. To quantify the carbon-fixing activity of the identified microbial populations a method should be used that allow fast throughput and an accurate quantification of $^{14}CO_2$ uptake by phylogenetically identified bacteria from sediments. Therefore, we applied for the first time a novel combination of molecular and isotopic tracer techniques to achieve these goals and thereby overcome limitations of other methods such as SIP, MAR or nanoSIMS.

(**3.2**) The microorganisms consuming $H_2$ in marine sediments are largely unknown. Therefore, I screened a metagenome from an intertidal sediment for potential $H_2$-oxidizing or -producing bacteria. Two additional coastal sediments should be further screened using functional gene (uptake hydrogenase) libraries for the major groups identified in the metagenome. As previously published hydrogenase primers would miss many sulfate reducers novel SRB-specific primers were designed. Together with metatranscriptomics, $H_2$-consumption experiments and immunohistochemistry I aimed to identify bacterial groups *in situ* relevant for $H_2$ scavenging.

(**3.3**) Acetate is a major product from fermentation and at the same time an important substrate for various microbes. Already decades ago, acetate was suggested to be among the most important substrates for SRB (Laanbroek and Pfennig, 1981; Thauer and Postgate, 1982). As many phylogenetically and physiologically distinct bacterial groups are able to assimilate acetate, I aimed to quantify acetate assimilation for particular bacterial populations in a coastal sediment including SRB. Here I used flow sorting of FISH-labeled cells that potentially incorporated $^{14}C$-labeled acetate (method introduced in **3.1**.)

# 3.) Manuscripts

**Ubiquitous *Gammaproteobacteria* dominate dark carbon fixation in coastal sediments**

Stefan Dyksma, Kerstin Bischof, Bernhard M. Fuchs, Katy Hoffmann, Dimitri Meier, Anke Meyerdierks, Petra Pjevac, David Probandt, Michael Richter, Ramunas Stepanauskas, and Marc Mußmann

Published (2016) in *The ISME Journal*

S.D., M.M. and B.M.F. developed ideas and designed research; S.D. and M.M. collected samples; Experimental work was done by S.D., M.M., K.B., K.H., D.P. and R.S.; Experimental data contribution by A.M., D.M., P.P. and M.R.; S.D. and M.M. conceived and wrote the manuscript; The manuscript was edited by K.B., B.M.F., K.H., D.M., A.M., P.P., D.P., M.R. and R.S.

**Metagenomes and metatranscriptomes suggest hydrogen consumption by *Desulfobacteraceae*, *Flavobacteriaceae* and *Gammaproteobacteria* in a marine sediment**

Stefan Dyksma, Petra Pjevac, Kin Ovanesov, Hanno Teeling and Marc Mußmann

Manuscript in preparation (2016). Intended to be published in *The ISME Journal*

S.D., and M.M. developed ideas and designed research; S.D., K.O. and M.M. collected samples; Experimental work was done by S.D. and K.O.; K.O. performed anoxic hydrogen oxidation experiments; Experimental data contribution by P.P. and H.T.; S.D. conceived and wrote the manuscript; The manuscript was edited by P.P., H.T. and M.M.

**Quantifying acetate assimilation by major bacterial populations in a marine sediment**

Stefan Dyksma, Sabine Lenk, Joanna E. Sawicka and Marc Mußmann

Manuscript submitted to *Environmental Microbiology* (2016)

S.D. and M.M. developed ideas and designed research; S.D., S.L. and M.M. collected samples; Experimental work was done by S.D. and S.L.; S.L. performed incubations and microautoradiography; HPLC analysis was done by J.E.S.; S.D. conceived and wrote the manuscript; The manuscript was edited by M.M.

**The ISME Journal (2016) 10,** 1939–1953

www.nature.com/ismej

ORIGINAL ARTICLE

# Ubiquitous *Gammaproteobacteria* dominate dark carbon fixation in coastal sediments

Stefan Dyksma[1], Kerstin Bischof[1], Bernhard M Fuchs[1], Katy Hoffmann[2,3], Dimitri Meier[1], Anke Meyerdierks[1], Petra Pjevac[1,4], David Probandt[1], Michael Richter[5], Ramunas Stepanauskas[6] and Marc Mußmann[1]

[1]*Department of Molecular Ecology, Max Planck Institute for Marine Microbiology, Bremen, Germany;* [2]*HGF-MPG Group for Deep Sea Ecology and Technology, Max Planck Institute for Marine Microbiology, Bremen, Germany;* [3]*Alfred Wegener Institute Helmholtz Centre for Polar and Marine Research, Bremerhaven, Germany;* [4]*Division of Microbial Ecology, Department of Microbiology and Ecosystem Science, University of Vienna, Vienna, Austria;* [5]*Microbial Genomics and Bioinformatics Research Group, Max Planck Institute for Marine Microbiology, Bremen, Germany and* [6]*Bigelow Laboratory for Ocean Sciences, East Boothbay, USA*

**Marine sediments are the largest carbon sink on earth. Nearly half of dark carbon fixation in the oceans occurs in coastal sediments, but the microorganisms responsible are largely unknown. By integrating the 16S rRNA approach, single-cell genomics, metagenomics and transcriptomics with $^{14}$C-carbon assimilation experiments, we show that uncultured *Gammaproteobacteria* account for 70–86% of dark carbon fixation in coastal sediments. First, we surveyed the bacterial 16S rRNA gene diversity of 13 tidal and sublittoral sediments across Europe and Australia to identify ubiquitous core groups of *Gammaproteobacteria* mainly affiliating with sulfur-oxidizing bacteria. These also accounted for a substantial fraction of the microbial community in anoxic, 490-cm-deep subsurface sediments. We then quantified dark carbon fixation by scintillography of specific microbial populations extracted and flow-sorted from sediments that were short-term incubated with $^{14}$C-bicarbonate. We identified three distinct gammaproteobacterial clades covering diversity ranges on family to order level (the *Acidiferrobacter*, JTB255 and SSr clades) that made up >50% of dark carbon fixation in a tidal sediment. Consistent with these activity measurements, environmental transcripts of sulfur oxidation and carbon fixation genes mainly affiliated with those of sulfur-oxidizing *Gammaproteobacteria*. The co-localization of key genes of sulfur and hydrogen oxidation pathways and their expression in genomes of uncultured *Gammaproteobacteria* illustrates an unknown metabolic plasticity for sulfur oxidizers in marine sediments. Given their global distribution and high abundance, we propose that a stable assemblage of metabolically flexible *Gammaproteobacteria* drives important parts of marine carbon and sulfur cycles.**
*The ISME Journal* (2016) **10,** 1939–1953; doi:10.1038/ISMEJ.2015.257; published online 12 February 2016

## Introduction

Marine coastal sediments are global hot spots of carbon remineralization and burial (Hedges and Keil, 1995). In current models of oceanic carbon cycling, the sequestration of microbially altered organic matter is the major mechanism of carbon preservation in sediments (Parkes *et al.*, 1993; Burdige, 2007). Marine sediments are sites not only of carbon remineralization but also of carbon fixation. Recent estimates suggest that marine microbes fix inorganic carbon independent of light (chemolithoautotrophy) in amounts that are in the same order of magnitude as the annual organic carbon burial (Middelburg, 2011). Chemolithoautotrophic microorganisms in marine sediments fix up to 370 Tg C/year, which equals 48% of carbon fixed chemolithoautotrophically in the ocean (Middelburg, 2011). Thereof, 47% are fixed in shallow, near-shore sediments (175 Tg C/year). Near-shore sediments, therefore, contribute more to oceanic carbon fixation than pelagic oxygen minimum zones (OMZs) and hydrothermal vents (Middelburg, 2011). In recent years, chemolithoautotrophy in these marine systems has received much attention. The ecophysiology and genetic composition of key players of carbon (and sulfur) cycling in OMZs and hydrothermal vents, such as the gammaproteobacterial SUP05 clade, have been extensively studied (Lavik *et al.*, 2009; Canfield *et al.*, 2010; Reinthaler *et al.*, 2010; Swan *et al.*, 2011; Grote *et al.*, 2012; Anantharaman *et al.*, 2013; Mattes *et al.*, 2013). This cosmopolitan clade is expected to

Correspondence: M Mußmann, Max Planck Institute for Marine Microbiology, Celsiusstrasse 1, 28359 Bremen, Germany.
E-mail: mmussman@mpi-bremen.de
Received 17 September 2015; revised 27 November 2015; accepted 1 December 2015; published online 12 February 2016

have an important role in attenuating atmospheric carbon dioxide concentrations, when OMZs expand in a warming climate (Hawley *et al*., 2014).

In contrast to pelagic OMZs, where the oxic-anoxic/sulfidic interface can be meters thick, in near-shore sediments this interface is only a few millimeters thick, and is characterized by steep biogeochemical gradients and approximately 1000-fold higher cell abundances per sample volume. Biogeochemical evidence indicates that sulfur oxidation is the dominant chemolithoautotrophic process in coastal sediments, while nitrification appears to play only a minor role (Middelburg, 2011; Boschker *et al*., 2014). Previous studies of benthic autotrophic sulfur oxidizers mostly focused on large, conspicuous sulfur bacteria such as *Beggiatoa*, which are widely distributed but occur in high abundances only in certain habitats (Salman *et al*., 2013; Ruff *et al*., 2015). Other *Gammaproteobacteria* affiliating with cultured sulfur oxidizers (*Acidithiobacillus, Thiohalophilus* and *Thiomicrospira*) or with uncultured symbiotic sulfur oxidizers among the *Chromaticaeae* and *Ectothiorhodospiracea* have been regularly found in marine and estuarine sediments (Bowman *et al*., 2005; Orcutt *et al*., 2011). Consistent with this, recent molecular and isotopic approaches suggest that some of these are indeed autotrophs (Lenk *et al*., 2011; Boschker *et al*., 2014; Vasquez-Cardenas *et al*., 2015).

Culture-independent molecular studies previously identified predominant carbon fixation pathways such as the Calvin-Benson-Bassham (CBB) cycle and the reductive tricarboxylic acid cycle in marine chemolithoautotrophic bacteria. The key genes encoding ribulose-1,5-bisphosphate carboxylase-oxygenase (RuBisCO) form I and form II (*cbbL*, *cbbM*) and the ATP citrate lyase (*aclAB*) in the reductive tricarboxylic acid cycle pathway have been frequently detected in environmental studies (reviewed by Hügler and Sievert, 2011). Likewise, genes encoding subunits of the reverse dissimilatory sulfite reductase (*dsrAB*), of the adenosine-5'-phosphosulfate reductase (*aprA*) and of the thiosulfate-oxidizing Sox-multienzyme complex (*soxB*) have been used to target the diversity of marine benthic sulfur oxidizers (Lenk *et al*., 2011; Thomas *et al*., 2014).

To understand how inorganic carbon at sediment surfaces is turned over and possibly buried, detailed knowledge of the microbes driving these processes is essential but currently still lacking. To fill this gap, we surveyed the diversity of candidate bacterial chemolithoautotrophs in 13 coastal surface sediments across Western Europe and Australia. Moreover, we studied whether these chemolithoautotrophic bacteria are also present in anoxic, 490-cm-deep subsurface sediments. We developed a new method to combine $^{14}$C-bicarbonate labeling of cells with fluorescence *in situ* hybridization (FISH), fluorescence-activated cell sorting (FACS) and scintillography to quantify dark carbon fixation by distinct taxonomic groups. Meta- and single-cell genomics along with metatranscriptomics provided evidence for a largely sulfur-based carbon fixation in a selected tidal sediment. Metatranscriptomic reads were mapped against reference databases containing *cbbL*, *cbbM* and *aclAB* sequences to identify active carbon fixation pathways. Metatranscriptomic reads mapped against reference databases containing *dsrAB*, *aprA* and *soxB* sequences indicated sulfur oxidation pathways active *in situ*. This unique combination of molecular and isotopic approaches provided unprecedented insights into the ecology and ecophysiology of cosmopolitan microorganisms driving a major part of global dark carbon fixation.

## Materials and methods

*Sediment sampling and characteristics*

Between October 2012 and December 2014, we sampled 10 tidal and 3 sublittoral sandy sediments

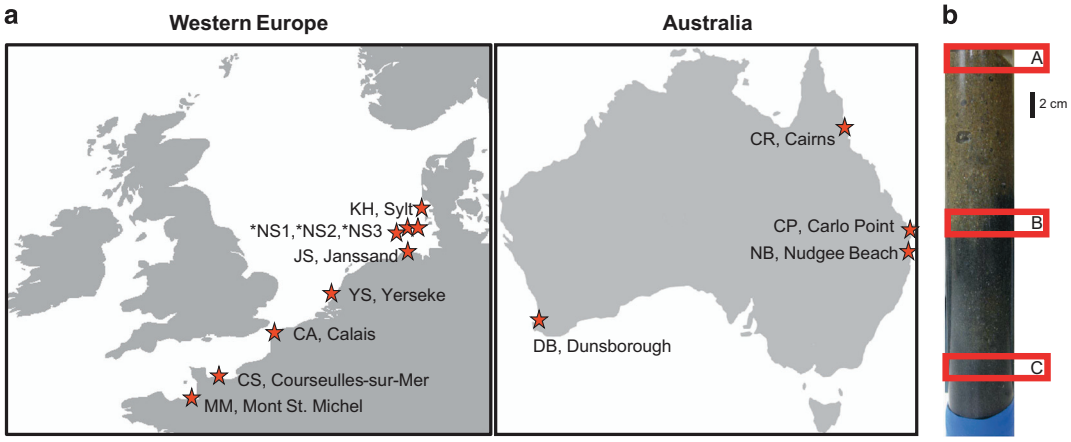


**Figure 1** Sampling sites of the 16S rRNA gene survey (**a**). Example for a typical stratification of a sediment core from coastal sandy sediments (**b**). A = uppermost sediment layer, B = sulfide transition zone and C = sulfidic layer refer to the different sampling depths in this study. During sampling, the sediment colors were used as an indicator for the presence of iron sulfide (dark gray to black). Asterisk indicates samples from sublittoral sediments.

in Western Europe and Australia (Figure 1 and Supplementary Table S1). The 10 tidal sediments were sampled during low tide using polyacryl-cores or cutoff syringes of up to 25 cm length. The three sublittoral, coastal sandy sediments were sampled during cruise He417 with the RV Heincke in March 2014 in the German Bight using multi- and boxcorers. At each site, two to three different sediment layers were selected for molecular analyses (16S rRNA gene amplicon sequencing, catalyzed reporter deposition (CARD)-FISH). Sediment for $^{14}C$ incubations was collected from sites Calais, Courseulles-sur-Mer and from Janssand (Supplementary Table S1). Sediment colors served as a proxy for redox state and active sulfide formation and oxidation (Figure 1). For most of the sites, sediment (i) from the uppermost cm (brownish sediment, sulfide-free), (ii) from the sulfide transition zone (brown to gray, reflecting the presence of iron sulfides) and (iii) from sediment of the sulfidic layer was sampled for molecular analyses (Supplementary Table S1). Sulfide concentrations in pore waters were measured for sites Calais and Courseulles-sur-Mer using the methylene blue method (Cline, 1969). More details on the biogeochemistry of sulfide and oxygen at the study sites Janssand and Königshafen in the German Wadden Sea have been published previously (de Beer *et al.*, 2005; Billerbeck *et al.*, 2006; Jansen *et al.*, 2009). In addition, in April 2005 we sampled a 490-cm-deep subsurface core at site Janssand as described in detail by Gittel *et al.* (2008). Sulfate and methane concentration profiles and lithological data from this core have been described previously (Gittel *et al.*, 2008; Seidel *et al.*, 2012).

*DNA extraction for barcoded 16S rRNA gene amplicon sequencing*

For all intertidal and subsurface sediment samples from Europe and Australia, DNA was extracted from 200 to 250 µl sediment recovered from distinct layers using the PowerSoil DNA isolation kit (MoBio Laboratories, Solana Beach, CA, USA). DNA from sites NoahA, NoahB and CCPδ was extracted from 5 g of homogenized surface sediments according to Zhou *et al.* (1996) including Proteinase K treatment for improved cell lysis.

*Barcoded 16S rRNA gene amplicon sequencing*

The bacterial diversity in all sediment samples was determined by analyzing the hypervariable V3–V4 region of the 16S rRNA gene using Roche 454 pyro- or Illumina MiSeq-sequencing of barcoded amplicons. Barcoded amplicons from all surface sediments were prepared using primers 341f/785rev (Herlemann *et al.*, 2011; Klindworth *et al.*, 2012). Barcoded amplicons from the 490 cm-deep subsurface sediment from site Janssand were prepared by replacing primer 785rev with 907rev (Muyzer *et al.*, 1998; Klindworth *et al.*, 2012). This primer covers a similar bacterial diversity as the reverse primer 785rev used for surface sediments (see above, Figure 2), but it is known to bias against some phyla that are, however, low abundant or absent in marine sediments (Klindworth *et al.*, 2012). In total, 311 196 bacterial 16S rRNA reads were kept for taxonomic classification using the SILVAngs pipeline v115 (Quast *et al.*, 2013) with a clustering at 98% identity. Details on PCR conditions, sequencing and processing are given as Supplementary Information.

*Sediment incubations with $^{14}C$-bicarbonate*

Sediment for $^{14}C$-DIC incubations was collected from sites Calais and Courseulles-sur-Mer in July 2013 and from Janssand in April 2014 (Supplementary Table S1). These cores were kept at *in situ* temperature (15–20 °C) and used for $^{14}C$-DIC incubations within 48 h after sampling. After slicing, 2 ml of the uppermost sediment layer and from the sulfide transition zone was transferred into 10 ml glass vials. In all, 1 ml of sterile filtered seawater and 1 ml of artificial seawater containing 1.5 mM $^{14}C$ bicarbonate (specific activity 54.7 mCi mmol$^{-1}$, Hartmann Analytic, Braunschweig, Germany) were added. Vials were sealed with lab-grade butyl rubber stoppers (GMT Inc., Ochelata, OK, USA) leaving 6 ml of headspace (air). Then, vials were incubated for 20 h with mild agitation (100 r.p.m.) at *in situ* temperature in the dark. In parallel incubations 1 mM thiosulfate was added to slurries from Courseulles-sur-Mer and Calais. Slurry incubations were performed in duplicates (Calais, Courseulles-sur-Mer) or in triplicates (Janssand). Dead controls were included for each site by adding formaldehyde (2%, final concentration) before the incubation.

*CARD-FISH and sample preparation for flow cytometry*

For CARD-FISH, sediment from sites Calais, Courseulles-sur-Mer and Janssand was fixed immediately after core retrieval as described in Lenk *et al.* (2011). Cells were detached from 100 to 200 µl sediment by ultrasonic treatment as described previously (Lenk *et al.*, 2011). Permeabilization and CARD-FISH were performed as described by Pernthaler *et al.* (2002) with the modifications detailed in Supplementary Information. Tyramides labeled with Alexa488 fluorescent dye (Molecular Probes, Eugene, OR, USA) were used for CARD signal amplification. An overview of oligonucleotide probes used in this study is shown in Supplementary Table S2. Novel oligonucleotide probes were designed for the JTB255 group using ARB and the SILVA 16S rRNA reference database release 117 (Pruesse *et al.*, 2007). Please note that the *Xanthomonadales,* which includes the JTB255 clade, are not targeted by probe GAM42a, specific for most *Gammaproteobacteria* (Siyambalapitiya and Blackall, 2005). In line with

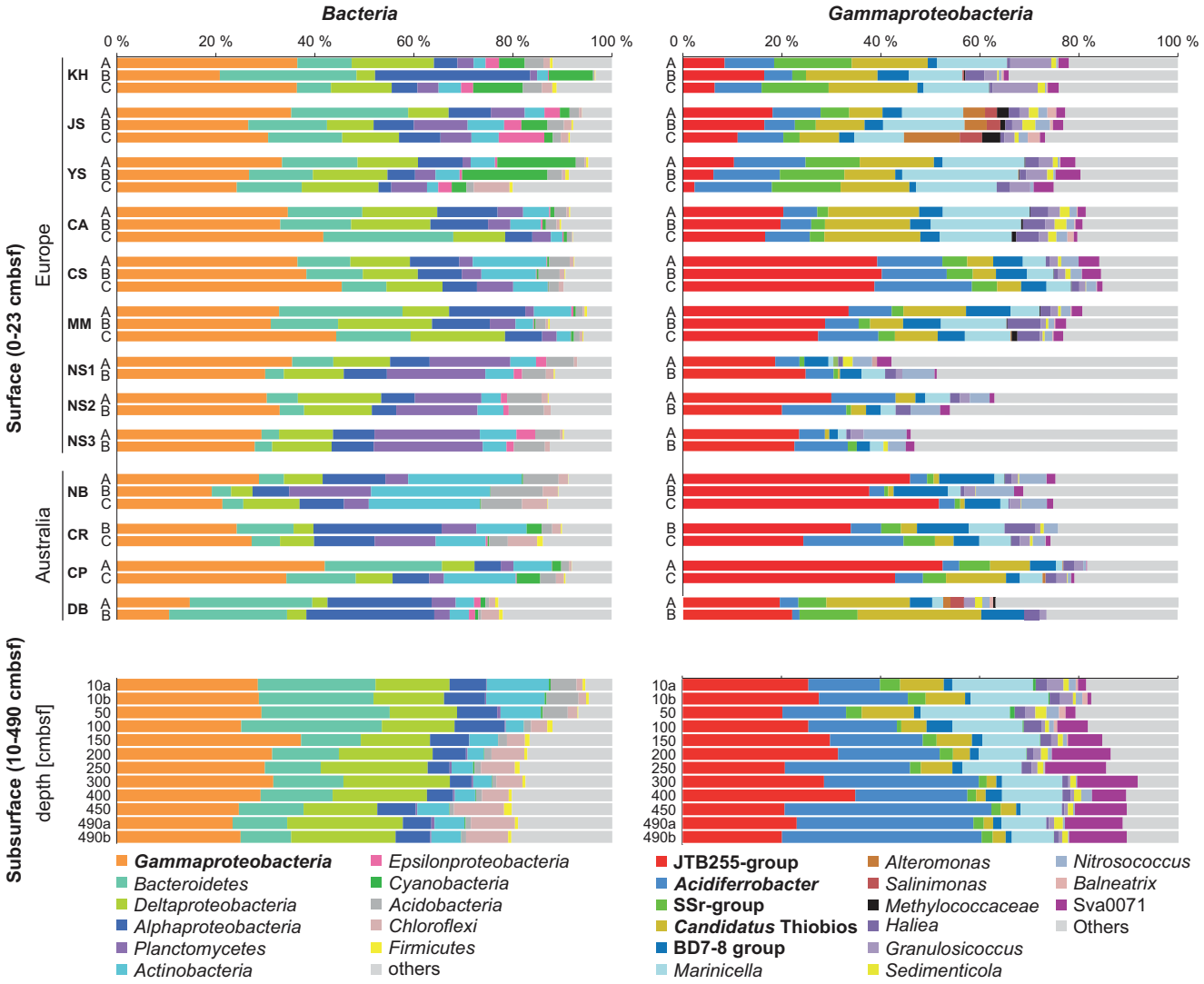


**Figure 2** Relative abundances of the bacterial 16S rRNA gene sequence (V3–V4 regions) in the 13 coastal sediments. Left panels: relative sequence abundance of most frequent bacterial phyla and classes. Right panels: relative sequence abundance of most frequent taxonomic groups (family to order level) within the class of *Gammaproteobacteria* according to the taxonomy of SILVA release 117 (Pruesse *et al*., 2007). The five candidate chemolithoautotrophic clades are given in bold. Upper panels: relative sequence abundance in 13 coastal surface sediments from 0 to 23 cm below surface (cmbsf) max. A = uppermost sediment layer (0.5 or 1 cmbsf), B = sulfide transition zone, C = sulfidic layer. For the detailed depth ranges, see Supplementary Table S1. Lower panels: relative sequence abundance in subsurface sediments at site Janssand (JS) from 50 to 490 cmbsf. For comparison, samples from 10 cmbsf are included. Sediment samples from 10 and 490 cmbsf were run in duplicate (10ab, 490ab). All but one amplicons were pyrosequenced, samples from DB were sequenced via the Illumina MiSeq platform.

this, the JTB255 clade could not be detected with probe GAM42a in double hybridizations with the JTB-probe mix (Supplementary Table S2). Therefore, we summed up FISH counts of the JTB255-probe mix and of probe GAM42a to yield the total relative abundance of FISH-detectable *Gammaproteobacteria*.

*FACS and scintillography of sorted cells*

We developed a novel protocol to quantify bulk assimilation of radiolabelled substrates in a defined number of cells phylogenetically identified via CARD-FISH before for flow sorting. To minimize cell loss, the filters were handled extremely carefully during the CARD-FISH procedure. Cells were scraped off from membrane filters by using a cell scraper or membrane filters were vortexed in 5 ml of 150 mM NaCl containing 0.05% Tween-80 according to Sekar *et al.* (2004). Before flow cytometry, large suspended particles were removed by filtration through 8-µm pore-size filter (Sartorius, Göttingen, Germany) to avoid clogging of the flow cytometer.

Flow sorting of cells that were fluorescently labeled by CARD-FISH was performed using a FACSCalibur flow cytometer equipped with cell sorter and a 15-mW argon ion laser exciting at 488 nm (Becton Dickinson, Oxford, UK). Autoclaved Milli-Q water was used as sheath fluid. Cell sorting

was done at low flow rate of $12 \pm 3$ µl $min^{-1}$ or med flow rate of $35 \pm 5$ µl $min^{-1}$ with single-cell sort mode to obtain the highest purity. The event rate was adjusted with a fluorescence threshold, and sorting was performed at a rate of approximately 25–100 particles $s^{-1}$. Hybridized cells were identified on scatter dot plots of green fluorescence versus 90° light scatter (Supplementary Figure S1). Sediment background such as clay particles was determined by flow-cytometric analysis of sediment hybridized with a nonsense probe (NON338) (Supplementary Figure S1). For subsequent measurements, 50 000 cells were sorted and filtered onto 0.2-µm polycarbonate filters (GTTP, Millipore, Eschborn, Germany). Dead controls of $^{14}C$ incubated sediments did not show any measurable assimilation of $^{14}C$, and were thus not used for cell sorting. Unspecifically adsorbed label in live samples caused only minor radioactive background as determined by spiking experiments with fluorescent beads and *Escherichia coli* cells (Supplementary Figure S2). Fluorescent beads (yellow-green, 1.0 µm, Polyscience, Warrington, PA, USA) or hybridized *E. coli* cells were flow-sorted from of a sample hybridized with the nonsense probe to determine radioactive background. *E. coli* cells were hybridized with EUBI-III probe beforehand. Beads and *E. coli* cells were mixed with the sample in approximately the same quantity as the target populations (10–20% of total cells). Two to three repeated sortings were applied to confirm the technical reproducibility from duplicate or triplicate incubations. Collected cell batches on polycarbonate filters were directly transferred into 5 ml scintillation vials and mixed with 5 ml Ultima-Gold XR (Perkin-Elmer, Boston, MA, USA) scintillation cocktail. Radioactivity of sorted cell batches was measured in a liquid scintillation counter (Tri-Carb 2900, Perkin-Elmer).

The purity of flow-cytometric enriched target cells was >93%, and was manually analyzed under an Axioplan epifluorescence microscope (Zeiss, Jena, Germany). For microscopic analysis, filters were counterstained with 1 µg $ml^{-1}$ 4′,6-diamidino-2-phenylindole (DAPI) and at least 1000 DAPI-stained cells were examined for CARD-FISH. Our approach was technically highly reproducible, and the radioactivity linearly increased with the number of sorted cells (Supplementary Figure S2).

For calculation of average cell-specific carbon fixation rates in our slurry experiments, we assumed a background concentration of dissolved inorganic carbon of 2 mM (Billerbeck *et al.*, 2006) as we used local seawater for our experiment (see Supplementary Information for calculations). The relative abundance of assimilating gammaproteobacterial cells in the sulfide transition zone from Calais, Courseulles-sur-Mer and Janssand sediments was determined by microautoradiography (MAR). MAR was performed according to Alonso and Pernthaler (2005) and Lenk *et al.* (2011) with an exposure time of 2 days. Relative abundance of MAR-positive cells was manually determined under an Axioplan epifluorescence microscope (Zeiss).

*A single-cell genome of the SSr clade from Janssand sediment*

In January 2011, the upper two centimetres of Janssand sediment were sampled for extraction and sorting of single bacterial cells for whole-genome amplification. After extraction, cells were cryopreserved with N,N,N-trimethylglycine ('glycine betaine') (Sigma-Aldrich, St Louis, MO, USA) at a final concentration of 4% according to Cleland *et al.* (2004), stored at −80 °C and shipped overseas. Single-cell sorting and whole-genome amplification via multiple displacement amplification were performed at the Bigelow Laboratory Single Cell Genomics Center (https://scgc.bigelow.org) as described by Swan *et al.* (2011). A single amplified genome (SAG) encoding a single, high quality 16S rRNA gene sequence affiliating with the SSr clade was sent to Max Planck Genome Centre (MP-GC) Cologne for MiSeq (Illumina) sequencing yielding 9 557 547 PE reads. The SAG assemblies were auto-annotated using the Joint Genome Institute IMG-ER pipeline (Markowitz *et al.*, 2012). Details on cell extraction, sequencing and quality control of the assembled genomic data are given as Supplementary information.

*cDNA libraries and metatranscriptomic mapping*

In April 2013, sediment was sampled from the sulfide transition zone at site Janssand and immediately frozen on dry ice. Total RNA was extracted from sediment in triplicates (one ml each) by the Vertis Biotechnologie AG (Freising, Germany), and bacterial rRNA was depleted with the Ribo-Zero Magnetic Kit (for *Bacteria*) (Epicentre, Madison, WI, USA). Barcoded RNA TrueSEQ libraries were constructed from RNA extractions and paired-end sequenced using Illumina HiSeq2000 (MP-GC, Cologne, Germany). After quality trimming at a Phred score 28 using Nesoni clip v.0.115 (http://www.vicbioinformatics.com/software.nesoni.shtml), reads were mapped to reference databases of nucleotide sequences encoding key genes for sulfur oxidation (Sox-multienzyme complex, *sox*B; reverse dissimilatory sulfite reductase, *dsr*AB; adenosine-5′-phosphosulfate reductase, *apr*A; uptake [NiFe]-hydrogenase, *hup*L; ammonia monooxygenase, *amo*A, ribulose-1,5-bisphosphate carboxylase/oxygenase form I, *cbbl,* and form II, *cbbm*; ATP citrate lyase, *acl*AB) and to the SAG using Bowtie2 (Langmead and Salzberg, 2012). Details on program settings and normalization are given as Supplementary information.

*Nucleotide accession numbers*

All nucleotide sequences obtained in this study have been deposited in GenBank. Sequences of 16S rRNA and hydrogenase gene libraries are available under

accession numbers KR824952–KR825244 and KR534775–KR534844, respectively. Amplicon sequences from the 16S rRNA gene surveys were deposited in NCBI BioProjects PRJNA283163 and PRJNA285206. All cDNA reads are available in BioProject PRJNA283210. Fosmid end sequences are available in NCBI's Genome Survey Sequences database (GSS) with the accession numbers KS297884–KS307053. The genome sequence of the SAG WSgam209 is accessible under the IMG Genome ID 2609459745 through the Joint Genome Institute portal IMG/ER (https://img.jgi.doe.gov/cgi-bin/er/main.cgi), the metagenomic bin *Acidiferrobacter*-a7 is accessible under the IMG Genome ID 2616644801.

## Results and Discussion

*Identification of candidate chemolithoautotrophs in coastal surface sediments*

To identify candidate chemolithoautotrophs in coastal sediments, we studied the bacterial diversity in 10 tidal and 3 sublittoral sandy sediments from Western Europe and Australia (Figure 1 and Supplementary Table S1). We sequenced the V3–V4 region (>300 bp) of tagged 16S rRNA gene amplicons. After quality trimming, 311 196 Illumina- and 454-tag reads were recovered. Taxonomic classification revealed that *Gammaproteobacteria* were consistently among the most abundant clades on class to phylum level, accounting for 12–45% of sequences regardless of sampling site, sediment depth or season (Figure 2). These data were supported by CARD-FISH, which showed that *Gammaproteobacteria* make up 19–22% of all bacteria at sites Janssand, Calais and Courseulles-sur-Mer (Supplementary Table S5). At all sites, we observed a recurring diversity pattern also at the family to order level within the *Gammaproteobacteria*. We consistently identified candidate chemoautotrophs most closely related to: (1) *Acidiferrobacter thiooxydans* of the family *Ectothiorhodospiraceae*, (2) symbionts of the siboglinid tubeworms such as *Oligobrachia* spp. (henceforth designated as *Siboglinidae* Symbionts related, SSr, see Supplementary Figures S3 and S4), (3) ciliate symbiont *Candidatus* Thiobios zoothamnicoli and (4) BD7-8 clade, including the γ3 symbiont of the marine gutless oligochaete *Olavius algarvensis* (Woyke *et al*., 2006). Sulfur-dependent chemolithoautotrophy for cultured or symbiotic relatives of these clades has been shown before (Rinke *et al*., 2006; Lösekann *et al*., 2008; Hallberg *et al*., 2011; Kleiner *et al*., 2012). *Acidiferrobacter thiooxydans* can also grow autotrophically with ferrous iron (Hallberg *et al*., 2011). Moreover, we previously showed carbon fixation by the SSr- and the *Acidiferrobacter*-related clades, and determined relative cell abundances of up to 8% at site Janssand in the German Wadden Sea (Lenk *et al*., 2011).

Strikingly, in all tested sediments up to 52% of gammaproteobacterial sequences grouped with the uncultured JTB255 clade. This clade is affiliated with the order *Xanthomonadales* and accounted for the largest fraction of gammaproteobacterial sequences at 10 out of 13 sites (Figure 2). In line with the sequence data, CARD-FISH targeting members of the JTB255 clade revealed rod-shaped cells (Supplementary Figure S5) that made up 3–6% of total cell counts in Janssand, Calais and Courseulles-sur-Mer sediments (Supplementary Table S6). So far, the exact environmental function of the JTB255 clade is unknown;however, a sulfur-oxidizing activity has been hypothesized (Bowman and McCuaig, 2003). In summary, we identified five candidate chemolithoautotrophs that accounted for 28–75% of *Gammaproteobacteria* and for 8–31% (average = 17%) of all bacterial sequences across all sites. Other potentially autotrophic populations such as sulfur-oxidizing *Epsilonproteobacteria*, anoxygenic phototrophs, the BD1-5/SN-2 clade, nitrifiers and cyanobacteria were found in low abundance or were patchily distributed (Figure 2).

*Gammaproteobacteria in subsurface sediments*

Because of the high sedimentation rates of >3 mm/year in the German Wadden Sea at site Janssand (Ziehe, 2009), a yet unknown fraction of the surface microbial community including the chemolithoautotrophic *Gammaproteobacteria* is buried into the anoxic subsurface. To study, how these organisms are affected by such a burial, we also analyzed the distribution of chemolithoautotrophic *Gammaproteobacteria* in a 490-cm-deep subsurface core from site Janssand, spanning a sedimentation record of 1000–2000 years (Ziehe, 2009). This sediment core displayed a typical sulfate-methane-transition zone in 150–200 cm below surface (cmbsf) (Gittel *et al*., 2008), reflecting the changes in the major metabolic pathways that are active along this depth range. Surprisingly, *Gammaproteobacteria* including the chemolithoautotrophic gammaproteobacterial clades also accounted for a dominant fraction of 16S rRNA gene pyrotags over the entire depth range (21–37% of all sequences, Figure 2). This observation was supported by 16S rRNA gene libraries from 200 and 490 cmbsf (Supplementary Figure S4), in which these clades accounted for 95 out of 289 clones (33%). To gain PCR-independent support for the dominance of *Gammaproteobacteria* in subsurface sediments, we fosmid-cloned large metagenomic fragments of ~40 kb in size from 490 cmbsf and taxonomically classified the end sequences (Supplementary Table S7), as FISH is commonly too insensitive to comprehensively target subsurface organisms with very low ribosome content (Schippers *et al*., 2005). In support of our 16S rRNA gene data, 24% of all prokaryote-affiliated fosmid end sequences ($n = 4052$) showed best hits to *Gammaproteobacteria*, while only approximately 1% affiliated with *Archaea* (Supplementary Table S7).

Collectively, these molecular data indicate a relatively stable community structure over the 5-m depth range, despite the measured strong biogeochemical gradients. These data are consistent with similar total cell abundances and a similar composition of major phospholipids over the entire 490 cm depth in the same sediment core (Gittel *et al*., 2008; Seidel *et al*., 2012).

Whether these gammaproteobacterial populations are active despite very different biogeochemical settings in the subsurface, or whether they are simply surviving in subsurface sediments with little or no turnover, are currently unclear. Upon burial, marine microbial cells may survive in the subsurface over geological time scales without significant growth (Jørgensen, 2011). Energy for maintenance and survival could be supplied by fermentation of refractory organic matter and by the slow transport and diffusion of dissolved organic compounds to subsurface sediments, which has been demonstrated for the subsurface at site Janssand (Røy *et al*., 2008; Seidel *et al*., 2012).

*Global occurrence of candidate chemolithoautotrophic Gammaproteobacteria*

Our 16S rRNA diversity and FISH data agree well with numerous studies showing a substantial contribution of *Gammaproteobacteria* to microbial communities in diverse marine surface sediments (Hunter *et al*., 2006; Kim *et al*., 2008; Schauer *et al*., 2009; Orcutt *et al*., 2011; Gobet *et al*., 2012; Ruff *et al*., 2015). To examine the geographic distribution of the five candidate chemoautotroph groups in more detail, we did a meta-analysis of 16S rRNA gene sequence data from 65 diversity studies of the sea floor (Figure 3). Although these published data sets hardly covered the extent of microbial diversity at the studied sites, sequences related to the *Acidiferrobacter*, SSr and to a lesser extent *Ca.* T. zoothamnicoli and BD7-8 groups were found in all types of benthic habitats ranging from intertidal sediments to deep-sea hydrothermal chimneys (Figure 3). Intriguingly, the JTB255 clade was detected in 92% of all studies (Figure 3) and accounted for the most frequent sequence group among *Bacteria* in Arctic, Antarctic and tropical deep-sea as well as shallow coastal sediments (Wang *et al*., 2013; Zheng *et al*., 2014; Liu *et al*., 2014; Emil Ruff *et al*., 2014). In temperate Tasmanian and in cold Antarctic coastal sediments, 16S rRNA gene copies of the JTB255 clade accounted for 6–9% of total bacterial 16S rRNA gene sequences (Bowman *et al*., 2005). In summary, our biogeographic survey shows that these five clades are important members of microbial communities in marine surface sediments worldwide, and clearly, the JTB255 clade is one of the most successful bacterial lineages in marine surface sediments.

*Measuring dark carbon fixation by Gammaproteobacteria in sediments*

Our 16S rRNA gene survey suggested that sulfur-oxidizing *Gammaproteobacteria* are potentially the major carbon fixers in dark coastal sediments.

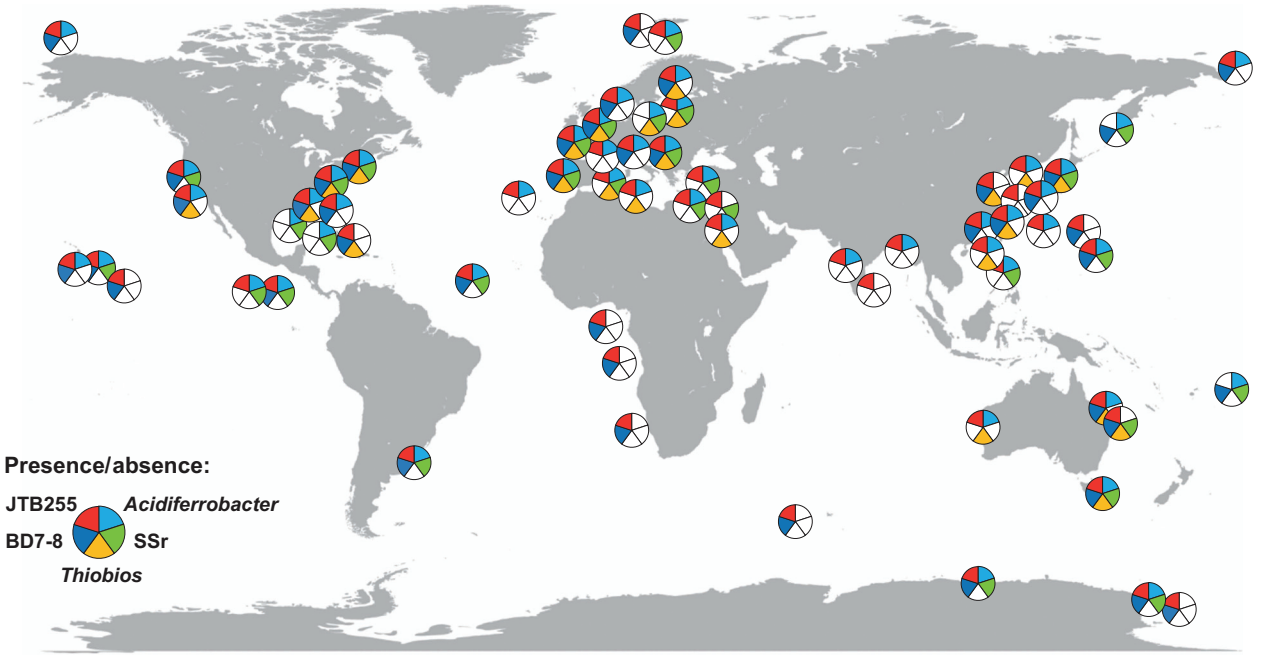


**Figure 3** Biogeographic survey of the major chemolithoautotrophic gammaproteobacterial clades identified in this study. Only clone sequences (presence/absence) from bacterial diversity studies from 65 marine sea floor surfaces have been considered, deposited in the SILVA database release 117 (Pruesse *et al*., 2007).

However, quantitative data on carbon fixation by distinct bacterial populations in marine sediments are lacking. To determine the contribution of *Gammaproteobacteria* to dark carbon fixation in sediments, we developed a novel approach to quantify assimilation of a radiolabeled compound by specific populations. Previous FACS experiments with autofluorescent, radiolabeled marine bacterioplankton and subsequent scintillography of sorted populations prompted us to use FISH signals instead of autofluorescence or unspecific DNA staining to identify and enrich populations from sediments (Zubkov *et al*., 2003; Jost *et al*., 2008). We incubated aerobic sediment slurries prepared from surface and from sulfide transition zone sediments from sites Calais, Courseulles-sur-Mer and Janssand with $^{14}$C-labeled bicarbonate and for 20 h in the dark. After detachment of cells from sand grains and CARD-FISH, we sorted fluorescently labeled *Bacteria* (probe EUBI-III) or *Gammaproteobacteria* (probe GAM42a). To account for potentially nitrifying autotrophic *Archaea*, we also sorted cells targeted by the archaeal probe Arch915. Fifty thousand cells were sorted per population, and bulk radioactivity was measured. This workflow allowed us to accurately quantify the bulk assimilation of radiolabeled substrates by a defined population in high throughput. At the analysis level of populations and communities it thereby overcomes limitations in throughput and precision of other methods such as MAR-FISH, HISH-SIMS and stable isotope probing (Boschker *et al*., 1998; Lee *et al*., 1999; Radajewski *et al*., 2000; Manefield *et al*., 2002; Musat *et al*., 2008).

Although the total amount of fixed carbon in sorted populations varied between sites and samples, the $^{14}$C-assimilation by sorted *Gammaproteobacteria* ranged from 2.4 to 10.3 Bq and was 2.5- to 5-fold higher than those of sorted *Bacteria* (0.5–2.1 Bq) (Figure 4a). At all three sites, the relative abundance of $^{14}$C-assimilating *Gammaproteobacteria* was approximately 40–50% as determined by MAR (Supplementary Table S8; Lenk *et al*., 2011) and is similar to the relative sequence frequency of chemoautotrophic subpopulations (Figure 2). The $^{14}$C-radioactivity of 50 000 archaeal cells accounted for 1.4–3.8 Bq, ranging between the average assimilation by *Bacteria* and *Gammaproteobacteria* (Figure 4b). Addition of nitrate did not stimulate $^{14}$C-assimilation in anoxic slurry incubations. The addition of 1 mM thiosulfate doubled the total carbon fixation by *Gammaproteobacteria* in the uppermost surface sediments, but not in the sulfide transition zone at Calais and Courseulles-sur-Mer (Figure 4a). Likewise, thiosulfate did not stimulate carbon fixation in the sulfide transition zone from site Janssand (Zerjatke, 2009). The oxidized surface sediments are possibly limited in electron donors, while the sulfide transition zone contained sufficient reduced sulfur compounds such as free and iron sulfides as energy sources for carbon fixation (Jansen *et al*., 2009; Supplementary Table S1).

*Dark carbon fixation in Gammaproteobacterial clades*

To quantify carbon fixed by the candidate chemolithoautotrophic clades, we used the FISH probes available for three of the five clades for cell sorting and subsequent scintillography. Our FISH probes for the SSr and *Acidiferrobacter* clades mostly target sequences retrieved from site Janssand (Supplementary Figure S4; Lenk *et al*., 2011); therefore, we measured carbon assimilation by specific subpopulations at this site. The *Acidiferrobacter* clade showed the highest $^{14}$C-assimilation (6.1–10 Bq), while the SSr clade assimilated 2.7–6.9 Bq (Figure 4b

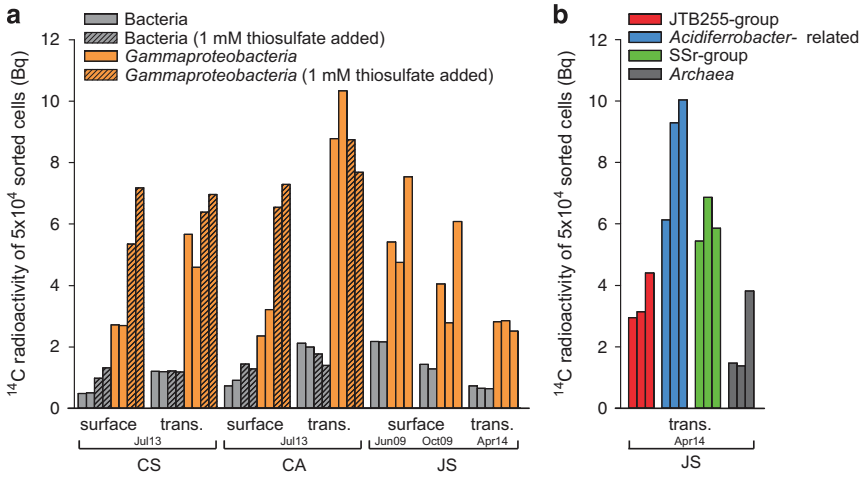


**Figure 4** $^{14}$C carbon fixed by *Bacteria, Gammaproteobacteria* and *Archaea* in three coastal sediments. Carbon fixation by flow-sorted populations of *Bacteria, Gammaproteobacteria* and *Archaea* from the uppermost sediment layer (surface, 0–1 cmbsf) and from the sulfide transition zone (trans.) incubated with $^{14}$C bicarbonate. $^{14}$C-assimilation by *Bacteria* and *Gammaproteobacteria* at three sampling sites (Courseulles-sur-Mer, Calais and Janssand) and in different seasons (**a**). $^{14}$C-assimilation by three gammaproteobacterial clades and *Archaea* (**b**). Batches of 50 000 cells were sorted per measurement. The $^{14}$C carbon activity is given in Becquerel (Bq).

and Supplementary Figure S6). This is consistent with the chemolithoautotrophic potential encoded in the corresponding genomes (Supplementary Table S5), and is confirmed by the previously detected $^{14}$C bicarbonate assimilation by single cells of both clades (Lenk *et al.*, 2011).

Our probes for the ubiquitous JTB255 clade display a wider target range; therefore, we used these probes to sort JTB255 cells from Janssand, Calais and Courseulles-sur-Mer. The $^{14}$C-assimilation by the JTB255 clade ranged from 3 to 4.4 Bq in Janssand sediment to up to 10.7 Bq in Calais sediment (Figure 4b and Supplementary Figure S6). The $^{14}$C-assimilation by the JTB255 clade was slightly less than that of the SSr clade. The addition of thiosulfate did not stimulate the $^{14}$C-assimilation by the JTB255 clade in Courseulles-sur-Mer but did slightly stimulate it in Calais sediments, which is consistent with the hypothesized thiotrophy of members of this clade (Bowman and McCuaig, 2003).

The $^{14}$C-assimilation by the three gammaproteobacterial clades was up to 10-fold higher than the $^{14}$C-assimilation by the entire bacterial community (Figures 4a and b), which largely consisted of heterotrophic bacteria (Figure 2). Using the carbon assimilated by the bulk bacterial community (targeted by probes EUBI-III) as an approximate reference for heterotrophic, anaplerotic carbon fixation (Wood and Werkman, 1936; Li, 1982; Roslev *et al.*, 2004), we conclude that heterotrophic carbon fixation was minor. Moreover, we calculated average carbon fixation rates per sorted gammaproteobacterial cell based on all sorted *Gammaproteobacteria* (1.1–3.0 fg C cell$^{-1}$ day$^{-1}$, Supplementary Table S8). Average carbon fixation rates per cell and for each of the three individual subpopulations ranged from 1.1 to 3.5 fg C cell$^{-1}$ day$^{-1}$. These rates are consistent with those of autotrophic freshwater green sulfur bacteria (1.4–5.8 fg C cell$^{-1}$ day$^{-1}$) (Musat *et al.*, 2008), and are in the lower range of rates measured for autotrophic marine bacterioplankton (3.5–24.7 fg C cell$^{-1}$ day$^{-1}$) (Jost *et al.*, 2008). Collectively, these data strongly support an autotrophic carbon fixation by the *Acidiferrobacter*, SSr and JTB255 clades.

### *Gammaproteobacteria dominate dark carbon fixation in coastal sediments*

The relative contribution of carbon fixed by the *Acidiferrobacter*, SSr and JTB255 clades amounted to 77% of gammaproteobacterial and to 50–62% of bacterial dark carbon fixation at Janssand (Figure 5). Although they make up only 19–22% of the total microbial community, *Gammaproteobacteria* in total accounted for 70–86% of the microbial dark carbon fixation irrespective of sampling site, season and sediment depth (Figure 5 and Supplementary Figure S7).

Although they can be important autotrophs in organic-poor deep-sea sediments (Molari *et al.*, 2013)

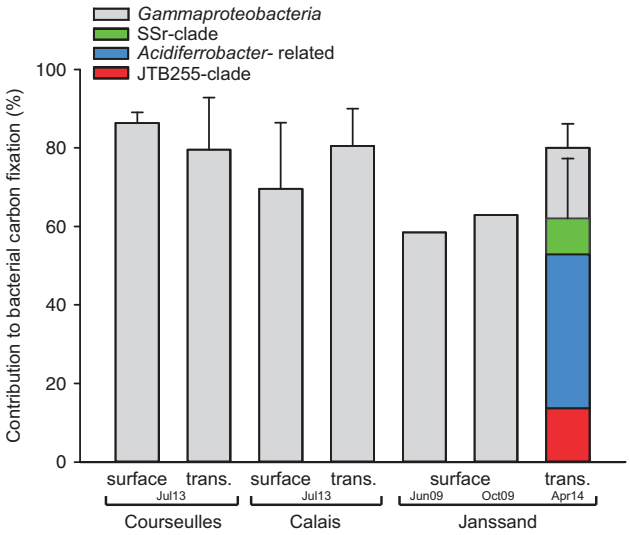


**Figure 5** Relative contribution of *Gammaproteobacteria* to total bacterial dark carbon fixation in three coastal sediments. The relative contribution of carbon fixed by total *Gammaproteobacteria* and by the *Acidiferrobacter*, SSr and JTB255 clade to total bacterial dark carbon fixation was calculated by integrating the $^{14}$C-carbon assimilation per population (dark gray bar) and the relative cell abundances of the respective populations in the sediments. Error bars represent the standard deviation (s.d.) of 3–4 replicate incubations. Values from 2009 (site Janssand) are depicted as average of duplicates only. Note that for experiments in 2009 $^{14}$C-assimilation by the JTB255 clade was not measured (for details, see Supplementary Information).

nitrifying *Archaea* have a minor role in dark carbon fixation in the sediments we measured. In our study, *Archaea* occurred at low relative abundances and assimilated less $^{14}$C than *Gammaproteobacteria* (Figures 4a and b and Supplementary Figure S7).

### *Genomics suggests thioautotrophy in uncultured Gammaproteobacteria*

We previously showed that key genes of sulfur oxidation in Janssand sediments are mainly affiliated with *Gammaproteobacteria* (Lenk *et al.*, 2011). To further investigate the metabolism of the candidate chemolithoautotrophic *Gammaproteobacteria*, we sequenced the amplified genomic DNA of a single cell of the SSr clade from Janssand sediment. In addition, we recovered a metagenomic bin of a member of the *Acidiferrobacter* clade from a deep-sea hydrothermal chimney that displayed 91% sequence identity to 16S rRNA gene sequences from site Janssand (Supplementary Figure S4).

The assembled SAG of the SSr cell ('WSgam209') consists of 1.9 Mbp on 311 scaffolds (Supplementary Table S3). In addition to the cytochrome c oxidase for oxygen respiration, the genome encoded a reverse dissimilatory adenosine-5′-phosphosulfate (APS)-reductase subunit A (AprA), a widely distributed enzyme catalyzing the oxidation of sulfite to sulfate (Meyer and Kuever, 2007). Similar to the 16S rRNA gene also the AprA is affiliated with the

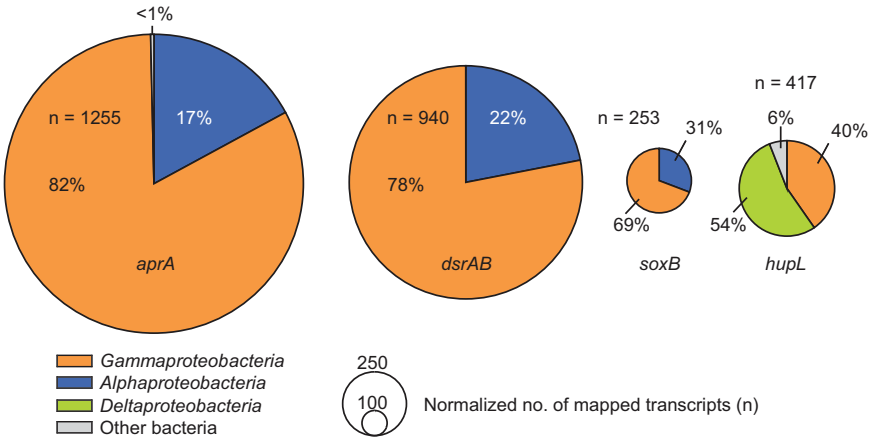


**Figure 6** Taxonomic affiliation of metatranscriptomic reads of key genes from sulfur and hydrogen oxidation pathways. Metatranscriptomic reads from the sulfide transition zone (Janssand surface sediments 2–3 cmbsf) were mapped to key genes of sulfur and hydrogen oxidation genes (*aprA*, adenosine-5′-phosphosulfate reductase; *dsrAB*, reverse dissimilatory sulfite reductase; *soxB*, Sox-multienzyme system; uptake [NiFe]-hydrogenase). Metatranscriptomes were sequenced in triplicates, and the average values are displayed. Transcript abundance is normalized for gene length and number of reads per data set.

sulfur-oxidizing symbionts of *Oligobrachia haakonmosbiensis* (Supplementary Figures S4 and S8), indicating a congruent phylogeny of both phylogenetic markers. Moreover, it encoded the large and small subunits of the RuBisCO form I (CbbL, CbbS) (Supplementary Table S5).

The metagenomic bin of the *Acidiferrobacter*-clade organism ('*Acidiferrobacter*-a7') consists of 2 Mbp on 66 scaffolds (Supplementary Table S3). It contained genes for thiosulfate oxidation (Sox-multienzyme complex, *soxABXYZ*), sulfite oxidation (*soeABC*) and carbon fixation (RuBisCO form I subunits *cbbL* and *cbbS*) (Supplementary Table S4). Together with the measured carbon fixation of SSr and the *Acidiferrobacter* clades at site Janssand, the identification of sulfur oxidation and carbon fixation genes in both clades provides the genetic background of their chemolithoautotrophic potential.

### *Metatranscriptomics underscores the role of Gammaproteobacteria in thioautotrophy*

To further test, whether *Gammaproteobacteria* in these sediments are the major active chemolithoautotrophs, we sequenced triplicate metatranscriptomes from the sulfide transition zone of Janssand sediments. Transcript reads were mapped to reference sequences from the GenBank database, functional gene libraries, metagenomic fragments and the SSr-single cell genome recovered from site Janssand (this study; Lenk *et al*., 2011, 2012).

To identify the expressed carbon fixation pathways, we mapped the metatranscriptomic reads to gene sequences of RuBisCO form I and form II (*cbbL*, *cbbM*) and of ATP citrate lyase (*aclAB*) from cultured representatives and environmental sequences from diverse aquatic environments including sediments. All transcripts of RuBisCO genes, on average 112 reads, mapped to those of sulfur-oxidizing *Gammaproteobacteria*, confirming active carbon fixation through the CBB-cycle in Janssand sediments. Only very few transcripts ($n \leqslant 6$) could be mapped on genes encoding an epsilonproteobacterial ATP citrate lyase (Supplementary Table S4), reflecting the low relative abundance and low activity of sulfur-oxidizing *Epsilonproteobacteria* in these sediments (Figure 2; Lenk *et al*., 2011).

To identify the expressed sulfur oxidation pathways and the respective organisms in the sulfur transition zone in Janssand sediments, we mapped the metatranscriptomic reads to references databases containing gene sequences encoding SoxB, AprA and subunits of the reverse dissimilatory sulfite reductase, DsrAB. The major fraction (69–82%) of transcripts mapped to *dsrAB, soxB* and *aprA* sequences that are affiliated with *Gammaproteobacteria* (Figure 6 and Supplementary Figure S8), further supporting their central role in chemolithoautotrophy. Here, *dsrAB* transcripts were fourfold higher than *soxB* transcripts. The identification of the sulfur oxidation pathway prevailing in marine sediments has important implications for modeling of carbon budgets, as the reverse Dsr (rDsr) pathway may allow a higher ATP gain that can be used for carbon fixation than the complete Sox-multienzyme complex (Klatt and Polerecky, 2015). In the rDsr pathway electrons finally enter the electron transport chain at the level of quinone (Holkenbrink *et al*., 2011), while the Sox-multienzyme complex donates electrons to cytochrome c (Kelly *et al*., 1997), probably resulting in higher energy yields for rDsr-encoding sulfur oxidizers. However, further *in situ* studies are essential to confirm this observation.

Very few reads mapped to bacterial ($n \leqslant 2$) and archaeal ($n \leqslant 5$) *amoA* genes encoding the ammonia monooxygenase subunit A (AmoA) (Supplementary Table S1). This is consistent with the minor role of *Archaea* in carbon assimilation measured in our

study (Supplementary Figure S7), and is also consistent with the very low nitrification rates measured at site Janssand (Marchant *et al.*, 2014). Overall our data confirm previous biogeochemical models suggesting a low impact of nitrification on chemolithoautotrophic production in coastal sediments (Middelburg, 2011; Boschker *et al.*, 2014).

*Hydrogen is likely an alternative energy source for sulfur-oxidizing Gammaproteobacteria*

Recently, uptake [NiFe]-hydrogenase genes were found in metagenomic bins of *Gammaproteobacteria* from estuarine sediments, indicating alternative energy sources for dark carbon fixation under oxic to suboxic conditions (Baker *et al.*, 2015). As the ability to oxidize hydrogen has been shown to confer metabolic plasticity to symbiotic and pelagic sulfur-oxidizing bacteria (Petersen *et al.*, 2011; Anantharaman *et al.*, 2013; Hansen and Perner, 2015), we tested whether hydrogen could serve as an alternative energy source also for gammaproteobacterial sulfur oxidizers in marine sediments, for example, to respire sulfur under anoxic conditions (Laurinavichene *et al.*, 2007). To overcome the lack of reference sequences from marine sediments, we constructed an uptake [NiFe]-hydrogenase gene library from Janssand sediments. The recovered hydrogenase gene diversity comprised different physiological groups from phyla such as *Proteobacteria* and *Bacteroidetes* (Supplementary Figure S9). A substantial fraction (40%) of all hydrogenase transcripts were assigned to sequences of diverse *Gammaproteobacteria,* in particular to those grouping with sulfur-oxidizing bacteria (Figure 6 and Supplementary Figure S9). Expression levels of hydrogenase genes were lower than those of sulfur oxidation genes, but were in the same order of magnitude (Figure 6).

To link a potential hydrogen-oxidizing activity with sulfur-oxidizing *Gammaproteobacteria*, we searched for co-localization and co-expression of key genes of both pathways. First, we identified a metagenomic fragment from Janssand, affiliated with *Gammaproteobacteria,* which encoded both the uptake [NiFe]-hydrogenase HupSL and the rDsr operon (Supplementary Figure S10). Notably, the SAG of the SSr-group recovered from site Janssand also encodes an uptake [NiFe]-hydrogenase gene in addition to *aprA* and *cbbLS*. Moreover, these genes were among the top 20 transcribed genes out of 2008 identified genes (Supplementary Figure S11).

Collectively, our single-cell genomic, metagenomic and metatranscriptomic data indicate that *Gammaproteobacteria* in marine surface sediments may use both reduced sulfur species and hydrogen as energy sources for carbon fixation. In fact, the thioautotroph *Sulfurimonas denitrificans* grows more efficiently with hydrogen than with thiosulfate, when the electron acceptor nitrate is limiting (Han and Perner, 2014). Hence, hydrogen oxidation could be a hitherto overlooked energy source for carbon fixation in marine sediments.

*Key functions of ubiquitous chemolithoautotrophic Gammaproteobacteria in sediments*

Overall, our molecular and $^{14}$C-assimilation data suggest that rather than a single group, a stable assemblage of *Gammaproteobacteria* drives dark carbon fixation in coastal surface sediments. In particular, we showed that members of the *Acidiferrobacter*, the JTB255 and the SSr clade occur in sediments worldwide and fix carbon in rates similar to those of uncultured sulfur-oxidizing bacteria from other aquatic habitats. Our genomic and metatranscriptomic evidence supports the previous assumption that chemolithoautotrophy in marine surface sediments is mainly driven by sulfur oxidation (Middelburg, 2011). However, the expression of uptake [NiFe]-hydrogenases in the SSr clade and other *Gammaproteobacteria* suggests that these organisms may also use hydrogen as an energy source for carbon fixation. On the basis of our data, we cannot exclude the possibility that other chemolithoautotrophic pathways such as ferrous iron oxidation also contributed to dark carbon fixation, but these are probably minor in organic- and sulfide-rich systems. Molecular, isotopic and physiological studies will be critical to determine, how other chemoautotrophic processes such as nitrification, metal oxidation, sulfur disproportionation (Jørgensen, 1990) and possibly also hydrogen-dependent sulfate respiration (Boschker *et al.*, 2014) contribute to dark carbon fixation in marine sediments. Intriguingly, sulfur-oxidizing, autotrophic *Gammaproteobacteria* including members of the SSr clade were recently shown to be associated with heterotrophic, electrogenic 'cable bacteria'. These were hypothesized to use cable bacteria as an electron sink during autotrophic sulfur oxidation (Vasquez-Cardenas *et al.*, 2015). Considering their cosmopolitan distribution, their metabolic lifestyle and their ecological importance, the *Acidiferrobacter*-, the JTB255-, and the three symbiont-related clades may be benthic counterparts to the gammaproteobacterial SUP05 clade, key organisms for sulfur and carbon cycling in hydrothermal plumes and OMZs (Canfield *et al.*, 2010; Wright *et al.*, 2012; Anantharaman *et al.*, 2013; Glaubitz *et al.*, 2013).

*Role of chemolithoautotrophic gammaproteobacteria in carbon cycling*

Coastal sediments are global hot spots of carbon cycling. The importance of marine vegetation such as sea grass, salt marshes and mangroves for carbon sequestration is already well established (Duarte *et al.*, 2005), but the role of coastal sediments as hot spots of microbial dark carbon fixation was only recently realized (Middelburg, 2011). According to our most conservative estimate, 70% of dark carbon

fixation in coastal sediments are driven by chemolithoautotrophic *Gammaproteobacteria* (Figure 5). These could fix 122 Tg C/year in Earth's coastal sediments (assuming a total of 175 Tg/year, from Middelburg 2011), which is similar to the 111 Tg carbon buried yearly by marine vegetated habitats worldwide (Duarte *et al.*, 2005). It is still unclear whether significant amounts of carbon fixed in the dark are buried into subsurface sediments. However, because identical/almost identical chemolithoautotrophic *Gammaproteobacteria* are frequently found in surface and subsurface sediments, they may have the potential to trap inorganic carbon and survive for centuries in subsurface sediments by tapping yet unknown sources of energy. Understanding whether the buried populations are in a state of dynamic equilibrium or whether they merely survive will be essential for assessing their role as a carbon sink.

Even though chemolithoautotrophy in shelf sediments mostly represents a 'secondary production', as it is ultimately based on energy from recycled organic matter (Middelburg, 2011), it may mitigate carbon (and sulfide) emissions from re-mineralized organic matter already at sediment surfaces. As marine sediments are the main site of global carbon sequestration, it is imperative to understand the processes and microorganisms that govern rates of burial of organic and inorganic carbon in these habitats. Here, our study provides first detailed insights into the microbiology of a largely overlooked aspect of the marine carbon cycle and highlights the environmental importance of widely distributed chemolithoautotrophic, most likely sulfur-oxidizing *Gammaproteobacteria*. As hypoxic events will expand and intensify in a warming ocean, sulfur-dependent carbon cycling will be more prevalent not only in pelagic OMZ, but also in organic-rich coastal sediments. Thus, sulfur-oxidizing and carbon-fixing microorganisms may have an increasingly important role in attenuating the rising emissions of sulfide and inorganic carbon to ocean waters and ultimately to the atmosphere.

## Conflict of Interest

The authors declare no conflict of interest.

## Acknowledgements

We greatly acknowledge the crew of R/V Navicula from the ICBM Oldenburg for ship time and assistance. We thank the crew of the R/V Meteor and R/V Sonne and the ROV team of the MARUM Quest 4000 m. We greatly acknowledge the chief scientist Wolfgang Bach for his excellent support during cruise SO216 with R/V Sonne, which was an integral part of the Cluster of Excellence of the MARUM 'The Ocean in the Earth System, Research Area GB: Geosphere-Biosphere Interactions' funded by the German Research Foundation (DFG). The cruise SO216 was funded by a grant (03G0216) from the *Bundesministerium für Bildung und Forschung* (*BMBF*) awarded to Wolfgang Bach and co-PIs. RS was supported by the US National Science Foundation grant OCE-1232982. We thank Falk Warnecke for support in sediment sampling and for sequencing of the subsurface samples. Special thanks go to Rudolf Amann for helpful discussions and continuous support. This study contributes to the project ABYSS funded by the European Research Council Advanced Investigator Grant 294757 to Antje Boetius. Further funding was provided by the Max Planck Society.

## References

Alonso C, Pernthaler J. (2005). Incorporation of glucose under anoxic conditions by bacterioplankton from coastal North Sea surface waters. *Appl Environ Microbiol* **71**: 1709–1716.

Anantharaman K, Breier JA, Sheik CS, Dick GJ. (2013). Evidence for hydrogen oxidation and metabolic plasticity in widespread deep-sea sulfur-oxidizing bacteria. *Proc Natl Acad Sci USA* **110**: 330–335.

Baker BJ, Lazar CS, Teske AP, Dick GJ. (2015). Genomic resolution of linkages in carbon, nitrogen, and sulfur cycling among widespread estuary sediment bacteria. *Microbiome* **3**: 14.

de Beer D, Wenzhöfer F, Ferdelman TG, Boehme SE, Huettel M, van Beusekom JEE *et al.* (2005). Transport and mineralization rates in North Sea sandy intertidal sediments, Sylt-Rømø Basin, Wadden Sea. *Limnol Oceanogr* **50**: 113–127.

Billerbeck M, Werner U, Polerecky L, Walpersdorf E, deBeer D, Huettel M. (2006). Surficial and deep pore water circulation governs spatial and temporal scales of nutrient recycling in intertidal sand flat sediment. *Mar Ecol Prog Ser* **326**: 61–76.

Boschker HTS, Nold SC, Wellsbury P, Bos D, de Graaf W, Pel R *et al.* (1998). Direct linking of microbial populations to specific biogeochemical processes by $^{13}$C-labelling of biomarkers. *Nature* **392**: 801–805.

Boschker HTS, Vasquez-Cardenas D, Bolhuis H, Moerdijk-Poortvliet TWC, Moodley L. (2014). Chemoautotrophic carbon fixation rates and active bacterial communities in intertidal marine sediments. *PLoS ONE* **9**: e101443.

Bowman JP, McCammon SA, Dann AL. (2005). Biogeographic and quantitative analyses of abundant uncultivated γ-proteobacterial clades from marine sediment. *Microb Ecol* **49**: 451–460.

Bowman JP, McCuaig RD. (2003). Biodiversity, community structural shifts, and biogeography of prokaryotes within Antarctic continental shelf sediment. *Appl Environ Microbiol* **69**: 2463–2483.

Burdige DJ. (2007). Preservation of organic matter in marine sediments: controls, mechanisms, and an imbalance in sediment organic carbon budgets? *Chem Rev* **107**: 467–485.

Canfield DE, Stewart FJ, Thamdrup B, Brabandere LD, Dalsgaard T, Delong EF *et al.* (2010). A cryptic sulfur cycle in oxygen-minimum-zone waters off the Chilean coast. *Science* **330**: 1375–1378.

Cleland D, Krader P, McCree C, Tang J, Emerson D. (2004). Glycine betaine as a cryoprotectant for prokaryotes. *J Microbiol Methods* **58**: 31–38.

Cline JD. (1969). Spectrophotometric determination of hydrogen sulfide in natural waters. *Limnol Oceanogr* **14**: 454–458.

Duarte CM, Middelburg JJ, Caraco N. (2005). Major role of marine vegetation on the oceanic carbon cycle. *Biogeosciences* **2**: 1–8.

Emil Ruff S, Probandt D, Zinkann A-C, Iversen MH, Klaas C, Würzberg L *et al.* (2014). Indications for algae-degrading benthic microbial communities in deep-sea sediments along the Antarctic Polar Front. *Deep Sea Res Part II Top Stud Oceanogr* **108**: 6–16.

Gittel A, Mußmann M, Sass H, Cypionka H, Könneke M. (2008). Identity and abundance of active sulfate-reducing bacteria in deep tidal flat sediments determined by directed cultivation and CARD-FISH analysis. *Environ Microbiol* **10**: 2645–2658.

Glaubitz S, Kießlich K, Meeske C, Labrenz M, Jürgens K. (2013). SUP05 dominates the gammaproteobacterial sulfur oxidizer assemblages in pelagic redoxclines of the central Baltic and Black Seas. *Appl Environ Microbiol* **79**: 2767–2776.

Gobet A, Böer SI, Huse SM, van Beusekom JEE, Quince C, Sogin ML *et al.* (2012). Diversity and dynamics of rare and of resident bacterial populations in coastal sands. *ISME J* **6**: 542–553.

Grote J, Schott T, Bruckner CG, Glöckner FO, Jost G, Teeling H *et al.* (2012). Genome and physiology of a model Epsilonproteobacterium responsible for sulfide detoxification in marine oxygen depletion zones. *Proc Natl Acad Sci USA* **109**: 506–510.

Hallberg KB, Hedrich S, Johnson DB. (2011). *Acidiferrobacter thiooxydans*, gen. nov. sp. nov.; an acidophilic, thermo-tolerant, facultatively anaerobic iron- and sulfur-oxidizer of the family Ectothiorhodospiraceae. *Extremophiles* **15**: 271–279.

Han Y, Perner M. (2014). The role of hydrogen for *Sulfurimonas denitrificans*' metabolism. *PLoS One* **9**: e106218.

Hansen M, Perner M. (2015). A novel hydrogen oxidizer amidst the sulfur-oxidizing *Thiomicrospira* lineage. *ISME J* **9**: 696–707.

Hawley AK, Brewer HM, Norbeck AD, Paša-Tolić L, Hallam SJ. (2014). Metaproteomics reveals differential modes of metabolic coupling among ubiquitous oxygen minimum zone microbes. *Proc Natl Acad Sci USA* **111**: 11395–11400.

Hedges JI, Keil RG. (1995). Sedimentary organic matter preservation: an assessment and speculative synthesis. *Mar Chem* **49**: 81–115.

Herlemann DP, Labrenz M, Jürgens K, Bertilsson S, Waniek JJ, Andersson AF. (2011). Transitions in bacterial communities along the 2000 km salinity gradient of the Baltic Sea. *ISME J* **5**: 1571–1579.

Holkenbrink C, Barbas SO, Mellerup A, Otaki H, Frigaard N-U. (2011). Sulfur globule oxidation in green sulfur bacteria is dependent on the dissimilatory sulfite reductase system. *Microbiology* **157**: 1229–1239.

Hügler M, Sievert SM. (2011). Beyond the Calvin cycle: autotrophic carbon fixation in the ocean. *Annu Rev Mar Sci* **3**: 261–289.

Hunter EM, Mills HJ, Kostka JE. (2006). Microbial community diversity associated with carbon and nitrogen cycling in permeable shelf sediments. *Appl Environ Microbiol* **72**: 5689–5701.

Jansen S, Walpersdorf E, Werner U, Billerbeck M, Böttcher ME, de Beer D. (2009). Functioning of intertidal flats inferred from temporal and spatial dynamics of $O_2$, $H_2S$ and pH in their surface sediment. *Ocean Dyn* **59**: 317–332.

Jørgensen BB. (1990). A thiosulfate shunt in the sulfur cycle of marine sediments. *Science* **249**: 152–154.

Jørgensen BB. (2011). Deep subseafloor microbial cells on physiological standby. *Proc Natl Acad Sci USA* **108**: 18193–18194.

Jost G, Zubkov MV, Yakushev E, Labrenz M, Jürgens K. (2008). High abundance and dark $CO_2$ fixation of chemolithoautotrophic prokaryotes in anoxic waters of the Baltic Sea. *Limnol Oceanogr* **53**: 14–22.

Kelly DP, Shergill JK, Lu W-P, Wood AP. (1997). Oxidative metabolism of inorganic sulfur compounds by bacteria. *Antonie Van Leeuwenhoek* **71**: 95–107.

Kim B-S, Kim BK, Lee J-H, Kim M, Lim YW, Chun J. (2008). Rapid phylogenetic dissection of prokaryotic community structure in tidal flat using pyrosequencing. *J Microbiol* **46**: 357–363.

Klatt JM, Polerecky L. (2015). Assessment of the stoichiometry and efficiency of $CO_2$ fixation coupled to reduced sulfur oxidation. *Aquat Microbiol* **6**: 484.

Kleiner M, Wentrup C, Lott C, Teeling H, Wetzel S, Young J *et al.* (2012). Metaproteomics of a gutless marine worm and its symbiotic microbial community reveal unusual pathways for carbon and energy use. *Proc Natl Acad Sci USA* **109**: E1173–E1182.

Klindworth A, Pruesse E, Schweer T, Peplies J, Quast C, Horn M *et al.* (2012). Evaluation of general 16S ribosomal RNA gene PCR primers for classical and next-generation sequencing-based diversity studies. *Nucleic Acids Res* **41**: e1.

Langmead B, Salzberg SL. (2012). Fast gapped-read alignment with Bowtie 2. *Nat Methods* **9**: 357–359.

Laurinavichene TV, Rákhely G, Kovács KL, Tsygankov AA. (2007). The effect of sulfur compounds on $H_2$ evolution/consumption reactions, mediated by various hydrogenases, in the purple sulfur bacterium *Thiocapsa roseopersicina*. *Arch Microbiol* **188**: 403–410.

Lavik G, Stührmann T, Brüchert V, Van der Plas A, Mohrholz V, Lam P *et al.* (2009). Detoxification of sulphidic African shelf waters by blooming chemolithotrophs. *Nature* **457**: 581–584.

Lee N, Nielsen PH, Andreasen KH, Juretschko S, Nielsen JL, Schleifer KH *et al.* (1999). Combination of fluorescent *in situ* hybridization and microautoradiography - a new tool for structure-function analyses in microbial ecology. *Appl Environ Microbiol* **65**: 1289–1297.

Lenk S, Arnds J, Zerjatke K, Musat N, Amann R, Mußmann M. (2011). Novel groups of *Gammaproteobacteria* catalyse sulfur oxidation and carbon fixation in a coastal, intertidal sediment. *Environ Microbiol* **13**: 758–774.

Lenk S, Moraru C, Hahnke S, Arnds J, Richter M, Kube M *et al.* (2012). *Roseobacter* clade bacteria are abundant in coastal sediments and encode a novel combination of sulfur oxidation genes. *ISME J* **6**: 2178–2187.

Li W. (1982). Estimating heterotrophic bacterial productivity by inorganic radiocarbon uptake - importance of establishing time courses of uptake. *Mar Ecol Prog Ser* **8**: 167–172.

Liu J, Liu X, Wang M, Qiao Y, Zheng Y, Zhang X-H. (2014). Bacterial and archaeal communities in sediments of the north Chinese marginal seas. *Microb Ecol* **70**: 105–117.

Lösekann T, Robador A, Niemann H, Knittel K, Boetius A, Dubilier N. (2008). Endosymbioses between bacteria and deep-sea siboglinid tubeworms from an Arctic

Cold Seep (Haakon Mosby Mud Volcano, Barents Sea). *Environ Microbiol* **10**: 3237–3254.

Manefield M, Whiteley AS, Griffiths RI, Bailey MJ. (2002). RNA stable isotope probing, a novel means of linking microbial community function to phylogeny. *Appl Environ Microbiol* **68**: 5367–5373.

Marchant HK, Lavik G, Holtappels M, Kuypers MMM. (2014). The fate of nitrate in intertidal permeable sediments. *PLoS ONE* **9**: e104517.

Markowitz VM, Chen I-MA, Palaniappan K, Chu K, Szeto E, Grechkin Y *et al.* (2012). IMG: the integrated microbial genomes database and comparative analysis system. *Nucleic Acids Res* **40**: D115–D122.

Mattes TE, Nunn BL, Marshall KT, Proskurowski G, Kelley DS, Kawka OE *et al.* (2013). Sulfur oxidizers dominate carbon fixation at a biogeochemical hot spot in the dark ocean. *ISME J* **7**: 2349–2360.

Meyer B, Kuever J. (2007). Molecular analysis of the diversity of sulfate-reducing and sulfur-oxidizing prokaryotes in the environment, using *aprA* as functional marker gene. *Appl Environ Microbiol* **73**: 7664–7679.

Middelburg JJ. (2011). Chemoautotrophy in the ocean. *Geophys Res Lett* **38**: 94–97.

Molari M, Manini E, Dell'Anno A. (2013). Dark inorganic carbon fixation sustains the functioning of benthic deep-sea ecosystems. *Glob Biogeochem Cycles* **27**: 212–221.

Musat N, Halm H, Winterholler B, Hoppe P, Peduzzi S, Hillion F *et al.* (2008). A single-cell view on the ecophysiology of anaerobic phototrophic bacteria. *Proc Natl Acad Sci USA* **105**: 17861–17866.

Muyzer G, Brinkhoff T, Nuebel U, Santegoeds C, Schaefer H, Waver C. (1998). Denaturing gradient gel electrophoresis (DGGE) in microbial ecology. In: Akkermans ADL, van Elsas JD, de Bruijn FJ (ed). *Molecular Microbial Ecology Manual*. Kluwer Academic Publishers: Dordrecht, The Netherlands, pp 1–27.

Orcutt BN, Sylvan JB, Knab NJ, Edwards KJ. (2011). Microbial ecology of the dark ocean above, at, and below the seafloor. *Microbiol Mol Biol Rev* **75**: 361–422.

Parkes RJ, Cragg BA, Getliff JM, Harvey SM, Fry JC, Lewis CA *et al.* (1993). A quantitative study of microbial decomposition of biopolymers in Recent sediments from the Peru Margin. *Mar Geol* **113**: 55–66.

Pernthaler A, Pernthaler J, Amann R. (2002). Fluorescence *in situ* hybridization and catalyzed reporter deposition for the identification of marine bacteria. *Appl Environ Microbiol* **68**: 3094–3101.

Petersen JM, Zielinski FU, Pape T, Seifert R, Moraru C, Amann R *et al.* (2011). Hydrogen is an energy source for hydrothermal vent symbioses. *Nature* **476**: 176–180.

Pruesse E, Quast C, Knittel K, Fuchs BM, Ludwig W, Peplies J *et al.* (2007). SILVA: a comprehensive online resource for quality checked and aligned ribosomal RNA sequence data compatible with ARB. *Nucleic Acids Res* **35**: 7188–7196.

Quast C, Pruesse E, Yilmaz P, Gerken J, Schweer T, Yarza P *et al.* (2013). The SILVA ribosomal RNA gene database project: improved data processing and web-based tools. *Nucleic Acids Res* **41**: D590–D596.

Radajewski S, Ineson P, Parekh NR, Murrell JC. (2000). Stable-isotope probing as a tool in microbial ecology. *Nature* **403**: 646–649.

Reinthaler T, van Aken HM, Herndl GJ. (2010). Major contribution of autotrophy to microbial carbon cycling in the deep North Atlantic's interior. *Deep Sea Res Part II Top Stud Oceanogr* **57**: 1572–1580.

Rinke C, Schmitz-Esser S, Stoecker K, Nussbaumer AD, Molnár DA, Vanura K *et al.* (2006). '*Candidatus* Thiobios zoothamnicoli,' an ectosymbiotic bacterium covering the giant marine ciliate *Zoothamnium niveum*. *Appl Environ Microbiol* **72**: 2014–2021.

Roslev P, Larsen MB, Jorgensen D, Hesselsoe M. (2004). Use of heterotrophic $CO_2$ assimilation as a measure of metabolic activity in planktonic and sessile bacteria. *J Microbiol Methods* **59**: 381–393.

Røy H, Lee JS, Jansen S, de Beer D. (2008). Tide-driven deep pore-water flow in intertidal sand flats. *Limnol Oceanogr* **53**: 1521–1530.

Ruff SE, Biddle JF, Teske AP, Knittel K, Boetius A, Ramette A. (2015). Global dispersion and local diversification of the methane seep microbiome. *Proc Natl Acad Sci USA* **112**: 4015–4020.

Salman V, Bailey JV, Teske A. (2013). Phylogenetic and morphologic complexity of giant sulphur bacteria. *Antonie Van Leeuwenhoek* **104**: 169–186.

Schauer R, Bienhold C, Ramette A, Harder J. (2009). Bacterial diversity and biogeography in deep-sea surface sediments of the South Atlantic Ocean. *ISME J* **4**: 159–170.

Schippers A, Neretin LN, Kallmeyer J, Ferdelman TG, Cragg BA, John Parkes R *et al.* (2005). Prokaryotic cells of the deep sub-seafloor biosphere identified as living bacteria. *Nature* **433**: 861–864.

Seidel M, Graue J, Engelen B, Köster J, Sass H, Rullkötter J. (2012). Advection and diffusion determine vertical distribution of microbial communities in intertidal sediments as revealed by combined biogeochemical and molecular biological analysis. *Org Geochem* **52**: 114–129.

Sekar R, Fuchs BM, Amann R, Pernthaler J. (2004). Flow sorting of marine bacterioplankton after fluorescence *in situ* hybridization. *Appl Environ Microbiol* **70**: 6210–6219.

Siyambalapitiya N, Blackall LL. (2005). Discrepancies in the widely applied GAM42a fluorescence *in situ* hybridisation probe for *Gammaproteobacteria*. *FEMS Microbiol Lett* **242**: 367–373.

Swan BK, Martinez-Garcia M, Preston CM, Sczyrba A, Woyke T, Lamy D *et al.* (2011). Potential for chemolithoautotrophy among ubiquitous bacteria lineages in the dark ocean. *Science* **333**: 1296–1300.

Thomas F, Giblin AE, Cardon ZG, Sievert SM. (2014). Rhizosphere heterogeneity shapes abundance and activity of sulfur-oxidizing bacteria in vegetated salt marsh sediments. *Front Microbiol* **5**: 1–14.

Vasquez-Cardenas D, van de Vossenberg J, Polerecky L, Malkin SY, Schauer R, Hidalgo-Martinez S *et al.* (2015). Microbial carbon metabolism associated with electrogenic sulphur oxidation in coastal sediments. *ISME J* **9**: 1966–1978.

Wang L, Liu L, Zheng B, Zhu Y, Wang X. (2013). Analysis of the bacterial community in the two typical intertidal sediments of Bohai Bay, China by pyrosequencing. *Mar Pollut Bull* **72**: 181–187.

Wood HG, Werkman CH. (1936). The utilisation of $CO_2$ in the dissimilation of glycerol by the propionic acid bacteria. *Biochem J* **30**: 48–53.

Woyke T, Teeling H, Ivanova NN, Huntemann M, Richter M, Gloeckner FO *et al.* (2006). Symbiosis

insights through metagenomic analysis of a microbial consortium. *Nature* **443**: 950–955.

Wright JJ, Konwar KM, Hallam SJ. (2012). Microbial ecology of expanding oxygen minimum zones. *Nat Rev Microbiol* **10**: 381–394.

Zerjatke K. (2009). Mikroautoradiographie und Genexpression von Bakterien im Oberflächensediment der Gezeitenzone des Wattenmeeres. *Diploma thesis*. University of Bremen: Bremen, Germany.

Zheng B, Wang L, Liu L. (2014). Bacterial community structure and its regulating factors in the intertidal sediment along the Liaodong Bay of Bohai Sea, China. *Microbiol Res* **169**: 585–592.

Zhou J, Bruns MA, Tiedje JM. (1996). DNA recovery from soils of diverse composition. *Appl Environ Microbiol* **62**: 316–322.

Ziehe D. (2009). *Aminosäure-D/L-Verhältnisse in biogenen Carbonaten als Schlüssel zur Datierung holozäner Sedimentationsvorgänge im norddeutschen Küstenraum* PhD thesis. University of Oldenburg: Oldenburg, Germany.

Zubkov MV, Fuchs BM, Tarran GA, Burkill PH, Amann R. (2003). High rate of uptake of organic nitrogen compounds by *Prochlorococcus* cyanobacteria as a key to their dominance in oligotrophic oceanic waters. *Appl Environ Microbiol* **69**: 1299–1304.

Supplementary Information accompanies this paper on The ISME Journal website (http://www.nature.com/ismej)

## Supplementary Information

### Methods

*Barcoded 16S rRNA gene amplicon sequencing*

The bacterial diversity in all sediment samples was determined by analyzing the hypervariable V3-V4 region of the 16S rRNA gene using Roche 454 pyro- or Illumina MiSeq-sequencing of barcoded amplicons. Barcoded amplicons from all surface sediments were prepared using primers 341f/785rev (Herlemann *et al.*, 2011; Klindworth *et al.*, 2012). PCR conditions were as follows: initial denaturation, 95°C for 5 min, followed by 20-28 cycles of 95°C for 30 s, 50°C for 1 min, 72°C for 1 min and final elongation of 72°C for 10 min. In general, the *Taq*-DNA polymerase (Eppendorf, Hamburg, Germany) was used, but for site Dunsborough we applied a high fidelity Phusion polymerase (Thermo Fisher Scientific Inc., USA). Pools of six replicates per sample were sequenced by Max Planck-Genome Centre (MP-GC, Cologne, Germany) using the Roche 454 GS junior sequencer. Barcoded amplicons from Dunsborough sediments were used for preparation of a TruSeq library and sequenced (paired end, 2x 250 bp) at MP-GC using an Illumina MiSeq instrument (Illumina Inc., USA). Barcoded amplicons from the 490 cm-deep subsurface sediment from site Janssand were prepared by replacing primer 785rev with 907rev (Muyzer *et al.*, rev 1998; Klindworth *et al.*, 2012). This primer covers a similar bacterial diversity as the reverse primer 785rev used for surface sediments (see above, Figure 2), but it is known to bias against some phyla that are, however, low abundant or absent in marine sediments (Klindworth *et al.*, 2012). PCR amplification and barcoded pyrosequencing was done by Research and Testing Laboratories, (Lubbock, Texas, USA) using a Roche 454 FLX sequencer. Samples from 10 cmbsf and 490 cmbsf were run in duplicate. Paired end reads were merged using the software package BBmap v4.3 (overlap >15 nucleotides). Finally, all amplicon reads were quality trimmed (>q20) and split by barcodes using MOTHUR (Schloss *et al.*, 2009). Sequences less than 300 bp and those containing ambiguous nucleotides and long homopolymers (>7) were removed. In total 311,196 bacterial 16S rRNA reads were kept for taxonomic classification using the SILVAngs pipeline v115 (Quast *et al.*, 2013) with a clustering at 98% identity.

*16S rRNA gene libraries from subsurface sediments and phylogenetic analysis*

From the 490 cm-deep subsurface core from Janssand sediment (April 2005) bulk DNA was extracted from 200 and 490 cmbsf according to Zhou *et al*. (1996) with an overnight incubation with proteinase K for improved cell lysis. The crude DNA extract obtained was purified using the Wizard DNA Cleanup system (Promega, Madison, WI, USA). PCRs were performed as described by Lenk *et al.* (2011) with the following thermocycler conditions: initial denaturation, 95°C for 5 min, followed by 25 cycles (490cmbsf) or 19 cycles (200

cmbsf) of 95°C for 1 min, 46°C for 1 min, 72°C for 3 min and final elongation of 72°C for 10 min using Master *Taq* DNA polymerase. The products of 6 (200 cmbsf) and 10 (490 cmbsf) parallel PCR amplifications were pooled and purified (QIAquick PCR purification Kit, Quiagen, Hilden, Germany). Preparative gels were used to get the right size of the PCR amplificates. The gel-excised and extracted (QIAquick Gel Extraction Kit, Quiagen, Hilden, Germany) PCR products were cloned using the TOPO TA Sequencing Kit (Invitrogen, Carlsbad, CA, USA) according to the manufacturer´s specifications. Clone inserts were sequenced using the BigDye Terminator cycle sequencing kit, version 3.1 (Applied Biosystems, Darmstadt, Germany). Selected nearly full-length sequences were retrieved using the Sequencher 4.9 DNA sequence assembly and analysis software (Gene Codes Corporation, Ann Arbor, MI, USA). All sequences were checked for chimera with the online tool Bellerophon from Greengenes (Huber *et al.*, 2004; DeSantis *et al.*, 2006) and possible chimera sequences were excluded from further analysis.

Phylogenetic trees were calculated by neighbor-joining (Jukes-Cantor correction) and PHYML (Guindon and Gascuel, 2003) maximum-likelihood analyses implemented in the ARB software package (Ludwig *et al.*, 2004) using a 50% base-frequency filter for *Gammaproteobacteria*. RAxML trees (Stamatakis *et al.*, 2004) were calculated using Gamma model of rate heterogeneity at the CIPRES cluster (version 7.2.745, http://www.phylo.org/46). Only sequences with more than 1200 base pairs (bp) were used for tree calculation. Topologies derived by the different approaches were compared to construct a consensus tree. Partial sequences were then inserted into the reconstructed tree by applying parsimony criteria, without allowing changes in the overall topology. Clones library preparation and nearly full-length 16S rRNA gene sequences from Janssand surface sediment have been published elsewhere (Lenk *et al.*, 2011).

*CARD-FISH and sample preparation for flow cytometry*

For catalyzed reporter deposition-fluorescence *in situ* hybridization (CARD-FISH) sediment from sites Calais, Courseulles-sur-Mer and Janssand was fixed immediately after core retrieval as described in Lenk *et al*. (2011). Cells were detached from 100-200 µl sediment by ultrasonic treatment as described previously (Lenk *et al.*, 2011). The sample was not centrifuged but directly after settlement of the sand grains the supernatant along with the detached cells were filtered onto 25 mm polycarbonate membrane filters with a 0.2 µm pore size (GTTP, Millipore, Eschborn, Germany). Permeabilization and CARD-FISH was performed as described by Pernthaler *et al*. (2002) without embedding in agarose with the following modifications. Endogenous peroxidases were inactivated in 3% $H_2O_2$ in Milli-Q water for 10 min at room temperature. The temperature for all hybridizations was 46°C and washing was performed at 48°C according to the protocol of Ishii *et al*. (2004). An overview

of oligonucleotide probes used in this study is shown in Supplementary Table 2. Novel oligonucleotide probes were designed for the JTB255-group using ARB and the SILVA 16S rRNA reference database release 117 (Pruesse *et al.*, 2007). Please note that the *Xanthomonadales,* which includes the JTB255-clade*,* is not targeted by probe GAM42a, specific for most *Gammaproteobacteria* (Siyambalapitiya and Blackall, 2005). In line with this, the JTB255-clade could not be detected with probe GAM42a in double hybridizations with the JTB probe mix (Supplementary Table 2). Therefore, we summed up FISH counts of the JTB255 probe mix and of probe GAM42a to yield the total relative abundance by FISH-detectable *Gammaproteobacteria*.

*Calculation of cell-specific carbon fixation rates*

The average cell-specific carbon fixation rates (g carbon/cell/h) were calculated from bulk measurements for a sorted population assuming 50,000 cells per sorting event according to the equation $R = (A * M) / (a * n * t * L)$. *A* represents the activity of the sorted cell batch (50,000 cells) in Becquerel (Bq), *M* represents the molar mass of carbon (g/mol), *a* equals the specific activity of the tracer (Bq/mol), *n* represents the number of sorted cells, *t* represents the incubation time in hours and *L* equals the ratio of total DIC/$^{14}$C DIC. Note that since the JTB255-group is not targeted by probe GAM42a, we added $^{14}$C carbon assimilation of the sorted JTB255-populations to the assimilation of cells sorted by probe GAM42a to yield the total amount of $^{14}$C assimilated by all FISH-detectable *Gammaproteobacteria*.

*Clone library of uptake [NiFe]-hydrogenase genes from Janssand sediment*

A library for the gene encoding the large subunit of an uptake [NiFe]-hydrogenase was established using DNA extracted from sediment of the upper cm, sulfide transition zone and sulfidic layer collected at site Janssand in March 2012. The hydrogenase gene was amplified with the general primers HUPLX1 (forward) and HUPLW2 (reverse) (Csáki *et al.*, 2001). PCR reactions (final volume of 20 µl) contained 10 pmol of each primer, 6.25 nmol of each dNTP, 1x Master *Taq* Buffer and 1U of *Taq* DNA. Thermocycler conditions were as follows: initial denaturation, 95°C for 5 min, followed by 35 cycles of 95°C for 30 s, 65°C for 30 s, 72°C for 2 min and final elongation of 72°C for 10 min. Amplified PCR products were cloned using TOPO TA kit for sequencing (pCR4-TOPO, Invitrogen, Germany) and sequenced with the Big Dye Terminator v3.1 Cycle Sequencing Kit (Applied Biosystems, Darmstadt, Germany) according to manufacturer's instructions. Alternatively, clones were sent for Sanger-sequencing to GATC Biotech AG (Konstanz, Germany). Phylogenetic trees from the deduced amino acid sequences were constructed in ARB (Ludwig *et al.*, 2004) using a maximum-likelihood algorithm (RAxML) (Stamatakis *et al.*, 2004) and the JTT amino acid substitution matrix with 100 bootstrap replicates.

*cDNA libraries and metatranscriptomic mapping*

In April 2013 sediment was sampled from the sulfide transition zone at site Janssand and immediately frozen on dry ice. Total RNA was extracted from sediment in triplicates (one ml each) by the Vertis Biotechnologie AG (Freising, Germany) and bacterial rRNA was depleted with the Ribo-Zero™ Magnetic Kit (for *Bacteria*) (Epicentre, Madison, *USA*). Barcoded RNA TrueSEQ libraries were constructed from RNA extractions and paired-end-sequenced using Illumina HiSeq2000 (MP-GC, Cologne, Germany). After quality trimming at a Phred score 28 using Nesoni clip (v.0.115) reads were mapped to reference databases of nucleotide sequences encoding key genes for sulfur oxidation (Sox multienzyme system, *sox*B; reverse dissimilatory sulfite reductase, *dsr*AB; adenosine-5'-phosphosulfate reductase, *apr*A), hydrogen oxidation (uptake [NiFe]-hydrogenase), ammonia oxidation (ammonia monooxygenase, *amo*A), carbon fixation (ribulose-1,5-bisphosphate carboxylase/oxygenase form I, cbbl; ribulose-1,5-bisphosphate carboxylase/oxygenase form II, cbbm; ATP citrate lyase, *acl*AB) and to the single amplified genome (SAG) using Bowtie2 (Langmead and Salzberg, 2012) with the following settings: match score = 0, mismatch penalty = 5, gap open penalty = 5, gap extension penalty = 5. The minimum alignment score for an alignment considered as valid was defined by -0.25 multiplied by read length for mapping to sulfur and hydrogen oxidation genes as well as for mapping on the SAG and -0.5 multiplied by read length for mapping to carbon fixation genes resulting in a percent identity cut-off of 95% and 90%, respectively. The percent identity cut-off for mapping to ammonia oxidation genes was set at 70%. The numbers of unique mapped reads were normalized by dividing the number of cDNA reads per gene by gene length multiplied by 1000 and adjusting for the total size of the data set. Details on reference databases are given in Supplementary Table 4. Reference sequences of sulfur oxidation genes (*apr*A, *dsr*AB and *sox*B) from site Janssand have been published previously (Lenk *et al.*, 2011; Lenk *et al.*, 2012).

*A single cell genome of the SSr-clade from Janssand sediment*

In January 2011, sediment from a 10 cm-deep sediment core was sampled at site Janssand. After immediate transfer to the lab the upper two cm including the oxidized and sulfide transition zone were mixed and one ml was transferred to a 15 ml plastic tube. After adding 3 ml of sterile-filtered sea water the slurry was vortexed at maximum speed for 5 min. After settlement of sand grains the supernatant was filtered through a 3 µm pore-size membrane. The filtrate was cryopreserved with N,N,N-trimethylglycine (“glycine betaine”) (Sigma-Aldrich, USA) at a final concentration of 4% according to Cleland *et al.* (2004), stored at -80°C and shipped overseas. Single-cell sorting and whole genome amplification via multiple displacement amplification (MDA) were performed at the Bigelow Laboratory Single Cell Genomics Center (https://scgc.bigelow.org) as described by Swan *et al.* (2011). PCR-

screening for 16S rRNA genes of amplified single cell genomes was performed at the MPI Bremen. A single amplified genome (SAG) encoding a single, high quality 16S rRNA gene sequence was sent to Max Planck Genome Centre Cologne for MiSeq (Illumina) sequencing yielding 9,557,547 PE-reads. Reads were assembled with the CLC Genomics software with standard settings. Details on assembled data are given in Supplementary Table 3. The SAG assemblies were auto-annotated using the Joint Genome Institute (JGI) IMG-ER pipeline (Markowitz *et al.*, 2012). The assembled data set was screened for contamination using k-mer analysis within the IMG-ER pipeline. Finally, two scaffolds showing a k-mer pattern divergent from bulk scaffolds were removed from the dataset. In addition, universal single copy genes (Ciccarelli *et al.*, 2006; Creevey *et al.*, 2011), ribosomal proteins and tRNA were manually checked for a possible contamination by examining their closest BLAST hits.

*Metagenomic sequencing from hydrothermal chimney (Manus Basin) and targeted re-assembly of metagenomic bins*

Total DNA from a hydrothermal chimney biofilm obtained from the Manus Basin hydrothermal field (Reeves *et al.*, 2011) was shotgun-sequenced on an Illumina HiSeq sequencer. After quality clipping, sequence reads were normalized to a k-mer depth value of 40 with BBnorm (BBmap package) and assembled using the IDBA-UD iterative assembler (Peng *et al.*, 2012). Scaffolds from the metagenome assembly larger than 1000 bp were imported into MetaWatt (Strous *et al.*, 2012) and binned by tetranucleotide (N4) frequencies (Teeling *et al.*, 2004) at a high confidence (98%) threshold. Open reading frames (ORFs) were predicted by Prodigal v 2.6.1 (Hyatt *et al.*, 2010) and scaffolds were taxonomically classified by a BLASTP search of the translated ORFs against the NCBI reference Genome database with the BLASTP based module of MetaWatt. N4 based bins were corrected manually based on GC content, coverage, and consistency of taxonomic classification. Selected genome bins were exported from MetaWatt and used as a reference for mapping of raw unassembled reads with BBmap. The initial mapping was performed with a minimum identity threshold of 80%. Mapped reads were subsequently assembled de-novo using the SPAdes assembler V3.1.1 (Bankevich *et al.*, 2012) in single cell mode with k-mer size ranging from 21 to 121 in steps of 10 and 121 as the maximum k-mer size. The new assembly was again binned by N4-frequency, classified with BLASTP and manually refined based on coverage and GC content in MetaWatt. Raw reads were again mapped onto the refined genome bin with more stringent parameters (minimum sequence identity of 95%) and de-novo assembled with SPAdes. Binning, mapping and de-novo assembly with SPAdes were repeated 7 times with increasing read mapping stringency (up to 98%). After the third round of re-assembly binned contigs larger than 10 kb were supplied to SPAdes as “trusted contigs”. The completeness and possible redundancy of the final genome bin was evaluated

by CheckM lineage-specific workflow and by the HMMER3 (Eddy, 2008) based "Six-frame Pfam" module search against a conserved single-copy gene set (Campbell *et al.*, 2013) in MetaWatt.

*Fosmid endsequence analysis*

DNA from the 490 cm-deep subsurface sediment core sampled in 2005 (Gittel *et al.*, 2008) was extracted according to Zhou *et al.* (1996). A metagenomic fosmid library was generated comprising 13,680 clones was established as described previously (Mussmann *et al.*, 2005). Five thousand clones were randomly selected for fosmids-end Sanger-sequencing on ABI3730XL capillary sequencers (PE Applied Biosystems, USA) by using fosmid-specific primers. End sequences were translated in all possible six reading frames. All reading frames were searched with BLAST against the NCBI-nr database. Reading frames with significant results (<1e-05 E-value) were considered as protein coding sequences. All protein coding sequences were taxonomically affiliated by BLAST against an in-house database of whole/draft genomes sequences (~10,000) by using a Lowest Common Ancestor (LCA) algorithm to assign an end-sequence to a particular taxonomic rank and group.

## References

Bankevich A, Nurk S, Antipov D, Gurevich AA, Dvorkin M, Kulikov AS, *et al.* (2012). SPAdes: a new genome assembly algorithm and its applications to single-cell sequencing. *J Comput Biol* **19**: 455–477.

Campbell JH, O'Donoghue P, Campbell AG, Schwientek P, Sczyrba A, Woyke T, *et al.* (2013). UGA is an additional glycine codon in uncultured SR1 bacteria from the human microbiota. *Proc Natl Acad Sci* **110**: 5540–5545.

Ciccarelli FD, Doerks T, Mering C von, Creevey CJ, Snel B, Bork P. (2006). Toward automatic reconstruction of a highly resolved tree of life. *Science* **311**: 1283–1287.

Cleland D, Krader P, McCree C, Tang J, Emerson D. (2004). Glycine betaine as a cryoprotectant for prokaryotes. *J Microbiol Methods* **58**: 31–38.

Creevey CJ, Doerks T, Fitzpatrick DA, Raes J, Bork P. (2011). Universally distributed single-copy genes indicate a constant rate of horizontal transfer. *PLoS ONE* **6**: e22099.

Csáki R, Hanczár T, Bodrossy L, Murrell J c., Kovács K l. (2001). Molecular characterization of structural genes coding for a membrane bound hydrogenase in *Methylococcus capsulatus* (Bath). *FEMS Microbiol Lett* **205**: 203–207.

DeSantis TZ, Hugenholtz P, Larsen N, Rojas M, Brodie EL, Keller K, *et al.* (2006). Greengenes, a chimera-checked 16S rRNA gene database and workbench compatible with ARB. *Appl Environ Microbiol* **72**: 5069–5072.

Eddy SR. (2008). A probabilistic model of local sequence alignment that simplifies statistical significance estimation. *PLoS Comput Biol* **4**: e1000069.

Gittel A, Mußmann M, Sass H, Cypionka H, Könneke M. (2008). Identity and abundance of active sulfate-reducing bacteria in deep tidal flat sediments determined by directed cultivation and CARD-FISH analysis. *Environ Microbiol* **10**: 2645–2658.

Guindon S, Gascuel O. (2003). A simple, fast, and accurate algorithm to estimate large phylogenies by maximum likelihood. *Syst Biol* **52**: 696–704.

Herlemann DP, Labrenz M, Jürgens K, Bertilsson S, Waniek JJ, Andersson AF. (2011). Transitions in bacterial communities along the 2000 km salinity gradient of the Baltic Sea. *ISME J* **5**: 1571–1579.

Huber T, Faulkner G, Hugenholtz P. (2004). Bellerophon: a program to detect chimeric sequences in multiple sequence alignments. *Bioinformatics* **20**: 2317–2319.

Hyatt D, Chen G-L, LoCascio PF, Land ML, Larimer FW, Hauser LJ. (2010). Prodigal: prokaryotic gene recognition and translation initiation site identification. *BMC Bioinformatics* **11**: 119.

Ishii K, Mußmann M, MacGregor BJ, Amann R. (2004). An improved fluorescence *in situ* hybridization protocol for the identification of bacteria and archaea in marine sediments. *FEMS Microbiol Ecol* **50**: 203–213.

Klindworth A, Pruesse E, Schweer T, Peplies J, Quast C, Horn M, *et al.* (2012). Evaluation of general 16S ribosomal RNA gene PCR primers for classical and next-generation sequencing-based diversity studies. *Nucleic Acids Res* 41:e1.

Langmead B, Salzberg SL. (2012). Fast gapped-read alignment with Bowtie 2. *Nat Methods* **9**: 357–359.

Lenk S, Arnds J, Zerjatke K, Musat N, Amann R, Mußmann M. (2011). Novel groups of *Gammaproteobacteria* catalyse sulfur oxidation and carbon fixation in a coastal, intertidal sediment. *Environ Microbiol* **13**: 758–774.

Lenk S, Moraru C, Hahnke S, Arnds J, Richter M, Kube M, *et al.* (2012). *Roseobacter* clade bacteria are abundant in coastal sediments and encode a novel combination of sulfur oxidation genes. *ISME J* **6**: 2178–2187.

Ludwig W, Strunk O, Westram R, Richter L, Meier H, Yadhukumar, *et al.* (2004). ARB: a software environment for sequence data. *Nucleic Acids Res* **32**: 1363–1371.

Markowitz VM, Chen I-MA, Palaniappan K, Chu K, Szeto E, Grechkin Y, *et al.* (2012). IMG: the integrated microbial genomes database and comparative analysis system. *Nucleic Acids Res* **40**: D115–D122.

Mussmann M, Richter M, Lombardot T, Meyerdierks A, Kuever J, Kube M, *et al.* (2005). Clustered genes related to sulfate respiration in uncultured prokaryotes support the theory of their concomitant horizontal transfer. *J Bacteriol* **187**: 7126–7137.

Muyzer G, Brinkhoff T, Nuebel U, Santegoeds C, Schaefer H, Waver C. (1998). Denaturing gradient gel electrophoresis (DGGE) in microbial ecology. In: Akkermans ADL, van Elsas JD, de Bruijn FJ, (ed). Molecular Microbial Ecology Manual. Dordrecht, The Netherlands: Kluwer Academic Publishers, pp. 1–27.

Peng Y, Leung HCM, Yiu SM, Chin FYL. (2012). IDBA-UD: a de novo assembler for single-cell and metagenomic sequencing data with highly uneven depth. *Bioinformatics* **28**: 1420–1428.

Pernthaler A, Pernthaler J, Amann R. (2002). Fluorescence *in situ* hybridization and catalyzed reporter deposition for the identification of marine bacteria. *Appl Environ Microbiol* **68**: 3094–3101.

Pruesse E, Quast C, Knittel K, Fuchs BM, Ludwig W, Peplies J, *et al.* (2007). SILVA: a comprehensive online resource for quality checked and aligned ribosomal RNA sequence data compatible with ARB. *Nucleic Acids Res* **35**: 7188–7196.

Quast C, Pruesse E, Yilmaz P, Gerken J, Schweer T, Yarza P, *et al.* (2013). The SILVA ribosomal RNA gene database project: improved data processing and web-based tools. *Nucleic Acids Res* **41**: D590–D596.

Reeves EP, Seewald JS, Saccocia P, Bach W, Craddock PR, Shanks WC, *et al.* (2011). Geochemistry of hydrothermal fluids from the PACMANUS, Northeast Pual and Vienna Woods hydrothermal fields, Manus Basin, Papua New Guinea. *Geochim Cosmochim Acta* **75**: 1088–1123.

Schloss PD, Westcott SL, Ryabin T, Hall JR, Hartmann M, Hollister EB, *et al.* (2009). Introducing mothur: open-source, platform-independent, community-supported software for describing and comparing microbial communities. *Appl Environ Microbiol* **75**: 7537–7541.

Siyambalapitiya N, Blackall LL. (2005). Discrepancies in the widely applied GAM42a fluorescence *in situ* hybridisation probe for *Gammaproteobacteria*. *FEMS Microbiol Lett* **242**: 367–373.

Stamatakis AP, Meier H, Ludwig T. (2004). New fast and accurate heuristics for inference of large phylogenetic trees. *Parallel and Distributed Processing Symposium, 2004. Proceedings. 18th International*, p. 193.

Strous M, Kraft B, Bisdorf R, Tegetmeyer HE. (2012). The binning of metagenomic contigs for microbial physiology of mixed cultures. *Front Microbiol* **3**: 410.

Swan BK, Martinez-Garcia M, Preston CM, Sczyrba A, Woyke T, Lamy D, *et al.* (2011). Potential for chemolithoautotrophy among ubiquitous bacteria lineages in the dark ocean. *Science* **333**: 1296–1300.

Teeling H, Waldmann J, Lombardot T, Bauer M, Glöckner FO. (2004). TETRA: a web-service and a stand-alone program for the analysis and comparison of tetranucleotide usage patterns in DNA sequences. *BMC Bioinformatics* **5**: 163.

Zhou J, Bruns MA, Tiedje JM. (1996). DNA recovery from soils of diverse composition. *Appl Environ Microbiol* **62**: 316–322.

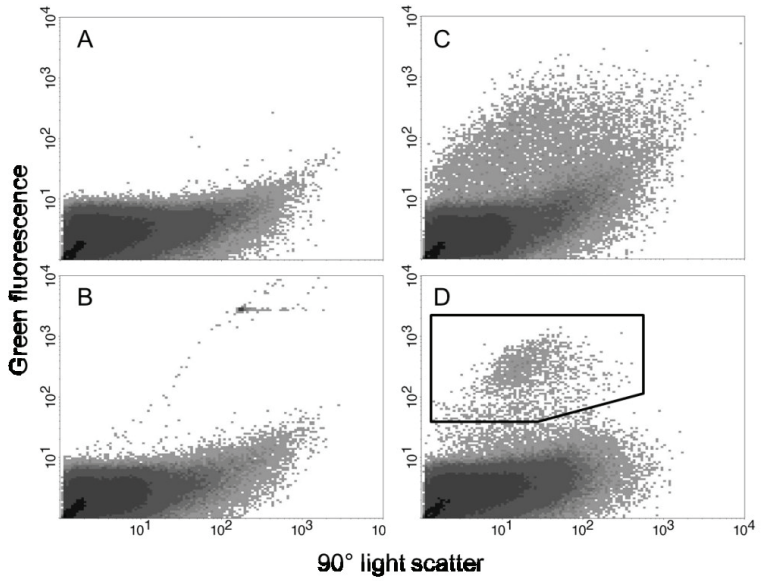


**Supplementary Figure 1** Characteristic signatures of sediment samples analyzed by flow cytometry. Density dot plot diagrams of green fluorescence plotted versus 90° light scatter. Each diagram showed 250,000 analyzed events from hybridization with the negative-control probe NON338 (a), NON338 mixed with fluorescent beads (b), EUBI-III (c) and GAM1030/GAM446 (d). The square indicates the sort-gate for cell sorting (d).

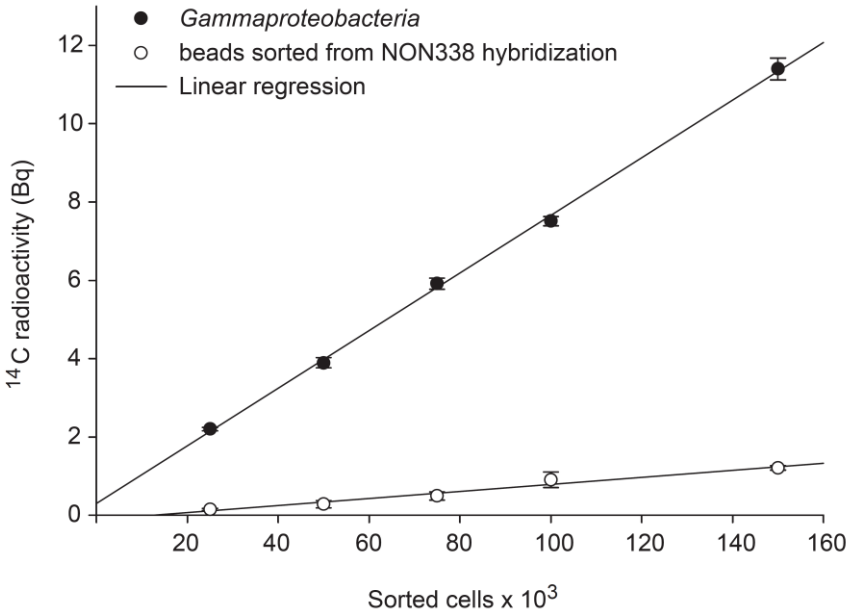


**Supplementary Figure 2** Correlation of $^{14}C$ carbon activity with abundances of sorted *Gammaproteobacteria* cells and fluorescent beads. To determine the unspecific background from $^{14}C$ bicarbonate incubations, sediments slurries were supplemented with fluorescent beads, hybridized with the negative control probe (NON338) and then sorted for liquid scintillography. $^{14}C$ carbon activity is given in Becquerel (Bq). Error bars indicate the standard deviation (SD) of triplicate sorting.

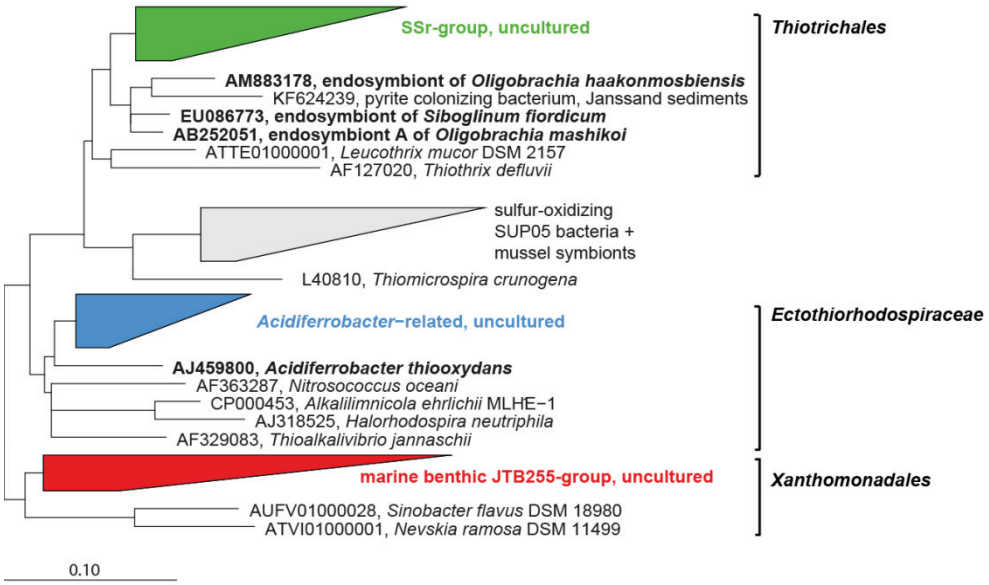


**Supplementary Figure 3** 16S rRNA phylogeny of the SSr-, the *Acidiferrobacter*-related and the JTB255-clades. Phylogenetic analysis of nearly full-length 16S rRNA gene sequences of three gammaproteobacterial clades abundant and widespread in marine sediments and their closest known relatives. A more detailed view is given in Supplementary Figure 4. The consensus tree was calculated using RAxML, and Phylip maximum likelihood and Neighbor joining algorithms. The taxonomy refers to the SILVA database, release 117 (Pruesse *et al.*, 2007).


**Supplementary Figure 4** Detailed phylogenetic reconstruction of nearly full length and partial 16S rRNA gene sequences of the SSr-, the *Acidiferrobacter*-related and the JTB255-clades. Sequences in blue were recovered from 200 or 490 cmbsf, sequences in red were recovered from the 0-12 cmbsf. OTUs were defined for sequences with 100% sequence identity. Target sequences of probes used for FISH counting and flow sorting are boxed in green. The consensus tree was calculated using RAxML, and Phylip maximum likelihood and Neighbor joining algorithms. Partial sequences were added using the quick-add parsimony tool in ARB. Note that in previous publications the JTB255-clade according to an outdated taxonomy were falsely classified as belonging to the *Sinobacteraceae*. The taxonomy used in this paper is based on to the SILVA database, release 117 (Pruesse *et al.*, 2007).

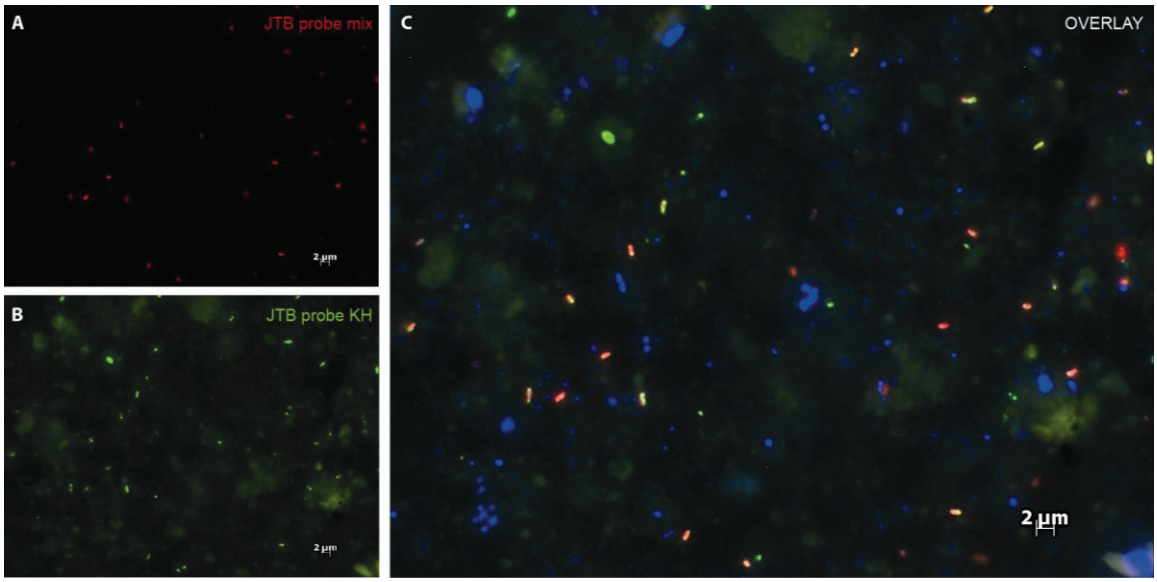


**Supplementary Figure 5** Epifluorescence images of cells of the gammaproteobacterial JTB255-clade in Janssand sediment (April 2014). To confirm identity of cells targeted by our "JTB probe mix" (probes JTB843 + JTB1275 + JTB1270), we performed a double hybridization with another JTB255-specific probe ("probe KH", unpublished, Katy Hoffmann). "JTB probe mix", Alexa594, red fluorescence (a), probe KH, Alexa488, green fluorescence (b), overlay of images (c). In blue: DAPI-stain.

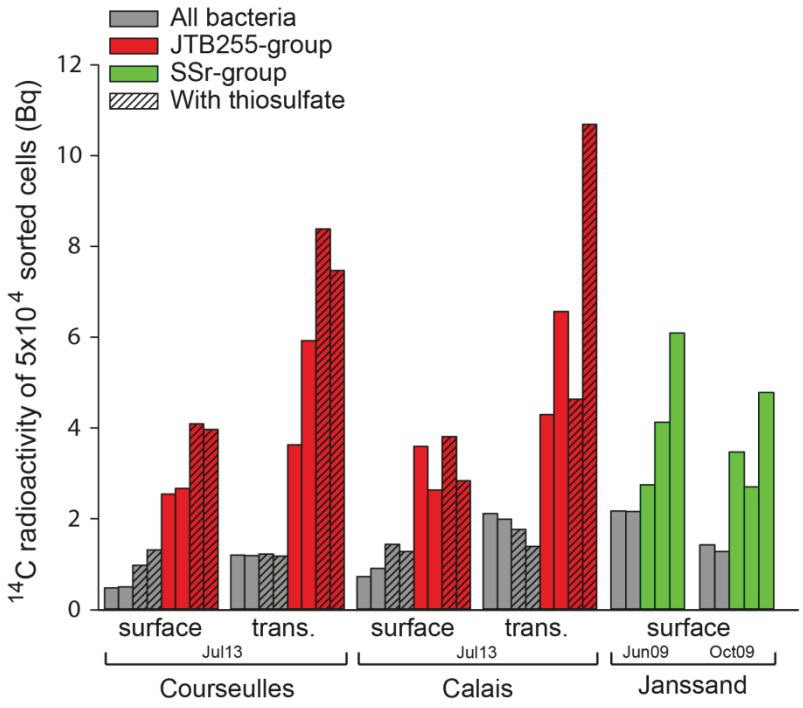


**Supplementary Figure 6** $^{14}$C carbon fixed by gammaproteobacterial clades identified in this study. $^{14}$C carbon fixation quantified in flow-sorted cells of the JTB255- and SSr-clades from the uppermost sediment layer (surface, 0-1 cmbsf) and from the sulfide transition zone (trans.) incubated with $^{14}$C bicarbonate. Batches of 50,000 cells were sorted for quantification. $^{14}$C carbon activity is given in Becquerel (Bq).

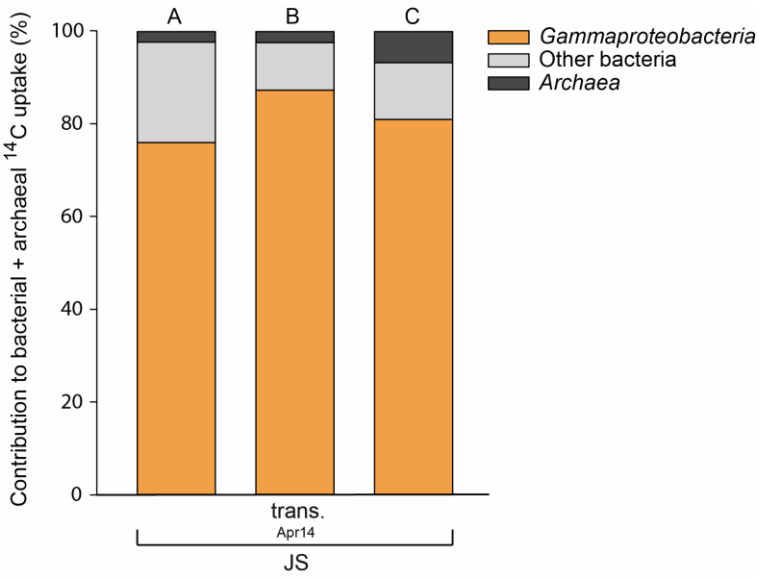


**Supplementary Figure 7** Relative contribution of bacterial and archaeal dark carbon fixation at site Janssand from triplicate incubations.

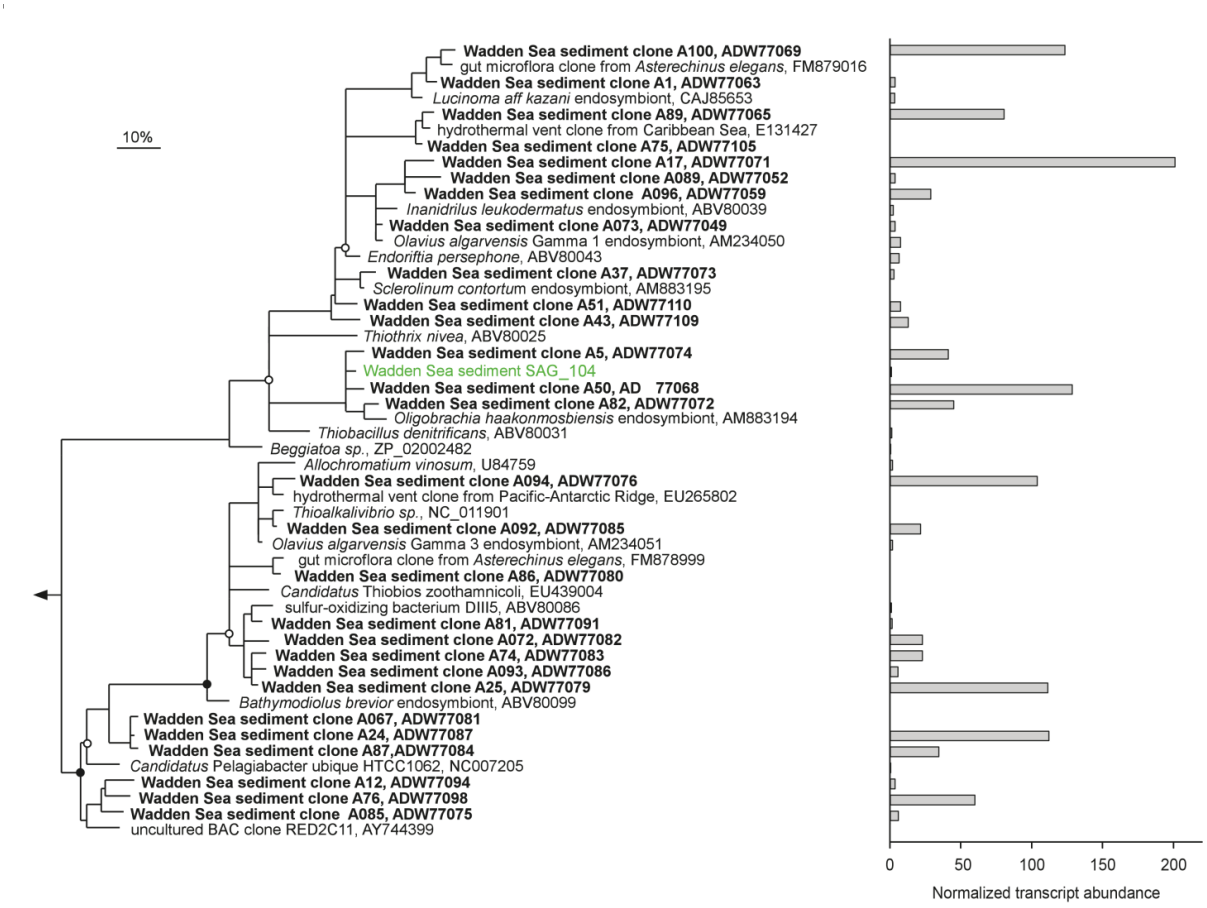


**Supplementary Figure 8** Phylogeny of AprA and abundance of metatranscriptomic reads. Phylogenetic tree based on maximum-likelihood (RAxML) of AprA amino acid sequences from site Janssand (in bold) and normalized abundance of their transcripts. Circles indicate lineages with > 70% (closed) and > 50% (open) RAxML bootstrap support. The bar indicates 10% sequence divergence.

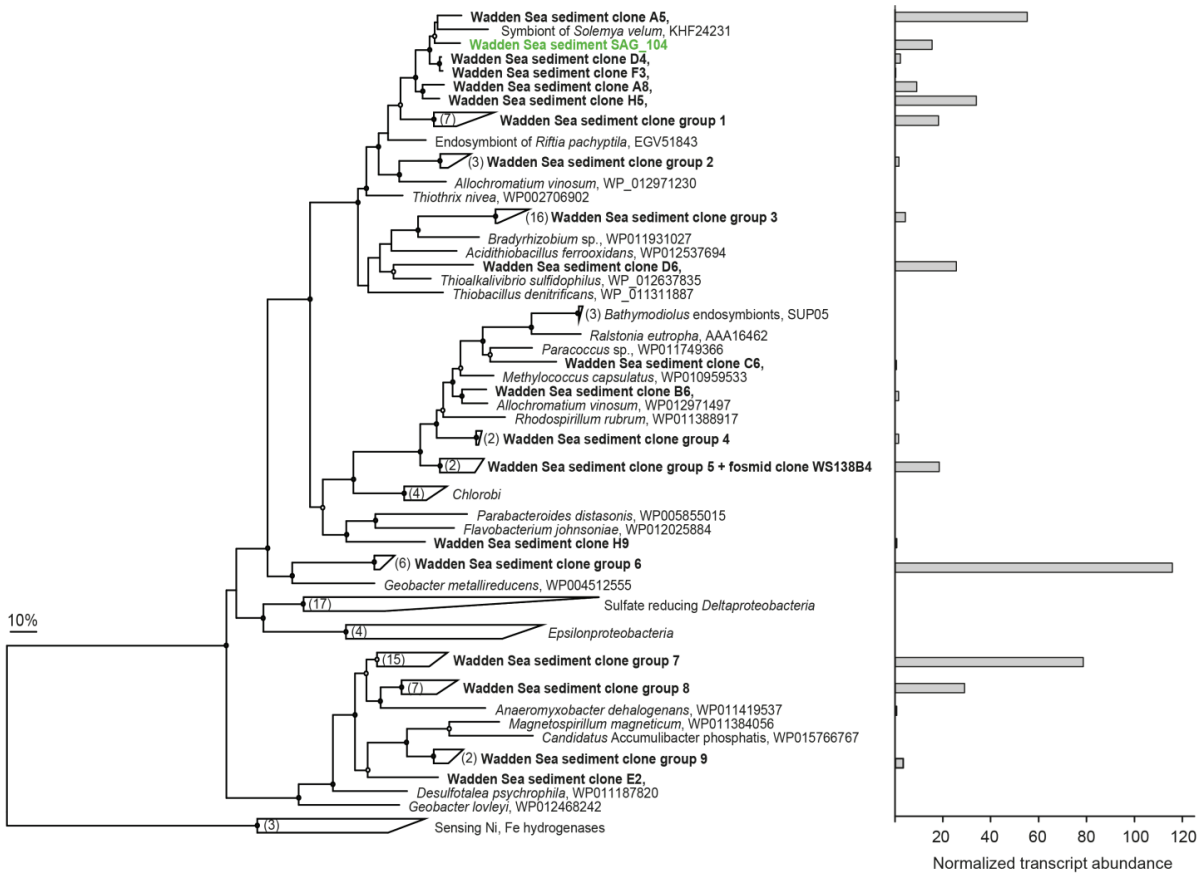


**Supplementary Figure 9** Phylogenetic tree based on maximum-likelihood (RAxML) of Uptake [NiFe]-hydrogenase amino acid sequences from site Janssand (in bold) and normalized abundance of their transcripts. Circles indicate branches with >70% (closed) and >50% (open) RAxML bootstrap support. The bar indicates 10% sequence divergence.

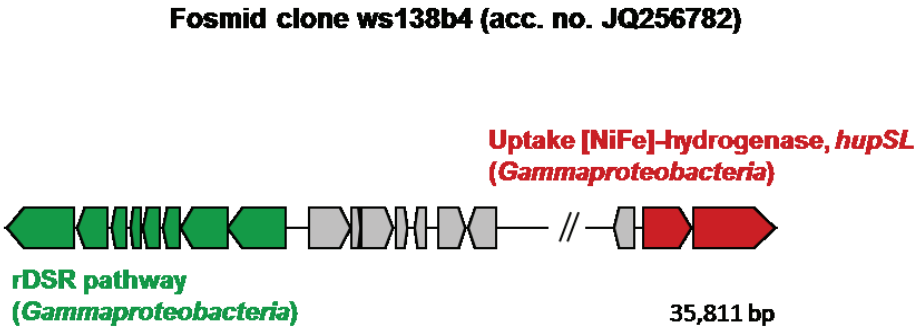


**Supplementary Figure 10** Co-localization of gammaproteobacterial rDsr-operon and *hupSL* genes encoding an uptake [NiFe]-hydrogenase on a metagenomic fosmid clone retrieved from Janssand sediments.

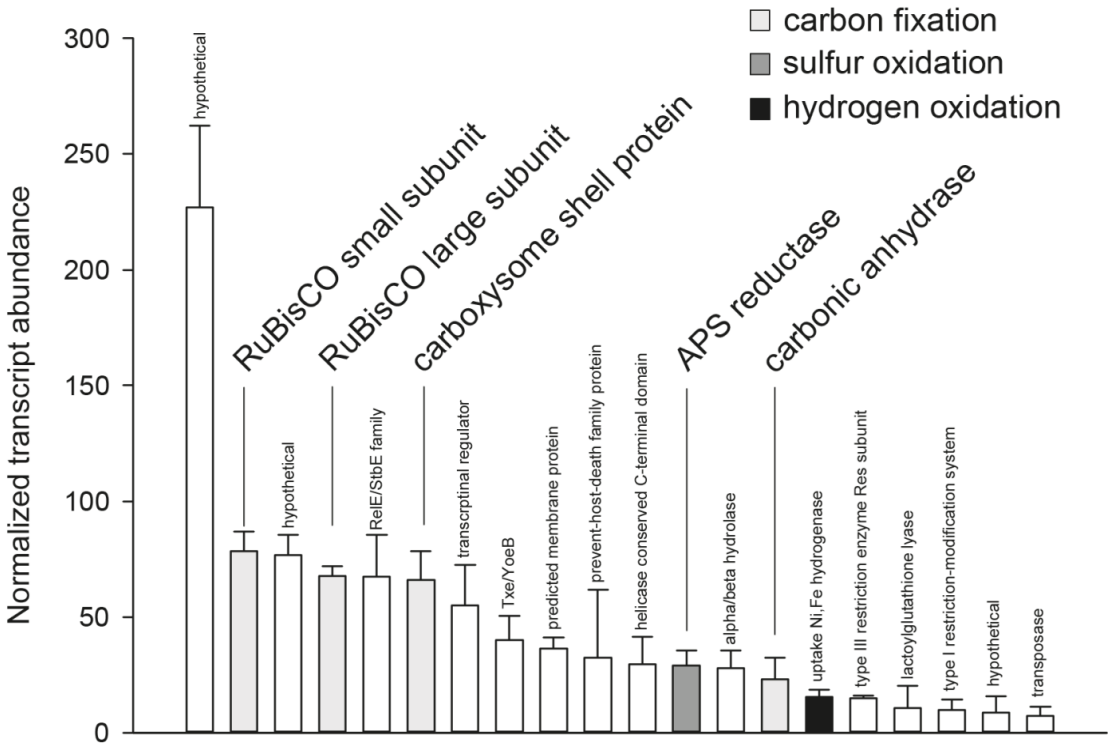


**Supplementary Figure 11** Normalized number of metatranscriptomic reads recruited by genes of a single cell genome affiliating with to the SSr-clade (WSgam209). The top 20 transcribed genes are shown including genes for carbon fixation, sulfur and hydrogen oxidation. IMG gene IDs: 2609851537=hypothetical, 2609851423=RuBisCO small subunit, 2609851536=hypothetical, 2609851422=RuBisCO large subunit, 2609852573=RelE/StbE family, 2609851428=carboxysome shell protein, 2609852572=transcriptional regulator, 2609852972=Txe/YoeB, 2609851841=predicted membrane protein, 2609852973=prevent-host-death family protein, 2609853218=helicase conserved C-terminal domain, 2609853000=APS reductase, 2609851840=alpha/beta hydrolase, 2609851425=carbonic anhydrase, 2609852733=type III restriction enzyme Res subunit, 2609852971=lactoylglutathione lyase, 2609851900=type I restriction-modification system, 2609851882=hypothetical, 2609853066=transposase. Note, that the sequence of the uptake [NiFe]-hydrogenase was recovered by PCR derived from MDA product of WSgam209 and is therefore not included in the IMG/ER of WSgam209 submission.

**Supplementary Table 1** Study sites and performed experiments

| Site/Country | Name code | Sampling position (Lat, Lon) | Sampling time | Surface temperature (°C) | Sulfide in sulfide transition zone (µM) | Sampling depth (cm) (A=surface, B= sulfide transition, C= sulfidic) | Performed experiments |
|---|---|---|---|---|---|---|---|
| **Intertidal sands:** | | | | | | | |
| Königshafen/GER | KH | 55.03432N, 8.42428E | April 2013 | 6 | 0-35*† | A: 0-1, B: 3-4, C: 9-10 | a |
| Janssand/GER | JS | 53.73668N, 7.69893E | October 2009 | - | 0-1000‡ | B: 1-2 | a, b§ |
| Janssand/GER | JS | 53.73668N, 7.69893E | March 2012 | 8 | 0-1000‡ | A: 0-1, B: 7-8, C: 12-13 | c |
| Janssand/GER | JS | 53.73668N, 7.69893E | April 2013 | 13 | 0-1000‡ | A: 0-1, B: 2-3, C: 6-7 | a, d |
| Janssand/GER | JS | 53.73668N, 7.69893E | April 2014 | - | 0-1000‡ | B: 2-3 | b, e |
| Yerseke/NL | YS | 51.45950N, 4.08026E | October 2012 | 15 | - | A: 0-1, B: 5-6, C: 7-8 | a |
| Calais/FRA | CA | 50.99695N, 1.98212E | October 2012 | 16 | - | A: 0-1, B 18-19, C: 22-23 | a |
| Calais/FRA | CA | 50.99695N, 1.98212E | July 2013 | 21 | 7-13 | A: 0-1, B: 2-3, C: 8-9 | b, e |
| Courseulles-sur-Mer/FRA | CS | 49.33955N, 0.46952W | October 2012 | 18 | - | A: 0-1, B: 2-3, C: 6-7 | a |
| Courseulles-sur-Mer/FRA | CS | 49.33955N, 0.46952W | July 2013 | 19 | 0 | A: 0-1, B: 15-16, C: 21-22 | b, e |
| Mont-St-Michel/FRA | MM | 48.61387N, 1.74368W | October 2012 | 18 | - | A: 0-1, B: 5-6, C: 7-8 | a |
| Cairns/AUS | CR | 16.91796S, 145.77678E | December 2013 | 25 | - | B: 1-1.5, C: 6.5-7 | a |
| Carlo Point/AUS | CP | 25.89598S, 153.05691E | December 2013 | 26 | - | A: 0-0.5, C: 6.5-7 | a |
| Nudgee Beach/AUS | NB | 27.34243S, 153.10273E | December 2013 | 26 | - | A: 0-0.5, B: 4.5-5, C: 8.5-9 | a |
| Dunsborough/AUS | DB | 33.61745S, 115.11572E | December 2014 | 25 | - | A: 0-1, B: 1-3, C: 6-7 | a |
| **Sublittoral sands¶:** | | | | | | | |
| Noah_A/GER | NS1 | 53.98767N, 6.23566E | March 2014 | - | - | A: 0-2, B: 2-5 | a |
| Noah_B/GER | NS2 | 53.98983N, 6.88150E | March 2014 | 7 | - | A: 0-2, B: 2-5 | a |
| CCPδ/GER | NS3 | 54.16883N, 7.99150E | March 2014 | 6 | - | A: 0-2, B: 2-5 | a |

**-** no information available; a 16S rRNA gene sequencing; b $^{14}$C DIC incubations; c hydrogenase gene library; d metatranscriptomics; e CARD-FISH

*(de Beer *et al.*, 2005); †(Thiermann *et al.*, 1996); ‡(Jansen *et al.*, 2009); §(Lenk *et al.*, 2011); ¶water depth: Noah_A, 29 m; Noah_B, 29 m; CCPδ, 20 m

**Supplementary Table 2** Oligonucleotide probes used in this study

| Probe | Specificity | Sequence (5'-3') | FA* (%) | Reference |
|---|---|---|---|---|
| EUB I-III† | *Bacteria* | GCWGCCWCCCGTAGGWGT | 35 | (Amann *et al.*, 1990; Daims *et al.*, 1999) |
| ARCH915† | *Archaea* | GTGCTCCCCCGCCAATTCCT | 35 | (Stahl and Amann, 1991) |
| NON338† | Nonsense probe | ACTCCTACGGGAGGCAGC | 35 | (Wallner *et al.*, 1993) |
| ROS537† | *Roseobacter*-clade bacteria | CAACGCTAACCCCCTCC | 35 | (Eilers *et al.*, 2001) |
| CF319a† | *Cytophaga/ Flavobacteria* | TGGTCCGTRTCTCAGTAC | 35 | (Manz *et al.*, 1996) |
| GAM42a†‡ | *Gamma-proteobacteria* | GCCTTCCCACATCGTTT | 35 | (Manz *et al.*, 1992) |
| BET42a§ | *Betaproteobacteria* | GCCTTCCCACTTCGTTT | 35 | (Manz *et al.*, 1992) |
| GAM209†‡ | SSr-group | CTACTAGTGCCAGGTCCG | 25 | (Lenk *et al.*, 2011) |
| GAM209c§ | | CTAATAGTGCCAGGTCCG | 25 | (Lenk *et al.*, 2011) |
| GAM1030† | *Acidiferrobacter*-related | CCTGTCAACCAGTTCCCG | 25 | (Lenk *et al.*, 2011) |
| GAM1030c§ | | CCTGTCAATCAGTTCCCG | 25 | (Lenk *et al.*, 2011) |
| GAM446† | *Acidiferrobacter*-related | ACCCGCAACTGTTTCCTC | 25 | (Lenk *et al.*, 2011) |
| GAM446c1§ | | ACCCTAAGCTTTTCCTC | 25 | (Lenk *et al.*, 2011) |
| GAM446c2§ | | ACCCTGAGCTTTTCTTC | 25 | (Lenk *et al.*, 2011) |
| GAM446c3§ | | ACCTTAAGCTTTTCTTC | 25 | (Lenk *et al.*, 2011) |
| GAM446c4§ | | ACCAAAAGCTTTTCTTC | 25 | (Lenk *et al.*, 2011) |
| GAM446c5§ | | ACCTTRAGCTTTTCCTC | 25 | (Lenk *et al.*, 2011) |
| GAM446h1§ | | GGTCGCGGGATATTA | 25 | (Lenk *et al.*, 2011) |
| GAM446h2§ | | CCYACTGAAAGTGCTT | 25 | (Lenk *et al.*, 2011) |
| JTB1270† | JTB255-group | GAGCTTTAAGGGATTAGCGCACCA | 40 | This study |
| JTB1270h¶ | | TTGCTGGTTGGCAACCCTCTGTAT | 40 | This study |
| JTB843†‡ | JTB255-group | TGCGACACCGAGGGACAR | 10 | This study |
| JTB843c1§ | | TTCGACACCGAGGGACAR | 10 | This study |
| JTB843c2§ | | TGCGACACCGAGGGGCAR | 10 | This study |
| JTB843c3§ | | TGCGACACCGAAAGACAR | 10 | This study |
| JTB843c4§ | | GGCGACACCGAGGGGCAR | 10 | This study |
| JTB843c5§ | | TGCGACACCGAAGGACTR | 10 | This study |
| JTB843us¶ | | TCCCCCAACATCTAGTTCTCA | 10 | This study |
| JTB843ds¶ | | CGGAGAACTTAACGCGTTAGC | 10 | This study |
| JTB1275†‡ | JTB255-group | AGCTTTAAGGGATTAGCG | 10 | This study |
| JTB1275c1§ | | AGCTTTAAGGGATTAGCG | 10 | This study |
| JTB1275c2§ | | AGCTTTAAGGGATTAGCA | 10 | This study |
| JTB1275c3§ | | AGCTTTAAGGGATTAGCT | 10 | This study |
| JTB1275c4§ | | CGCTTTAAGGGATTAGCT | 10 | This study |
| JTB1275us¶ | | TTGGCAACCCTCTGTACTCGC | 10 | This study |
| JTB1275ds¶ | | ACTCCATACCGGACTACGACG | 10 | This study |

* Formamide concentration (v/v) in hybridization buffer

† Probe labeled with horseradish peroxidase (HRP)

‡ Probe was applied with competitor

§ Unlabeled competitor oligonucleotide

¶ Unlabeled helper oligonucleotide

**Supplementary Table 3** General statistics of assemblies of a single cell genome (recovered from site Janssand) affiliating with the SSr-clade (WSgam209) and a metagenomic bin affiliating with the *Acidiferrobacter*-clade (recovered from a deep-sea hydrothermal chimney)

| | WSgam209 | | Uncultured *Acidiferrobacter* | |
|---|---|---|---|---|
| | # | % of total | # | % of total |
| DNA, total number of bases | 1,922,127 | 100 | 2,041,809 | 100 |
| DNA coding number of bases | 1,660,663 | 86.4 | 1,933,109 | 94.7 |
| G+C content | | 43.8 | | 68.9 |
| DNA scaffolds | 311 | | 66 | |
| Genes total number | 2,008 | 100 | 2,092 | 100 |
| Protein coding genes | 1,989 | 99.1 | 2,059 | 98.5 |
| Protein coding genes with function prediction | 1,488 | 74 | 1,748 | 83.6 |
| Protein coding genes without function prediction | 501 | 25 | 311 | 14.9 |
| RNA genes | 19 | 1 | 33 | 1.6 |
| tRNA genes | 11 | 0.5 | 27 | 1.3 |
| estimated completeness | 20%*/22%† | | | 89%‡/71.9%§ |

* expressed as % of tRNAs is next cultured relative *Leucothrix mucor* (Grabovich *et al.*, 1999).

† expressed as % of universal single copy genes in SSr_104 (28) out of 40 (Ciccarelli *et al.*, 2006; Creevey *et al.*, 2011).

‡ CheckM (Matsen *et al.*, 2010; Hyatt *et al.*, 2012; Parks *et al.*, 2015)

§ Six Frame PFAM embedded in Metawatt (Strous *et al.*, 2012; Campbell *et al.*, 2013)

**Supplementary Table 4** Overview of metatranscriptomic reads mapped on reference databases

| Reference database | No. of unique mapped cDNA reads | | |
|---|---|---|---|
| | Replicate A (29029446 reads) | Replicate B (29726577 reads) | Replicate C (33590664 reads) |
| *aprA* (220 sequences) | 603 | 582 | 669 |
| *dsrAB* (133 sequences) | 1927 | 1972 | 2078 |
| *soxB* (166 sequences) | 226 | 202 | 293 |
| Uptake Ni, Fe hydrogenase (203 sequences) | 658 | 532 | 685 |
| cbbm/cbbl (250 sequences) | 196 | 190 | 260 |
| *aclAB* (269 sequences) | 0 | 6 | 2 |
| *amoA* (bacteria) (6999 sequences) | 2 | 0 | 1 |
| *amoA* (archaea) (8544 sequences) | 3 | 5 | 3 |

**Supplementary Table 5** Selected IMG gene IDs for WSgam209 and the *Acidiferrobacter* metagenomic bin

| IMG/ER Gene ID | Gene product name (IMG/ER) | Type of genome: organism (origin) | Sequence length (aa) | COG ID | COG name | Pfam ID |
|---|---|---|---|---|---|---|
| 2609851422 | Ribulose 1,5-bisphosphate carboxylase, large subunit, or a RuBisCO-like protein | single cell genome SSr-group: WSgam209 (Janssand sediment) | 471 | COG1850 | Ribulose 1,5-bisphosphate carboxylase, large subunit, or a RuBisCO-like protein | pfam02788 |
| 2609851423 | Ribulose bisphosphate carboxylase small subunit | single cell genome SSr-group: WSgam209 (Janssand sediment) | 113 | COG4451 | Ribulose bisphosphate carboxylase small subunit | pfam00101 |
| 2609851424 | Carboxysome shell peptide mid-region | single cell genome SSr-group: WSgam209 (Janssand sediment) | 791 | | | pfam12288 |
| 2609851425 | carboxysome shell carbonic anhydrase | single cell genome SSr-group: WSgam209 (Janssand sediment) | 514 | | | pfam08936 |
| 2609851426 | carboxysome peptide A | single cell genome SSr-group: WSgam209 (Janssand sediment) | 84 | COG4576 | Carboxysome shell and ethanolamine utilization microcompartment protein CcmK/EutM | pfam03319 |
| 2609851427 | carboxysome peptide B | single cell genome SSr-group: WSgam209 (Janssand sediment) | 84 | COG4576 | Carboxysome shell and ethanolamine utilization microcompartment protein CcmK/EutM | pfam03319 |
| 2609851482 | cytochrome c oxidase, subunit I | single cell genome SSr-group: WSgam209 (Janssand sediment) | 531 | COG0843 | Heme/copper-type cytochrome/quinol oxidase, subunit 1 | pfam00115 |
| 2609851483 | cytochrome c oxidase, subunit II | single cell genome SSr-group: WSgam209 (Janssand sediment) | 377 | COG1622 | Heme/copper-type cytochrome/quinol oxidase, subunit 2 | pfam13442 |
| 2609851866 | hydrogenase expression/formation protein HypE | single cell genome SSr-group: WSgam209 (Janssand sediment) | 333 | COG0309 | Hydrogenase maturation factor | pfam00586 |
| 2609851868 | hydrogenase expression/formation protein HypD | single cell genome SSr-group: WSgam209 (Janssand sediment) | 364 | COG0409 | Hydrogenase maturation factor | pfam01924 |
| 2609851869 | hydrogenase accessory protein HypB | single cell genome SSr-group: WSgam209 (Janssand sediment) | 278 | COG0378 | Ni+binding GTPase involved in regulation of expression and maturation of urease and hydrogenase | pfam02492 |
| 2609851881 | hydrogenase (Ni,Fe) small | single cell genome SSr-group: | 271 | | | pfam01058 |

| | | | | | | |
|---|---|---|---|---|---|---|
| | subunit (hydA) | WSgam209 (Janssand sediment) | | | | |
| 2609852594 | Ni,Fe, NiFeSe hydrogenase small subunit C-terminal | single cell genome SSr-group: WSgam209 (Janssand sediment) | 144 | | | pfam14720 |
| 2609852596 | Ni,Fe-hydrogenase 2 integral membrane subunit HybB | single cell genome SSr-group: WSgam209 (Janssand sediment) | 377 | COG5557 | Ni/Fe-hydrogenase 2 integral membrane subunit HybB | pfam03916 |
| 2609852597 | Ni,Fe-hydrogenase I large subunit | single cell genome SSr-group: WSgam209 (Janssand sediment) | 575 | COG0374 | Ni,Fe-hydrogenase I large subunit | pfam00374 |
| 2609852598 | hydrogenase expression/formation protein | single cell genome SSr-group: WSgam209 (Janssand sediment) | 199 | COG0680 | Ni,Fe-hydrogenase maturation factor | pfam01750 |
| 2609852649 | Carbonic anhydrase | single cell genome SSr-group: WSgam209 (Janssand sediment) | 202 | COG0288 | Carbonic anhydrase | pfam00484 |
| 2609852672 | hydrogenase maturation protease | single cell genome SSr-group: WSgam209 (Janssand sediment) | 173 | COG0680 | Ni,Fe-hydrogenase maturation factor | |
| 2609853000 | dissimilatory adenylylsulfate reductase alpha subunit precursor (EC 1.8.99.2) | single cell genome SSr-group: WSgam209 (Janssand sediment) | 524 | COG1053 | Succinate dehydrogenase/fumarate reductase, flavoprotein subunit | pfam00890 |
| 2616652017 | Sulfite oxidase subunit A (SoeA) | metagenomic bin Acidiferrobacter_a7 (black smoker chimney, Manus Basin) | 943 | COG0243 | Anaerobic selenocysteine-containing dehydrogenase | pfam04879 |
| 2616652018 | Sulfite oxidase subunit A (SoeB) | metagenomic bin Acidiferrobacter_a7 (black smoker chimney, Manus Basin) | 212 | COG0437 | Fe-S-cluster-containing dehydrogenase component | pfam13247 |
| 2616652019 | Sulfite oxidase subunit A (SoeC) | metagenomic bin Acidiferrobacter_a7 (black smoker chimney, Manus Basin) | 313 | COG3302 | DMSO reductase anchor subunit | pfam04976 |
| 2616652250 | ribulose 1,5-bisphosphate carboxylase large subunit (EC 4.1.1.39) | metagenomic bin Acidiferrobacter_a7 (black smoker chimney, Manus Basin) | 472 | COG1850 | Ribulose 1,5-bisphosphate carboxylase, large subunit, or a RuBisCO-like protein | pfam02788 |
| 2616652251 | ribulose 1,5-bisphosphate carboxylase small subunit (EC 4.1.1.39) | metagenomic bin Acidiferrobacter_a7 (black smoker chimney, Manus Basin) | 121 | COG4451 | Ribulose bisphosphate carboxylase small subunit | pfam00101 |
| 2616652516 | thiosulfate oxidation protein SoxX | metagenomic bin Acidiferrobacter_a7 (black smoker chimney, Manus Basin) | 122 | | | pfam00034 |
| 2616652517 | thiosulfate oxidation protein SoxY | metagenomic bin Acidiferrobacter_a7 (black smoker chimney, Manus Basin) | 155 | COG5501 | Predicted secreted protein | pfam13501 |

| | | | | | | |
|---|---|---|---|---|---|---|
| 2616652518 | thiosulfate oxidation protein SoxZ | metagenomic bin Acidiferrobacter_a7 (black smoker chimney, Manus Basin) | 105 | | | pfam08770 |
| 2616652519 | thiosulfate oxidation protein SoxA | metagenomic bin Acidiferrobacter_a7 (black smoker chimney, Manus Basin) | 278 | | | |
| 2616652520 | thiosulfate oxidation protein SoxB | metagenomic bin Acidiferrobacter_a7 (black smoker chimney, Manus Basin) | 579 | COG0737 | 2',3'-cyclic-nucleotide 2'-phosphodiesterase/5'- or 3'-nucleotidase, 5'-nucleotidase family | pfam02872 |

**Supplementary Table 6** Relative cell abundance at site Courseulles-sur-Mer (CS), Calais (CA) and Janssand (JS)

| | | Relative Abundance (%) | | | | |
|---|---|---|---|---|---|---|
| | | CS | | CA | | JS May 2014 |
| Probes | Specificity | Surface | Trans. | Surface | Trans. | Trans. |
| EUBI-III | *Bacteria* | 95.3 | 92.1 | 94.7 | 90.9 | 94.4 |
| ARCH915 | *Archaea* | 0.9 | 0.9 | 1.3 | 1.2 | 1.2 |
| GAM42a | *Gammaproteobacteria* | 13.5 | 14.6 | 15.1 | 15.3 | 16.3 |
| JTB1270 | JTB255-group | 6.2 | 5.1 | 5.1 | 3.4 | 5.3 |
| GAM209 | SSr-group | 0.6 | 1.1 | 0.9 | 0.5 | 1.0 |
| GAM1030/ GAM446 | *Acidiferrobacter*-related | 2.1 | 2.1 | 1.7 | 0.9 | 3.1 |

Note: GAM42a + JTB1270 target most of the *Gammaproteobacteria* (Siyambalapitiya and Blackall, 2005)

**Supplementary Table 7** Phylogenetic affiliation of fosmid endsequences recovered from a metagenomic fosmid library from shallow subsurface sediments (490 cm sediment depth), Janssand April 2004

| | No. of reads | % of total archaeal and bacterial reads |
|---|---|---|
| *Archaea* | 60 | 1 |
| *Bacteria* | 3992 | |
| Bacterial and archaeal reads | 4052 | |
| *Gammaproteobacteria* | 979 | 24 |
| *Planctomycetes* | 505 | 12 |
| *Alphaproteobacteria* | 303 | 7 |
| *Deltaproteobacteria* | 301 | 7 |
| *Actinobacteria* | 289 | 7 |
| *Firmicutes* | 173 | 4 |
| *Betaproteobacteria* | 112 | 3 |
| *Bacteroidetes* | 95 | 2 |
| *Cyanobacteria* | 71 | 2 |
| *Chloroflexi* | 72 | 2 |
| *Acidobacteria* | 16 | 0.4 |
| Other *Bacteria* | 1076 | 26 |
| unassigned reads | 5118 | |
| **all reads** | **9170** | |

**Supplementary Table 8** Cell-specific carbon fixation rates and relative abundance of cells labeled by microautoradiography

| Sampling site | Population | Population-specific $CO_2$ fixation rate (fg C cell$^{-1}$ d$^{-1}$) | MAR positive cells (%) | Cell-specific $CO_2$ fixation rate (fg C cell$^{-1}$ d$^{-1}$) |
|---|---|---|---|---|
| Courseulles | All bacteria | 0.3 | - | - |
| surface | *Gammaproteobacteria* | 1.5 | 46 | 3.2 |
| Jul13 | JTB255-group | 1.1 | - | - |
| Courseulles | All bacteria | 0.4 | - | - |
| transition | *Gammaproteobacteria* | 2.0 | 49 | 4.0 |
| Jul13 | JTB255-group | 2.1 | - | - |
| Calais | All bacteria | 0.4 | - | - |
| surface | *Gammaproteobacteria* | 1.6 | - | - |
| Jul13 | JTB255-group | 1.1 | - | - |
| Calais | All bacteria | 0.6 | - | - |
| transition | *Gammaproteobacteria* | 3.0 | 50 | 5.9 |
| Jul13 | JTB255-group | 2.2 | - | - |
| Janssand | All bacteria | 0.3 | - | - |
| transition | *Gammaproteobacteria* | 1.1 | - | - |
| Apr14 | JTB255-group | 1.5 | - | - |
| | *Acidiferrobacter*-related | 3.5 | - | - |
| | SSr-group | 2.5 | - | - |
| | *Archaea* | 0.9 | - | - |
| Janssand | All bacteria | 0.9 | 22 (Lenk *et al.*, 2011) | 4.2 |
| surface | *Gammaproteobacteria* | 2.4 | 40 (Lenk *et al.*, 2011) | 6.4 |
| Jun09 | SSr-group | 1.9 | 25 (Lenk *et al.*, 2011) | 7.5 |
| Janssand | All bacteria | 0.6 | 18 (Lenk *et al.*, 2011) | 3.3 |
| surface | *Gammaproteobacteria* | 1.9 | 43 (Lenk *et al.*, 2011) | 4.4 |
| Oct09 | SSr-group | 1.6 | 25 (Lenk *et al.*, 2011) | 6.4 |

- not determined

Amann RI, Binder BJ, Olson RJ, Chisholm SW, Devereux R, Stahl DA. (1990). Combination of 16S rRNA-targeted oligonucleotide probes with flow cytometry for analyzing mixed microbial populations. *Appl Environ Microbiol* **56**:1919–1925.

Beer D de, Wenzhöfer F, Ferdelman TG, Boehme SE, Huettel M, van Beusekom JEE, *et al.* (2005). Transport and mineralization rates in North Sea sandy intertidal sediments, Sylt-Rømø Basin, Wadden Sea. *Limnol Oceanogr* **50**:113–127.

Campbell JH, O'Donoghue P, Campbell AG, Schwientek P, Sczyrba A, Woyke T, *et al.* (2013). UGA is an additional glycine codon in uncultured SR1 bacteria from the human microbiota. *Proc Natl Acad Sci* **110**:5540–5545.

Ciccarelli FD, Doerks T, Mering C von, Creevey CJ, Snel B, Bork P. (2006). Toward automatic reconstruction of a highly resolved tree of life. *Science* **311**:1283–1287.

Creevey CJ, Doerks T, Fitzpatrick DA, Raes J, Bork P. (2011). Universally distributed single-copy genes indicate a constant rate of horizontal transfer. *PLoS ONE* **6**:e22099.

Daims H, Brühl A, Amann R, Schleifer KH, Wagner M. (1999). The domain-specific probe EUB338 is insufficient for the detection of all bacteria: development and evaluation of a more comprehensive probe set. *Syst Appl Microbiol* **22**:434–444.

Eilers H, Pernthaler J, Peplies J, Glöckner FO, Gerdts G, Amann R. (2001). Isolation of novel pelagic bacteria from the German Bight and their seasonal contributions to surface picoplankton. *Appl Environ Microbiol* **67**:5134–5142.

Grabovich MY, Muntyan MS, Lebedeva VY, Ustiyan VS, Dubinina GA. (1999). Lithoheterotrophic growth and electron transfer chain components of the filamentous gliding bacterium *Leucothrix mucor* DSM 2157 during oxidation of sulfur compounds. *FEMS Microbiol Lett* **178**:155–161.

Hyatt D, LoCascio PF, Hauser LJ, Uberbacher EC. (2012). Gene and translation initiation site prediction in metagenomic sequences. *Bioinformatics* **28**:2223–2230.

Jansen S, Walpersdorf E, Werner U, Billerbeck M, Böttcher ME, Beer D de. (2009). Functioning of intertidal flats inferred from temporal and spatial dynamics of $O_2$, $H_2S$ and pH in their surface sediment. *Ocean Dyn* **59**:317–332.

Lenk S, Arnds J, Zerjatke K, Musat N, Amann R, Mußmann M. (2011). Novel groups of *Gammaproteobacteria* catalyse sulfur oxidation and carbon fixation in a coastal, intertidal sediment. *Environ Microbiol* **13**:758–774.

Manz W, Amann R, Ludwig W, Vancanneyt M, Schleifer K-H. (1996). Application of a suite of 16S rRNA-specific oligonucleotide probes designed to investigate bacteria of the phylum cytophaga-flavobacter-bacteroides in the natural environment. *Microbiology* **142**:1097–1106.

Manz W, Amann R, Ludwig W, Wagner M, Schleifer K. (1992). Phylogenetic oligodeoxynucleotide probes for the major subclasses of proteobacteria - problems and solutions. *Syst Appl Microbiol* **15**:593–600.

Matsen FA, Kodner RB, Armbrust EV. (2010). pplacer: linear time maximum-likelihood and Bayesian phylogenetic placement of sequences onto a fixed reference tree. *BMC Bioinformatics* **11**:538.

Parks DH, Imelfort M, Skennerton CT, Hugenholtz P, Tyson GW. (2015). CheckM: assessing the quality of microbial genomes recovered from isolates, single cells, and metagenomes. *Genome Res* **25**:1043–1055.

Siyambalapitiya N, Blackall LL. (2005). Discrepancies in the widely applied GAM42a fluorescence *in situ* hybridisation probe for *Gammaproteobacteria*. *FEMS Microbiol Lett* **242**:367–373.

Stahl DA, Amann RI. (1991). Development and application of nucleic acid probes. 205-248. In E. Stackebrandt and M. Goodfellow (ed.), Nucleic acid techniques in bacterial systematics. John Wiley & Sons Ltd., Chichester, England.

Strous M, Kraft B, Bisdorf R, Tegetmeyer HE. (2012). The binning of metagenomic contigs for microbial physiology of mixed cultures. *Front Microbiol* **3**. doi:10.3389/fmicb.2012.00410.

Thiermann F, Niemeyer A-S, Giere O. (1996). Variations in the sulfide regime and the distribution of macrofauna in an intertidal flat in the North Sea. *Helgoländer Meeresunters* **50**:87–104.

Wallner G, Amann R, Beisker W. (1993). Optimizing fluorescent *in situ* hybridization with rRNA-targeted oligonucleotide probes for flow cytometric identification of microorganisms. *Cytometry* **14**:136–143.

# Metagenomes and metatranscriptomes suggest hydrogen consumption by *Desulfobacteraceae*, *Flavobacteriaceae* and *Gammaproteobacteria* in a marine sediment

Stefan Dyksma[a], Petra Pjevac[b], Kin Ovanesov[c], Hanno Teeling[a] and Marc Mussmann[a,b]*

[a] Department of Molecular Ecology, Max Planck Institute for Marine Microbiology, Bremen, Germany

[b] University of Vienna, Department of Microbiology and Ecosystem Science, Division of Microbial Ecology, Vienna, Austria

[c] Department of Microbiology, Max Planck Institute for Marine Microbiology, Bremen, Germany

*To whom correspondence should be addressed: University of Vienna, Department of Microbiology and Ecosystem Science, Division of Microbial Ecology, A-1090 Vienna, Austria, Tel +43 1 4277 54207, mussmann@microbial-ecology.net

Running title: Hydrogenases in a marine sediment

Keywords: sulfate-reducing bacteria, single cell genomes, Sva0081-MBG, JTB255-MBG, molecular hydrogen, Eudoraea

**Abstract**

Molecular hydrogen ($H_2$) is the key intermediate in the anaerobic degradation of organic matter, as it controls the thermodynamic balance between fermentation and terminal respiration. Marine sediments are global hot spots of anaerobic carbon mineralization and sequestration, and thus $H_2$ cycling, but the involved $H_2$ases and the corresponding microorganisms are unknown. We combined metagenomics, single-cell (meta)genomics and metatranscriptomics to investigate the diversity and expression of $H_2$ase genes in a marine sediment that was shown to consume $H_2$ under micro-oxic and anoxic conditions. Metagenomic analysis revealed exceptionally high frequencies of $H_2$ase reads, the majority of which belonged to $H_2$-evolving [FeFe]- and to group 1 uptake and group 3 bidirectional [NiFe]-$H_2$ases. Corresponding transcriptome reads suggested that $O_2$-tolerant 1d uptake [NiFe]-$H_2$ases were relatively more abundant in the uppermost sediment layer (0-1 cm), while $O_2$-sensitive 1b uptake [NiFe]-$H_2$ases were relatively more abundant in the deeper layers (2-8 cm). Single-cell genomics allowed us to identify the organisms encoding highly expressed $H_2$ases. In oxic sediments, the JTB255-marine benthic group (MBG)/*Gammaproteobacteria* and *Flavobacteriaceae/Bacteroidetes* were the most likely $H_2$ consumers, whereas sulfate-reducing *Desulfobacteraceae/Deltaproteobacteria* likely oxidized $H_2$ in deeper, anoxic sediments. Notably, the uncultured, sulfate-reducing Sva0081-MBG consistently accounted for around half of transcripts of detected uptake [NiFe]-$H_2$ases from sulfate-reducing microorganisms. These distinct bacterial groups are ubiquitous and abundant in marine sediments and likely scavenge $H_2$ under distinct oxygen regimes. In particular, sulfate-reducing *Desulfobacteraceae* seem to play a central role in maintaining the anaerobic food chain by removing $H_2$.

## Introduction

Coastal sediments are hot spots of organic matter mineralization in the oceans (Hedges and Keil, 1995). Since oxygen is rapidly consumed in organic-rich marine sediments, a large fraction of organic matter is degraded anaerobically, e.g. via fermentation and sulfate respiration (Jørgensen, 1982). When oxygen is depleted, fermenting bacteria release organic acids, alcohols and molecular hydrogen ($H_2$) as main end products that are in turn consumed by different anaerobic terminal respiration processes. In this anaerobic food chain, $H_2$ is central for energy transfer and thermodynamic control of "virtually every step of organic matter breakdown" (Hoehler *et al,* 1998). Accumulation of $H_2$ inhibits fermentative reactions, hence scavenging of $H_2$ by $H_2$-consuming bacteria is essential to make fermentation thermodynamically possible (Monetti and Scranton, 1992). Therefore, the production and consumption of $H_2$ are tightly coupled so that $H_2$ is generally short-lived and present only in nanomolar concentrations in marine sediments (Novelli *et al*, 1987; Novelli *et al*, 1988; Michener *et al,* 1988).

Diverse *Bacteria* and *Archaea* consume $H_2$, e.g. during sulfate reduction, acetogenesis, methanogenesis and anoxygenic phototrophy (Schwartz *et al,* 2013). In anoxic aquatic sediments and water-logged soils sulfate-reducing microorganisms (SRM) and methanogenic *Archaea* compete for $H_2$ in the terminal steps of the anaerobic food chain (Winfrey and Zeikus, 1977; Oremland and Taylor, 1978; Oremland and Polcin, 1982). Since SRM have a higher affinity to $H_2$, they can successfully outcompete methanogens even at low sulfate concentrations (Pester *et al,* 2012). Thus, sulfate respiration is the major $H_2$ consuming process in marine surface sediments (Oremland and Taylor, 1978), whereas methanogenesis is prevalent in the sulfate-depleted subsurface sediments (D'Hondt *et al,* 2002).

Hydrogenases ($H_2$ases) are the key enzymes of $H_2$ cycling. They catalyze the reversible cleavage of $H_2$ to protons and electrons ($H_2 \leftrightarrow 2H^+ + 2e^-$). Hydrogenases are classified according to the metal cofactor at the catalytic site as [NiFe]-, [FeFe]- and [Fe]-$H_2$ases. These hydrogenase-types have evolved independently (Schwartz *et al,* 2013). [NiFe]-$H_2$ases represent the most widespread type and comprise four subgroups that catalyze $H_2$ oxidation and/or $H_2$ evolution. The phylogeny of group 1 [NiFe]-$H_2$ases has been strongly affected by diversification and adaptation to specific environmental conditions (Pandelia *et al,* 2012; Greening *et al,* 2015). Distinct phylogenetic clades appear to correspond to functionally homologous groups according to e.g. $O_2$ tolerance and the preferred terminal electron acceptor (Vignais *et al,* 2001; Vignais and Billoud, 2007; Pandelia *et al,* 2012; Greening *et al,* 2015). Few $H_2$ases, such as group 1d [NiFe]-$H_2$ases, can function at $O_2$-saturation, whereas most tolerate only 1-2% $O_2$ and others are inactivated by even trace amounts of $O_2$ (Goris *et al,* 2011; Vargas *et al,* 2011; Pandelia *et al,* 2012; Fritsch *et al,* 2013). In a recent survey,

Greening *et al.* (2015) found that $H_2$ases are widespread and abundant in metagenomes from diverse ecosystems including soil, gut, freshwater and seawater habitats. Notably, group 1 [NiFe]-$H_2$ases were proposed to play a major role in catalyzing $H_2$ consumption in many ecosystems.

Many molecular studies used 16S rRNA or dissimilatory sulfite reductase (DsrAB) genes as molecular markers to identify deltaproteobacterial SRM, in particular *Desulfobacterales* as the dominant SRM in diverse marine sediments (Rabus *et al,* 2015). Although $H_2$ is a key substrate for SRM, those responsible for $H_2$-dependent sulfate respiration are still unidentified. Besides SRM, other functional groups may consume $H_2$. For instance, primarily thioautotrophic *Gammaproteobacteria* from hydrothermal vent systems can also oxidize $H_2$ with oxygen or nitrate (Petersen *et al,* 2011; Anantharaman *et al,* 2013; Hansen and Perner, 2015). Moreover, (meta)genomes from coastal and estuarine sediments recently identified the potential for $H_2$ oxidation in *Gammaproteobacteria* (Baker *et al,* 2015; Dyksma *et al,* 2016). Recently, Hamann and colleagues (2016) reported an anaerobic consortium of a $H_2$-releasing nanoflagellate and $H_2$-consuming *Epsilonproteobacteria* isolated from a tidal sediment in the German Wadden Sea.

In our study, we revisited this tidal sediment and investigated the overall diversity and expression of $H_2$ase genes in a metagenome and in replicated transcriptomes from different sediment layers. We hypothesized that group 1 uptake [NiFe]-$H_2$ases from *Desulfobacterales* and thiotrophic *Gammaproteobacteria* account for a major fraction of metagenomic and -transcriptomic $H_2$ase reads. Moreover, we designed primers to specifically target group 1 [NiFe]-$H_2$ase genes of a subset of environmentally relevant SRM. Using PCR-based clone libraries we studied the geographic distribution of group 1b-e [NiFe]-$H_2$ases in two additional sediments along the European Atlantic coast. To link frequently detected clusters of $H_2$ase genes with the corresponding microorganisms we screened selected metagenomes derived from pooled single-cell genomes (SAGs). Finally, incubations with $H_2$ under anoxic and micro-oxic conditions demonstrated an active $H_2$ consumption in sediment from our main study site.

## Materials and methods

### Study sites and sampling

Between January 2011 and July 2015 we sampled sandy tidal sediments during low tide at three sites along the European coastline for molecular analysis and $H_2$ oxidation experiments (see Supplementary Table 1 for geographic positions of samples used for the different experiments). Our main sampling site "Janssand" is a tidal flat in the German Wadden Sea in approximately 10 km distance from the coastline. In addition, we sampled two tidal sandy sediments close to Mt. St. Michel and Courseulles-sur-Mer (France) for molecular analysis (see Dyksma *et al,* 2016).

Sediment was retrieved by 3.7 cm diameter polyacryl cores and sliced according to the sediment color that commonly serves as proxy for sulfide formation by sulfate respiration. Sediment from the uppermost oxidized (0-1 cm, brownish color, sulfide-free), from the sulfide transition zone (2-4 cm, interface of brown- to grey-color, reflecting formation/oxidation of iron-sulfides) and from the sulfidic layers (6-8 cm, grey to black color due to formation of iron-sulfides by sulfate respiration) were recovered. Detailed exemplary oxygen, sulfide and pH profiles of Janssand sediments were published by Jansen *et al.* (2009).

### Metagenomics and targeted screening for uptake $H_2$ases

In April 2013 we sampled the sulfide transition zone comprising both oxidized (brown) and sulfidic (grey) sediments for metagenomic analysis. The uppermost surface layer was removed in order to avoid excess eukaryotic DNA. The bacterial community composition in the upper 8 cm of Janssand sediments is largely homogeneous (Lenk *et al,* 2011; Dyksma *et al,* 2016) as the studied sediments are characterized by constant re-shuffling and periodic changes from oxic to suboxic/anoxic conditions during the tidal cycles (Jansen *et al,* 2009). DNA was extracted according to the protocol by Zhou *et al*. (1996). DNA was then paired-end sequenced (2x 150 bp) in a single Illumina (San Diego, CA, USA) HiSeq 2000 run (one lane) at the Max Planck Genome Centre (MP-GC, Cologne, Germany). $H_2$ase reads were extracted as follows: the metagenome was screened using blastx (Camacho *et al,* 2009) against a reference database that was recently introduced by Greening *et al*. (2015) containing 3,286 $H_2$ase sequences. The translated BLAST (Altschul *et al,* 1990) screening was performed with the following settings: word size 3, e-value 0.1 and minimum percentage query coverage 75% (Greening *et al,* 2015). To minimize false positive hits, the minimum percentage identity cut-off was set to 60%.

In order to assemble nucleotide sequences of group 1 [NiFe]-$H_2$ases for phylogenetic analysis we mapped 141,031,806 metagenomic reads to a reference database. Bowtie2 (Langmead and Salzberg, 2012) was used with local alignment. The reference database comprised 271 environmental sequences from clone libraries (site Janssand) and published

sequences of group 1 [NiFe]-$H_2$ases. In total, 26,425 reads (0.02% of the total) mapped to reference sequences. These reads were assembled using SPAdes (Bankevich *et al,* 2012) and contigs larger than 500 bp (n=109) were kept for phylogenetic analysis and as reference for metatranscriptome mapping.

**Metatranscriptome sequencing and analysis**

In April 2013 and in July 2015 triplicate sediment cores were sampled at site Janssand during low tide. In April 2013, sediment was sampled at late low tide after the sand flat was bare of sea water for approximately one hour. In July 2015 during late low tide, the sand flat was still water-covered (approximately 5 cm water depth) and flushed with sea water by slight waves. Immediately after retrieval the cores were sliced (Supplementary Table 1), 9-14 g of sediment of each layer were transferred to 50 ml tubes and stored at dry ice/-80°C until further processing. Care was taken that the sediment slices were not disturbed and transferred within 20 s to minimize oxygen penetration.

Total RNA was extracted from one gram of each sampled layer from the triplicate cores, DNAase-treated and purified by Vertis Biotechnologie AG (Freising, Germany). Bacterial rRNA was depleted with the Ribo-Zero™ Magnetic Kit (for *Bacteria*) (Epicentre, Madison, WI, USA*)*. Barcoded RNA TrueSEQ libraries were constructed from RNA extractions and paired-end sequenced using Illumina HiSeq 2500 (MP-GC). Quality trimming was performed at phred score 28 using Nesoni v.0.115 (https://github.com/Victorian-Bioinformatics-Consortium/nesoni) with the clip option. Sequencing results are provided in Supplementary Table 2. All metatranscriptomes were analyzed using blastx against the reference database from Greening *et al*. (2015) as described above.

Transcript reads were mapped to the reference database of group 1 [NiFe]-$H_2$ase nucleotide sequences from GenBank, environmental clone libraries and metagenomic assemblies recovered from site Janssand (total of 380 sequences). For mapping we used Bowtie2 with settings: match score = 0, mismatch penalty = 5, gap open penalty = 5, gap extension penalty = 5. The minimum alignment score for an alignment considered as valid was defined by -0.25 multiplied by read length resulting in a percent identity cut-off of 95%. Abundances of unique mapped reads were normalized for gene length and adjusted for the total number of cDNA reads. On average, 3,376 cDNA reads per replicate mapped to the reference database.

**$H_2$ase genes from single–cell (meta)genomes**

In January 2011, the upper two and in August 2015, the upper three centimeters comprising the oxic and sulfide transition layers of Janssand sediment were sampled for extraction and sorting of single bacterial cells for whole genome amplification. After immediate transfer to

the lab the sediment was mixed and 1 ml was transferred to a 15 ml plastic tube. After adding 3 ml of sterile-filtered sea water slurries were vortexed at maximum speed for 3 or 5 min, respectively. Sand grains were allowed to settle and the supernatant was filtered through a 3 or 5 µm pore-size membrane, respectively. The cell extracts were cryopreserved with N,N,N-trimethylglycine ("glycine betaine") (Sigma-Aldrich, St. Louis, MO, USA) at a final concentration of 4% according to Cleland *et al.* (2004), stored at -80°C and shipped overseas.

Single-cell sorting and whole-genome amplification via multiple displacement amplification (MDA) were performed at the Bigelow Laboratory Single Cell Genomics Center (East Boothbay, ME, https://scgc.bigelow.org) as described by Swan *et al.* (2011) or at the Microbial Single Cell Genomics facility at SciLifeLab in Uppsala, Sweden (https://www.scilifelab.se/facilities/single-cell) as described by Mussmann *et al.* (submitted).

SAGs were screened for 16S rRNA genes (described in Dyksma *et al,* 2016; Mussmann *et al,* submitted) affiliating with flavobacterial *Eudoraea* spp. or the deltaproteobacterial Sva0081-marine benthic group (Supplementary Table 3). To minimize costs two SAGs of the *Eudoraea*-group were pooled before sequencing. The 16S rRNA gene sequences displayed 99.8% sequence identity (SI) to each other and 98% to the type strain *Eudoraea adriatica* (Alain *et al,* 2008). Furthermore, we pooled 11 SAGs from the Sva0081-MBG into 4 SAG-pools. The 16S rRNA gene sequences displayed 96-99% SI. The pooling scheme of the individual SAGs and the corresponding 16S rRNA genes sequences is given in Supplementary Table 3. The recovery and analysis of a SAG belonging to the JTB255-MBG is described by Mussmann *et al.* (submitted). The pooled SAGs were sequenced at the Department of Energy Joint Genome Institute (DOE-JGI, Walnut Creek, CA, USA) or at the MP-GC.

The three SAG-pools "pSCGC" were sequenced (Illumina HiSeq 2000, Illumina HiSeq 2500) and assembled at the DOE-JGI, and auto-annotated using the IMG-ER pipeline (Markowitz *et al,* 2012). The assembled dataset was screened for contamination using k-mer analysis within the IMG-ER pipeline. In addition, universal single copy genes (Ciccarelli *et al,* 2006; Creevey *et al,* 2011), ribosomal proteins and tRNA were manually checked for a possible contamination by examining their closest BLAST hits.

The SAG-pools 1868_C and 1868_D were sequenced (Illumina MiSeq) at the MP-GC. Sequence reads were quality trimmed with BBmap (v35.82; https://sourceforge.net/projects/bbmap, using bbduk.sh) at a minimum quality cut-off of 15. Single cell genome assembly was performed with SPAdes v 3.6.2 using the single-cell mode (--sc), the "-careful" option and suggested kmer-sizes between 21 and 99. Purity of the assembly was checked with Metawatt v 3.5.2 (Strous *et al,* 2012) using tetramer frequencies and GC-content. The completeness and possible redundancy of the SAG assembly and the

final genome bin was evaluated with the HMMER3 (Eddy, 2008) based "Six-frame Pfam" module search against a conserved single-copy gene set (Campbell *et al,* 2013) in Metawatt. The SAG-pools 1868_C and 1868_D were auto-annotated using the IMG-ER pipeline (Markowitz *et al,* 2012) and manually checked. After sequencing we recovered a 16S rRNA gene sequence and a group 1 [NiFe]-$H_2$ase sequence per SAG-pool (n=5) (Supplementary Table 3). The metagenomic sequences of all SAG pools described in this study will be published elsewhere (Mussmann *et al,* in preparation).

**Design of $H_2$ase primers for clone library construction**

As primers previously published by Csáki *et al,* (2001) and Kim *et al*, (2007) mainly target alpha-, beta- and gammaproteobacterial group 1 [NiFe]-$H_2$ase genes, we designed novel primer sets to cover a broader diversity of $H_2$ases from sulfate-reducing *Deltaproteobacteria*. Details on design of primers to target group 1b and 1c uptake [NiFe]-$H_2$ases of SRM, PCR and phylogenetic reconstructions of group 1 [NiFe]-$H_2$ase and 16S rRNA genes are provided in the Supplementary Material and Methods. Furthermore, nucleotide accession numbers of $H_2$ase and 16S rRNA gene sequences recovered from metagenomes, -transcriptomes, clone libraries and SAGs are given in the Supplementary Material and Methods

**$H_2$ oxidation experiments in Janssand sediments**

Sediments were sampled at site Janssand in January 2012 (anoxic incubations) and April 2013 (micro-oxic incubations). Portions of 3 ml of sediment were transferred into 50 ml serum bottles with 2 ml sterile filtered seawater. The headspace was replaced by either nitrogen ($N_2$) gas with 3,600 nmol $l^{-1}$ $H_2$ for anoxic, sulfate-dependent incubations or $N_2$ with 210 nmol $l^{-1}$ $H_2$ and 1% oxygen for micro-oxic experiments. The triplicate incubations were mildly agitated for 52-96 h at 14 °C. Residual sulfate reduction in micro-oxic treatments was inhibited in parallel incubations by adding sodium molybdate (28 mmol $l^{-1}$ final concentration). For measuring $H_2$ one ml of the headspace was sampled and analyzed using gas chromatography (GC-8A, Shimadzu) with an HgO-reducing detector (RGD2, Trace Analytical, Gemany). Concentrations of dissolved $H_2$ was calculated according to Weiss (1970) and Crozier and Yamamoto (1974).

**Results**

**$H_2$ase diversity and expression in a coastal sediment**

To study the diversity and relative abundance of genes of the catalytic subunit of $H_2$ases in coastal sediments, we first recruited reads of all types of $H_2$ases from the Janssand metagenome. Overall, 0.1% (n=275,328) of all metagenomic sequence reads were assigned to $H_2$ases and were classified according to a revised scheme recently introduced by

Greening *et al.* (2015). Three types accounted for the majority of the $H_2$ase reads: 77% corresponded to [FeFe]-$H_2$ases (mainly $H_2$-evolving), 11% to group 1 [NiFe]-$H_2$ases (mainly uptake) and 9% to cytosolic, bidirectional group 3 [NiFe] $H_2$ases (Figure 1).

To study the vertical expression profile of the distinct types of $H_2$ase genes we sequenced triplicate metatranscriptomes from the surface, sulfide transition and sulfidic sediment layers in July 2015. In addition, we recovered a triplicate metatranscriptome from the sulfide transition layer in April 2013. $H_2$ase genes of all groups and subgroups were expressed in both seasons and in all tested sediment layers (Figure 1 and Supplementary Figure 1). While normalized, total read abundances varied strongly between the triplicate metatranscriptomes of July 2015 (not shown), the relative expression of the different $H_2$ase types showed clear trends with sediment depth (Figure 1). The oxygen-sensitive, mainly $H_2$-evolving [FeFe]-$H_2$ases were relatively higher expressed in the sulfide transition and in the sulfidic layer, whereas group 1 and 3 [NiFe]-$H_2$ases were relatively more expressed in the surface layer than in deeper layers (Figure 1).

**Diversity of group 1 [NiFe]-$H_2$ase genes in three tidal sediments**

$H_2$ is an energy source for diverse but still unidentified microorganisms in marine sediments. Thus, we studied the diversity and expression of genes of $H_2$-oxidizing $H_2$ases in more detail. Since metagenomic reads of group 1 [NiFe]-$H_2$ases clearly prevailed over those of group 2 [NiFe]-$H_2$ases, we focused our diversity and expression analysis on group 1 [NiFe]-$H_2$ases.

Among all metagenomic reads of group 1 [NiFe]-$H_2$ases, 89% belonged to subgroups 1b-e (Figure 1: 1e, Isp/Hyn, 40%; 1d, $O_2$-tolerant, 19%; 1c, Hyb-type, 17%; and 1b, prototypical, 13%). Only few reads were assigned to subgroups 1a, 1g and 1h.

Similar to the overall $H_2$ase expression (Figure 1) the subgroup 1d-e NiFe $H_2$ases showed a depth-dependent expression pattern (Figure 1). While group 1d and 1e NiFe $H_2$ases together were relatively more expressed in the surface layer (56%) than in sulfidic layer (29%), the SRM-type group 1b [NiFe]-$H_2$ases followed an inverse pattern, accounting for in average 12% in the upper cm to in average 36% in the sulfidic layer of all group 1 uptake [NiFe]-$H_2$ase transcripts (Figure 1).

For a detailed phylogenetic analysis of the metagenomic group 1 [NiFe]-$H_2$ases we assembled 98 partial sequences (>500 bp) of group 1 [NiFe]-$H_2$ase genes with diverse phylogenetic origin (Supplementary Figure 1). To cover a larger diversity of potential group 1 uptake [NiFe]-$H_2$ases, we established gene libraries from Janssand sediment (Germany) and from two additional coastal sediments (Western France). As the published primer set (Csáki *et al,* 2001; Kim *et al,* 2007) mostly targets group 1d and 1e [NiFe]-$H_2$ase genes of sulfur-oxidizing and Knallgas-bacteria, we designed a novel primer set to include a broader diversity of 1b and 1c [NiFe]-$H_2$ase of mostly cultured, environmentally abundant

*Desulfobulbaceae* and *Desulfobacteraceae* SRM (Supplementary Tables 4, 5). These target 50 genes sequences of group 1 [NiFe]-$H_2$ases of cultured and uncultured SRM (see Supplementary Information). Using both newly designed and previously published primers we yielded a total of 317 [NiFe]-$H_2$ase clone sequences.

Together, the PCR-derived and metagenomic group 1 [NiFe]-$H_2$ase sequences formed 24 monophyletic sequence clusters among bacterial group 1b-f [NiFe] $H_2$ases (Supplementary Figure 1). The sequence diversity recovered from clone libraries and from the metagenome largely overlapped, however, the cloning approach revealed a higher microdiversity and entire sequence clusters that were underrepresented in the metagenome (Figure 2 and Supplementary Figure 1). Of the 24 sediment clusters, 18 were represented in at least two of three study sites indicating a more widespread occurrence of the corresponding organisms. The retrieved [NiFe]-$H_2$ase sequences affiliated with different phylogenetic and functional groups including sulfate-reducing bacteria, sulfur-oxidizing bacteria and others (Supplementary Figure 1).

**Group 1e [NiFe]-$H_2$ases: diversity and expression**

Group 1e [NiFe]-$H_2$ases catalyze different $H_2$-cyling reactions including dark $H_2$ oxidation, light-dependent $H_2$ evolution and intracellular $H_2$ cycling. These accounted for a substantial fraction of all group 1 [NiFe]-$H_2$ases in the metagenome (40%), in clone libraries (24-34%) and also in the metatranscriptomes (16-37%) (Figure 1). Nine out of twelve sediment clusters exhibited transcriptional activity, but no depth-related trend (Supplementary Figure 1), except for sediment cluster 11, which was more expressed in the uppermost sediment layer (Supplementary Figure 1). Most of the clone and metagenome-derived sequences of group 1e [NiFe]-$H_2$ases were related to those of sulfur-oxidizing *Gammaproteobacteria* such as endosymbionts, *Thiothrix* spp. or *Thioalkalivibrio* spp. (Supplementary Figure 1). The corresponding 16S rRNA gene sequences are unknown except for sediment cluster 2, which contains a $H_2$ases sequence derived from a SAG of the gammaproteobacterial, sulfur-oxidizing SSr-clade recovered from Janssand sediment (Dyksma *et al*, 2016).

**$O_2$-tolerant, group 1d uptake [NiFe]-$H_2$ases: diversity and expression**

The $O_2$-tolerant group 1d uptake [NiFe]-$H_2$ases accounted for 19% of metagenomic and for 12-21% of metatranscriptomic group 1 [NiFe]-$H_2$ase reads (Figure 1). Within this group only sediment clusters 13 and 15 were significantly expressed, in particular in the surface layer (Figure 2).

The sediment cluster 15 accounted for 23% of all group 1d [NiFe]-$H_2$ase transcripts and grouped with [NiFe]-$H_2$ase sequences of $H_2$-oxidizing *Bacteroidetes*, such as the soil-dwelling *Flavobacterium johnsoniae* (Figure 2). To show the potential for $H_2$ oxidation in

marine benthic *Flavobacteriaceae*, we identified a 1d [NiFe]-$H_2$ase sequence among two pooled flavobacterial SAGs from the *Eudoraea*-group retrieved from site Janssand. The 16S rRNA gene sequences of the individual SAGs displayed 99.8% sequence identity to each other and 98% to the heterotrophic, aerobic flavobacterium *Eudoraea adriatica* (Figure 3, Alain *et al*, 2008). This *Eudoraea*-related [NiFe]-$H_2$ase groups with sediment cluster 15 and with other flavobacterial $O_2$-tolerant 1d [NiFe]-$H_2$ase sequences (Figure 2).

Notably, cluster 13 accounted for >75% of all group 1d uptake [NiFe]-$H_2$ases in the surface layer, suggesting a pivotal role of this cluster in $O_2$-tolerant $H_2$-oxidation. Six sequences of sediment cluster 13 were relatively less expressed in deeper sediment layers than at the sediment surface (Figure 2). The corresponding organisms are still unknown, however, we recently identified a closely related $H_2$ase sequence retrieved from a SAG of the uncultured gammaproteobacterial JTB255-marine benthic group (Mussmann *et al,* submitted) (Figure 2). This SAG has been recovered from the same site during our sampling campaign in July 2015. Consistent with this finding we identified a closely related 1d [NiFe]-$H_2$ase in a metagenomic bin from the White Oak River, USA, that is also affiliated with the JTB255-marine benthic group (Figure 2, Baker *et al,* 2015; Mussmann *et al,* submitted). We therefore propose that the 1d [NiFe]-$H_2$ases sediment cluster 13 most likely corresponds to the uncultured JTB255-marine benthic group.

**Group 1b and 1c uptake [NiFe]-$H_2$ases of sulfate-reducing bacteria**

We retrieved 117 clone and 11 metagenomic sequences that are affiliated with cultured and uncultured *Desulfobacteraceae* (Figure 2). Only few group 1c [NiFe]-$H_2$ases of *Desulfobulbaceae* were encoded in the metagenome (n=3) and in clone libraries (n=3) (Figure 2 and Supplementary Figure 2).

$H_2$ases of sediment clusters 17 to 19 comprised the majority of clone and metagenome-derived $H_2$ase sequences of SRM and are most closely related to $H_2$ases of *Desulfosarcina* spp. as next cultured relatives (Figure 2). Interestingly, clone and metagenomic sequences of sediment cluster 17 consistently grouped with a $H_2$ase of the sulfate-reducing □1-symbiont of the gutless marine oligochaete *Olavius algarvensis* (Figure 3*).* To identify the corresponding microorganisms, we sequenced 4 metagenomes derived from 11 pooled closely related SAGs from site Janssand (Figure 3). The 16S rRNA gene sequences of the SAGs displayed a 96-99% sequence identity to those of *Olavius* ssp. sulfate-reducing δ-endosymbionts (Figure 3) and are affiliated with the uncultured Sva0081-marine benthic group (MBG)/*Desulfobacteraceae* (ARB-Silva taxonomy, Ref NR99_SSU release 117 as of April 2015, Quast *et al,* 2013). As the phylogeny of the 1b uptake [NiFe]-$H_2$ase and of 16S rRNA are largely congruent, the 1b [NiFe]-$H_2$ase sediment cluster 17 therefore most likely corresponds to the Sva0081-MBG (Figures 2 and 3).

Consistent with the metagenomic data, the group 1b [NiFe]-$H_2$ases of *Desulfobacteraceae* (sediment clusters 17-19, Figure 2) accounted for a majority of transcripts of SRM-related $H_2$ases (82-89%, Figure 2, Supplementary Figure 2). In all metatranscriptomes from April 2013 and July 2015 the largest fraction of mapped transcripts (49-69%) affiliated with the sediment cluster 17, the putative Sva0081-MBG. $H_2$ase sequences more closely related to *D. variabilis* (sediment clusters 18, 19) and to *Desulfobulbaceae* (sediment cluster 23) recruited only 14-30% and 11-18% of SRM-$H_2$ase transcripts, respectively (Figure 2, Supplementary Figure 2). Transcripts of epsilonproteobacterial $H_2$ases were not found.

**Potential $H_2$ oxidation rates in Janssand sediments**

As sulfate respiration is considered the major $H_2$-consuming process in marine sediments, we initially focused our measurements on anaerobic $H_2$-oxidation in Janssand sediments. In January 2012 $H_2$ (3,600 nmol $l^{-1}$) in sediments slurries was completely consumed within 48 h equaling a $H_2$ oxidation rate of 31 nmol $ml^{-1}$ $h^{-1}$ (Figure 4).

Since the detected diversity of group 1 [NiFe]-$H_2$ase genes in our sediments unexpectedly indicated also a $H_2$ consumption in the presence of $O_2$ we then measured the potential $H_2$ oxidation rates in micro-oxic sediment slurries in April 2013. Here, $O_2$ and $H_2$ concentrations were adjusted to 210 nmol $l^{-1}$ $H_2$ and to 1% $O_2$ to account for inhibitory effects. A potential residual sulfate-dependent $H_2$ consumption was inhibited by the addition of molybdate. Under these micro-oxic conditions $H_2$ was consumed at a rate of 0.97 nmol $ml^{-1}$ $h^{-1}$ (Figure 4).

**Discussion**

Evidence is accumulating that various types of $H_2$ases drive $H_2$-cycling in natural and anthropogenic ecosystems, while the $H_2$ases themselves and the corresponding microorganisms in marine sediments are still unknown. In our study we show that the metagenome from Janssand tidal sediment contained more than twice as many $H_2$ase-assigned reads (0.1%) as in any of the recently investigated ecosystem (up to 0.045% in 20 ecosystems), including aerated soils, hypoxic water-clogged soils, marine water bodies and anoxic termite and human guts (Greening *et al,* 2015). This underscores the vital role of $H_2$ for energy transfer in marine sediments (Hoehler *et al,* 1998). In particular, in anoxic sediments the $H_2$-evolving [FeFe]-$H_2$ases may be as important for $H_2$ production as in digestive systems (Greening *et al,* 2015), while distinct group 1 [NiFe]-$H_2$ases may mostly oxidize $H_2$. Other $H_2$ases such as the abundant bidirectional group 3 [NiFe]-$H_2$ases could also play a still unknown role in oxic and suboxic sediment layers.

An explanation for the observed high frequency of $H_2$ase reads is possibly the dynamic nature of the studied ecosystem: tidal cycles cause strong short-termed spatial and temporal gradients in e.g. oxygen and sulfide levels (Jansen *et al,* 2009), thus the microbial

communities experience alternating oxic and sub-/anoxic conditions. This provides many distinct ecological niches on a narrow spatial and temporal scale that foster the co-existence of diverse $O_2$-tolerant/-sensitive and $H_2$-producing/-consuming microorganisms. Moreover, marine SRM use $H_2$ to reduce and detoxify $O_2$ under micro-oxic conditions (Krekeler *et al,* 1997) and therefore also express $H_2$ase genes in oxic surface sediments (Figures 1, 2). Thus, we can also not exclude that SRM oxidized $H_2$ in our micro-oxic experiment despite the addition of SR-inhibiting molybdate (Figure 4). Together, these habitat-specific factors may be the reason, why virtually all types of $H_2$ases, including $O_2$-sensitive $H_2$ases, were expressed at relatively similar levels in the three distinct sediment layers. Likewise, the expression of the same group 1 [NiFe]-$H_2$ase gene clusters in April 2013 and in July 2015 in the three distinct sediment layers (Figure 2, Supplementary Figures 1, 2), indicates a stable bacterial $H_2$-cycling community structure over time. This agrees with the generally similar bacterial 16S rRNA diversity found in the upper 7 to 10 cm of sandy tidal surface sediments across the ocean (Dyksma *et al,* 2016). It would be intriguing to reveal, whether and how tightly these distinct $H_2$ases are regulated under the highly fluctuating conditions. As deep metaproteome analysis from such complex communities is still virtually impossible, additional, internally standardized metatranscriptomes (Gifford *et al,* 2011) need to be sequenced in a higher spatial and temporal resolution to reveal the extent of constitutive and tightly regulated expression during a tidal cycle.

**Group 1 [NiFe]-$H_2$ase genes are abundant and frequently expressed**

Group 1 [NiFe]-$H_2$ases accounted for the largest fraction of potential uptake [NiFe]-$H_2$ase reads in the metagenome. In fact, group 1 [NiFe]-$H_2$ases are the most widespread $H_2$-metabolizing enzymes and are encoded in many *Bacteria* and *Archaea* isolated from diverse ecosystems (Vignais and Billoud, 2007; Schwartz *et al,* 2013; Greening *et al*, 2015). A significant subset of metagenomic and -transcriptomic reads affiliated with $O_2$-sensitive, group 1e (Hyn-type) [NiFe]-$H_2$ases related to sulfur-oxidizing *Gammaproteobacteria* (Figure 2). However, this type of $H_2$ase can exert different metabolic functions: Hyn-type $H_2$ases are involved in dark $H_2$ oxidation but also in $H_2$ evolution under light in the phototrophic purple sulfur bacterium *Thiocapsa roseopersicina* (Laurinavichene *et al,* 2007; Tengölics *et al,* 2014). Moreover, the expression of Hyn-type $H_2$ase is up-regulated in *Allochromatium vinosum* when growing on sulfide, thiosulfate or $S^0$ in the absence of $H_2$ (Weissgerber *et al,* 2014). Recently, Kreutzmann and Schulz-Vogt (2016) showed that the marine aerobic sulfide-oxidizing strain *Beggiatoa* sp. 35Flor reaches higher biomass using $H_2$ probably as a supplemental energy source for maintenance or for disposing excess intracellular sulfur. In line with this, a group 1e [NiFe]-$H_2$ase gene in the SAG of the sulfur-oxidizing SSr-group was among the top 20 expressed genes along with sulfite-oxidation and carbon-fixation genes,

suggesting a possibly multifunctional role of group 1e [NiFe]-$H_2$ases in chemoautotrophy (Dyksma *et al*, 2016). It is therefore conceivable that the generally high expression of $O_2$-sensitive group 1e [NiFe]-$H_2$ases even in the oxygen-exposed, uppermost sediment layer reflects an intracellular $H_2$ recycling during sulfur oxidation and not necessarily the oxidation of ambient $H_2$.

**$O_2$-tolerant oxidation of $H_2$ by Flavobacteriaceae and Gammaproteobacteria**

Our data show that sediment clusters 13 (putative JTB255-MBG) and 15 (putative *Eudoraea*-group) contributed almost all transcripts of $O_2$-tolerant, group 1d uptake [NiFe]-$H_2$ases at all depths and seasons (Figure 2). This is consistent with the observed oxidation of $H_2$ under micro-oxic conditions in parallel samples in April 2013 (Figure 4, Supplementary Figure 1). Thus, it is likely that mostly these two groups are responsible for oxidation of $H_2$ at ambient $O_2$ levels, e.g. in the uppermost sediment surface or at high tide, when also deeper sediments are temporarily flushed with fully oxygenated sea water (Jansen *et al*, 2009).

Recently, we showed that members of the JTB255-MBG fix $CO_2$ (Dyksma *et al,* 2016), and encode RubisCO form I and a thiosulfate oxidation pathway, suggesting carbon fixation powered by thiosulfate or $H_2$ (Mussmann *et al,* submitted). The high transcript frequency and the more widespread occurrence of $H_2$ase genes of the putative JTB255-MBG (Figure 2) agrees with the fact that JTB255-MBG is a cosmopolitan, abundant core member of microbial communities in diverse types of marine sediments, (Dyksma *et al,* 2016, Mussmann *et al*, submitted). While few other marine *Gammaproteobacteria*, such as symbiotic and pelagic members of the SUP05-clade, do thrive on $H_2$ (Petersen *et al,* 2011; Anantharaman *et al,* 2013), we propose that the JTB255-MBG could be an important aerotolerant $H_2$-oxidizing *Gammaproteobacteria* also in marine surface sediments.

Consistent with the relatively high transcript frequency of putative *Eudoraea*-group $H_2$ases, cells closely related to *Eudoraea adriatica* accounted for up to 4% of total cells in coastal sediments including site Janssand (Rizvi, 2014). Although $H_2$ oxidation has so far been only been shown for soil *Flavobacteria* (Maimaiti *et al,* 2007), evidence is accumulating for flavobacterial group 1d [NiFe]-$H_2$ases also in marine water and sediment metagenomes (Figure 2, Barz *et al*, 2010). In fact, $H_2$ could be an attractive energy source for marine bacterioplankton since seawater can be supersaturated with $H_2$ that is formed by nitrogen fixation or photochemical $H_2O$ lysis (Hoehler *et al,* 2001; Punshon and Moore, 2008; Moore *et al,* 2014).

**Desulfobacteraceae likely oxidize $H_2$ in anoxic coastal sediments**

In line with our initial hypothesis the *Desulfobacterales*, in particular the *Desulfobacteraceae*, accounted for most of SRM-related $H_2$ase genes and transcripts and may therefore drive

sulfate-dependent $H_2$ oxidation at site Janssand and perhaps also at sites Mt. St. Michel and Courseulles-sur-Mer. Although *Desulfovibrio*-like $H_2$ase genes have earlier been detected in coastal sediments (Wawer and Muyzer, 1995), we did not find any indication for *Desulfovibrio*-related organisms in our samples. Accordingly, *Desulfobacteraceae* commonly dominate SRM communities and outnumber *Desulfobulbaceae* and *Desulfovibrionaceae* in most marine sites including Janssand and other Wadden Sea sediments (Llobet-Brossa *et al,* 1998; Ravenschlag *et al,* 2000; Ishii *et al,* 2004; Mußmann *et al,* 2005). Moreover, the low relative frequency of group 1c [NiFe]-$H_2$ase reads may also reflect the relatively low abundance of *Desulfobulbaceae* in these sediments. However, a better coverage of group 1c [NiFe]-$H_2$ases via additional metagenome sequencing could provide a more comprehensive reference data set for efficient metatranscriptome mapping.

**The uncultured Sva0081-MBG are possible key players in the anaerobic food chain**

Notably, $H_2$ase sequences of the SRM-related sediment cluster 17 accounted for in total approximately ~50% of all SRM-related group 1b and 1c [NiFe]-$H_2$ase transcripts in April 2013 and in July 2015. We could link these $H_2$ase sequences to the uncultured, deltaproteobacterial Sva0081-MBG by sequencing the metagenome of 11 pooled SAGs from site Janssand and by analyzing symbiotic Sva0081-MBG in a metagenomes of the bacterial symbionts of gutless marine oligochaetes *O. algarvensis*. Consistent with this, the high $H_2$ consumption rates by *O. algarvensis* symbionts and the detection of a Sva0081-specific [NiFe]-$H_2$ase in corresponding proteomes (Kleiner *et al*, 2012, 2015) strongly corroborate the capability of the Sva0081-MBG to actively oxidize $H_2$ in marine sediments. Since this a chemolithotrophic process, a concomitant carbon fixation seems plausible. However, previous isotopic tracer experiments did not indicate any carbon fixation in the *Olavius* sp. worms despite high $H_2$ oxidation rates (Kleiner *et al,* 2015). Likewise, $CO_2$ assimilation in sulfidic sediment layers at site Janssand was very low (Lenk *et al,* 2011). Presumably, the Sva0081-MBG oxidizes $H_2$ chemolithoheterotrophically, as other SRM do, by using e.g. acetate as carbon source (Kleiner *et al,* 2015, Rabus *et al,* 2015).

$H_2$ase sequences of the putative Sva0081-MBG occurred in all three studied coastal sediment sites and in other North Sea sediments (Figure 2). In line with this, the Sva0081-MBG has been frequently identified in 16S rRNA gene surveys in marine sediments (Ravenschlag *et al,* 2000; Wang *et al,* 2013; Liu *et al,* 2014; Zheng *et al,* 2014) and accounts for up to 6-8% of total cell counts in different marine sediments worldwide including site Janssand (Mussmann *et al,* in prep.; Ovanesov, 2012). If the genetic potential to oxidize $H_2$ is common to members of the Sva0081-MBG in sediments worldwide, these SRM are candidate key players in the marine anaerobic food chain.

**Ecological significance of the candidate $H_2$-consumers in coastal sediments**

Here, we provide first molecular evidence that a complex community of mostly uncultured microorganisms drives $H_2$-cycling, in particular $H_2$ consumption in marine coastal sediments. By analyzing single cell-derived (meta)genomes, we identified putative bacterial representatives of significant $H_2$ase sequence clusters of group 1 uptake [NiFe]-$H_2$ases. Since production, flux and consumption rates of $H_2$ are generally low in oxic sediments, the metabolically flexible JTB255-MBG and *Eudoraea*-group probably consume $H_2$ only as a supplemental energy source. However, by employing $O_2$-tolerant $H_2$ases they might be able to monopolize $H_2$ at ambient $O_2$ concentrations.

While it has been known for decades that $H_2$ is a central energy source for marine sulfate respiration, we now propose that widely distributed and abundant family *Desulfobacteraceae*, in particular the uncultured Sva0081-MBG, are the probable key players in consuming $H_2$ released by fermentative hydrolysis of organic matter. Importantly, these SRM may outcompete hydrogenoclastic methanogens and thereby suppress the production and emission of methane in organic-rich coastal surface sediments. In general, marine sediments may harbor a multitude of hidden syntrophic interactions between novel $H_2$-forming and -consuming microorganisms that ultimately control the anaerobic food chain and carbon sequestration in earth´s largest carbon sink.

**Acknowledgement**

We greatly acknowledge the crew of R/V Navicula from the ICBM Oldenburg for ship time and assistance. We thank Stefan Becker, Jörg Wulf and Thomas Holler for great technical assistance and advice. Special thanks go to Rudolf Amann for the continuous and excellent support. We greatly acknowledge the Department of Energy-Joint Genome Institute (Walnut Creek, CA, USA) for sequencing of the pooled single amplified genomes (Community Science Program Proposal ID1118, granted to Marc Mussmann and Community Science Program proposal ID1049158 granted to Hanno Teeling. The latter is supported by the Office of Science of the U.S. DOE under Contract No. DE-AC02-05CH11231). Moreover, this study was funded by the Max Planck Society/Germany.

**References**

Alain K, Intertaglia L, Catala P, Lebaron P (2008). *Eudoraea adriatica* gen. nov, sp. nov, a novel marine bacterium of the family *Flavobacteriaceae*. *Int. J. Syst. Evol. Microbiol.* **58**: 2275–2281.

Altschul SF, Gish W, Miller W, Myers EW, Lipman DJ (1990). Basic local alignment search tool. *J. Mol. Biol.* **215**: 403–410.

Anantharaman K, Breier JA, Sheik CS, Dick GJ (2013). Evidence for hydrogen oxidation and metabolic plasticity in widespread deep-sea sulfur-oxidizing bacteria. *Proc. Natl. Acad. Sci.* **110**: 330–335.

Baker BJ, Lazar CS, Teske AP, Dick GJ (2015). Genomic resolution of linkages in carbon, nitrogen, and sulfur cycling among widespread estuary sediment bacteria. *Microbiome* **3**: 14.

Bankevich A, Nurk S, Antipov D, Gurevich AA, Dvorkin M, Kulikov AS, *et al*. (2012). SPAdes: a new genome assembly algorithm and its applications to single-cell sequencing. *J. Comput. Biol.* **19**: 455–477.

Barz M, Beimgraben C, Staller T, Germer F, Opitz F, Marquardt C*, et al*. (2010). Distribution analysis of hydrogenases in surface waters of marine and freshwater environments. *PLOS ONE* **5**: e13846.

Camacho C, Coulouris G, Avagyan V, Ma N, Papadopoulos J, Bealer K, Madden TL (2009). BLAST+: architecture and applications. *BMC Bioinformatics* **10**: 421.

Campbell AG, Campbell JH, Schwientek P, Woyke T, Sczyrba A, Allman S, *et al.* (2013). Multiple single-cell genomes provide insight into functions of uncultured *Deltaproteobacteria* in the human oral cavity. *PLOS ONE* **8**: e59361.

Ciccarelli FD, Doerks T, von Mering C, Creevey CJ, Snel B, Bork P (2006). Toward automatic reconstruction of a highly resolved tree of life. *Science* **311**: 1283–1287.

Cleland D, Krader P, McCree C, Tang J, Emerson D. (2004). Glycine betaine as a cryoprotectant for prokaryotes. *J. Microbiol. Methods* **58**: 31–38.

Creevey CJ, Doerks T, Fitzpatrick DA, Raes J, Bork P (2011). Universally distributed single-copy genes indicate a constant rate of horizontal transfer. *PLoS ONE* **6**: e22099.

Crozier TE,n Yamamoto S (1974). Solubility of hydrogen in water, sea water, and sodium chloride solutions. *J. Chem. Eng. Data* **19**: 242–244.

Csáki R, Hanczár T, Bodrossy L, Murrell JC, Kovács KL. (2001). Molecular characterization of structural genes coding for a membrane bound hydrogenase in *Methylococcus capsulatus* (Bath). *FEMS Microbiol Lett* **205**: 203–207.

D'Hondt S, Rutherford S, Spivack AJ. (2002). Metabolic activity of subsurface life in deep-sea sediments. *Science* **295**: 2067–2070.

Dyksma S, Bischof K, Fuchs BM, Hoffmann K, Meier D, Meyerdierks A, *et al*. (2016). Ubiquitous *Gammaproteobacteria* dominate dark carbon fixation in coastal sediments. *ISME J.* doi: 10.1038/ismej.2015.257.

Eddy SR. (2008). A probabilistic model of local sequence alignment that simplifies statistical significance estimation. *PLOS Comput Biol* **4**: e1000069.

Fritsch J, Lenz O, Friedrich B (2013). Structure, function and biosynthesis of $O_2$-tolerant hydrogenases. *Nat. Rev. Microbiol.* **11**: 106–114.

Gifford SM, Sharma S, Rinta-Kanto JM, Moran MA. (2011). Quantitative analysis of a deeply sequenced marine microbial metatranscriptome. *ISME J* **5**: 461–472.

Goris, T, Wait, A.F, Saggu, M, Fritsch, J, Heidary, N, Stein, M, *et al*. (2011). A unique iron-sulfur cluster is crucial for oxygen tolerance of a [NiFe]-hydrogenase. *Nat. Chem. Biol.* **7**: 310–318.

Greening, C, Biswas, A, Carere, C.R, Jackson, C.J, Taylor, M.C, Stott, M.B, et al. (2015). Genomic and metagenomic surveys of hydrogenase distribution indicate $H_2$ is a widely utilised energy source for microbial growth and survival. *ISME J* **10**: 761–777.

Hansen M, Perner M. (2015). A novel hydrogen oxidizer amidst the sulfur-oxidizing *Thiomicrospira* lineage. *ISME J.* **9**: 696–707.

Hedges JI, Keil RG. (1995). Sedimentary organic matter preservation: an assessment and speculative synthesis. *Mar. Chem.* **49**: 81–115.

Hamann E, Gruber-Vodicka H, Kleiner M, Tegetmeyer HE, Riedel D, Littmann S, *et al.* (2016). Environmental Breviatea harbour mutualistic *Arcobacter* epibionts. *Nature* **534**: 254–258.

Hoehler TM, Alperin MJ, Albert DB, Martens CS. (1998). Thermodynamic control on hydrogen concentrations in anoxic sediments. *Geochim Cosmochim Acta* **62**: 1745–1756.

Hoehler, T.M, Bebout, B.M, and Des Marais, D.J. (2001). The role of microbial mats in the production of reduced gases on the early Earth. *Nature* **412**: 324–327.

Ishii K, Mußmann M, MacGregor BJ, Amann R. (2004). An improved fluorescence *in situ* hybridization protocol for the identification of bacteria and archaea in marine sediments. *FEMS Microbiol. Ecol.* **50**: 203–213.

Jansen S, Walpersdorf E, Werner U, Billerbeck M, Böttcher ME, deBeer D. (2009). Functioning of intertidal flats inferred from temporal and spatial dynamics of $O_2$, $H_2S$ and pH in their surface sediment. *Ocean Dyn.* **59**: 317–332.

Jørgensen, BB. (1982). Mineralization of organic matter in the sea bed-the role of sulphate reduction. *Nature* **296**: 643–645.

Kim JYH, Jung HJ, Cha HJ. (2007). Universal degenerate oligonucleotide-primed-polymerase chain reaction for detection and amplification of NiFe-hydrogenase genes. *Enzyme Microb Technol* **42**: 1–5.

Kleiner M, Wentrup C, Lott C, Teeling H, Wetzel S, Young J, *et al.* (2012). Metaproteomics of a gutless marine worm and its symbiotic microbial community reveal unusual pathways for carbon and energy use. *Proc Natl Acad Sci U S A* **109**: 1173–1182.

Kleiner M, Wentrup C, Holler T, Lavik G, Harder J, Lott C, *et al*. (2015). Use of carbon monoxide and hydrogen by a bacteria–animal symbiosis from seagrass sediments. *Environ. Microbiol.* **17:** 5023–5035.

Krekeler D, Sigalevich P, Teske A, Cypionka H, Cohen Y. (1997). A sulfate-reducing bacterium from the oxic layer of a microbial mat from Solar Lake (Sinai), *Desulfovibrio oxyclinae* sp. nov. *Arch Microbiol* **167**: 369–375.

Kreutzmann AC, Schulz-Vogt HN. (2016). Oxidation of molecular hydrogen by a chemolithoautotrophic *Beggiatoa* strain. *Appl Environ Microbiol* **82**: 2527–2536.

Langmead B, Salzberg SL. (2012). Fast gapped-read alignment with Bowtie 2. *Nat. Methods* **9**: 357–359.

Laurinavichene TV, Rákhely G, Kovács KL, and Tsygankov AA. (2007). The effect of sulfur compounds on $H_2$ evolution/consumption reactions, mediated by various hydrogenases, in the purple sulfur bacterium, *Thiocapsa roseopersicina*. *Arch. Microbiol.* **188**: 403–410.

Lenk S, Arnds J, Zerjatke K, Musat N, Amann R, Mußmann M. (2011). Novel groups of *Gammaproteobacteria* catalyse sulfur oxidation and carbon fixation in a coastal, intertidal sediment. *Environ. Microbiol.* **13**: 758–774.

Liu J, Liu X, Wang M, Qiao Y, Zheng Y, Zhang XH. (2014). Bacterial and archaeal communities in sediments of the North Chinese Marginal Seas. *Microb. Ecol.* **70:** 105–117

Llobet-Brossa E, Rosselló-Mora R, Amann R. (1998). Microbial community composition of Wadden Sea sediments as revealed by fluorescence *in situ* hybridization. *Appl. Environ. Microbiol.* **64**: 2691–2696.

Maimaiti J, Zhang Y, Yang J, Cen Y-P, Layzell DB, Peoples M, *et al.* (2007). Isolation and characterization of hydrogen-oxidizing bacteria induced following exposure of soil to hydrogen gas and their impact on plant growth. *Environ Microbiol* **9**: 435–444.

Markowitz VM, Chen I-MA, Palaniappan K, Chu K, Szeto E, Grechkin Y, *et al.* (2012). IMG: the integrated microbial genomes database and comparative analysis system. *Nucleic Acids Res* **40**: D115–D122.

Michener RH, Scranton MI, and Novelli P. (1988). Hydrogen ($H_2$) distributions in the carmans river estuary. *Estuar. Coast. Shelf Sci.* **27**: 223–235.

Monetti MA, Scranton MI. (1992). Fatty acid oxidation in anoxic marine sediments: the importance of hydrogen sensitive reactions. *Biogeochemistry* **17**: 23–47.

Moore RM, Kienast M, Fraser M, Cullen JJ, Deutsch C, Dutkiewicz S, *et al.* (2014). Extensive hydrogen supersaturations in the western South Atlantic Ocean suggest substantial underestimation of nitrogen fixation. *J Geophys Res Oceans* **119**: 4340–4350.

Mußmann, M, Ishii, K, Rabus, R, and Amann, R. (2005). Diversity and vertical distribution of cultured and uncultured *Deltaproteobacteria* in an intertidal mud flat of the Wadden Sea. *Environ. Microbiol.* **7**: 405–418.

Novelli PC, Scranton MI, Michener RH. (1987). Hydrogen distributions in marine sediments. *Limnol. Oceanogr.* **32**: 565–576.

Novelli P, Michelson A, Scranton M, Banta G, Hobbie J, Howarth, R. (1988). Hydrogen and acetate cycling in two sulfate-reducing sediments: Buzzards Bay and Town Cove, Mass. *Geochim. Cosmochim. Acta* **52**: 2477–2486.

Oremland RS, Polcin S. (1982). Methanogenesis and sulfate reduction: competitive and noncompetitive substrates in estuarine sediments. *Appl. Environ. Microbiol.* **44**: 1270–1276.

Oremland RS, Taylor BF. (1978). Sulfate reduction and methanogenesis in marine sediments. *Geochim. Cosmochim. Acta* **42**: 209–214.

Ovanesov K. (2012). Abundance, distribution, and first insights into metabolism of an environmentally important group of sulfate-reducing bacteria. Master thesis. University of Bremen, Bremen, Germany

Pandelia ME, Lubitz W, Nitschke W. (2012). Evolution and diversification of group 1 [NiFe] hydrogenases. Is there a phylogenetic marker for $O_2$-tolerance? *Biochim. Biophys. Acta* **1817**: 1565–1575.

Pester M, Knorr KH, Friedrich MW, Wagner M, Loy A. (2012). Sulfate-reducing microorganisms in wetlands - fameless actors in carbon cycling and climate change. *Front. Microbiol.* **3**: 72.

Petersen JM, Zielinski FU, Pape T, Seifert R, Moraru C, Amann R, *et al*. (2011). Hydrogen is an energy source for hydrothermal vent symbioses. *Nature* **476**: 176–180.

Punshon S, Moore RM. (2008). Photochemical production of molecular hydrogen in lake water and coastal seawater. *Mar. Chem.* **108**: 215–220.

Quast C, Pruesse E, Yilmaz P, Gerken J, Schweer T, Yarza P, *et al.* (2013). The SILVA ribosomal RNA gene database project: improved data processing and web-based tools. *Nucleic Acids Res* **41**: D590–D596.

Rabus R, Venceslau SS, Wöhlbrand L, Voordouw G, Wall JD, Pereira IAC. (2015). A post-genomic view of the ecophysiology, catabolism and biotechnological relevance of sulphate-reducing prokaryotes. In: Poole RK (ed) Vol. 66. *Advances in Microbial Physiology*. Academic Press, pp 55–321.

Ravenschlag K, Sahm K, Knoblauch C, Jørgensen BB, Amann R. (2000). Community structure, cellular rRNA content, and activity of sulfate-reducing bacteria in marine Arctic sediments. *Appl. Environ. Microbiol.* **66**: 3592–3602.

Rizv, R. (2014). Ecology and cultivation of unknown *Flavobacteria* in tidal sediments. Master thesis. Georg-August-University, Göttingen, Germany

Schwartz DE., Fritsch J, Friedrich B. (2013). $H_2$-metabolizing prokaryotes. In Rosenberg E, DeLong EF, Lory S, Stackebrandt E, Thompson F. (eds), *The Prokaryotes*. Springer Berlin Heidelberg, pp. 119–199.

Strous M, Kraft B, Bisdorf R, Tegetmeyer HE. (2012). The binning of metagenomic contigs for microbial physiology of mixed cultures. *Front Microbiol* **3**: 410.

Swan BK, Martinez-Garcia M, Preston CM, Sczyrba A, Woyke T, Lamy D, *et al*. (2011) Potential for chemolithoautotrophy among ubiquitous bacteria lineages in the dark ocean. *Science* **333**: 1296–1300.

Tengölics R, Mészáros L, Győri E, Doffkay Z, Kovács KL, Rákhely G. (2014). Connection between the membrane electron transport system and Hyn hydrogenase in the purple sulfur bacterium, *Thiocapsa roseopersicina* BBS. *Biochim. Biophys. Acta BBA - Bioenerg.* **1837**: 1691–1698.

Vargas WA, Weyman PD, Tong Y, Smith HO, Xu Q. (2011). [NiFe] hydrogenase from *Alteromonas macleodii* with unusual stability in the presence of oxygen and high temperature. *Appl. Environ. Microbiol.* **77**: 1990–1998.

Vignais PM, Billoud B. (2007). Occurrence, classification, and biological function of hydrogenases: An Overview. *Chem. Rev.* **107**: 4206–4272.

Vignais PM, Billoud B, Meyer J. (2001). Classification and phylogeny of hydrogenases. *FEMS Microbiol. Rev.* **25**: 455–501.

Wang L, Liu L, Zheng B, Zhu Y, Wang X. (2013). Analysis of the bacterial community in the two typical intertidal sediments of Bohai Bay, China by pyrosequencing. *Mar. Pollut. Bull.* **72**: 181–187.

Wawer C, Muyzer G. (1995). Genetic diversity of *Desulfovibrio* spp. in environmental samples analyzed by denaturing gradient gel electrophoresis of [NiFe] hydrogenase gene fragments. *Appl. Environ. Microbiol.* **61**: 2203–2210.

Weiss RF. (1970). The solubility of nitrogen, oxygen and argon in water and seawater. *Deep Sea Res. Oceanogr. Abstr.* **17**: 721–735.

Weissgerber T, Sylveste, M, Kröninger L, Dahl C. (2014). A comparative quantitative proteomic study identifies new proteins relevant for sulfur oxidation in the purple sulfur bacterium *Allochromatium vinosum*. *Appl. Environ. Microbiol.* **80**: 2279–2292.

Winfrey MR, Zeikus JG. (1977). Effect of sulfate on carbon and electron flow during microbial methanogenesis in freshwater sediments. *Appl. Environ. Microbiol.* **33**: 275–281.

Zheng B, Wang L, Liu L. (2014). Bacterial community structure and its regulating factors in the intertidal sediment along the Liaodong Bay of Bohai Sea, China. *Microbiol. Res.* **169**: 585–592.

Zhou J, Bruns MA, Tiedje JM. (1996). DNA recovery from soils of diverse composition. *Appl. Environ. Microbiol.* **62**: 316–322.

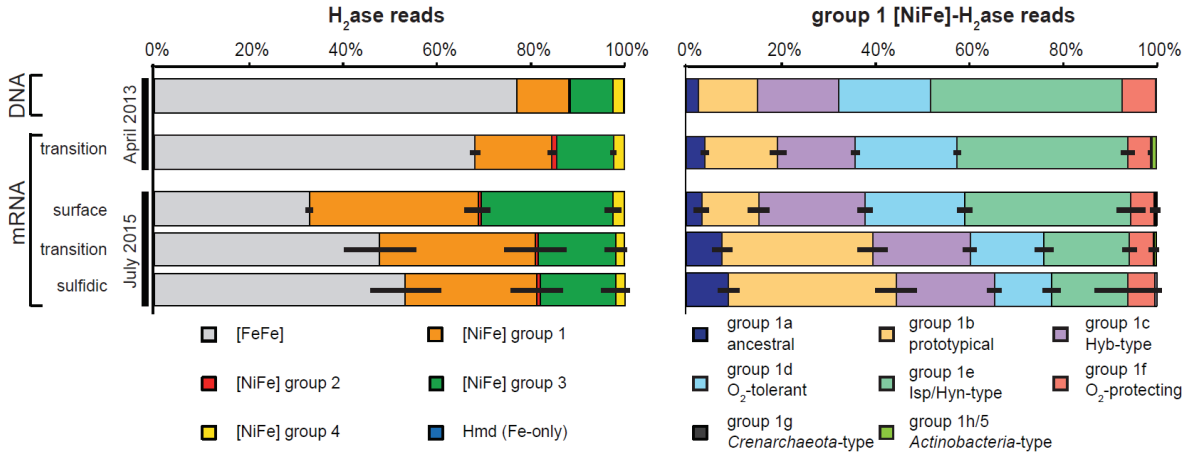


**Figure 1.** Relative frequency of metagenomic and metatranscriptomic sequence reads of $H_2$ases in Janssand sediments in April 2013 and July 2015. Left panel: relative frequency of sequence reads of $H_2$ases with different metal co-factors. Right panel: relative frequency of sequence reads of group 1a-1h [NiFe]-$H_2$ases. In July 2015 samples were taken during low tide at different sediment depth (cm below surface, cmbsf): surface= 0-1 cmbsf, transition=sulfide transition zone 2-3 or 3-4 cmbsf, and sulfidic=sulfidic sediment layer 7-8 cmbsf. All metatranscriptomic samples were taken in triplicate.

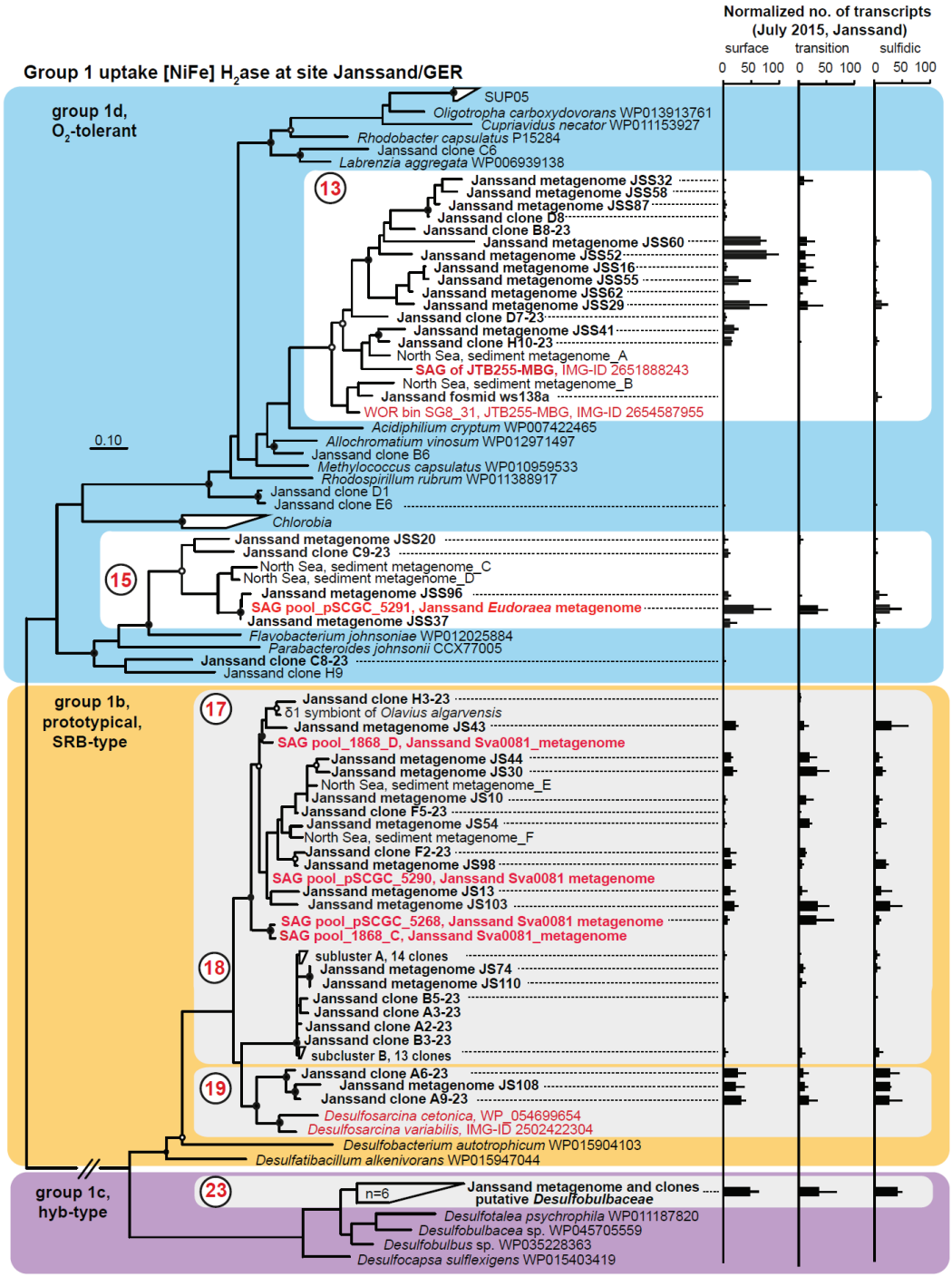


**Figure 2.** Phylogenetic tree of group 1 [NiFe]-$H_2$ase sediment sequence clusters 13, 15, 17-19 (see Supplementary Figure 1 for overview). It displays the prototypic group 1b and $O_2$-tolerant group 1d [NiFe]-$H_2$ase amino acid sequences and the normalized abundance of transcripts from three distinct sediment layers (Janssand, July 2015). Metatranscriptomes were sampled in triplicates. The guide tree was calculated using RAx-Maximum Likelihood and the overall topology was supported by Neighbor-Joining. Circles indicate branches with >70% (closed) and >50% (open) RAxML bootstrap support (100 replicates). For simplicity sequence accession numbers reference sequences of North Sea sediments are provided in Supplementary Table 6. The scale bar indicates 10% sequence divergence.

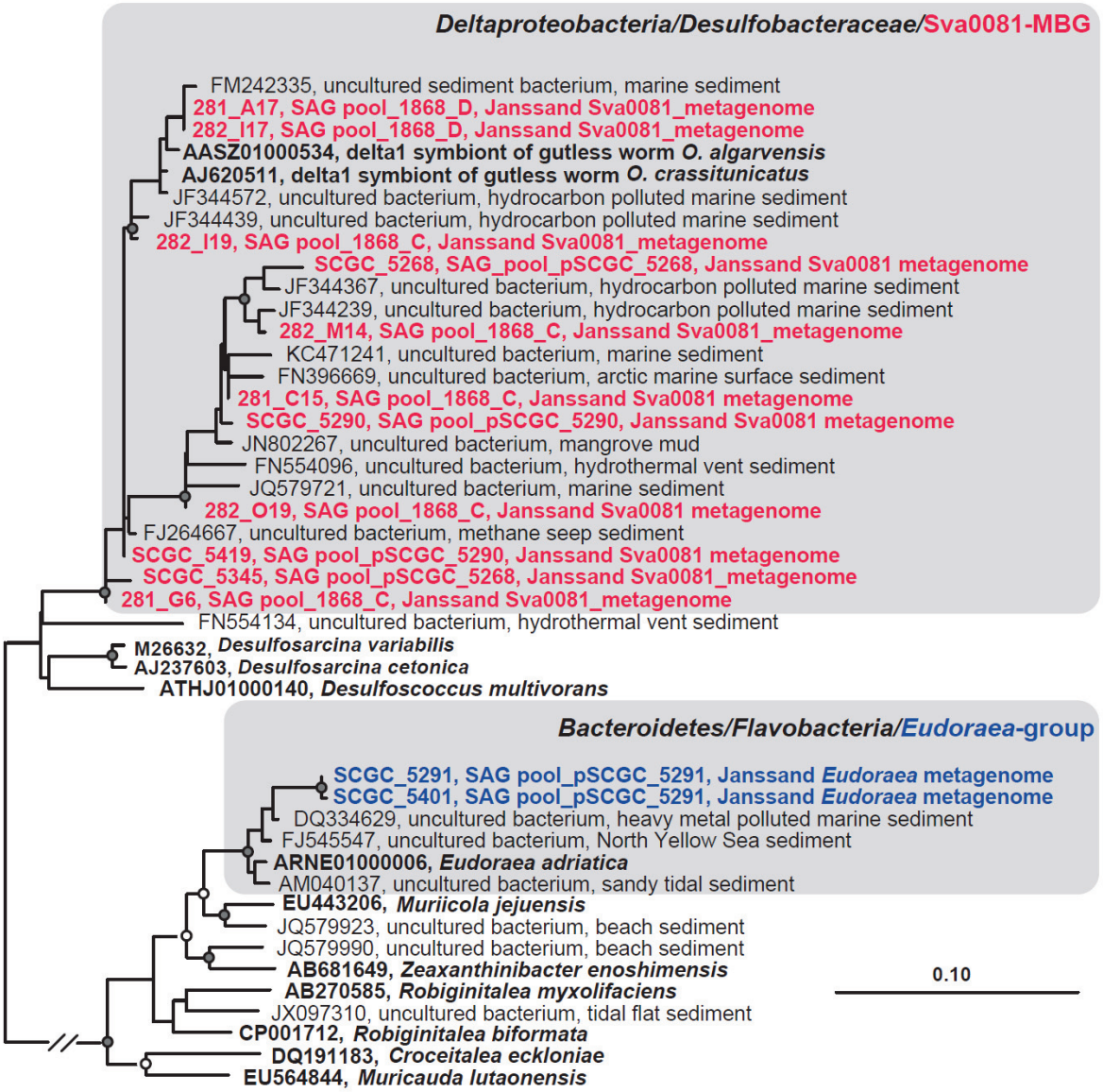


**Figure 3.** Phylogenetic tree of 16S rRNA genes from single amplified (meta)genomes (SAGs) of the Sva0081-MBG/*Desulfobacteraceae* and of *Eudoraea* spp.-group/*Flavobacteriaceae*. The guide tree was calculated with RAxML (100 bootstraps). The overall topology was supported by Neighbor-joining. The scale bar indicates 10% sequence divergence.

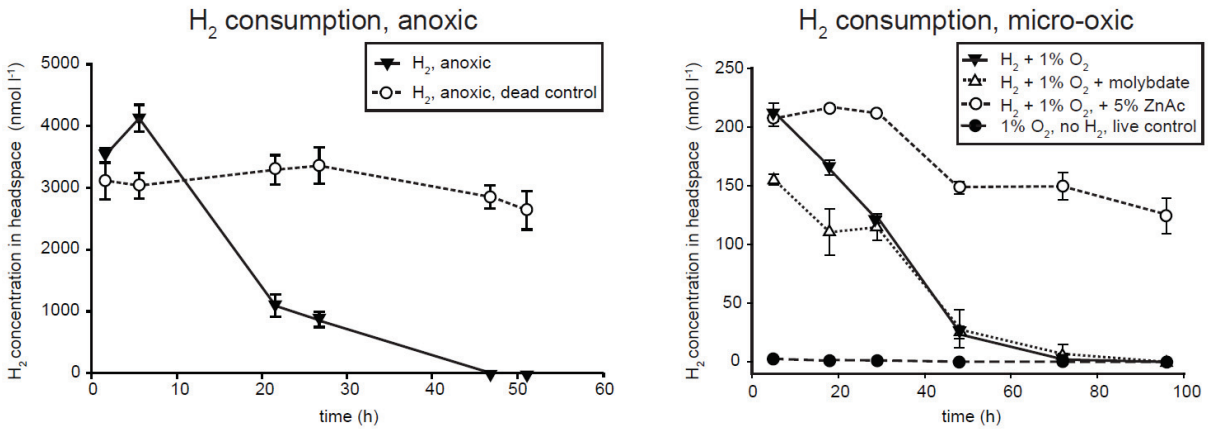


**Figure 4**. Potential $H_2$ consumption rates in sediment slurries from site Janssand. Left panel: sulfidic sediment incubated with 3,600 nmol $H_2$ $l^{-1}$ under anoxic conditions (January 2012). Right panel: sediment from 0-1 cmbsf incubated with 210 nmol $H_2$ $l^{-1}$ under micro-oxic (1% $O_2$) conditions (April 2013). Sodium molybdate (28 mM) was added to inhibit residual sulfate respiration. For dead controls sediments were either inactivated by addition of 5% zinc acetate or were autoclaved. All experiments were performed in triplicates.

**Supplementary Material and Methods**

*Design of $H_2$ase primers for clone library construction*

As primers previously published by Csáki *et al.* (2001) and Kim *et al*. (2007) mainly target alpha-, beta- and gammaproteobacterial group 1 [NiFe]-$H_2$ase genes, we designed novel primer sets to cover a broader diversity of $H_2$ases from sulfate-reducing *Deltaproteobacteria*. An alignment of selected $H_2$ase sequences from SRM (Appendix I) was used as reference and primer sequences were selected using Primrose 2.17 (Ashelford *et al.*, 2002). For evaluation of the novel oligonucleotides (Supplementary Table 4), the gene encoding the large subunit of group 1 [NiFe]-$H_2$ases was amplified from a set of pure cultures (Supplementary Table 5). Details on primer coverage are provided in the Appendix I.

*PCR amplification and sequencing of uptake [NiFe]-$H_2$ases*

Clone libraries of genes encoding the large subunit of group 1 [NiFe]-$H_2$ase were established using DNA extracted from sediment sampled in 2012 at sites Janssand, Mt. St. Michel and Courseulles-sur-Mer (Supplementary Table 1). DNA extraction from three distinct layers was performed using the MoBio Power Soil kit (MoBio Laboratories, Solana Beach, CA, USA) according to the manufacturer's instructions. PCR reactions were performed with primers HUPLX1 (forward) and HUPLW2 (reverse) (Csáki *et al.*, 2001), hupLSRB2f/hupLSRB2r and hupLSRB3f/hupLSRB3r (Supplementary Table 3). The primer HUPLW1, HUPLXF, and HUPLXY (Csáki *et al.*, 2001) were also tested but no amplicon with the specific size was recovered. Each reaction (final volume of 20 µl) contained 10 pmol of each primer, 6.25 nmol of each dNTP, 1x Master *Taq* Buffer and 1U of *Taq* DNA polymerase (Eppendorf, Hamburg, Germany). Thermocycler conditions were as follows: initial denaturation, 95 °C for 5 min, followed by 35 cycles of 95 °C for 60 s, annealing (for temperature see Supplementary Table 3) for 60 s, 72 °C for 2 min and final elongation of 72 °C for 10 min. The expected amplicon length for the primers hupLSRB2f/hupLSRB2r is approximately 1200 bp and approximately 1300 bp for primers hupLSRB3f/hupLSRB3r. Amplified PCR products were cloned using TOPO TA kit for sequencing (pCR4-TOPO, Invitrogen, Germany) or cloned into pGEM-T Easy vector (Promega, Madison, WI, USA) and sequenced with the Big Dye Terminator v3.1 Cycle Sequencing Kit (Applied Biosystems, CA, USA) according to manufacturer's instructions or clones were sent for Sanger-sequencing to GATC Biotech AG (Konstanz, Germany). We recovered 142 sequences from site Janssand (Germany), 84 sequences from Courseulles-sur-Mer (France) and 91 sequences from Mont St. Michel (France).

*Phylogenetic analysis of uptake [NiFe]-$H_2$ases and 16S rRNA genes*

All $H_2$ase sequences were aligned using MAFFT version 7 (Katoh and Standley, 2013) and imported into ARB (Ludwig *et al.*, 2004). Partial sequences of ~600-900 bp from sites

Courseulles-sur-Mer and Mont St. Michel and nearly full-length sequences of ~1200-1500 bp from site Janssand were included for phylogenetic analyses. The alignment was manually corrected. Trees from the corresponding amino acid sequences were constructed in ARB using the maximum-likelihood algorithm RAxML (100 bootstrap resamples, JTT amino acid substitution matrix, Stamatakis *et al.*, 2004) and by Neighbor-Joining trees (1000 bootstrap resamples, Kimura substitution). Detailed trees were calculated for group 1b and 1d [NiFe]-Hases using RAxML and Neighbor-Joining as described above. Only sequences >300 aa and 50% amino acid frequency filters were used for construction of guide trees. Partial sequences were added without changing the overall tree topology using the *Quick Add* parsimony tool in ARB.

For phylogenetic reconstruction of the 16S rRNA genes from pooled SAGs (Supplementary Table 3) we used the SILVA Ref NR99_SSU 117 dataset (Pruesse *et al.,* 2007). For the guide tree, only sequences >1200 bp were used. Trees were calculated by RAxML (100 bootstraps) and Neighbor-Joining (Jukes-Cantor correction, 1000 bootstraps) using 50% base frequency filters. Partial sequences were added without changing the overall tree topology using the *Quick Add* parsimony tool in ARB.

*Nucleotide accession numbers*

$H_2$ase metagenomic and –transcriptomic reads are available in BioProject PRJNA324597. Sequences of group 1 [NiFe]-$H_2$ases gene libraries are available under accession numbers KX352470-KX352722. The genome sequence of the JTB255-MBG SAG is accessible through the Joint Genome Institute portal IMG/ER (https://img.jgi.doe.gov/cgi-bin/er/main.cgi) under the IMG Genome ID 2651869504. The 16S rRNA gene sequences and group 1 [NiFe]-$H_2$ase of SAGs and SAG-pools (Supplementary Table 3) are available under accession no. (pending).

**References**

Ashelford, K.E., Weightman, A.J., and Fry, J.C. (2002) PRIMROSE: a computer program for generating and estimating the phylogenetic range of 16S rRNA oligonucleotide probes and primers in conjunction with the RDP-II database. *Nucleic Acids Res.* **30**: 3481–3489.

Csáki, R., Hanczár, T., Bodrossy, L., Murrell, J. c., and Kovács, K. l. (2001) Molecular characterization of structural genes coding for a membrane bound hydrogenase in *Methylococcus capsulatus* (Bath). *FEMS Microbiol. Lett.* **205**: 203–207.

Katoh, K. and Standley, D.M. (2013) MAFFT multiple sequence alignment software version 7: improvements in performance and usability. *Mol. Biol. Evol.* **30**: 772–780.

Kim JYH, Jung HJ, Cha HJ. (2007). Universal degenerate oligonucleotide-primed-polymerase chain reaction for detection and amplification of NiFe-hydrogenase genes. *Enzyme Microb Technol* **42**: 1–5.

Ludwig, W., Strunk, O., Westram, R., Richter, L., Meier, H., Yadhukumar, et al. (2004) ARB: a software environment for sequence data. *Nucleic Acids Res.* **32**: 1363–1371.

Pruesse E, Quast C, Knittel K, Fuchs BM, Ludwig W, Peplies J et al. (2007). SILVA: a comprehensive online resource for quality checked and aligned ribosomal RNA sequence data compatible with ARB. *Nucleic Acids Res* **35**: 7188–7196.

Stamatakis, A.P., Meier, H., and Ludwig, T. (2004) New fast and accurate heuristics for inference of large phylogenetic trees. In, *Parallel and Distributed Processing Symposium, 2004. Proceedings. 18th International*., p. 193.

**Supplementary Figure 1.** Overview phylogenetic guide tree using maximum-likelihood (RAxML) including all sequences from clone libraries, metagenome and single-cell (meta)genome-derived group 1 uptake [NiFe]-$H_2$ase sequences recovered from site Janssand (JS), Courseulles-sur-Mer (CS) and Mont St. Michel (MM). Abundance and source of sequences in sediment cluster is indicated in parentheses as follows (PCR: JS-CS-MM, metagenome, SAG). Note that sequences from sites Courseulles-sur-Mer and Mt. St. Michel were recovered by PCR-based clone libraries only. The normalized abundance of transcripts from three distinct sediment layers (Janssand April 2013: only sulfide transition layer, July 2015: all three layers, see Figure 2) is given as average of triplicate metatranscriptomes. Standard deviations were omitted for simplicity as they indicated no significant differential expression for the individual sediment clusters except for sediment cluster 17 (see Figure 2). The scale bar indicates 10% sequence divergence.

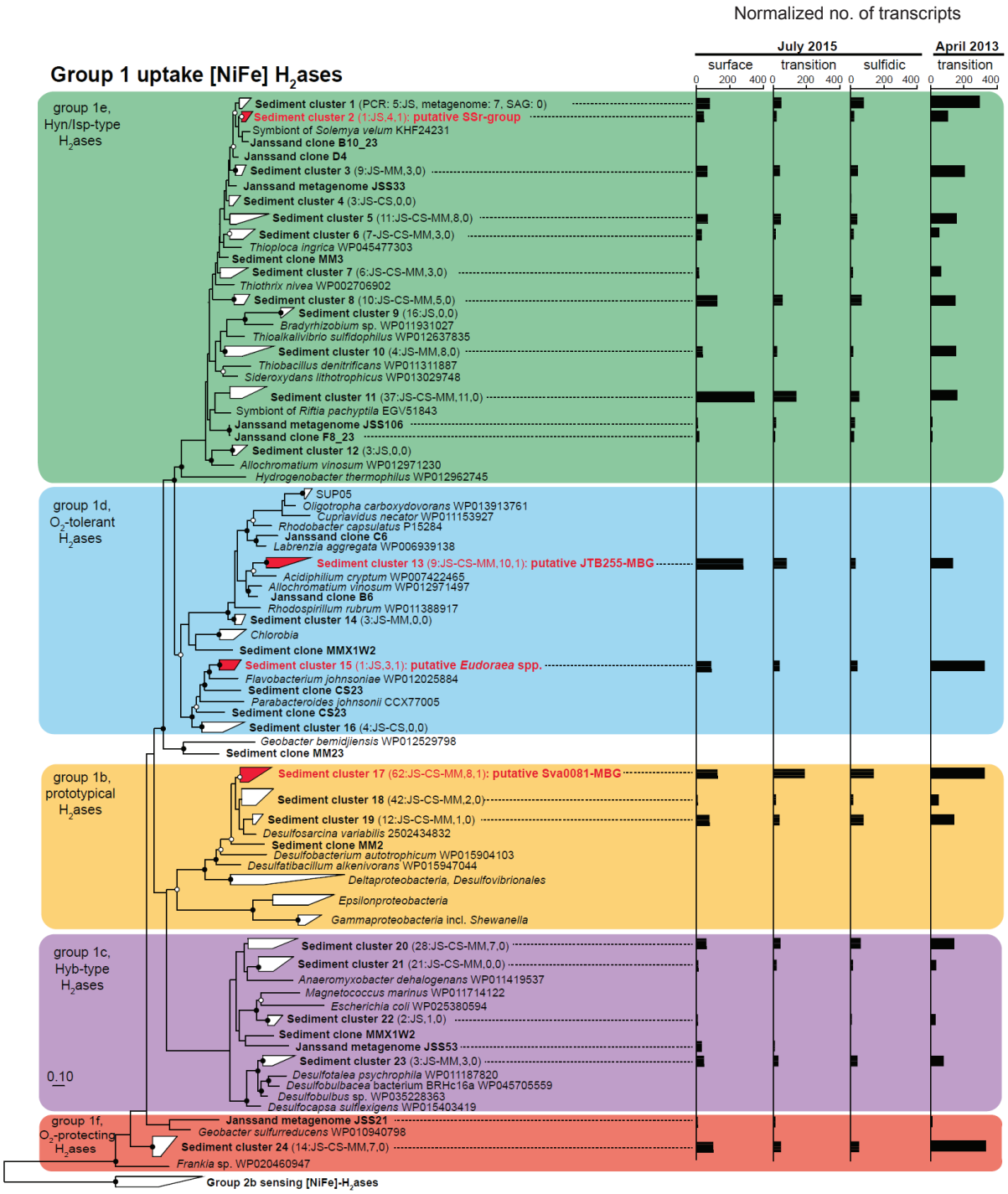
Normalized no. of transcripts
July 2015
April 2013
surface
transition
sulfidic
transition
0 200 400
Group 1 uptake [NiFe] H2ases
group 1e, Hyn/Isp-type H2ases
Sediment cluster 1 (PCR: 5:JS, metagenome: 7, SAG: 0)
Sediment cluster 2 (1:JS,4,1): putative SSr-group
Symbiont of Solemya velum KHF24231
Janssand clone B10_23
Janssand clone D4
Sediment cluster 3 (9:JS-MM,3,0)
Janssand metagenome JSS33
Sediment cluster 4 (3:JS-CS,0,0)
Sediment cluster 5 (11:JS-CS-MM,8,0)
Sediment cluster 6 (7-JS-CS-MM,3,0)
Thioploca ingrica WP045477303
Sediment clone MM3
Sediment cluster 7 (6:JS-CS-MM,3,0)
Thiothrix nivea WP002706902
Sediment cluster 8 (10:JS-CS-MM,5,0)
Sediment cluster 9 (16:JS,0,0)
Bradyrhizobium sp. WP011931027
Thioalkalivibrio sulfidophilus WP012637835
Sediment cluster 10 (4:JS-MM,8,0)
Thiobacillus denitrificans WP011311887
Sideroxydans lithotrophicus WP013029748
Sediment cluster 11 (37:JS-CS-MM,11,0)
Symbiont of Riftia pachyptila EGV51843
Janssand metagenome JSS106
Janssand clone F8_23
Sediment cluster 12 (3:JS,0,0)
Allochromatium vinosum WP012971230
Hydrogenobacter thermophilus WP012962745
group 1d, O2-tolerant H2ases
SUP05
Oligotropha carboxydovorans WP013913761
Cupriavidus necator WP011153927
Rhodobacter capsulatus P15284
Janssand clone C6
Labrenzia aggregata WP006939138
Sediment cluster 13 (9:JS-CS-MM,10,1): putative JTB255-MBG
Acidiphilium cryptum WP007422465
Allochromatium vinosum WP012971497
Janssand clone B6
Rhodospirillum rubrum WP011388917
Sediment cluster 14 (3:JS-MM,0,0)
Chlorobia
Sediment clone MMX1W2
Sediment cluster 15 (1:JS,3,1): putative Eudoraea spp.
Flavobacterium johnsoniae WP012025884
Sediment clone CS23
Parabacteroides johnsonii CCX77005
Sediment clone CS23
Sediment cluster 16 (4:JS-CS,0,0)
Geobacter bemidjiensis WP012529798
Sediment clone MM23
group 1b, prototypical H2ases
Sediment cluster 17 (62:JS-CS-MM,8,1): putative Sva0081-MBG
Sediment cluster 18 (42:JS-CS-MM,2,0)
Sediment cluster 19 (12:JS-CS-MM,1,0)
Desulfosarcina variabilis 2502434832
Sediment clone MM2
Desulfobacterium autotrophicum WP015904103
Desulfatibacillum alkenivorans WP015947044
Deltaproteobacteria, Desulfovibrionales
Epsilonproteobacteria
Gammaproteobacteria incl. Shewanella
group 1c, Hyb-type H2ases
Sediment cluster 20 (28:JS-CS-MM,7,0)
Sediment cluster 21 (21:JS-CS-MM,0,0)
Anaeromyxobacter dehalogenans WP011419537
Magnetococcus marinus WP011714122
Escherichia coli WP025380594
Sediment cluster 22 (2:JS,1,0)
Sediment clone MMX1W2
Janssand metagenome JSS53
Sediment cluster 23 (3:JS-MM,3,0)
Desulfotalea psychrophila WP011187820
Desulfobulbacea bacterium BRHc16a WP045705559
Desulfobulbus sp. WP035228363
Desulfocapsa sulfiexigens WP015403419
0.10
group 1f, O2-protecting H2ases
Janssand metagenome JSS21
Geobacter sulfurreducens WP010940798
Sediment cluster 24 (14:JS-CS-MM,7,0)
Frankia sp. WP020460947
Group 2b sensing [NiFe]-H2ases

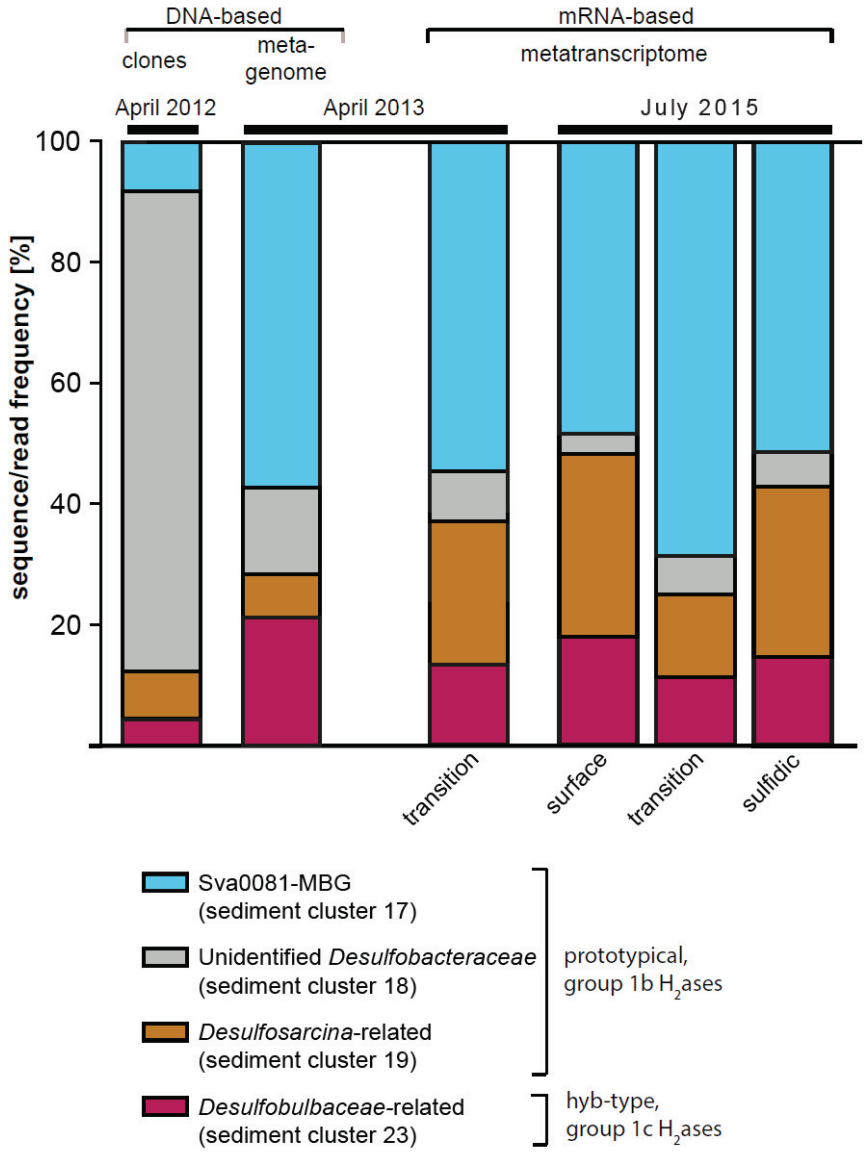


**Supplementary Figure 2.** Relative frequency of clone sequences, assembled metagenomic fragments and metatranscriptomic reads affiliated with sulfate-reducing microorganisms at site Janssand. Sediment clusters 17-19 belong to prototypic group 1b [NiFe]-$H_2$ases of *Desulfobacteraceae*, sediment cluster 23 belong to group 1c [NiFe]-$H_2$ases related to *Desulfobulbaceae*.

**Supplementary Table 1.** Sampling sites and performed experiments

| Site, country | Sampling position (Lat, Lon) | Sampling date | Surface temperature (°C) | Sampling depth (cmbsf) (A=surface, B= sulfide transition, C= sulfidic) | Performed experiments |
|---|---|---|---|---|---|
| Janssand, GER | 52.7366N, 7.6989E | January 2011 | | A: 0-1, B: 1-2 | [a] |
| Janssand, GER | 52.7366N, 7.6989E | January 2012 | 5 | C: 3-5 | [b] |
| Janssand, GER | 53.7368N, 7.6989E | March 2012 | 8 | A: 0-1, B: 7-8, C: 12-13 | [c] |
| Janssand, GER | 53.7366N, 7.6989E | April 2013 | 13 | A: 0-1, B: 2-3, C: 6-7 | [b, d, e] |
| Janssand, GER | 53.7375N, 7.6988E | July 2015 | 18 | Supplementary Table 2 | [e] |
| Courseulles-sur-Mer, FRA | 49.3395N, 0.4695W | October 2012 | 18 | A: 0-1, B: 2-3, C: 6-7 | [c] |
| Mont St. Michel, FRA | 48.6138N, 1.7436W | October 2012 | 18 | A: 0-1, B: 5-6, C: 7-8 | [c] |

[a] single cell genomics; [b] $H_2$ oxidation experiments; [c] clone libraries; [d] metagenomics; [e] metatranscriptomics

**Supplementary Table 2.** Sample IDs and reads abundances of metatranscriptomes from site Janssand

| Sampling date | Sediment depth | Layer | Sample ID | core no. | Reads* |
|---|---|---|---|---|---|
| April 2013 | 2-3 cm | transition | A | | 29,029,446 |
| | 2-3 cm | transition | B | | 29,726,577 |
| | 2-3 cm | transition | C | | 33,590,664 |
| July 2015 | 0-1 cm | surface | A | 1 | 30,334,650 |
| | 3-4 cm | transition | B | 1 | 23,645,294 |
| | 7-8 cm | sulfidic | C | 1 | 22,259,685 |
| | 0-1 cm | surface | D | 2 | 28,626,609 |
| | 2-3 cm | transition | E | 2 | 20,595,041 |
| | 7-8 cm | sulfidic | F | 2 | 29,235,314 |
| | 0-1 cm | surface | G | 3 | 29,610,575 |
| | 2-3 cm | transition | H | 3 | 21,066,755 |
| | 7-8 cm | sulfidic | I | 3 | 20,830,901 |

* Number of paired reads kept after quality trimming

**Supplementary Table 3.** Pooling scheme of single amplified genomes (SAGs), accession no. and service institutions.

| | 16S rRNA gene acc. no of individual SAG | SAG pool identifier | 16S rRNA gene acc. no from SAG pool after sequencing | WGA[a] by sequenced by |
|---|---|---|---|---|
| **SAG identifier** | | | | |
| *Eudoraea* spp. | | | | |
| SCGC_5401 | Pending | pSCGC_5291* | Pending | SCGC[b] JGI[c] |
| SCGC_5291* | Pending | | | |
| Sva0081-MBG | | | | |
| SCGC_5345 | Pending | pSCGC_5268* | Pending | SCGC[b] JGI[c] |
| SCGC_5268* | Pending | | | |
| SCGC_5290* | Pending | pSCGC_5290* | Pending | SCGC[b] JGI[c] |
| SCGC_5419 | Pending | | | |
| 282_O19 | Pending | 1868_C | Pending | SciLifeLab[d] MP-GC[e] |
| 281_G6 | Pending | | | |
| 281_C15 | Pending | | | |
| 282_I19 | Pending | | | |
| 282_M14 | Pending | | | |
| 282_I17 | Pending | 1868_D | Pending | SciLifeLab[d] MP-GC[e] |
| 281_A17 | Pending | | | |

[a] whole genome amplification
[b] Bigelow Laboratory Single Cell Genomics Centre, Bigelow, USA
[c] Joint Genome Institute, Walnut Creek, USA
[d] Microbial Single Cell Genomics facility at SciLifeLab, University of Uppsala, Sweden
[e] Max Planck Genome Centre, Cologne, Germany

**Supplementary Table 4.** PCR primers used in this study

| Primer | Sequence (5'-3') | Annealing Temperature (°C) | Reference |
|---|---|---|---|
| HUPLX1 | GACCCSGTBACSCGNATYGARGG | 65 | (Csáki *et al.*, 2001) |
| HUPLW2 | RCANGCNAGRCASGGGTCGAA | 65 | (Csáki *et al.*, 2001) |
| HupLSRB2f | GSAGCCCAGTTYCAGCAC | 53 | This study |
| HupLSRB2r | CCAGGTKGAGGGAACMAC | 53 | This study |
| HupLSRB3f | GCCCTSGACTGGGTBGAYRT | 55 | This study |
| HupLSRB3r | CAGGCVAKRCABGGRTCRAA | 55 | This study |

**Supplementary Table 5.** Evaluation of novel PCR primer sets on pure cultures of sulfate-reducing bacteria

| | | Amplicon with primers set | | |
|---|---|---|---|---|
| **Species** | DSM no. | hupLX1/W2 (Csaki et al., 2001) | hupLSRB2f/r (This study) | hupLSRB3f/r (This study) |
| *Syntrophobacter fumaroxidans* | 10017 | + | + | + |
| *Desulfatibacillum alkenivorans* | 16219 | - | + | - |
| *Desulfobacterium autotrophicum* | 3382 | - | + | - |
| *Desulfosarcina variabilis* | 2060 | - | + | + |
| *Desulfobacter postgatei* | 2034 | + | - | - |
| *Desulfobulbus propionicus* | 2032 | - | - | + |
| *Desulfotalea psychophila* | 12343 | - | - | + |
| *Desulfovibrio fructosivorans* | 3604 | + | - | + |
| *Sulfurimonas denitrificans** | 1251 | - | + | - |

+ specific PCR product, - no PCR product, * non-sulfate-reducing *Epsilonproteobacteria*

**Supplementary Table 6.** Accession numbers of group 1 [NiFe]-$H_2$ase reference sequences from North Sea sediment metagenomes in Figure 2.

| **Sequence name in tree (Figure 2)** | **IMG gene ID** |
|---|---|
| North Sea, sediment metagenome_A | Ga0065183_110804171 |
| North Sea, sediment metagenome_B | Ga0065183_107219501 |
| North Sea, sediment metagenome_C | Ga0055584_1022313581 |
| North Sea, sediment metagenome_D | Ga0055584_1000122545 |
| North Sea, sediment metagenome_E | Ga0065183_102383401 |
| North Sea, sediment metagenome_F | Ga0055584_1002724581 |

## References

Csáki R, Hanczár T, Bodrossy L, Murrell J c., Kovács K l. (2001). Molecular characterization of structural genes coding for a membrane bound hydrogenase in *Methylococcus capsulatus* (Bath). *FEMS Microbiol Lett* **205**: 203–207

## Supporting Information

**Appendix S1:** Primer evaluation on hydrogenase genes in SRM (meta)genomes (available at Joint Genome Institute, IMG platform, May 2016).

| IMG: Gene ID or Locus tag | IMG: gene product name | targeted by | | | |
|---|---|---|---|---|---|
| | | HupLSRB2f | HupLSRB2r | HupLSRB3f | HupLSRB3r |
| 644405509 | Nickel-dependent hydrogenase large subunit | | | | |
| 2595078610 | NiFe hydrogenase large subunit | | | | |
| orf68 0100 5 | Nickel-dependent hydrogenase, large subunit | | | | |
| JGI24668J20090_100028693 | NiFe-hydrogenase I large subunit | | | | |
| JGI24669J20092_100009643 | NiFe-hydrogenase I large subunit | | | | |
| JGI24670J26820_116366605 | NiFe-hydrogenase I large subunit | | | | |
| JGI25716J29047_114730585 | NiFe-hydrogenase I large subunit | | | | |
| Ga0052190_1016636 | NiFe-hydrogenase I large subunit | | | | |
| Ga0065184_100008933 | NiFe-hydrogenase I large subunit | | | | |
| Ga0065185_100007893 | NiFe-hydrogenase I large subunit | | | | |
| 2503007996 | NiFe hydrogenase large subunit | | | | |
| 2523114984 | NiFe hydrogenase large subunit | | | | |
| 643720967 | HynA | | | | |
| 648711125 | Nickel-dependent hydrogenase large subunit | | | | |
| 2502436589 | NiFe-hydrogenase I large subunit | | | | |
| 2537414111 | NiFe hydrogenase large subunit | | | | |
| 645000006 | Nickel-dependent hydrogenase large subunit | | | | |
| 2595072046 | NiFe hydrogenase large subunit | | | | |
| 2597044397 | NiFe hydrogenase large subunit | | | | |
| 637527826 | Ni/Fe-hydrogenase, large subunit | | | | |
| 2525210765 | NiFe hydrogenase large subunit | | | | |
| 2612205264 | NiFe hydrogenase large subunit | | | | |
| 2638626507 | NiFe hydrogenase large subunit | | | | |
| 644801811 | NiFe hydrogenase large subunit | | | | |
| 647337628 | Nickel-dependent hydrogenase large subunit | | | | |
| 2508669373 | NiFe hydrogenase large subunit | | | | |
| 2558086154 | hydrogenase large subunit | | | | |
| 2639033377 | NiFe hydrogenase large subunit | | | | |
| 649928178 | Nickel-dependent hydrogenase large subunit | | | | |
| 2563384592 | NiFe hydrogenase large subunit | | | | |
| 648112620 | Nickel-dependent hydrogenase large subunit | | | | |
| 2516165900 | NiFe hydrogenase large subunit | | | | |
| 2514920201 | hydrogenase large subunit | | | | |
| 2523326328 | NiFe hydrogenase large subunit | | | | |
| 2541022611 | NiFe hydrogenase large subunit | | | | |
| 2541022315 | NiFe hydrogenase large subunit | | | | |

| | |
|---|---|
| 2541022313 | NiFe-hydrogenase I apoprotein, large subunit |
| 2623443530 | NiFe hydrogenase large subunit |
| 2656899711 | hydrogenase large subunit |
| 645036831 | Nickel-dependent hydrogenase large subunit |
| 2562215499 | NiFe hydrogenase large subunit |
| 2562334896 | hydrogenase large subunit |
| 2588171282 | NiFe hydrogenase large subunit |
| JGI24672J20091_100017575 | NiFe-hydrogenase I large subunit |
| 2515197362 | NiFe hydrogenase large subunit |
| 2523422185 | NiFe hydrogenase large subunit |
| Ga0056138_100053411 | NiFe-hydrogenase I large subunit |
| Ga0056113_10004878 | NiFe-hydrogenase I large subunit |
| Ga0056137_10010493 | NiFe-hydrogenase I large subunit |
| Ga0056112_10004959 | NiFe-hydrogenase I large subunit |
| 2523914283 | hydrogenase large subunit |
| 2524113310 | NiFe hydrogenase large subunit |
| 2623322204 | NiFe hydrogenase large subunit |
| 637123769 | periplasmicNiFe hydrogenase, large subunit, isozyme 2 |
| 2508700825 | ferredoxin hydrogenase large subunit |
| 2508699307 | NiFe hydrogenase large subunit |
| 2523845531 | hydrogenase large subunit |
| 2524232440 | NiFe hydrogenase large subunit |
| 2582525997 | hydrogenase large subunit |
| 2597044293 | NiFe hydrogenase large subunit |
| 2598074110 | ferredoxin hydrogenase large subunit |
| 649843381 | Nickel-dependent hydrogenase large subunit |
| 2525928439 | NiFe hydrogenase large subunit |
| 2540825772 | ferredoxin hydrogenase large subunit |
| 2563206737 | NiFe hydrogenase large subunit |
| 2563206505 | hydrogenase large subunit |
| 2568551726 | ferredoxin hydrogenase large subunit |
| 2583208918 | NiFe hydrogenase large subunit |
| 2587818225 | hydrogenase large subunit |
| 2612204691 | NiFe hydrogenase large subunit |
| 2646275835 | ferredoxin hydrogenase large subunit |
| 2654383969 | NiFe hydrogenase large subunit |
| 637784678 | periplasmic (NiFe) hydrogenase, large subunit, isozyme 2 |
| 637783027 | periplasmic (NiFe) hydrogenase, large subunit, isozyme 1 |
| 643139751 | NiFe-hydrogenase I large subunit |
| 2574173340 | NiFe hydrogenase large subunit |

| | |
|---|---|
| 2587790109 | NiFe hydrogenase large subunit |
| 639819476 | Nickel-dependent hydrogenase, large subunit |
| 639818936 | Nickel-dependent hydrogenase, large subunit |
| 2518924523 | NiFe hydrogenase large subunit |
| 2523307157 | NiFe hydrogenase large subunit |
| 2524894892 | NiFe hydrogenase large subunit |
| 2524893616 | NiFe-hydrogenase I apoprotein, large subunit |
| 2528591788 | NiFe hydrogenase large subunit |
| 2572190346 | ferredoxin hydrogenase large subunit |
| 2621232412 | hydrogenase large subunit |
| 648112215 | Cytochrome-c3 hydrogenase |
| 2507228726 | hydrogenase large subunit |
| 643581839 | Nickel-dependent hydrogenase large subunit |
| 643581633 | NiFe-hydrogenase I apoprotein, large subunit |
| 2514390240 | ferredoxin hydrogenase large subunit |
| 2514388568 | NiFe hydrogenase large subunit |
| 2588094852 | NiFe hydrogenase large subunit |
| 646846126 | Nickel-dependent hydrogenase large subunit |
| 2514486646 | hydrogenase large subunit |
| 2514486499 | NiFe hydrogenase large subunit |
| 2595154195 | NiFe hydrogenase large subunit |
| 2595151730 | hydrogenase large subunit |
| 643540248 | Nickel-dependent hydrogenase large subunit |
| 643538766 | Nickel-dependent hydrogenase large subunit |
| 2508601824 , | hydrogenase large subunit |
| 2527180206 | NiFe hydrogenase large subunit |
| 2574508305 | NiFe hydrogenase large subunit |
| 2576856899 | NiFe hydrogenase large subunit |
| 2576856829 | ferredoxin hydrogenase large subunit |
| 2585089270 | hydrogenase large subunit |
| JGI24673J20094_1000031411 | NiFe-hydrogenase I large subunit |
| JGI24669J20092_1000019416 | NiFe-hydrogenase I large subunit |
| JGI24670J26820_1163752548 | NiFe-hydrogenase I large subunit |
| JGI25716J29047_1147383648 | NiFe-hydrogenase I large subunit |
| Ga0049118_1000002535 | NiFe-hydrogenase I large subunit |
| Ga0049118_100857211 | NiFe-hydrogenase I large subunit |
| Ga0056122_1000003235 | NiFe-hydrogenase I large subunit |
| Ga0056122_1000003829 | NiFe-hydrogenase I large subunit |
| Ga0056122_100057871 | NiFe-hydrogenase I large subunit |
| Ga0056137_100001428 | NiFe-hydrogenase I large subunit |
| Ga0056137_10016624 | NiFe-hydrogenase I large subunit |

| | |
|---|---|
| Ga0049117 100005389 | NiFe-hydrogenase I large subunit |
| Ga0049119_10001214 | NiFe-hydrogenase I large subunit |
| Ga0049119_10709271 | NiFe-hydrogenase I large subunit |
| Ga0065184_1000000779 | NiFe-hydrogenase I large subunit |
| Ga0065185_1000000935 | NiFe-hydrogenase I large subunit |
| 2598073802 | NiFe hydrogenase large subunit |
| 639703724 | Nickel-dependent hydrogenase, large subunit |
| 2574153587 | NiFe hydrogenase large subunit |
| 2638625652 | NiFe-hydrogenase I apoprotein, large subunit |
| 2541188942 | NiFe hydrogenase large subunit |
| 2574147102 | NiFe hydrogenase large subunit |
| 2574204277 | NiFe hydrogenase large subunit |
| 2620573311 | NiFe hydrogenase large subunit |
| 2524272668 | NiFe hydrogenase large subunit |
| 2515940352 | NiFe hydrogenase large subunit |
| 2523531168 | NiFe hydrogenase large subunit |
| JGI24672J20091_1000003416 | NiFe-hydrogenase I large subunit |
| Ga0056138_100000496 | NiFe-hydrogenase I large subunit |
| Ga0056113_100003029 | NiFe-hydrogenase I large subunit |
| Ga0114885_1083856 | NiFe hydrogenase large subunit |
| 649853399 | Nickel-dependent hydrogenase large subunit |
| 2526261803 | NiFe-hydrogenase I large subunit |
| 2574158876 | NiFe hydrogenase large subunit |
| 2515863299 | NiFe hydrogenase large subunit |
| 2588105827 | NiFe hydrogenase large subunit |
| JGI24673J20094_100279691 | NiFe-hydrogenase I large subunit |
| JGI24672J20091_100074731 | NiFe-hydrogenase I large subunit |
| Ga0049117_100001461 | NiFe-hydrogenase I large subunit |
| 648708799 | Cytochrome-c3 hydrogenase |
| 2501939430 | F420-non-reducing hydrogenase subunit A |
| 2501938422 | hydrogenase large subunit |
| 2510244675 | hydrogenase large subunit |
| 2510242326 | hydrogenase large subunit |
| 2510241718 | hydrogenase large subunit |
| 2502438970 | NiFe-hydrogenase III large subunit |
| 2502438769 | NiFe-hydrogenase III large subunit |
| 2502434832 | NiFe-hydrogenase I large subunit |
| 2522159913 | Nickel-dependent hydrogenase |
| 2523967573 | hydrogenase large subunit |
| 2562527838 | NiFe hydrogenase large subunit |
| 2579732409 | NiFe hydrogenase large subunit |
| 2588508210 | hydrogenase large subunit |
| 2648644610 | hydrogenase large subunit |
| 637123154 | periplasmicNiFe hydrogenase, large subunit, isozyme 1 |

| | |
|---|---|
| 637123150 | periplasmic |
| 645001194 | Nickel-dependent hydrogenase large subunit |
| 2507427916 | hydrogenase large subunit |
| 2507427835 | hydrogenase large subunit |
| 2507427304 | hydrogenase large subunit |
| 2507425773 | hydrogenase large subunit |
| 2508699310 | hydrogenase large subunit |
| 2505283578 | hydrogenase large subunit |
| 2503788802 | NiFe hydrogenase large subunit |
| 2523908838 | Nickel-dependent hydrogenase |
| 2523908837 | NiFe hydrogenase large subunit |
| 2597044294 | Nickel-dependent hydrogenase |
| 637529521 | NAD(P)-dependent Nickel-iron dehydrogenase catalytic subunit |
| 637527407 | similar to cytochrome-c3 hydrogenase (NiFeSe), large subunit |
| 649842741 | Nickel-dependent hydrogenase large subunit |
| 650891413 | Nickel-dependent hydrogenase large subunit |
| 2503788087 | NiFe hydrogenase large subunit |
| 2525728026 | hydrogenase large subunit |
| 2525725080 | hydrogenase large subunit |
| 2540825143 | NiFe hydrogenase large subunit |
| 2568551616 | NiFe hydrogenase large subunit |
| 2612205263 | Nickel-dependent hydrogenase |
| 2620502094 | NiFe hydrogenase large subunit |
| 2646274870 | NiFe hydrogenase large subunit |
| 2656812246 | hydrogenase large subunit |
| 2656812245 | hydrogenase large subunit |
| 637783024 | NiFeSe) hydrogenase, large subunit, selenocysteine-containing |
| 643137516 | NiFe-hydrogenase I large subunit |
| 644840202 | Nickel-dependent hydrogenase large subunit |
| 644840066 | Nickel-dependent hydrogenase large subunit |
| 2507127932 | hydrogenase large subunit |
| 2507126251 | hydrogenase large subunit |
| 2507124978 | hydrogenase large subunit |
| 2524001555 | NiFe hydrogenase large subunit |
| 2568540186 | NiFe hydrogenase large subunit |
| 2595078611 | Nickel-dependent hydrogenase |
| 637912001 | NiFe-hydrogenase large subunit |
| 637911861 | NiFe-hydrogenase large subunit |
| 637911350 | NiFe-hydrogenase large subunit |
| 637910522 | NiFe-hydrogenase large subunit |
| 639819479 | Nickel-dependent hydrogenase, large subunit |

| | |
|---|---|
| 644401216 | Nickel-dependent hydrogenase large subunit |
| 646853416 | Nickel-dependent hydrogenase large subunit |
| 649926633 | Nickel-dependent hydrogenase large subunit |
| 649988675 | Cytochrome-c3 hydrogenase |
| 2509273730 | hydrogenase large subunit |
| 2509270523 | hydrogenase large subunit |
| 2509269915 | hydrogenase large subunit |
| 2514680147 | hydrogenase large subunit |
| 2511486587 | NiFe-hydrogenase I large subunit |
| 2511486368 | NiFe-hydrogenase I large subunit |
| 2511486004 | hydrogenase large subunit |
| 2506602637 | hydrogenase large subunit |
| 2523631346 | NiFe hydrogenase large subunit |
| 2523711418 | NiFe hydrogenase large subunit |
| 2527068693 | NiFe hydrogenase large subunit |
| 2572192879 | NiFe hydrogenase large subunit |
| 2651739353 | NiFe hydrogenase large subunit |
| 643563290 | Nickel-dependent hydrogenase large subunit |
| 643563191 | Nickel-dependent hydrogenase large subunit |
| 643562662 | hydrogen:quinone oxidoreductase |
| 643560720 | Nickel-dependent hydrogenase large subunit |
| 2507228328 | hydrogenase large subunit |
| 2507227045 | hydrogenase large subunit |
| 2507226995 | hydrogenase large subunit |
| 2509741687 | NiFe hydrogenase large subunit |
| 2512873150 | quinone-reactive Ni/Fe-hydrogenase large subunit |
| 2516167362 | NiFe hydrogenase large subunit |
| 2656900525 | hydrogenase large subunit |
| 646845900 | Cytochrome-c3 hydrogenase |
| 646845739 | Nickel-dependent hydrogenase large subunit |
| 2508512363 | hydrogenase large subunit |
| 2508512196 | hydrogenase large subunit |
| 2502445612 | NiFe-hydrogenase I large subunit |
| 2502444211 | NiFe-hydrogenase I large subunit |
| 2502443232 | NiFe-hydrogenase I large subunit |
| 2502443231 | NiFe-hydrogenase I large subunit |
| 2502442079 | NiFe-hydrogenase I large subunit |
| 2523311096 | NiFe hydrogenase large subunit |
| 2566033826 | NiFe hydrogenase large subunit |
| 2571096069 | NiFe hydrogenase large subunit |
| 2583134717 | NiFe hydrogenase large subunit |
| 2653076074 | hydrogenase large subunit |
| 2653074786 | hydrogenase large subunit |

| | |
|---|---|
| 643538769 | Nickel-dependent hydrogenase large subunit |
| 643719900 | HysA |
| 2508601061 | hydrogenase large subunit |
| 2508506329 | hydrogenase large subunit |
| 2508505836 | hydrogenase large subunit |
| 2520044566 | NiFe hydrogenase large subunit |
| 2524221153 | hydrogenase large subunit |
| 2524277342 | NiFe hydrogenase large subunit |
| 2524275249 | hydrogenase large subunit |
| 2574444789 | hydrogenase large subunit |
| 2600105052 | NiFe hydrogenase large subunit |
| 2620818713 | NiFe hydrogenase large subunit |

# Quantifying acetate assimilation by major bacterial populations in a marine sediment

Stefan Dyksma[a], Sabine Lenk[a], Joanna E. Sawicka[b], and Marc Mußmann[a,c*]

[a] Department of Molecular Ecology, Max Planck Institute for Marine Microbiology, Bremen, Germany

[b] Department of Biogeochemistry, Max Planck Institute for Marine Microbiology, Bremen, Germany

[c] University of Vienna, Department of Microbiology and Ecosystem Science, Division of Microbial Ecology, Vienna, Austria

[*]To whom correspondence should be addressed: University of Vienna, Department of Microbiology and Ecosystem Science, Division of Microbial Ecology, A-1090 Vienna, Austria, Tel +43 1 4277 54207, mussmann@microbial-ecology.net

Running title: Acetate-assimilating bacteria in a marine sediment

Keywords: sulfate-reducing bacteria, *Desulfobacteraceae*, *Desulfobulbaceae*, *Gammaproteobacteria*, *Roseobacter*-clade bacteria, polyhydroxyalkanoates, flow cytometry

**Abstract**

Acetate is a key intermediate in organic matter mineralization in aquatic sediments. To quantify acetate assimilation by distinct bacterial populations in marine sediments, we incubated sediment cores with $^{14}$C-labeled acetate and flow-sorted cells identified by fluorescence *in situ* hybridization or stained by Nile Red, a fluorescent dye for polyhydroxyalkanoates (PHA). Subsequently, scintillography determined the amount of $^{14}$C-acetate assimilated by distinct populations. By integrating $^{14}$C-acetate assimilation rates and cell abundances, we measured total uptake and the relative contribution of individual populations to the overall acetate uptake by *Bacteria*. Acetate uptake was highest in the surface layer (0-1 cm) for all sorted populations. Although cell-specific uptake rates were highest in *Roseobacter*-clade bacteria, they contributed only up to 11% to total bacterial acetate assimilation because of their low cell abundance *in situ*. Sulfate-reducing *Desulfobacterales* accounted for up to 32% of total bacterial acetate assimilation, while *Gammaproteobacteria* dominated acetate uptake in all sediment layers with a relative acetate uptake of 31-62%. Flow-sorting of Nile Red-stained cells demonstrated that some yet unidentified microorganisms assimilated $^{14}$C-acetate into PHA with rates exceeding those of the sorted bacterial population by 3-fold. Our results suggest that phylogenetically and metabolically diverse bacteria consume acetate in distinct layers of tidal sediments.

## Introduction

In organic-rich coastal and ocean margin sediments oxygen is already depleted in a few millimetres depth below the sediment surface, thus a large fraction of organic matter is degraded anaerobically (Jørgensen, 1977; Jørgensen, 1982). Under anoxic conditions complex organic matter is fermented and molecular hydrogen and volatile fatty acids such as propionate and acetate are released and respired by different terminal electron accepting processes (Christensen and Blackburn, 1982; Reeburgh, 1983; Novelli *et al.*, 1988). In marine sediments acetate is quickly turned over and pore water concentrations are typically in the micromolar range (Sørensen *et al.*, 1981; Christensen, 1984; Parkes *et al.*, 1989; Kristensen, 1994; Finke *et al.*, 2007; Valdemarsen and Kristensen, 2010). Several studies have shown that acetate stimulates in particular sulfate respiration in marine sediments (Oremland and Polcin, 1982; Werner *et al.*, 2006). Consistent with this acetate was suggested to be the quantitatively most important substrate for sulfate-reducing bacteria (SRB) that are capable of completely oxidizing organic substrates to $CO_2$ (Laanbroek and Pfennig, 1981; Thauer and Postgate, 1982). Thus, acetate is considered to be a central substrate for sulfate respiration, a process accounting for up to 50% of total carbon mineralization (Jørgensen, 1982).

Stable isotope probing (SIP) has been frequently used to track the consumption of isotopically labelled model substrates into cellular biomarkers such as nucleic acids (DNA-SIP, RNA-SIP) or phospholipid fatty acids (PLFA-SIP) (Boschker *et al.*, 1998; Webster *et al.*, 2006; MacGregor *et al.*, 2006; Miyatake *et al.*, 2009; Webster *et al.*, 2010; Vandieken *et al.*, 2012; Vandieken and Thamdrup, 2013; Na *et al.*, 2015). These studies helped in detecting acetate assimilation by sulfate-reducing *Desulfobacteraceae*, *Firmicutes*, *Crenarchaeota* and others (Boschker *et al.*, 1998; Webster *et al.*, 2006; Webster *et al.*, 2010; Seyler *et al.*, 2014; Na *et al.*, 2015). Moreover, diverse *Gammaproteobacteria* like *Alteromonadales*, *Oceanospirillales* and *Acidithiobacillales* and the epsilonproteobacterial *Arcobacter* respire acetate using oxygen, nitrate and manganese oxide as electron acceptors (Vandieken *et al.*, 2012; Vandieken and Thamdrup, 2013). Because of relatively long incubation periods in DNA-SIP, cross-feeding and population shifts are well known limitations (Dumont and Murrell, 2005). In these SIP approaches, the uptake of an isotopically labelled model compound by a defined population cannot or only indirectly be quantified. Moreover, microbes assimilating isotopic labels into compounds other than nucleic acids or PFLAs escape detection by SIP. To overcome these limitations, we recently introduced a novel methodological approach, in which we combined $^{14}$C-labeling of cells with catalyzed-reporter deposition fluorescence *in situ* hybridization (CARD-FISH), fluorescence-activated cell sorting (FACS) and scintillography to quantify carbon uptake by a given number of cells of a phylogenetically identified populations (Dyksma *et al.*, 2016).

In our study, we applied this approach to identify the major acetate-assimilating bacterial populations in tidal sediments of the German Wadden Sea. These sediments are characterized by high nutrient concentrations, high aerobic respiration rates and intense sulfur cycling (Billerbeck *et al.*, 2006; Beck *et al.*, 2008; Al-Raei *et al.*, 2009; Jansen *et al.*, 2009). To identify major contributors to acetate assimilation in distinct sediment layers we incubated whole sediment cores and slurries with $^{14}$C-acetate. After CARD-FISH we flow-sorted cell batches of 50,000 cells from major phylogenetic groups for scintillography. Thereby, we aimed at quantifying $^{14}$C-acetate assimilation by *in situ* abundant groups such as *Gammaproteobacteria*, *Roseobacter*-clade bacteria (RCB), sulfate reducing *Desulfobulbaceae* and some *Desulfobacteraceae* (*Desulfosarcina*/*Desulfococcus*-clade). Given their abundance and their metabolic potential to completely oxidize organic compounds to $CO_2$, members of the *Desulfobacteraceae* were suggested to be the key players in carbon- and sulfur-cycling in organic rich marine sediments (Rabus *et al.*, 2015). . In addition, flow-sorting of cells containing fluorescently stained polyhydroxyalkanoates (PHAs) revealed an assimilation of $^{14}$C-acetate into storage compounds.

## Results

*Pore water concentrations of acetate, formate and lactate*

In June 2009 we exemplarily determined the concentrations of acetate, formate and lactate in distinct sediment layers at site Janssand. In the top 10 cm of the sediment concentrations were in the lower micromolar range (Fig. S1). Acetate and lactate concentrations varied between 0 and 12 µM, whereas formate concentrations were below 5 µM.

*Bulk assimilation of acetate and abundance of acetate-assimilating cells*

To quantify acetate assimilation by the bulk sediment and by *in situ* abundant bacterial populations we percolated two sediment cores with seawater containing 100 µM of [1,2-$^{14}$C]-labelled acetate and incubated them for 8h. We used oxic seawater in order to mimic flushing of even deeper sediment layers with fully oxygenated seawater during high tide (de Beer *et al.*, 2005; Jansen *et al.*, 2009). The relative abundance of $^{14}$C-acetate-assimilating cells was determined by microautoradiography (MAR) of DAPI-stained cells. The abundance of acetate-assimilating cells was highest in 0-1 cm depth, equalling 17% of total cell counts and decreased to 2% in 9-10 cm depth (Fig. 1). Similarly, bulk acetate assimilation was highest at in 0-1 cm reaching 7.6 µmol $l^{-1}$ $h^{-1}$ and steeply decreased to 0.2 µmol $l^{-1}$ $h^{-1}$ in 9-10 cm sediment depth (Fig. 1).

*Quantification of acetate assimilation in FISH-identified bacterial populations*

First, we used MAR-FISH to identify major candidate acetate-assimilating populations in the surface layer (0-1 cm) of the whole cores incubated with $^{14}$C-acetate. *Gammaproteobacteria* accounted for about 60% of all MAR-positive cells, whereas *Deltaproteobacteria* and RCB made up only for 6-8% each (Table S1). Approximately 19% of *Gammaproteobacteria*, 40% of RCB and 8% of *Deltaproteobacteria* displayed a MAR-signal (Fig. 2 and Table S1).

Since MAR-FISH is only semi-quantitative and has a low dynamic range of sensitivity we quantified $^{14}$C-acetate assimilation by measuring the bulk substrate uptake by pooling a defined number of phylogenetically identified cells. To this end, we sorted different populations from three distinct sediment layers from the duplicate cores, 50,000 cells each. Our target populations were I) *Bacteria* (probe EUBI-III), II) *Gammaproteobacteria* (probe GAM42a), III) *Roseobacter*-clade bacteria (RCB, probe ROS537), IV) some members of the *Desulfobacteraceae* (probe DSS658) and V) *Desulfobulbaceae* (probe DSB706). For each measurement the flow-sorted batches of 50,000 cells were used for subsequent quantitative scintillography. To estimate background assimilation of acetate we sorted fluorescent beads added to dead controls and fluorescent particles from probe NON33-targeted samples (control for unspecific staining). Background radioactivity was minimal and was subtracted from values of the sorted bacterial populations (Fig. S2).

As a general trend, all studied populations assimilated most acetate in the upper 0-1 cm and assimilated less with increasing sediment depth (Fig. 3a). The $^{14}C$ radioactivity of 50,000 sorted *Bacteria* ranged between 9.8 Bq in the uppermost cm to 0.5 Bq at 6-7 cm sediment depth. In the top cm of the sediment cores *Roseobacter*-clade bacteria (RCB) showed highest $^{14}C$-acetate assimilation (20.1-24.8 Bq), while *Gammaproteobacteria* assimilated 10.1 to 14.2 Bq (Fig. 3a). Also sulfate-reducing *Desulfobacteraceae* and *Desulfobulbaceae* assimilated acetate in the upper one cm ranging from 6.3 to 8.4 Bq and 12.6 to 18.2 Bq, respectively.

By dividing the total amount of assimilated $^{14}C$-acetate per population by the number of sorted cells cell (50,000 per measurement), we calculated the average cell-specific $^{14}C$-acetate uptake. RCB displayed highest cell-specific carbon assimilation rates amounting to 9.7 fg C cell$^{-1}$ d$^{-1}$ (Table 1). The measured cell-specific assimilation rates for *Gammaproteobacteria* were approximately half (5.5 fg C cell$^{-1}$ d$^{-1}$) and sulfate-reducing *Desulfobulbaceae* assimilated acetate up to 7.1 fg C cell$^{-1}$ d$^{-1}$, while *Desulfobacteraceae* showed lower cell-specific rates of up to 3.3 fg C cell$^{-1}$ d$^{-1}$.

*Relative contribution of populations to total bacterial acetate assimilation*

We then calculated the relative contribution of the sorted populations to total acetate assimilation by integrating the relative *in situ* cell abundances in the sediment cores (Fig. S3), the cell-specific $^{14}C$-carbon assimilation and the $^{14}C$-carbon assimilated by *Bacteria*. The relative abundances of the individual target populations were highly similar throughout the upper 7 cm in both cores (Fig. S3). Irrespective of the sediment depth, *Gammaproteobacteria* assimilated most acetate, accounting for 31-62% of total bacterial acetate assimilation (Fig. 3b). The relative contribution of *Desulfobulbaceae* to total acetate assimilation slightly increased with sediment depth, while such an effect was unclear for *Desulfobacteraceae*. Together, SRB contributed up to 32% of total bacterial acetate assimilation (Fig. 3b). Although RCB showed highest $^{14}C$-acetate assimilation per cell, they contributed only 1-11% to bacterial acetate assimilation because of their lower cell abundances (1-2% of total cell counts).

*Sediment slurry incubations in October 2009*

To study acetate assimilation by the individual groups in more detail, we prepared oxic sediment slurries from 0-1 cm depth and anoxic slurries from 10-11 cm depth in October 2009. As whole cores slurries were incubated under similar conditions at 100 µM $^{14}C$-acetate for 6-8 h. In contrast to whole core incubations from June 2009, *Gammaproteobacteria* displayed a 3-fold higher acetate uptake per 50,000 sorted cells than RCB (Fig. 4). *Desulfobulbaceae* and *Desulfobacteraceae* assimilated acetate in oxic and anoxic slurry

incubations but 2 to 3-fold less than in the whole core incubations (Fig. 4). Similar to whole core incubations *Desulfobacteraceae* from surface layers seemed to assimilate more acetate than cells from deeper layers, while this trend was not clear for *Desulfobulbaceae*. Consistent with the whole core incubations *Desulfobulbaceae* assimilated in average more acetate than *Desulfobacteraceae* (Figs. 3a, 4 and Table 1).

In addition, we sorted cells of the uncultured Sva0081-MBG using a newly designed probe DSS_1431 (Fig. S4). The Sva0081-MBG forms a monophyletic subcluster within the *Desulfobacteraceae* and partial 16S rRNA gene sequences of this group have been recovered from site Janssand during earlier sampling and sequencing efforts (Lenk *et al*., 2011). The Sva0081-MBG assimilated acetate in similar rates as *Desulfobacteraceae* and *Desulfobulbaceae* (Table 1).

*Acetate uptake and polyhydroxyalkanoates (PHAs)*

To test, whether acetate is used to build up storage compounds (Anderson and Dawes, 1990), we used the lipophilic, fluorescent dye Nile Red to stain polyhydroxyalkanoates (PHA) in bacterial cells from the oxic and anoxic slurry incubations. We observed strongly fluorescent intracellular inclusions in cells extracted from incubated sediments (Fig. S5). As the intracellular PHA concentration and Nile Red fluorescence intensity correlate linearly (Greenspan *et al.*, 1985; Vidal-Mas *et al.*, 2001) we flow-sorted Nile Red-stained cells according to four fluorescence intensity classes (Fig. S6) and measured $^{14}C$ radioactivity in batches of 50,000 cells.

In the sorted cell fractions, the fluorescence intensity of Nile Red stained cells correlated well with $^{14}C$ radioactivity, suggesting that unidentified microorganisms formed PHAs from acetate (Fig. 5). In oxic incubations, PHA formation from acetate was slightly higher (Fig. 5). Cells with the highest intracellular PHA concentration showed average carbon assimilation rates between 19.8 and 26.4 fg C cell$^{-1}$ d$^{-1}$ (Table S2), which exceeded all cell-specific uptake rates measured for the phylogenetically identified populations (Table 1).

## Discussion

We combined a radioactive labeling of bacterial cells with CARD-FISH and flow-sorting to exactly quantify the assimilation of acetate by a given number of cells of a phylogenetically identified population. Our approach provides a high sample throughput and a precision at the level of populations that complements readily existing methods such as MAR-FISH, HISH-SIMS and DNA/RNA-SIP (Boschker *et al.*, 1998; Nielsen and Nielsen, 2002; Vandieken *et al.*, 2012; Vandieken and Thamdrup, 2013; Na *et al.*, 2015). The scintillography of 50,000 FISH-stained cells thus also includes cells that are labeled below detection limits of techniques such as SIP or MAR-FISH. Single cell methods could be applied after sorting to

achieve a resolution at the single cell level in a higher throughput. These would allow including biovolumes to more accurately infer population-specific uptake rates. To facilitate accurate modelling of carbon budgets, the amount of $^{14}CO_2$ released by respired acetate should be quantified in future experiments.

*Acetate assimilation rates in distinct sediment layers*

The average cell-specific acetate assimilation rates in whole core incubations amounted to 9.7 fg C cell$^{-1}$ d$^{-1}$ (Table 1), which is three orders of magnitude lower than rates reported for activated sludge communities (1.1-7.6 pg C cell$^{-1}$ d$^{-1}$; Nielsen and Nielsen, 2002) but are in the range of rates known for freshwater bacterioplankton (approximately 5-57 fg C cell$^{-1}$ d$^{-1}$; Buck *et al.*, 2009). Bulk sediment uptake and population-specific substrate incorporation were highest in 0-1 cm for all groups investigated in this study (Figs. 1, 3a). This is consistent with earlier studies that showed highest acetate assimilation in oxygenated surface layers (Christensen and Blackburn, 1980; Christensen and Blackburn, 1982). In our experiment, the surface layer (0-1 cm) also comprised the oxic-anoxic interface as indicated by transition of brownish to black-coloured sediment in approximately one cm depth and exemplary $O_2$-microsensor measurements at site Janssand (Jansen *et al*., 2009). In this transition zone nitrate, manganese, ferric iron and sulfate serve as alternative electron acceptors (Kowalski *et al.*, 2012) which likely supported anaerobic acetate uptake during our experiments. Apparently, the incubation conditions and the vertical resolution in our core experiment were not sufficient to clearly discriminate aerobic from anaerobic acetate uptake as it was out of scope of our study to ultimately evaluate acetate uptake under fully oxic versus fully anoxic conditions. Such experiments require a more sophisticated experimental set-up, e.g. as described by Gao *et al.* (2010). However, our data clearly demonstrate that the microbial community displayed a generally higher acetate-assimilating activity at the sediment surface than in deeper layers. In the transition zone, the onset of microbial fermentations fosters the production of $H_2$ and acetate, which in turn stimulate sulfate respiration. Our data also agree with the observation that e.g. sulfate reduction rates can peak right below the oxic-anoxic interface in tidal surface sediments (de Beer *et al.*, 2005; Al-Raei *et al.*, 2009).

Roseobacter*-clade bacteria showed the highest bulk assimilation of $^{14}$C-acetate*

*Roseobacter*-clade bacteria (RCB) are metabolically versatile and thrive as heterotrophs, anoxygenic phototrophs and oxidize inorganic and organic sulfur compounds (Sorokin, 1995; González *et al.*, 1999; Howard *et al.*, 2006; Sass *et al.*, 2010; Curson *et al.*, 2011). In the incubated sediment cores the RCB assimilated most acetate per 50,000 cells of all sorted populations including the total bacterial fraction (Fig. 3, Table 1), but they contributed only up to 11% to bacterial acetate assimilation because of their low cell abundance. However, since

relative cell abundances of RCB seasonally vary in these tidal sediments (Lenk *et al.*, 2012), their contribution to acetate consumption may also shift significantly during a seasonal cycle.
In contrast to whole core incubations, in slurry incubations RCB assimilated less acetate than *Gammaproteobacteria* cells despite identical acetate concentrations and the use of oxic seawater (Figs. 3a, 4, Table 1). RCB and *Gammaproteobacteria* comprise many distinct physiological groups that possibly respond differently to incubations in either undisturbed sediment or slurries. In addition, Vandieken and Thamdrup (2013) observed the accumulation of added acetate in slurry incubations and suggested a lower acetate oxidizing capacity in slurries compared to intact core incubations, possible because of a limitation of electron acceptors. Together, these observations suggest a severe impact of the applied incubation conditions on the measured acetate uptake.

Gammaproteobacteria *dominate bacterial acetate assimilation*

Both MAR-FISH and scintillography of sorted populations suggested that *Gammaproteobacteria* are major acetate consumers in Janssand sediments accounting for up to 62% of total bacterial acetate assimilation (Fig 3b). This is consistent with the previous observation that gammaproteobacterial groups such as *Alteromonadales*, *Acidithiobacillales* and *Oceanospirillales* incorporated acetate in marine sediments using manganese and likely other electron acceptors (Vandieken *et al.*, 2012; Vandieken and Thamdrup, 2013). *Gammaproteobacteria* account for up to 20-25% to total cell counts in Janssand sediments and are central members of the microbial communities in coastal sediments (Fig. S3, Dyksma *et al.*, 2016). These comprise distinct physiological groups including autotrophic and heterotrophic members that possibly assimilated acetate in our experiments. However, our MAR-FISH results indicated that only approximately 20% of *Gammaproteobacteria* assimilated acetate in amounts detectable at the single cell level (Fig. 2 and Table S1), suggesting that only few gammaproteobacterial groups assimilated high amounts of acetate.
The accumulation of high amounts of substrate by a relatively few number of cells within a short incubation period is typical for formation of storage compounds such as PHA. In line with this, the high correlation of acetate uptake and PHA concentrations (Fig. 5) along with the high cellular uptake rates (Table S2) indicate that some, still unknown microorganisms took up relatively large amounts of $^{14}$C-acetate and formed PHA. Our observation that relatively few *Gammaproteobacteria* accounted for most of bacterial acetate assimilation, lets us hypothesize that these formed PHAs during the short-term experiments. However, double labelling of cells with Nile Red and CARD-FISH provided inconclusive results and requires methodological optimization.
In general, PHAs are formed at elevated carbon-to-nitrogen ratios or under nutrient limitation (Macrae and Wilkinson, 1958; Dawes and Senior, 1973; Repaske and Repaske, 1976). In

our incubations, we used 10-fold higher acetate concentrations than in pore waters (Fig. S1) to minimize substrate limitation during the course of our incubations. However, as for most isotopic tracer studies it has to be taken into account that such artificially high acetate concentrations can blur results, as they may favour opportunistic microorganisms adapted to high substrate concentrations. Consistent with this notion, our results suggest that the rapid build-up of PHA under the experimentally introduced nutritional imbalance may have favoured PHA-forming bacteria, possibly some *Gammaproteobacteria*. In the future, the application of specific probes for gammaproteobacterial subgroups along with optimized Nile Red stains may unravel their contribution to bacterial acetate assimilation. Moreover, we recommend semi-continuous culture-like set-ups to guarantee both low substrate concentrations and sufficient isotopic labeling of cells (Pester *et al.*, 2010).

*Sulfate-reducing* Desulfobacteraceae *and* Desulfobulbaceae *assimilated acetate*

In both whole core and slurry experiments the *Desulfobacteraceae* contributed more to total acetate assimilation than *Desulfobulbaceae* (Fig. 3b), although the *Desulfobulbaceae* consistently showed a higher acetate uptake rate both in core and slurry incubations (Figs. 3a, 4, Table 1). The higher *in situ* cell abundances of the *Desulfobacteraceae* made up for the lower cell-specific rates, which explains their prevalent contribution to acetate uptake among SRB (Fig. 3b). *Desulfobacteraceae*, in particular members of the *Desulfosarcina/Desulfococcus*-group and *Desulfobulbaceae* have been regularly identified as the key SRB in marine sediments by 16S rRNA gene libraries and FISH (Devereux *et al.*, 1992; Edgcomb *et al.*, 1999; Ravenschlag *et al.*, 2000; Knittel *et al.*, 2003; Mußmann *et al.*, 2005; Musat *et al.*, 2006). Moreover, *Desulfobacteraceae* have been identified as acetate consumers in SIP approaches using nucleic acids or PFLAs but quantitative data are lacking (Boschker *et al.*, 1998; Webster *et al.*, 2006; Webster *et al.*, 2010; Na *et al*., 2015). Generally, *Desulfobulbaceae* can utilize acetate only as carbon source, whereas most *Desulfobacteraceae* use acetate also energy source (Kuever, 2014; Rabus et al., 2015). According to this distinct pattern of acetate utilization, the *Desulfobulbaceae* in our experiments may have consumed acetate mostly for assimilation into biomass, while *Desulfobacteraceae* probably also respired acetate and thus assimilated a smaller fraction of the consumed acetate.

Unexpectedly, both *Desulfobacteraceae* and *Desulfobulbaceae* assimilated similar amounts of acetate in oxic and anoxic slurry incubations (Table 1, Fig. 4). Here, despite vigorous shaking we cannot rule out the existence of anoxic micro-niches that could have supported sulfate respiration. Alternatively, instead of respiring acetate with sulfate these SRB might have channelled acetate into storage compounds such as PHA or glycogen, which are commonly used by SRB to detoxify oxygen (Dolla *et al.*, 2006). In addition, even a slight

growth in presence of oxygen was reported for some SRB (reviewed in Rabus *et al.*, 2015). Future experiments require a higher spatial and temporal resolution and more defined incubation conditions to test for a potential acetate uptake by SRB in under fully oxic conditions.

To further resolve the acetate assimilation of *Desulfobacteraceae* in more detail we studied the activity of Sva0081-MBG in the sediment slurries. This group assimilated acetate in higher rates than the average *Desulfobacteraceae* population (Fig. 4 and Table 1). Within the highly diverse *Desulfobacteraceae* the Sva0081-MBG has been frequently detected in various types of marine sediments (Wang *et al.*, 2013; Liu *et al.*, 2014; Zheng *et al.*, 2014) and was found in high cell abundance in Wadden Sea sediments (up to 8% of total cell counts, Ovanesov, 2012). Thus, we hypothesize that the Sva0081-MBG could be an important acetate-consuming SRB also in other marine coastal sediments.

**Conclusion**

Our approach complements earlier studies on microbial acetate assimilation in marine sediments, as we can now accurately quantify the acetate uptake by distinct bulk populations and determine their relative contribution to the total bacterial acetate uptake. We show that physiologically and phylogenetically distinct bacterial groups assimilated acetate, whereby *Gammaproteobacteria* and sulfate-reducing *Desulfobacteraceae* accounted for most of the bacterial acetate assimilation, in particular in the upper one cm of the sediment, which generally is the microbially most active zone in coastal sediments. Future experiments using different electron acceptors facilitate to track the varying contributions of distinct microbial populations to acetate consumption in a high spatial and temporal resolution, for instance during a full tidal cycle. By quantifying acetate uptake in distinct bacterial populations, we provide deeper insights into the activity of key players involved in acetate consumption, which is essential for our understanding of re-mineralization of organic matter in marine sediments.

## Experimental procedures

*Study site and sampling*

In June and October 2009 sediment was sampled by 3.7 cm diameter polyacryl cores at the tidal flat Janssand (53.7366N, 7.6989E) located in the German Wadden Sea. This site represents a typical sand flat with predominantly sandy sediment (Beck *et al.*, 2009). Biogeochemical data and sediment characteristics of this site are published elsewhere (Billerbeck *et al.*, 2006; Jansen *et al.*, 2009). Sediment cores of 20 cm length were taken, stored at *in situ* temperatures and processed within 24 to 48 h after sampling.

*Concentrations of volatile fatty acids and lactate*

Concentrations of volatile fatty acids and lactate were analyzed in two sediment cores sampled in June 2009. Sediment from seven distinct sediment layers was sampled. High-performance liquid chromatography (HPLC), collection and analysis of pore water were performed as described by Sawicka and colleagues (2009). In brief, sediment samples from respective depths were centrifuged in SphinexR 135 filters at 4000 rpm at 4°C for 15 min. Collected pore water was filtered into 1-ml brown borosilicate glass vials that were pre-combusted at 480°C for 4 h to minimize possible contamination. The acids were derivatized with *p*-nitrophenyl hydrazine, separated by HPLC using a LiChrosphere 80/100 (Knauer, Berlin, Germany) column at 25°C, and the concentrations were determined from the absorption on a UV/VIS detector (Linear) at 400 nm.

*Whole sediment core and slurry incubations with $^{14}$C-acetate*

Intact sediment cores from the same sampling campaign in June 2009 were percolated with 50 ml of sterile filtered pore-water containing 100 µM [1,2-$^{14}$C]-acetate (specific activity 100 mCi/mmol (Hartmann Analytic, Braunschweig, Germany) to displace natural pore water (as described earlier (Lenk *et al*., 2011) and incubated for 8 h at *in situ* temperature (20 °C). After incubation, sediment cores were washed by percolating 2×50 ml of sterile filtered seawater to remove free $^{14}$C-acetate and sliced into 1 cm thick sections. From each layer 0.5 ml were fixed for FISH as described previously (Lenk *et al.*, 2011).

In October 2009 we prepared additional sediment slurries from 0-1 cm depth for oxic incubations and from 10-11 cm depth for anoxic incubations. We added 100 µM [1,2-$^{14}$C]-acetate to 1 ml of sediment and 1 ml of medium and incubated under ambient air at 200 rpm. For sediment from 0-1 cm depth we used the local sterile-filtered seawater as medium, while for sediment from 10-11 cm depth we used 1 ml of sterile-filtered pore water, extracted from sediment of 8-12 cm depth and incubated under a $N_2/CO_2$ (80/20 v/v) atmosphere. The slurries were incubated in 5 ml vials for 8 h before inactivation. All sediment samples were fixed by adding 1.8% formaldehyde overnight at 4 °C and processed for CARD-FISH

analysis according to Ishii *et al*. (2004). From this experiment cells either labeled by CARD-FISH or by Nile Red for PHA stain were used. As controls we used formaldehyde-inactivated sediment. These dead controls did not show any significant $^{14}C$ incorporation.

*Microautoradiography*

The relative abundance of $^{14}C$-acetate-assimilating cells in sediment cores from June 2009 was determined by microautoradiography (MAR). MAR was performed according to Alonso and Pernthaler (2005) and Lenk *et al*. (2011) with an exposure time of two days. Relative abundance of MAR-positive cells was manually determined under an Axioplan epifluorescence microscope (Zeiss, Jena, Germany).

*Measurements of acetate uptake by the bulk microbial community*

Bulk uptake of acetate by the microbial community in whole core incubations and time-series experiment (June 2009) was measured in cells separated from large sediment particles. Therefore, fixed cells were detached from sediment grains by ultrasonic treatment as described previously (Lenk *et al.*, 2011). After sonication 10 µl of the supernatant containing the detached cells was mixed with 5 ml UltimaGold XR (Perkin Elmer, Boston, USA) scintillation cocktail and the radioactivity was measured in a liquid scintillation counter (Tri-Carb 2900, Perkin Elmer, USA). Scintillation counts of formaldehyde-inactivated dead controls were minor and were subtracted from the samples.

*CARD-FISH and sample preparation for flow cytometry*

For catalyzed reporter deposition-fluorescence *in situ* hybridization (CARD-FISH) sediment was fixed immediately after core retrieval as described in Lenk *et al*. (2011). Cells were detached from sediment particles by ultrasonic treatment as described previously (Lenk *et al.*, 2011). Cells were detached from 100-200 µl sediment by ultrasonic treatment as described previously (Lenk *et al.*, 2011). The sample was not centrifuged but directly after settlement of the sand grains the supernatant along with the detached cells were filtered onto 25 mm polycarbonate membrane filters with a 0.2 µm pore size (GTTP, Millipore, Eschborn, Germany). Permeabilization and CARD-FISH was performed as described by Pernthaler *et al*. (2002) without embedding in agarose with the following modifications. Endogenous peroxidases were inactivated in 3% $H_2O_2$ in Milli-Q water for 10 min at room temperature. The temperature for all hybridizations was 46°C and washing was performed at 48°C according to the protocol of Ishii *et al*. (2004). An overview of oligonucleotide probes used in this study is shown in Table S3. Tyramides labeled with Alexa488 fluorescent dye (Molecular Probes, USA) were used for CARD signal amplification. For detachment of cells filters were vortexed in 5 ml of 150 mM NaCl containing 0.05% Tween 80 according to Sekar *et al*.

(2004) or using a cell scraper. Prior to flow cytometry, large suspended particles were removed by filtration through 8 µm pore-size filter (Sartorius, Göttingen, Germany) to avoid clogging of the flow cytometer.

*Fluorescence activated flow sorting (FACS) and scintillography of sorted cells*

Flow sorting of FISH-identified cells and scintillation counting of sorted cell fractions were performed as described previously (Dyksma *et al*., 2016). In brief, cells were sorted using a FACSCalibur flow cytometer (Becton Dickinson, Oxford, UK). Hybridized cells were identified on scatter dot plots of green fluorescence versus 90° light scatter and sediment background was determined by flow cytometric analysis of hybridizations with a nonsense probe (NON338) prior to flow sorting. Collected cell batches on polycarbonate filters were transferred into 5 ml scintillation vials and mixed with 5 ml UltimaGold XR (Perkin Elmer, Boston, USA) scintillation cocktail. Radioactivity of sorted cell batches was measured in a liquid scintillation counter (Tri-Carb 2900, Perkin Elmer, USA). Unspecifically adsorbed label in live samples caused only minor radioactive background as determined by spiking experiments with fluorescent beads (Fig. S2).

For measuring assimilation of $^{14}$C-acetate into PHAs we sampled oxic sediment slurries from 0-1 cm depth sampled in October 2009 (see above). For Nile red staining of PHAs, cells were detached from the sediment as described above and stained with 10 µg/ml (final concentration) Nile red from a stock solution of 1 mg/ml dissolved in dimethylsulfoxide (DMSO). Cells were stained for 30 min at 37 °C and a fraction of the stained sample was manually checked under an epifluorescence microscope (Zeiss, Jena, Germany) (Fig. S5). Prior to flow cytometry large suspended particles were removed by filtration through 5 µm pore-size filters (Sartorius, Göttingen, Germany). Target cells for flow cytometry were identified on scatter dot plots of orange fluorescence (detected wavelength 585 ±21 nm) versus 90° light scatter. Regions with four different fluorescence intensities were selected for sorting (Fig. S6). Sorted cell batches were collected on polycarbonate filters and radioactivity was measured as described above.

*Calculation of cell-specific carbon assimilation rates*

The average cell-specific carbon assimilation rates (g carbon/cell/h) were calculated from bulk measurements for a sorted population according to the equation $R = (A * M) / (a * n * t * L)$. $A$ represents the activity of the sorted cell batch in Becquerel (Bq), $M$ represents the molar mass of carbon (g/mol), $a$ equals the specific activity of the tracer (Bq/mol), $n$ represents the number of sorted cells, $t$ represents the incubation time in hours and $L$ equals the ratio of total acetate/$^{14}$C-acetate.

*16S rRNA gene phylogeny of Sva0081-MBG and probe design*

From previous sampling and sequencing efforts at site Janssand (Lenk *et al*., 2011, 2012) we recovered 19 partial clone sequences (644 to 907 bp) belonging to the Sva0081-MBG/*Desulfobacteraceae*. For phylogenetic reconstruction these sequences were imported into the SILVA Ref NR99_SSU 117 dataset (Pruesse *et al.*, 2007) using the ARB software package (Ludwig *et al.*, 2004). For the guide tree, only sequences >1200 bp were considered. Trees were calculated by RAxML, Maximum Parsimony, Neighbor-Joining (Jukes-Cantor correction) and MrBayes using 50% base frequency filters. A subset of partial sequences of Sva0081-MBG from site Janssand were added without changing the overall tree topology using the *Quick Add* parsimony tool in ARB.

The probe_design-tool implemented in ARB was used to design a specific probe for those sequences >1,200 bp of the Sva0081-MBG that grouped with the only partial sequences recovered from site Janssand (Fig. S4). As positive control for probe DSS1431 we used cross-sections of the marine gutless oligochaete *Olavius algarvensis* harboring the □1-symbiont that were kindly provided by Nicole Dubilier and Mario Schimak, MPI Bremen. Helper and competitor probes were applied at 30% formamide in the hybridization buffer (Table S3), yielding an optimal signal-to-noise-ratio in the tested sediment from site Janssand. Double-hybridizations with probe DSS658 targeting most members of the *Desulfoarcina/Desulfococcus*-group within the *Desulfobacteraceae* was performed to ensure specificity. Therefore, consecutive CARD-FISH using Alexa488- and Alexa546-labeleld tyramides were performed with an intermediate inactivation of HRP-enzyme after the probe applied first. All FISH signals for probe DSS1431 overlapped with signals of probe DSS658. Unspecific signals were neglectable

*Nucleotide accession numbers*

The partial 16S rRNA gene sequences of the Sva0081-MBG are available under accession no. (pending).

**Acknowledgement**

We greatly acknowledge the crew of R/V Navicula from the ICBM Oldenburg for ship time and assistance. We thank Katrice Zerjatke, Josephine Rapp, Kin Ovanesov and Jörg Wulf for technical assistance. Special thanks go to Rudolf Amann for helpful discussions and the excellent continuous support. This study was funded by the Max Planck Society.

**References**

Alonso, C. and Pernthaler, J. (2005) Incorporation of glucose under anoxic conditions by bacterioplankton from coastal North Sea surface waters. *Appl. Environ. Microbiol.* **71**: 1709–1716.

Al-Raei, A.M., Bosselmann, K., Böttcher, M.E., Hespenheide, B., and Tauber, F. (2009) Seasonal dynamics of microbial sulfate reduction in temperate intertidal surface sediments: controls by temperature and organic matter. *Ocean Dyn* **59**: 351–370.

Anderson, A.J. and Dawes, E.A. (1990) Occurrence, metabolism, metabolic role, and industrial uses of bacterial polyhydroxyalkanoates. *Microbiol. Rev.* **54**: 450–472.

Beck, M., Dellwig, O., Liebezeit, G., Schnetger, B., and Brumsack, H.-J. (2008) Spatial and seasonal variations of sulphate, dissolved organic carbon, and nutrients in deep pore waters of intertidal flat sediments. *Estuar. Coast. Shelf Sci.* **79**: 307–316.

Beck, M., Köster, J., Engelen, B., Holstein, J.M., Gittel, A., Könneke, M., *et al*. (2009) Deep pore water profiles reflect enhanced microbial activity towards tidal flat margins. *Ocean Dyn.* **59**: 371–383.

Billerbeck, M., Werner, U., Polerecky, L., Walpersdorf, E., deBeer, D., and Huettel, M. (2006) Surficial and deep pore water circulation governs spatial and temporal scales of nutrient recycling in intertidal sand flat sediment. *Mar. Ecol. Prog. Ser.* **326**: 61–76.

Boschker, H.T.S., Nold, S.C., Wellsbury, P., Bos, D., Graaf, W. de, Pel, R., *et al*. (1998) Direct linking of microbial populations to specific biogeochemical processes by $^{13}$C-labelling of biomarkers. *Nature* **392**: 801–805.

Buck, U., Grossart, H.-P., Amann, R., and Pernthaler, J. (2009) Substrate incorporation patterns of bacterioplankton populations in stratified and mixed waters of a humic lake. *Environ. Microbiol.* **11**: 1854–1865.

Christensen, D. and Blackburn, T.H. (1980) Turnover of tracer ($^{14}$C, $^{3}$H labelled) alanine in inshore marine sediments. *Mar. Biol.* **58**: 97–103.

Christensen, D. and Blackburn, T.H. (1982) Turnover of $^{14}$C-labelled acetate in marine sediments. *Mar. Biol.* **71**: 113–119.

Christensen, D. (1984) Determination of substrates oxidized by sulfate reduction in intact cores of marine sediments. *Limnol. Oceanogr.* **29**: 189–191.

Curson, A.R.J., Todd, J.D., Sullivan, M.J., and Johnston, A.W.B. (2011) Catabolism of dimethylsulphoniopropionate: microorganisms, enzymes and genes. *Nat. Rev. Microbiol.* **9**: 849–859.

Dawes, E.A. and Senior, P.J. (1973) The role and regulation of energy reserve polymers in micro-organisms. *Adv. Microb. Physiol.* **10**: 135–266.

Devereux, R., Kane, M.D., Winfrey, J., and Stahl, D.A. (1992) Genus- and group-specific hybridization probes for determinative and environmental studies of sulfate-reducing bacteria. *Syst. Appl. Microbiol.* **15**: 601–609.

Dolla, A., Fournier, M., and Dermoun, Z. (2006) Oxygen defense in sulfate-reducing bacteria. *J Biotechnol* **126**: 87–100.

Dumont, M.G. and Murrell, J.C. (2005) Stable isotope probing - linking microbial identity to function. *Nat. Rev. Microbiol.* **3**: 499–504.

Dyksma, S., Bischof, K., Fuchs, B.M., Hoffmann, K., Meier, D., Meyerdierks, A., *et al.* (2016) Ubiquitous *Gammaproteobacteria* dominate dark carbon fixation in coastal sediments. *ISME J*. e-pub ahead of print, doi: 10.1038/ismej.2015.257.

Edgcomb, V.P., McDonald, J.H., Devereux, R., and Smith, D.W. (1999) Estimation of bacterial cell numbers in humic acid-rich salt marsh sediments with probes directed to 16S ribosomal DNA. *Appl. Environ. Microbiol.* **65**: 1516–1523.

Finke, N., Vandieken, V., and Jørgensen, B.B. (2007) Acetate, lactate, propionate, and isobutyrate as electron donors for iron and sulfate reduction in Arctic marine sediments, Svalbard. *FEMS Microbiol. Ecol.* **59**: 10–22.

Gao, H., Schreiber, F., Collins, G., Jensen, M.M., Kostka, J.E., Lavik, G., et al. (2009) Aerobic denitrification in permeable Wadden Sea sediments. *ISME J.* **4**: 417–426.

González, J.M., Kiene, R.P., and Moran, M.A. (1999) Transformation of sulfur compounds by an abundant lineage of marine bacteria in the alpha-subclass of the class *Proteobacteria*. *Appl. Environ. Microbiol.* **65**: 3810–3819.

Greenspan, P., Mayer, E.P., and Fowler, S.D. (1985) Nile red: a selective fluorescent stain for intracellular lipid droplets. *J. Cell Biol.* **100**: 965–973.

Howard, E.C., Henriksen, J.R., Buchan, A., Reisch, C.R., Bürgmann, H., Welsh, R., *et al*. (2006) Bacterial taxa that limit sulfur flux from the ocean. *Science* **314**: 649–652.

Ishii, K., Mußmann, M., MacGregor, B.J., and Amann, R. (2004) An improved fluorescence *in situ* hybridization protocol for the identification of bacteria and archaea in marine sediments. *FEMS Microbiol. Ecol.* **50**: 203–213.

Jansen, S., Walpersdorf, E., Werner, U., Billerbeck, M., Böttcher, M.E., and Beer, D. de (2009) Functioning of intertidal flats inferred from temporal and spatial dynamics of $O_2$, $H_2S$ and pH in their surface sediment. *Ocean Dyn.* **59**: 317–332.

Jørgensen, B.B. (1977) The sulfur cycle of a coastal marine sediment (Limfjorden, Denmark). *Limnol. Oceanogr.* **22**: 814–832.

Jørgensen, B.B. (1982) Mineralization of organic matter in the sea bed - the role of sulphate reduction. *Nature* **296**: 643–645.

Knittel, K., Boetius, A., Lemke, A., Eilers, H., Lochte, K., Pfannkuche, O., *et al*. (2003) Activity, distribution, and diversity of sulfate reducers and other bacteria in sediments above gas hydrate (Cascadia margin, Oregon). *Geomicrobiol. J.* **20**: 269–294.

Kowalski, N., Dellwig, O., Beck, M., Grunwald, M., Dürselen, C.-D., Badewien, T.H., *et al*. (2012) A comparative study of manganese dynamics in the water column and sediments of intertidal systems of the North Sea. *Estuar. Coast. Shelf Sci.* **100**: 3–17.

Kristensen, G.K. (1994) Sulfate reduction, acetate turnover and carbon metabolism in sediments of the Ao-Nam-Bor Mangrove, Phuket, Thailand. *Mar. Ecol. Prog. Ser.* **111**: 245–255.

Kuever, J. (2014) The Family *Desulfobulbaceae*. In, Rosenberg,E., DeLong,E.F., Lory,S., Stackebrandt,E., and Thompson,F. (eds), *The Prokaryotes*. Springer Berlin Heidelberg, pp. 75–86.

Laanbroek, H.J. and Pfennig, N. (1981) Oxidation of short-chain fatty acids by sulfate-reducing bacteria in freshwater and in marine sediments. *Arch. Microbiol.* **128**: 330–335.

Lenk, S., Arnds, J., Zerjatke, K., Musat, N., Amann, R., and Mußmann, M. (2011) Novel groups of *Gammaproteobacteria* catalyse sulfur oxidation and carbon fixation in a coastal, intertidal sediment. *Environ. Microbiol.* **13**: 758–774.

Lenk, S., Moraru, C., Hahnke, S., Arnds, J., Richter, M., Kube, M., *et al*. (2012) *Roseobacter* clade bacteria are abundant in coastal sediments and encode a novel combination of sulfur oxidation genes. *ISME J.* **6**: 2178–2187.

Liu, J., Liu, X., Wang, M., Qiao, Y., Zheng, Y., and Zhang, X.-H. (2014) Bacterial and archaeal communities in sediments of the North Chinese Marginal Seas. *Microb. Ecol.* 1–13.

Ludwig, W., Strunk, O., Westram, R., Richter, L., Meier, H., Yadhukumar, *et al.* (2004) ARB: a software environment for sequence data. *Nucleic Acids Res* **32**: 1363–1371.

MacGregor, B.J., Boschker, H.T.S., and Amann, R. (2006) Comparison of rRNA and polar-lipid-derived fatty acid biomarkers for assessment of $^{13}$C-substrate incorporation by microorganisms in marine sediments. *Appl. Environ. Microbiol.* **72**: 5246–5253.

Macrae, R.M. and Wilkinson, J.F. (1958) Poly-β-hyroxybutyrate metabolism in washed suspensions of *Bacillus cereus* and *Bacillus megaterium*. *J. Gen. Microbiol.* **19**: 210–222.

Miyatake, T., MacGregor, B.J., and Boschker, E. (2009) Stable isotope probing combined with magnetic bead capture hybridization of 16S rRNA: linking microbial community function to phylogeny of sulfate-reducing *Deltaproteobacteria* in marine sediments. *Appl. Environ. Microbiol.*

Musat, N., Halm, H., Winterholler, B., Hoppe, P., Peduzzi, S., Hillion, F., *et al*. (2008) A single-cell view on the ecophysiology of anaerobic phototrophic bacteria. *Proc. Natl. Acad. Sci.* **105**: 17861–17866.

Musat, N., Werner, U., Knittel, K., Kolb, S., Dodenhof, T., van Beusekom, J.E.E., *et al*. (2006) Microbial community structure of sandy intertidal sediments in the North Sea, Sylt-Rømø Basin, Wadden Sea. *Syst. Appl. Microbiol.* **29**: 333–348.

Mußmann, M., Ishii, K., Rabus, R., and Amann, R. (2005) Diversity and vertical distribution of cultured and uncultured *Deltaproteobacteria* in an intertidal mud flat of the Wadden Sea. *Environ. Microbiol.* **7**: 405–418.

Na, H., Lever, M.A., Kjeldsen, K.U., Schulz, F., and Jørgensen, B.B. (2015) Uncultured *Desulfobacteraceae* and Crenarchaeotal group C3 incorporate $^{13}$C-acetate in coastal marine sediment. *Environ. Microbiol. Rep.* **7**: 614–622.

Nielsen, J.L. and Nielsen, P.H. (2002) Enumeration of acetate-consuming bacteria by microautoradiography under oxygen and nitrate respiring conditions in activated sludge. *Water Res.* **36**: 421–428.

Novelli, P., Michelson, A., Scranton, M., Banta, G., Hobbie, J., and Howarth, R. (1988) Hydrogen and acetate cycling in two sulfate-reducing sediments: Buzzards Bay and Town Cove, Mass. *Geochim. Cosmochim. Acta* **52**: 2477–2486.

Oremland, R.S. and Polcin, S. (1982) Methanogenesis and sulfate reduction: competitive and noncompetitive substrates in estuarine sediments. *Appl. Environ. Microbiol.* **44**: 1270–1276.

Ovanesov, K. (2012) Abundance, distribution, and first insights into metabolism of an environmentally important group of sulfate-reducing bacteria. Master thesis. University of Bremen, Bremen, Germany

Parkes, R.J., Gibson, G.R., Mueller-Harvey, I., Buckingham, W.J., and Herbert, R.A. (1989) Determination of the substrates for sulphate-reducing bacteria within marine and esturaine sediments with different rates of sulphate reduction. *Microbiology* **135**: 175–187.

Pernthaler, A., Pernthaler, J., and Amann, R. (2002) Fluorescence *in situ* hybridization and catalyzed reporter deposition for the identification of marine bacteria. *Appl. Environ. Microbiol.* **68**: 3094–3101.

Pester, M., Bittner, N., Deevong, P., Wagner, M., and Loy, A. (2010) A 'rare biosphere' microorganism contributes to sulfate reduction in a peatland. *ISME J* **4**: 1591–1602.

Pruesse, E., Quast, C., Knittel, K., Fuchs, B.M., Ludwig, W., Peplies, J., *et al.* (2007) SILVA: a comprehensive online resource for quality checked and aligned ribosomal RNA sequence data compatible with ARB. *Nucleic Acids Res* **35**: 7188–7196.

Rabus, R., Venceslau, S.S., Wöhlbrand, L., Voordouw, G., Wall, J.D., and Pereira, I.A.C. (2015) A post-genomic view of the ecophysiology, catabolism and biotechnological relevance of sulphate-reducing prokaryotes. In: Poole RK (ed) Vol. 66. *Advances in Microbial Physiology*. Academic Press, pp 55–321.

Ravenschlag, K., Sahm, K., Knoblauch, C., Jørgensen, B.B., and Amann, R. (2000) Community structure, cellular rRNA content, and activity of sulfate-reducing bacteria in marine Arctic sediments. *Appl. Environ. Microbiol.* **66**: 3592–3602.

Reeburgh, W.S. (1983) Rates of biogeochemical processes in anoxic sediments. *Annu. Rev. Earth Planet. Sci.* **11**: 269–298.

Repaske, R. and Repaske, A.C. (1976) Quantitative requirements for exponential growth of *Alcaligenes eutrophus*. *Appl. Environ. Microbiol.* **32**: 585–591.

Sass, H., Kopke, B., Rutters, H., Feuerlein, T., Droge, S., Cypionka, H., and Engelen, B. (2010) *Tateyamaria pelophila* sp. nov., a facultatively anaerobic alphaproteobacterium isolated from tidal-flat sediment, and emended descriptions of the genus *Tateyamaria* and of *Tateyamaria omphalii*. *Int. J. Syst. Evol. Microbiol.* **60**: 1770–1777.

Sawicka, J.E., Robador, A., Hubert, C., Jørgensen, B.B., and Brüchert, V. (2010) Effects of freeze–thaw cycles on anaerobic microbial processes in an Arctic intertidal mud flat. *ISME J.* **4**: 585–594.

Sekar, R., Fuchs, B.M., Amann, R., and Pernthaler, J. (2004) Flow sorting of marine bacterioplankton after fluorescence *in situ* hybridization. *Appl. Environ. Microbiol.* **70**: 6210–6219.

Seyler, L.M., McGuinness, L.M., and Kerkhof, L.J. (2014) Crenarchaeal heterotrophy in salt marsh sediments. *ISME J.* **8**: 1534–1543.

Sørensen, J., Christensen, D., and Jørgensen, B.B. (1981) Volatile fatty acids and hydrogen as substrates for sulfate-reducing bacteria in anaerobic marine sediment. *Appl. Environ. Microbiol.* **42**: 5–11.

Sorokin, D.Y. (1995) *Sulfitobacter pontiacus* gen. nov., sp. nov. - A new heterotrophic bacterium from the black sea, specialized on sulfite oxidation. *Microbiology* **64**: 295–305.

Thauer, R.K. and Postgate, J.R. (1982) Dissimilatory sulphate reduction with acetate as electron donor. *Philos. Trans. R. Soc. Lond. B Biol. Sci.* **298**: 467–471.

Valdemarsen, T. and Kristensen, E. (2010) Degradation of dissolved organic monomers and short-chain fatty acids in sandy marine sediment by fermentation and sulfate reduction. *Geochim. Cosmochim. Acta* **74**: 1593–1605.

Vandieken, V., Pester, M., Finke, N., Hyun, J.-H., Friedrich, M.W., Loy, A., and Thamdrup, B. (2012) Three manganese oxide-rich marine sediments harbor similar communities of acetate-oxidizing manganese-reducing bacteria. *ISME J.* **6**: 2078–2090.

Vandieken, V. and Thamdrup, B. (2013) Identification of acetate-oxidizing bacteria in a coastal marine surface sediment by RNA-stable isotope probing in anoxic slurries and intact cores. *FEMS Microbiol. Ecol.* **84**: 373–386.

Vidal-Mas, J., Resina-Pelfort, O., Haba, E., Comas, J., Manresa, A., and Vives-Rego, J. (2001) Rapid flow cytometry - Nile red assessment of PHA cellular content and heterogeneity in cultures of *Pseudomonas aeruginosa* 47T2 (NCIB 40044) grown in waste frying oil. *Antonie Van Leeuwenhoek* **80**: 57–63.

Wang, L., Liu, L., Zheng, B., Zhu, Y., and Wang, X. (2013) Analysis of the bacterial community in the two typical intertidal sediments of Bohai Bay, China by pyrosequencing. *Mar. Pollut. Bull.* **72**: 181–187.

Webster, G., Watt, L.C., Rinna, J., Fry, J.C., Evershed, R.P., Parkes, R.J., and Weightman, A.J. (2006) A comparison of stable-isotope probing of DNA and phospholipid fatty acids to study prokaryotic functional diversity in sulfate-reducing marine sediment enrichment slurries. *Environ. Microbiol.* **8**: 1575–1589.

Webster, G., Rinna, J., Roussel, E.G., Fry, J.C., Weightman, A.J., and Parkes, R.J. (2010) Prokaryotic functional diversity in different biogeochemical depth zones in tidal sediments of the Severn Estuary, UK, revealed by stable-isotope probing. *FEMS Microbiol. Ecol.* **72**: 179–197.

Werner, U., Billerbeck, M., Polerecky, L., Franke, U., Huettel, M., van Beusekom, J.E.E., and de Beer, D. (2006) Spatial and temporal patterns of mineralization rates and oxygen distribution in a permeable intertidal sand flat (Sylt, Germany). *Limnol. Oceanogr.* **51**: 2549–2563.

Zheng, B., Wang, L., and Liu, L. (2014) Bacterial community structure and its regulating factors in the intertidal sediment along the Liaodong Bay of Bohai Sea, China. *Microbiol. Res.* **169**: 585–592.

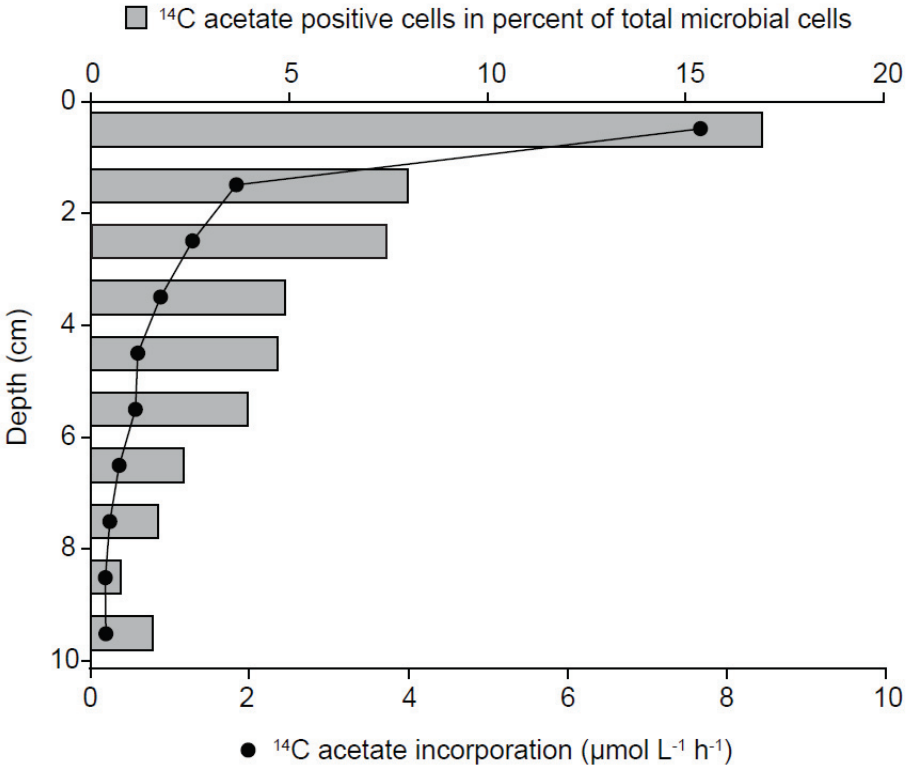


**Fig. 1.** Bulk $^{14}$C-carbon activity given in Becquerel (Bq) and relative abundance of $^{14}$C-acetate-assimilating cells determined by microautoradiography after 8h incubations of whole sediment cores (June 2009).

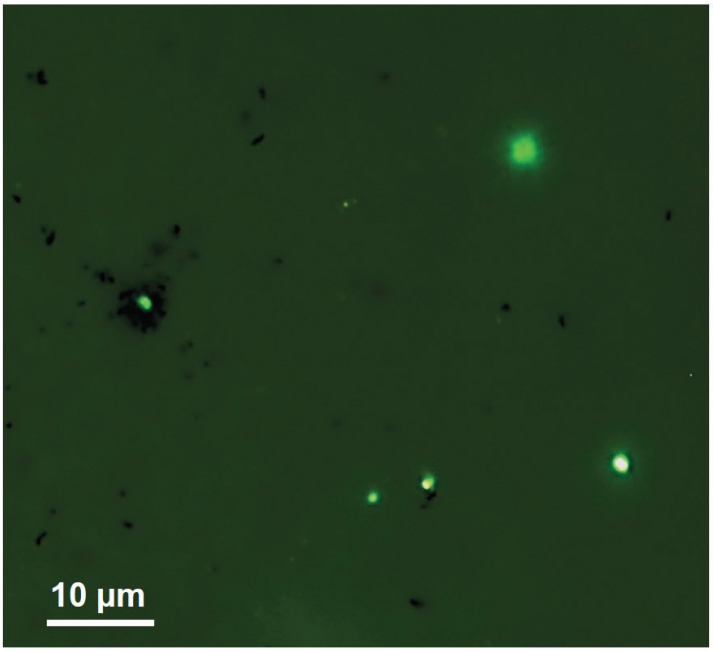


**Fig. 2.** Microautoradiography combined with CARD-FISH demonstrating $^{14}$C-acetate uptake by *Gammaproteobacteria*. Epifluorescence micrograph showing *Gammaproteobacteria* labeled by probe GAM42a (Alexa488, green signals) and silver grains indicate uptake of $^{14}$C-acetate.

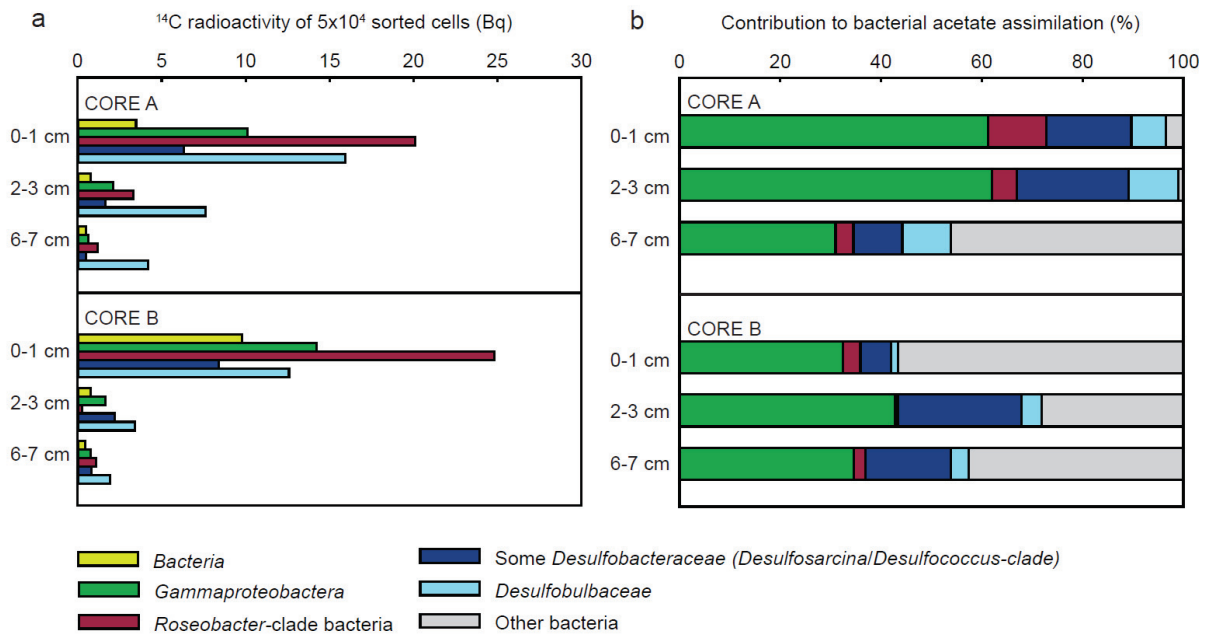


**Fig. 3.** $^{14}$C-carbon activity in 50,000 cells flow-sorted after CARD-FISH from incubations of whole sediment cores (June 2009). The following populations were flow-sorted according to their CARD-FISH signal: *Bacteria* (probe EUBI-III), *Gammaproteobacteria* (probe GAM42a), *Roseobacter*-clade bacteria (RCB, probe ROS537), *Desulfobulbaceae* (probe DSB706) and some members of the *Desulfobacteraceae* (probe DSS658). Batches of 50,000 cells were sorted for quantification (a). Integration of relative cell abundances of flow-sorted populations and their average cell-specific $^{14}$C-acetate assimilation rates shows the relative contribution to total bacterial $^{14}$C-acetate assimilation (b).

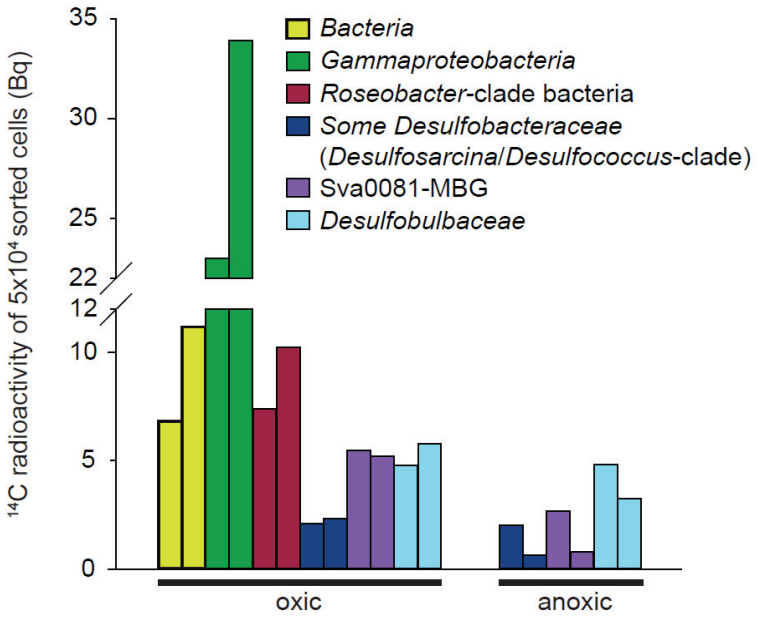


**Fig. 4.** $^{14}$C-carbon activity in 50,000 cells flow-sorted after CARD-FISH from duplicate sediment slurries incubated under oxic or anoxic conditions (October 2009).

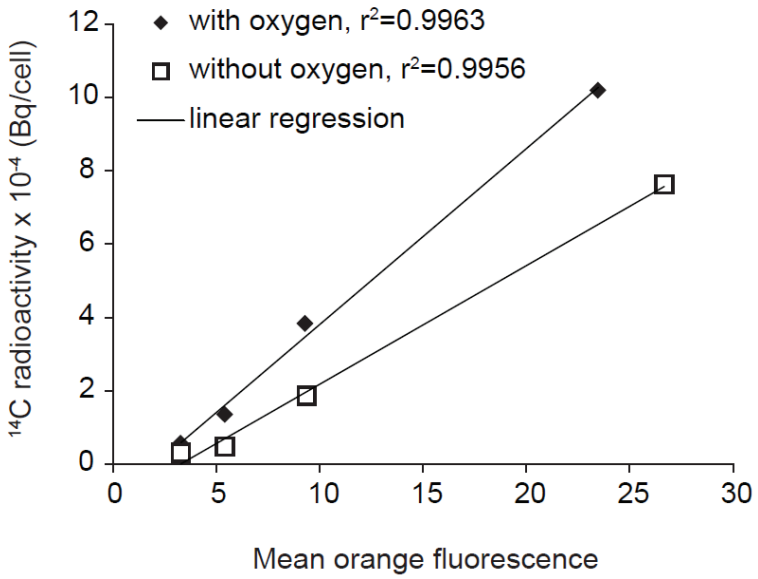


**Fig. 5.** $^{14}$C-carbon activity in 50,000 flow-sorted cells after Nile Red-staining. Four different mean fluorescence intensity classes were defined for flow-sorting (see Fig. S6). Values are depicted as average of duplicate sediment slurries incubated under oxic or anoxic conditions (June 2009).

**Table 1.** Average cell-specific $^{14}$C-acetate assimilation rates of flow-sorted populations (50,000 cells each) from duplicate whole core and slurry incubations. Cells were either labeled by CARD-FISH (16S rRNA) or by Nile Red-staining (polyhydroxyalkanoate, PHA).

| | **Cell-specific assimilation rates (fg C cell$^{-1}$ d$^{-1}$)** core A/B | | | | | | |
|---|---|---|---|---|---|---|---|
| **Sample type** | ***Bacteria*** | ***Gamma-proteob.*** | **RCB** | ***Desulfobacteraceae*** Sva0081 | | ***Desulfo-bulbaceae*** | **PHA*** (min-max) |
| core incubations A/B: | | | | | | | |
| 0-1 cm | 3.8/1.3 | 5.5/3.9 | 9.7/7.8 | 3.3/2.5 | n.d. | 4.9/7.1 | |
| 2-3 cm | 0.2/0.3 | 0.6/0.8 | 0.1/1.3 | 0.9/0.6 | n.d. | 1.3/3.0 | |
| 6-7 cm | 0.2/0.2 | 0.3/0.2 | 0.4/0.5 | 0.3/0.2 | n.d. | 0.8/1.6 | |
| slurry incubations A/B: | | | | | | | |
| oxic | 3.5/5.8 | 11.9/17.6 | 3.8/5.3 | 1.1/1.2 | 2.7/2.8 | 2.5/3.0 | 1-26 |
| anoxic | n.d. | n.d. | n.d. | 0.3/1.0 | 0.4/1.4 | 1.7/2.5 | 1-20 |

n.d, not determined; * polyhydroxyalkanoates stained with Nile Red

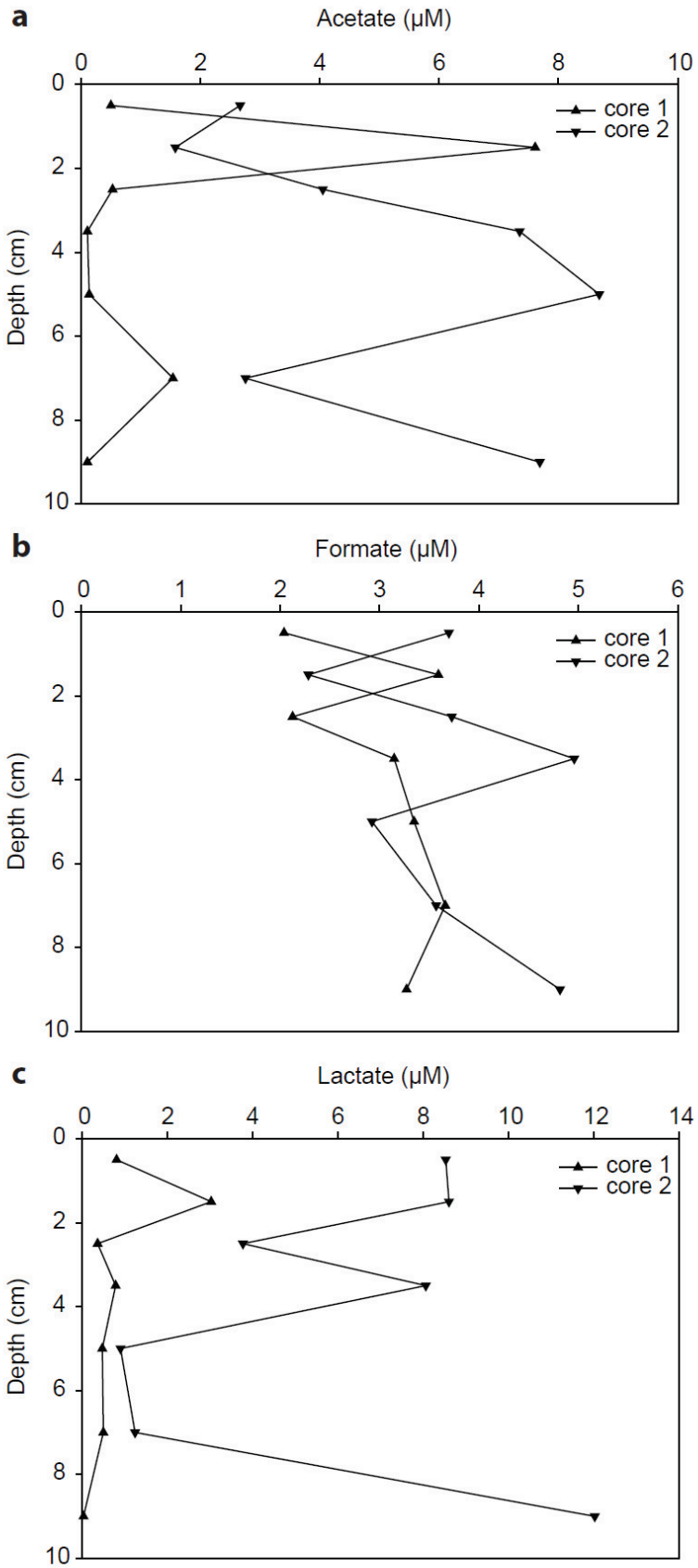


**Fig. S1.** *In situ* pore water concentrations of acetate (a), formate (b) and lactate (c) in sediment cores sampled in duplicates at site Janssand in June 2009.

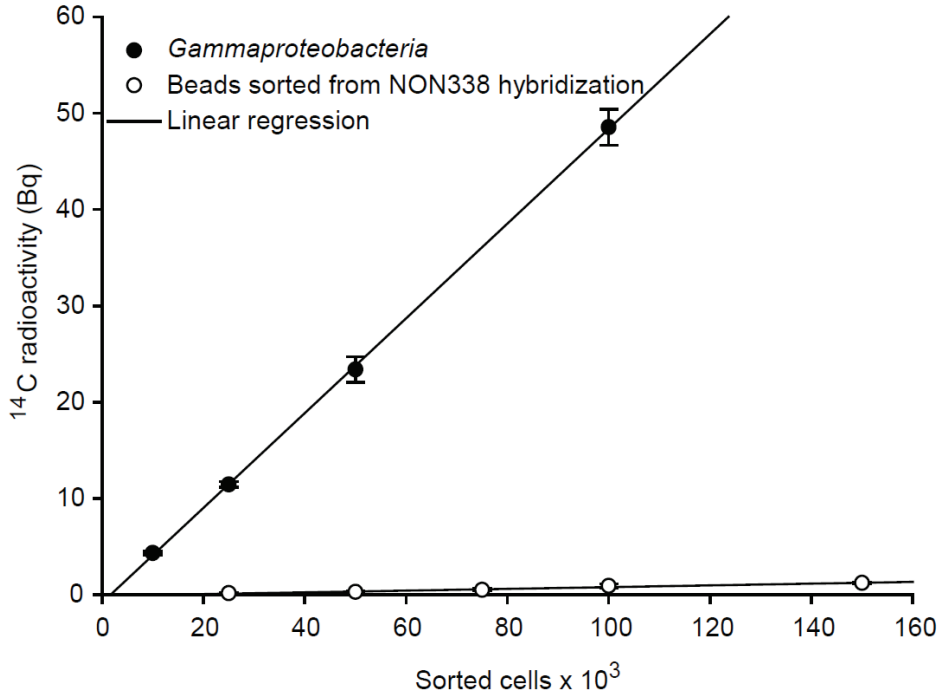


**Fig. S2.** Correlation of $^{14}$C-carbon activity with abundances of flow-sorted cells of *Gammaproteobacteria* and fluorescent beads. To determine the unspecific background from $^{14}$C-acetate incubations, sediments slurries were supplemented with fluorescent beads and hybridized with the negative control probe (NON338). Fluorescent beads were then flow-sorted before liquid scintillography. $^{14}$C-carbon activity is given in Becquerel (Bq). Error bars indicate the standard deviation (SD) of triplicate flow-sorting.

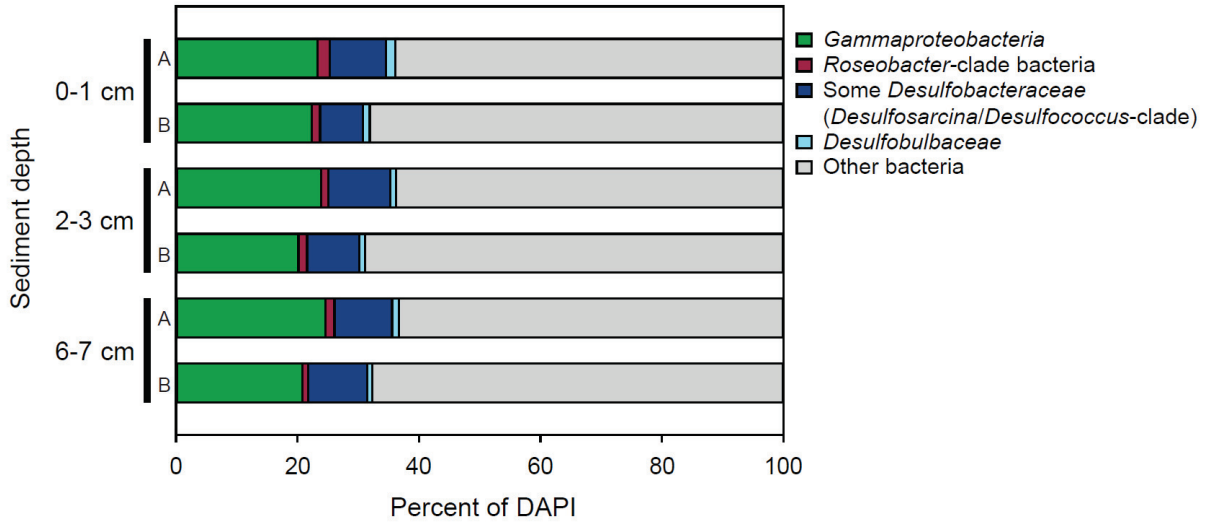


**Fig. S3.** Relative cell abundance over sediment depth in percent of total cell counts (DAPI) in two sediment cores (A, B) used for radiotracer incubations.

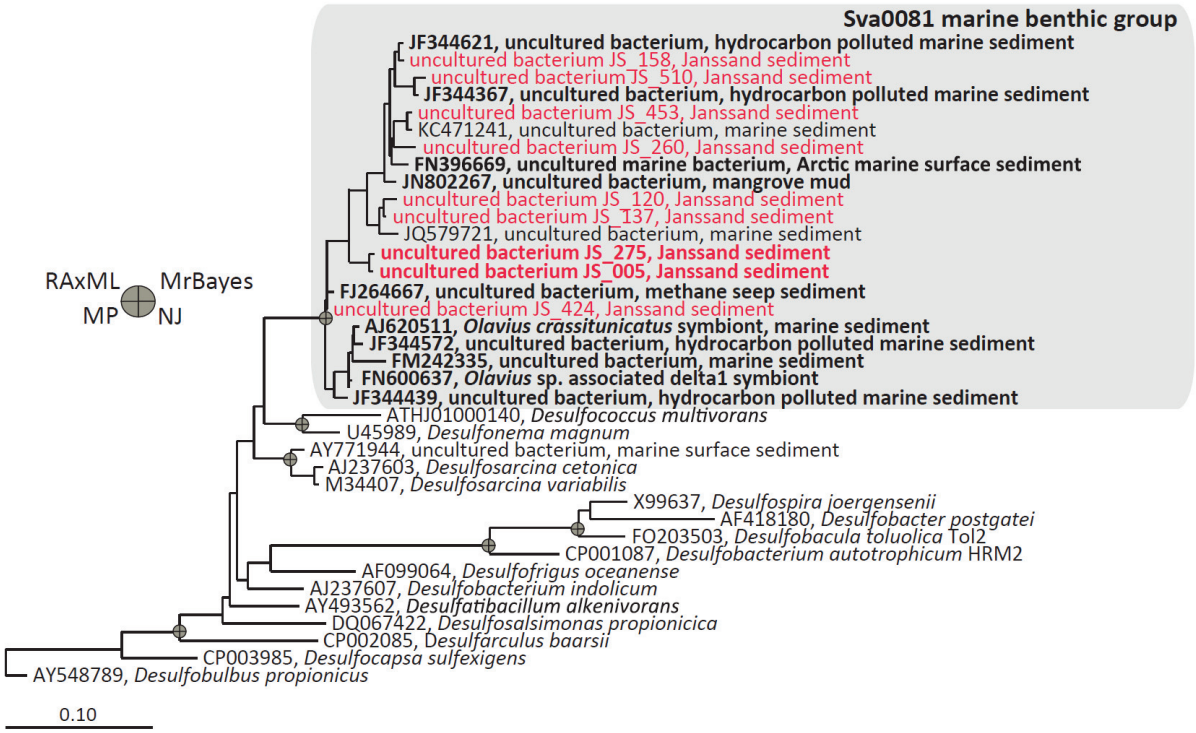


**Fig. S4.** Phylogenetic reconstruction of 16S rRNA gene sequences of selected *Desulfobacterales* based on RAxML. Only branching patterns supported by all 4 treeing methods are indicated. Partial Sva0081-MBG sequences retrieved from Janssand sediments are given in red. Sequences given in bold are targeted by the Sva0081-MBG specific probe DSS1431. Note that some partial sequences were too short to cover the target site of probe DSS1431. The scale bar refers to 10% sequence divergence.

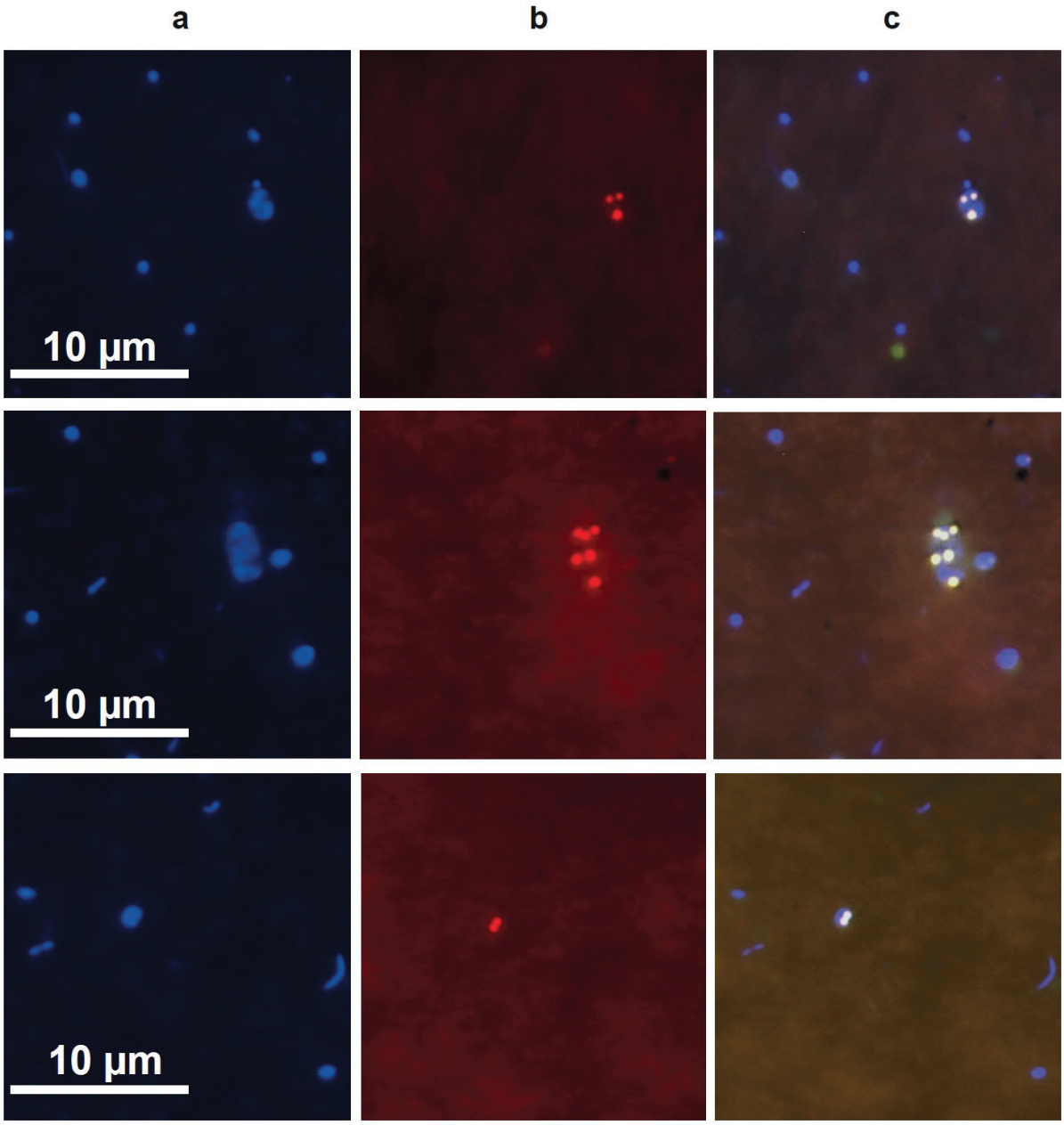


**Fig. S5.** Epifluorescence images of samples from sediment slurry incubations (October 2009) stained with DAPI and Nile Red. DAPI-stained cells panel a, Nile Red-stain panel b and overlay of images panel c.

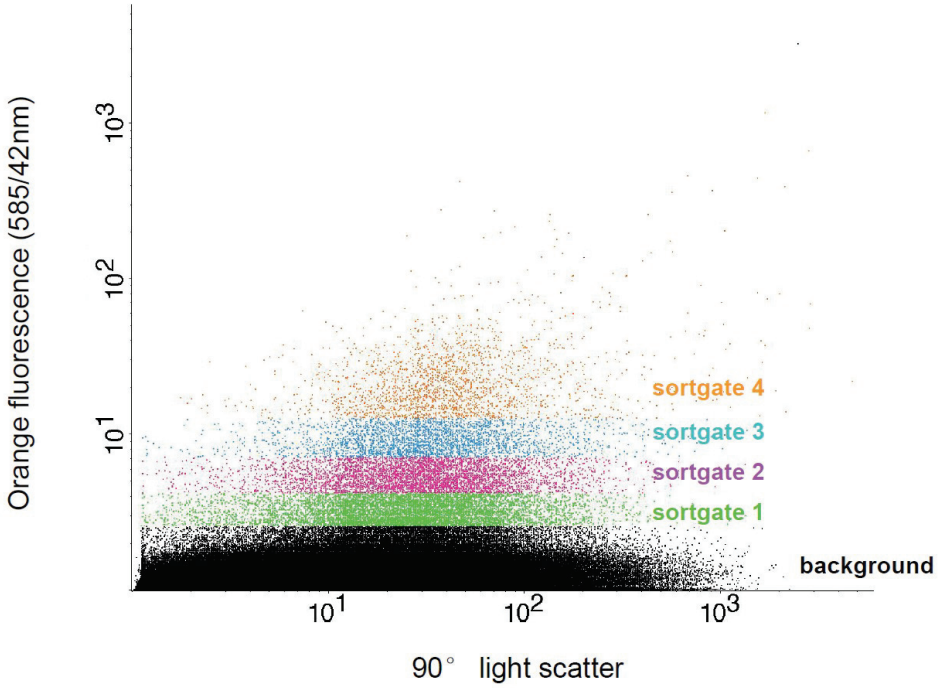


**Fig. S6.** Characteristic signatures of sediment samples stained with Nile Red and analysed by flow cytometry. Dot plot diagram of orange fluorescence plotted versus 90° light scatter. The gates used for cell sorting are indicated (sortgate 1-4).

**Table S1.** Relative abundances of $^{14}$C-acetate-assimilating cells as determined by microautoradiography and DAPI staining or hybridization with specific CARD-FISH probes in duplicate whole sediment cores incubated with $^{14}$C-acetate.

| **Sorted population** | **% of all MAR-positive cells** (core A/B) | **% MAR-positive of hybridized cells** (core A/B) |
|---|---|---|
| *Gammaproteobacteria* | *59/61* | 19/19 |
| *Roseobacter*-clade bacteria (RCB) | 6/8 | 48/32 |
| *Deltaproteobacteria* | 8/4 | 9/7 |

**Table S2.** Average cell-specific $^{14}$C-acetate assimilation rates of flow-sorted populations after Nile Red-staining. Four distinct fluorescence intensity classes (Fig. S6) were defined for sorting from duplicate sediment slurries incubated under oxic and anoxic conditions.

| **Fluorescence intensity of Nile Red-stained cells** | **Cell-specific carbon assimilation rates (fg C cell$^{-1}$ d$^{-1}$)** | |
|---|---|---|
| | with oxygen | without oxygen |
| ++++ (bright fluorescence) | 26.4 | 19.8 |
| +++ | 9.9 | 4.8 |
| ++ | 3.5 | 1.2 |
| + (weak fluorescence) | 1.5 | 0.8 |

**Table S3.** Horseradish peroxidase (HRP)-labeled oligonucleotide probes used for CARD-FISH. Helper and competitor oligonucleotides were not labeled.

| Probe | Specificity | Sequence (5'-3') | FA (%) | Reference |
|---|---|---|---|---|
| EUB I-III | most Bacteria | GCWGCCWCCCGTAGGWGT | 35 | Amann *et al.* (1990) Daims *et al.* (1999) |
| NON338 | Negative control | ACTCCTACGGGAGGCAGC | | Wallner *et al.* (1993) |
| GAM42a* | most *Gammaproteobacteria* | GCCTTCCCACATCGTTT | 35 | Manz *et al.* (1992) |
| ROS537 | *Roseobacter*-clade bacteria (RCB) | CAACGCTAACCCCCTCC | 35 | Eilers *et al.* (2000) |
| DSS658 | many marine *Desulfobacteraceae* including the *Desulfosarcina/ Desulfococcus*-group | TCCACTTCCCTCTCCCAT | 50 | Manz *et al.* (1998) |
| DSB706 | many marine *Desulfobulbaceae* | ACCGGTATTCCTCCCGAT | 40 | Loy *et al.* (2002) |
| Delta495 a-c* | most *Deltaproteobacteria* | AGTTAGCCGGTGCTTCCT AGTTAGCCGGCGCTTCCT AATTAGCCGGTGCTTCCT | 35 | Lücker *et al.* (2007) |
| DSS1431* | subgroup of Sva0081-MBG | GGTTTGCCCAACGACTTC | 30 | This study |
| cDSS1431a† | Competitor to probe DSS1431 | GGTTTGCCCAACAACTTC | 30 | This study |
| cDSS1431b† | Competitor to probe DSS1431 | GGTTAGCCCAACAACTTC | 30 | This study |
| cDSS1431c† | Competitor to probe DSS1431 | GGTTCGCCCACCAACTTC | 30 | This study |
| cDSS1431d† | Competitor to probe DSS1431 | AGTTTGCCCAACAACTTC | 30 | This study |
| cDSS1431e† | Competitor to probe DSS1431 | GGTTGGCCCAACAACTTC | 30 | This study |
| DSS1431us‡ | Helper to probe DSS1431 | TGGTACAACCAACTCTCATGG | 30 | This study |
| DSS1431us‡ | Helper to probe DSS1431 | TTAGGCGCCTGCATCCCCGAA | 30 | This study |
| DSS1431us‡ | Helper to probe DSS1431 | TTAGGCGCCTGCATCCTGTAAA | 30 | This study |

FA, formamide; * probes were used with published competitors; † competitor oligonucleotide; ‡ helper oligonucleotide

## References

Amann, R.I., Binder, B.J., Olson, R.J., Chisholm, S.W., Devereux, R., and Stahl, D.A. (1990) Combination of 16S rRNA-targeted oligonucleotide probes with flow cytometry for analyzing mixed microbial populations. *Appl. Environ. Microbiol.* **56**: 1919–1925.

Daims, H., Brühl, A., Amann, R., Schleifer, K.H., and Wagner, M. (1999) The domain-specific probe EUB338 is insufficient for the detection of all *Bacteria*: development and evaluation of a more comprehensive probe set. *Syst. Appl. Microbiol.* **22**: 434–444.

Eilers, H., Pernthaler, J., Glöckner, F.O., and Amann, R. (2000) Culturability and *in situ* abundance of pelagic bacteria from the North Sea. *Appl. Environ. Microbiol.* **66**: 3044–3051.

Loy, A., Lehner, A., Lee, N., Adamczyk, J., Meier, H., Ernst, J., *et al.* (2002) Oligonucleotide microarray for 16S rRNA gene-based detection of all recognized lineages of sulfate-reducing prokaryotes in the environment. *Appl. Environ. Microbiol.* **68**: 5064–5081.

Lücker, S., Steger, D., Kjeldsen, K.U., MacGregor, B.J., Wagner, M., and Loy, A. (2007) Improved 16S rRNA-targeted probe set for analysis of sulfate-reducing bacteria by fluorescence *in situ* hybridization. *J. Microbiol. Methods* **69**: 523–528.

Manz, W., Amann, R., Ludwig, W., Wagner, M., and Schleifer, K.-H. (1992) Phylogenetic oligodeoxynucleotide probes for the major subclasses of *Proteobacteria*: problems and solutions. *Syst. Appl. Microbiol.* **15**: 593–600.

Manz, W., Eisenbrecher, M., Neu, T.R., and Szewzyk, U. (1998) Abundance and spatial organization of Gram-negative sulfate-reducing bacteria in activated sludge investigated by *in situ* probing with specific 16S rRNA targeted oligonucleotides. *FEMS Microbiol. Ecol.* **25**: 43–61.

Wallner, G., Amann, R., and Beisker, W. (1993) Optimizing fluorescent *in situ* hybridization with rRNA-targeted oligonucleotide probes for flow cytometric identification of microorganisms. *Cytometry* **14**: 136–143.

# 4.) General discussion

Key intermediates of organic matter remineralization in aquatic sediments are $CO_2$, $H_2$ and acetate. In the past, several studies addressed acetate- (e.g., Christensen and Blackburn, 1982; Sansone and Martens, 1982; Wellsbury and Parkes, 1995; Graaf *et al.*, 1996; Finke *et al.*, 2007) and $H_2$ turnover (Lovley *et al.*, 1982; Lovley and Goodwin, 1988; Goodwin *et al.*, 1988; Hoehler *et al.*, 1998) as well as chemoautotrophy (Lenk *et al.*, 2011; Boschker *et al.*, 2014; Vasquez-Cardenas *et al.*, 2015) in marine sediments but the involved organisms are still largely unexplored. Goals of this thesis were the identification of key players, to understand their metabolic potential and how they contribute to these important processes. Cultivation independent molecular tools such as fluorescence *in situ* hybridization, metagenomics and metatranscriptomics have been used to identify organisms, quantify their *in situ* abundance and to investigate their potential function. However, it is important to integrate these merely molecular data with quantitative activity measurements to study the ecological role of key microbes within complex microbial communities. I therefore developed a novel methodological approach to exactly quantify $^{14}C$ carbon uptake by phylogenetically identified microorganisms. The following chapter summarizes the collective findings of this study and describes potential impact of my research on the current knowledge about the ecology of sulfur and carbon cycling bacteria in marine sediments.

## 4.1) Groups of *Gammaproteobacteria* are key players in inorganic carbon fixation

Among the most important outcomes of my dissertation is that particular groups within the *Gammaproteobacteria* dominate chemoautotrophy in coastal sediments regardless of the site and season. Consistently 40 to 50% of the *Gammaproteobacteria* in coastal sediments fixed $^{14}CO_2$ in the dark and were therefore identified as potential chemoautotrophs (**Manuscript I**). Intriguingly, these chemoautotrophic gammaproteobacteria accounted for up to 86% of the bacterial chemoautotrophy. *Gammaproteobacteria* are globally distributed and abundant members of the bacterial community in nearly all types of marine sediments (Hunter *et al.*, 2006; Kim *et al.*, 2008; Schauer *et al.*, 2009; Orcutt *et al.*, 2011; Gobet *et al.*, 2012; Ruff *et al.*, 2015). Primary production by chemoautotrophic bacteria at hydrothermal vents and dark carbon fixation in pelagic oxygen minimum zones has been extensively studied in the past. Here, key players for carbon and sulfur cycling such as the gammaproteobacterial SUP05-clade have been identified and their ecophysiology and environmental impacts are well described (Lavik *et al.*, 2009; Canfield *et al.*, 2010; Reinthaler *et al.*, 2010; Grote *et al.*, 2012; Anantharaman *et al.*, 2013; Mattes *et al.*, 2013; Hawley *et al.*, 2014). However, the identity and activity of chemolithoautotrophic bacteria (and archaea) in

coastal and shelf sediments are still understudied although this environment contribute more to oceanic dark carbon fixation than pelagic oxygen minimum zones and hydrothermal vents (Middelburg, 2011). According to Middelburg (2011), 291 Tg C $y^{-1}$ are fixed in coastal and shelf sediments. Intriguingly, the area of theses sediments accounts for only ~5% of the total marine benthic environment, but they are responsible for 78% of sedimentary dark carbon fixation (Dunne *et al.*, 2007; Middelburg, 2011). On average we observed a cell-specific carbon fixation rate for *Gammaproteobacteria* accounting for 5 fg C $cell^{-1}$ $d^{-1}$ in sediments from the uppermost centimetre and a total cell abundance of chemoautotrophic *Gammaproteobacteria* of approximately $10^8$ cells $cm^{-3}$. Assuming an even distribution and similar activity across coastal and shelf sediments these *Gammaproteobacteria* would account for 30.3 Tg carbon fixed per year, only considering the top cm of the sediment (surface area estimation was taken from Dunne *et al.* (2007)). We surveyed the bacterial 16S rRNA gene diversity of 13 tidal and sublittoral sediments across Europe and Australia and indeed we identified putatively chemoautotrophic core groups of *Gammaproteobacteria* mainly affiliating with sulfur-oxidizing bacteria that were ubiquitous distributed in theses sediments, which indicates that microbial community structures may be similar. At all sites we identified candidate chemoautotrophs related to *Acidiferrobacter*, to symbionts of the siboglinid tubeworms (*Siboglinidae* Symbionts related, SSr), to the ciliate symbiont *Candidatus* Thiobios zoothamnicoli, to the BD7-8 group including mussel and worm symbionts and the JTB255-clade. Moreover, three of these clades (the *Acidiferrobacter*-, JTB255- and the SSr-clade) made up more than 50% of dark carbon fixation, largely fuelled by sulfur oxidation, in a tidal sediment and by FISH we further confirmed their *in situ* abundance (Figure 10). We then re-visited the 16S rRNA gene diversity data collected in 65 diversity studies from marine surface sediments and found those groups globally distributed in various types of sediments. Microbial respirations generally lead to a net release of $CO_2$ from the sediment and inorganic carbon fixation counteracts these processes (Howarth, 1984; Dunne *et al.*, 2007). Thus, chemoautotrophy driven by few ubiquitous gammaproteobacterial populations at sediment surfaces could attenuate $CO_2$ emissions to the ocean and ultimately to the atmosphere. Given their ubiquity and frequent dominance as well as the major contribution to dark carbon fixation these groups of chemolithoautotrophic *Gammaproteobacteria* are important not only for carbon fixation but also for sulfide detoxification at sediment surfaces, thereby effectively preventing oxygen minimum zones to build up. Therefore, the stable assemblage of the *Acidiferrobacter*-, JTB255- and the SSr-clade may be benthic counterparts to pelagic sulfur-oxidizing and carbon-fixing SUP05, however, more widely distributed and abundant.

### 4.2) The enigmatic and cosmopolitan JTB255-clade

Further attention should be paid to the enigmatic JTB255-clade. This group consistently accounted not only for one the largest sequence fraction within the *Gammaproteobacteria* (**Manuscript I**), but also for one of the most abundant sequence fraction at the family/order level across all phyla at 13 investigated sites. Using CARD-FISH we identified the JTB255-clade as abundant, accounting for 3-6 % of total cell counts in coastal sediments. In our meta-analysis of 16S rRNA gene sequence data from 65 diversity studies of the sea floor around the world the JTB255-group was detected in 92% of all studies and often accounted for the most frequent sequence group of *Bacteria* in deep-sea (Bowman *et al.*, 2005; Schauer *et al.*, 2009) and in shallow coastal sediments (Wang *et al.*, 2013; Zheng *et al.*, 2014; Liu *et al.*, 2014; Ruff *et al.*, 2014). Moreover, in a comprehensive 16S rRNA gene survey Bienhold *et al.* (2016) identified the JTB255-clade as a true cosmopolitan group in 27 investigated deep sea sediments while a significant part of the bacterial community appears to be geographically restricted. The 16S rRNA gene divergence within the JTB255-clade is high (family to order level). Whether different sequence clusters exists that reflect distinct groups adapted to specific environmental conditions is still an open question. So far the environmental function of the JTB255-group is largely unknown. In the past, a sulfur-oxidizing activity of the JTB255-group has been speculated (Bowman and McCuaig, 2003). In this thesis we provided first indication that the JTB255-clade fix inorganic carbon and may use reduced sulfur compounds as we observed a stimulation of dark carbon fixation by this group in some incubation experiments when thiosulfate was added. However, this group may not be obligate autotroph or they can grow mixotrophically. It is of fundamental interest for our understanding of ecosystem functioning to decipher the prevalent physiological mechanisms that makes this clade globally successful in nearly all types of marine sediments. Like the alphaproteobacterial SAR11-clade, which appears to be the most abundant bacteria in the pelagic zone, the gammaproteobacterial JTB255-clade may be equally predominant in marine sediments.

### 4.3) Burial of microorganisms as mechanism for long-term carbon storage

An important implication that can be drawn from the first manuscript presented in my dissertation is that burial of chemolithoautotrophic bacteria may be a yet unrecognized mechanism carbon sequestration. Coastal vegetation such salt marshes and seagrass meadows are already well known for their importance in carbon sequestration as they not only hold a large standing stock of carbon but also bury carbon into sediments (Duarte *et al.*, 2005; Kennedy *et al.*, 2010; Fourqurean *et al.*, 2012). In current models of oceanic carbon cycling the burial of refractory organic matter is the major mechanism of carbon preservation in sediments, while the microbial contribution to carbon burial in sediments to date focused

on the diagenesis and assimilation of organic carbon (Burdige, 2007). The ability of chemolithoautotrophs to trap carbon and to survive a long-term burial in subsurface sediments is unknown. Recently, biogeochemical budgeting revealed coastal sediments also as hot spots of dark carbon fixation (175 Tg C/yr), exceeding total carbon fixed in the dark ocean (Middelburg, 2011). We also searched for burial of candidate chemolithoautotrophic *Gammaproteobacteria* in subsurface sediment at site Janssand with an estimated age of 1,000 to 2,000 years in the deepest layer (Seidel *et al.*, 2012). Likewise, we observed the same candidate subpopulations (JTB255, *Acidiferrobacter*, symbiont-relatives) with up to 100% identity to sequences from the surface (**Manuscript I**) even though they are may secluded from potential electron acceptors. A large fraction of microbial cells in marine sediments are inactive (Luna *et al.*, 2002) but can persist millions of years in the subsurface (Morono *et al.*, 2009; Jørgensen, 2011; Røy *et al.*, 2012). The slow, but steady advective transport of dissolved organic matter in these sediments (Røy *et al.*, 2008; Seidel *et al.*, 2012) may have supplied the buried populations with sufficient nutrients for maintenance and long-term survival in an otherwise unfavourable environment for chemoautotrophic bacteria. Despite strong biogeochemical gradients in the upper 500 cm below sea floor (cmbsf) bacterial communities and cell abundances in surface and subsurface sediments appear to be surprisingly similar also in other benthic habitats (Kirchman *et al.*, 2014; Treude *et al.*, 2014; Walsh *et al.*, 2015). However, other surface-associated populations such as the sulfate-reducing, deltaproteobacterial Sva0081-clade almost disappeared at site Janssand below 100 cmbsf and in other subsurface sediments strong changes in the entire microbial community were observed with sediment depth (Wilms *et al.*, 2006; Jorgensen *et al.*, 2012; Walsh *et al.*, 2015).

Given the high sedimentation rate in the German Wadden Sea of >3 mm/yr (Ziehe, 2009), a large fraction of microorganisms is buried in the subsurface. By their ability to persist in subsurface sediments for hundreds to thousands of years they may substantially contribute to long-term burial of carbon. Consequently, carbon fixation by chemolithoautotrophs at sediment surfaces and their subsequent burial may represent a previously unrecognized but significant mechanism in carbon sequestration. It is fundamental to decipher processes and microorganisms that govern rates of carbon burial. Detangling the microbial contribution of inorganic and organic carbon assimilation to carbon flux into the subsurface will be an important future task and will help to improve modelling of global carbon budgets.

### 4.4) Important role of $H_2$ in energy transfer in marine sediments

Evidence is accumulating that microbial metabolism of $H_2$ is widely distributed rather than a niche process. Greening *et al.* (2015) screened 20 published metagenomic datasets from different environments including soil, gut and water samples for enzymes involved in $H_2$

production and consumption and reported that $H_2$ is a major electron donor for respiration in various oxic and anoxic ecosystems as well as that fermentative $H_2$ production is widely distributed. Moreover, the ubiquity of $H_2$ utilization also in subsurface sediments under a wide range of environmental conditions and biogeochemical zones has been suggested recently (Adhikari *et al.*, 2016). However, until now, no comprehensive metagenomic study of $H_2$ases in marine sediments was available and the involved groups were largely unknown. Therefore we screened single cell genomes, a metagenome and 4 replicated metatranscriptomes from a coastal sediment for $H_2$ases and the involved organisms. Overall, we found the highest number of $H_2$ase-assigned reads so far reported for an environmental ecosystem, suggesting that coastal sediments are hot spots of $H_2$ cycling and pointing to a central role of $H_2$ in energy transfer. In particular, a large fraction of metagenome and transcriptome reads were assigned to [FeFe]-$H_2$ases. Coastal sediments are largely anoxic habitat as oxygen is only the uppermost millimeters to centimeters of the surface layer available (Jørgensen, 1982; Jansen *et al.*, 2009). Here, fermentation processes are an integral part of organic carbon remineralization (Schmitz *et al.*, 2006). Obligate and facultative fermenters possess [FeFe]-$H_2$ases that are most likely responsible for the release excess reducing equivalents in form of $H_2$.

On the contrary, group 1 [NiFe]-$H_2$ases were also abundant in the metagenome as well as in the metatranscriptomes and thereby identified as major determinant for $H_2$ oxidation. An oxygen-tolerant subclass of group 1 [NiFe]-$H_2$ases from the flavobacterial *Eudoraea* spp. and from sulfur-oxidizing *Gammaproteobacteria* appear to play a more important role in $H_2$-cycling at the oxic sediment surface. Among sulfate-reducing bacteria $H_2$ase sequences affiliating with *Desulfobacteraceae* and *Desulfobulbaceae* were consistently found in three tidal sediments at the European Atlantic coast and sediment slurry incubation experiments with $H_2$ suggested a rather sulfate-dependent $H_2$ oxidation. In particular, the sulfate-reducing Sva0081-clade within the *Desulfobacteraceae* accounted for 50% of all SRB-related transcripts. Scavenging of $H_2$ is an essential process in anoxic marine sediments to keep $H_2$ concentrations low and thereby making $H_2$-forming fermentation thermodynamically possible, which is central to organic carbon degradation. Here, some sulfur-oxidizing *Gammaproteobacteria*, *Eudoraea* spp. and particularly sulfate-reducing *Desulfobacteraceae* may be essential for ecosystem functioning by scavenging $H_2$ (Figure 10).

### 4.5) Acetate consuming bacteria in coastal sediments

Acetate is a product of organic matter remineralization and at the same time a source of energy and carbon for bacteria and archaea not only in marine sediments. We were able to unravel the identity of physiologically and phylogenetically distinct bacterial groups that assimilated acetate in a coastal sediment such as *Gammaproteobacteria*, sulfate-reducing

*Desulfobacteraceae* and *Desulfobulbaceae* as well as sulfur-oxidizing *Roseobacter*-clade bacteria (Figure 10). Acetate incorporation was generally highest in the top layer of the sediment for all groups investigated in this study which is consistent with earlier studies that showed highest acetate assimilation in oxygenated surface layers (Christensen and Blackburn, 1980; Christensen and Blackburn, 1982). In marine surface sediments there is a high functional redundancy for the oxidation of rather simple organic compounds such as acetate, in particular in the top layer of the sediment (Böer *et al.*, 2009; Miyatake *et al.*, 2013; Baker *et al.*, 2015). Although acetate assimilating *Gammaproteobacteria* contributed only approximately 5% to the microbial community they accounted for up to 62% of the bacterial acetate assimilation thereby contributing the largest fraction to total acetate assimilation under both oxic and anoxic conditions. *Roseobacter*-clade bacteria showed highest cell-specific acetate uptake rates but they contributed only up to 11% to total bacterial acetate assimilation because of their low cell abundance *in situ*. However, high cell abundances (up to 10%) have been reported for lithoheterotrophic sulfur-oxidizing members of the *Roseobacter*-clade in coastal sediments (Lenk *et al.*, 2012). Thus *Roseobacter*-clade bacteria may be important for acetate turnover linked to oxidative sulfur cycling whereas the *Desulfobulbaceae* and the *Desulfobacteraceae* assimilated acetate likely during sulfate reduction (Figure 10).

### 4.6) Key functions of the sulfate-reducing Sva0081-clade in coastal sediments

Acetate is a central substrate for sulfate-reducing bacteria in marine sediments. In sediment slurry and intact sediment core incubations we showed acetate incorporation among uncultured relatives of *Desulfosarcina variabilis* (*Desulfosarcina/Desulfococcus*-group). In particular, we identified the Sva0081-clade as important acetate consumers within the *Desulfosarcina/Desulfococcus*-group. Intriguingly, members of the Sva0081-clade were found in high cell abundance accounting for up to 10% of cell counts in various tidal, seagrass and deep-sea sediments (Mussmann *et al.*, in prep.) and have been frequently identified in 16S rRNA gene surveys in various types of marine sediments (Ravenschlag *et al.*, 2000; Wang *et al.*, 2013; Liu *et al.*, 2014; Zheng *et al.*, 2014). Acetate was suggested to be the quantitatively most important substrate for complete oxidizing SRB (Laanbroek and Pfennig, 1981; Thauer and Postgate, 1982). Given their abundance and their metabolic potential to completely oxidize organic compounds to $CO_2$, the Sva0081 may be a key player in carbon- and sulfur-cycling in organic rich marine sediments (Figure 10).

Using single cell genomics we could link a cluster of [NiFe]-hydrogenase genes with the 16S rRNA gene of the Sva0081-clade. This cluster occurred in all three tested sediments and accounted for ~50% of all SRB-type $H_2$ase transcripts at site Janssand indicating a predominant role of the sulfate-reducing Sva0081-clade in $H_2$ consumption. In support of this,

the δ1-endosymbiont of *O. algarvensis*, also a member of Sva0081-clade, has been suggested to oxidize $H_2$ in Mediterranean sediments (Kleiner *et al.*, 2012; Kleiner *et al.*, 2015). Above all, we provide first molecular evidence that widely distributed and abundant sulfate reducers of the Sva0081-clade could be important drivers of $H_2$- and acetate oxidation in marine sediments. By keeping $H_2$ and acetate levels low they make fermentations thermodynamically feasible. SRB of the Sva0081-clade may also be important to global carbon cycling as they probably outcompete hydrogenoclastic methanogens in organic-rich marine surface sediments, thereby preventing the production of the potent greenhouse gas and therefore unwanted methane. Their cosmopolitan distribution, their metabolically versatile lifestyle and their ecological importance, make the Sva0081-clade a candidate key player in the marine anaerobic food chain.

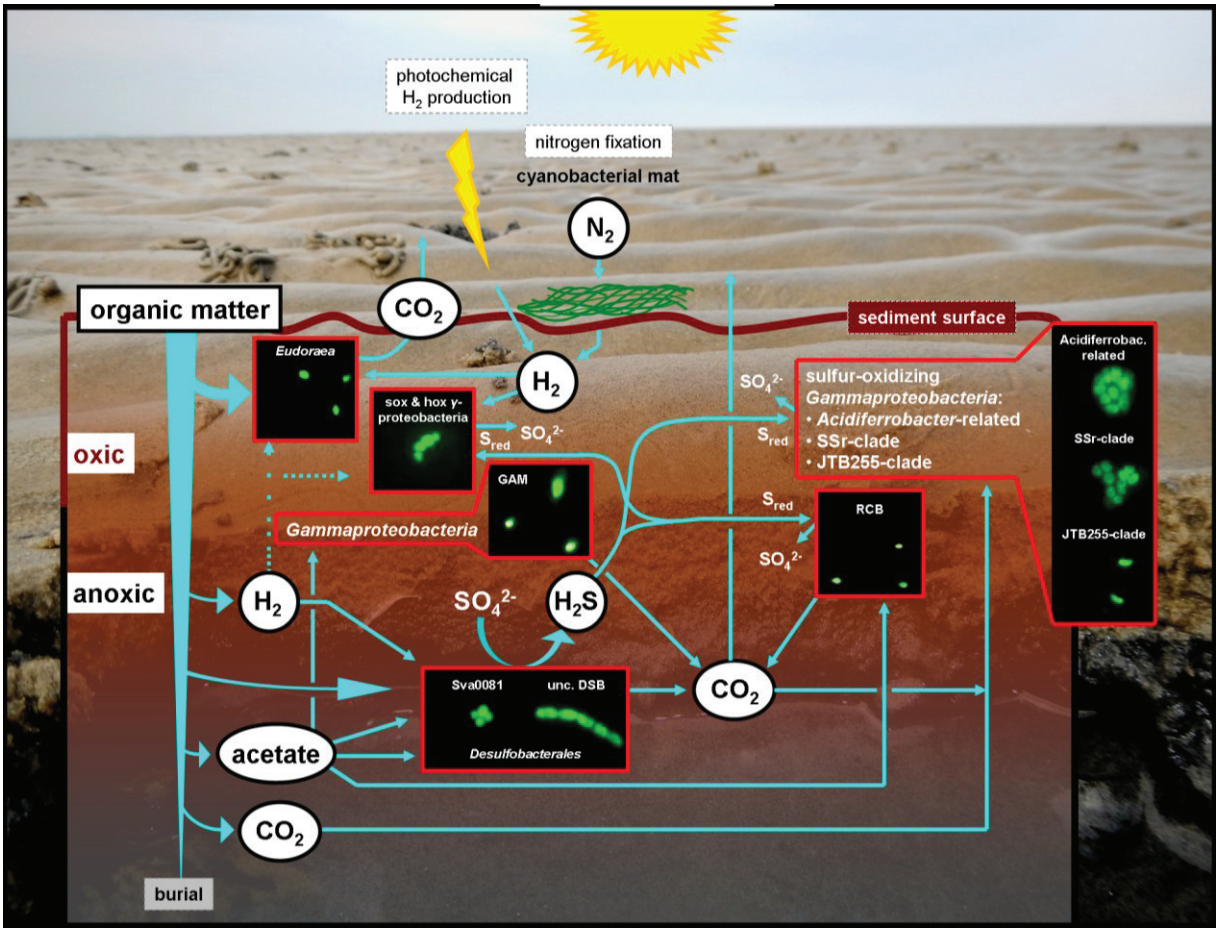


**Figure 10.** A simplified scheme depicting bacterial key players that consume intermediates and products from the remineralization of organic matter in marine sediments based on data presented in this dissertation. Organisms targeted in this study are highlighted (red boxes). $S_{red}$, reduced sulfur compound. Unc., uncultured. RCB, *Roseobacter*-clade bacteria. DSB, *Desulfobulbaceae*. Image of *Eudoraea* provided by M. Mußmann.

## 4.7) Methodological considerations: linking the identity of uncultured microbes with their activity

There are versatile applications of flow cytometry and cell sorting for molecular microbial ecology. Sorting of single cells or small cell batches of up to hundreds of cells is widely applied for subsequent genomic analysis (Woyke *et al.*, 2009; Swan *et al.*, 2011; Lloyd *et al.*, 2013; Kashtan *et al.*, 2014). Single cells were randomly sorted followed by whole genome amplification (WGA) and sequencing. In combination with tools such as the multi-labeled FISH approach (MiL-FISH; Schimak *et al.*, 2016) or hybridization chain reaction-FISH (HCR-FISH; Yamaguchi *et al.*, 2015) it allows the identification and flow cytometric enrichment of target cells prior to downstream processing. The sorted cell batch of FISH-identified and thereby phylogenetically related organisms can then be used for genomic analysis. This is of particular importance, if the target organisms are low abundant. Furthermore, HRC-FISH as well as MiL-FISH can be applied to living samples and thereby allow omitting fixation, which can greatly affect the accessibility of nucleic acids for further analysis (Yamaguchi *et al.*, 2015; Schimak *et al.*, 2016).

FACS of marine bacterioplankton after CARD-FISH was already described more than a decade ago (Sekar *et al.*, 2004). However, the application of flow cytometry to sediments is more challenging due to strongly enhanced background. First, cells need to be detached from the sediment particles (e.g., by ultrasonication) for a subsequent flow cytometric analysis. The cells in suspension are separated from sediment grains and larger particles to avoid clogging of the flow cytometer. Usually the orifice of the nozzle of a jet-in-air flow cytometer has a diameter between 50-200 µm. In this range is also the largest possible particle size that can be analyzed by flow cytometry. In order to purify cells from sediments density gradient centrifugation has been successfully applied for flow cytometric cell sorting and further downstream analysis (Lenk, 2011; Lloyd *et al.*, 2013). Flow cytometry is a high-throughput method and FACS together with radio-labeling has been used to measure the assimilation of radioactive substrates into individual populations of marine bacterioplankton (Zubkov *et al.*, 2004; Zubkov *et al.*, 2007; Jost *et al.*, 2008). Using nucleic acid or protein staining techniques different populations of a microbial community could be distinguished by flow cytometry based on their DNA or protein content. However, DNA- or protein-staining is rather unspecific and does not allow a phylogenetic identification.

With this research project I present a novel method combining radioisotope probing of sediment bacteria with cell detachment and flow cytometric sorting based on CARD-FISH identification of particular phylogenetic clades (**Manuscript I** and Figure 11).

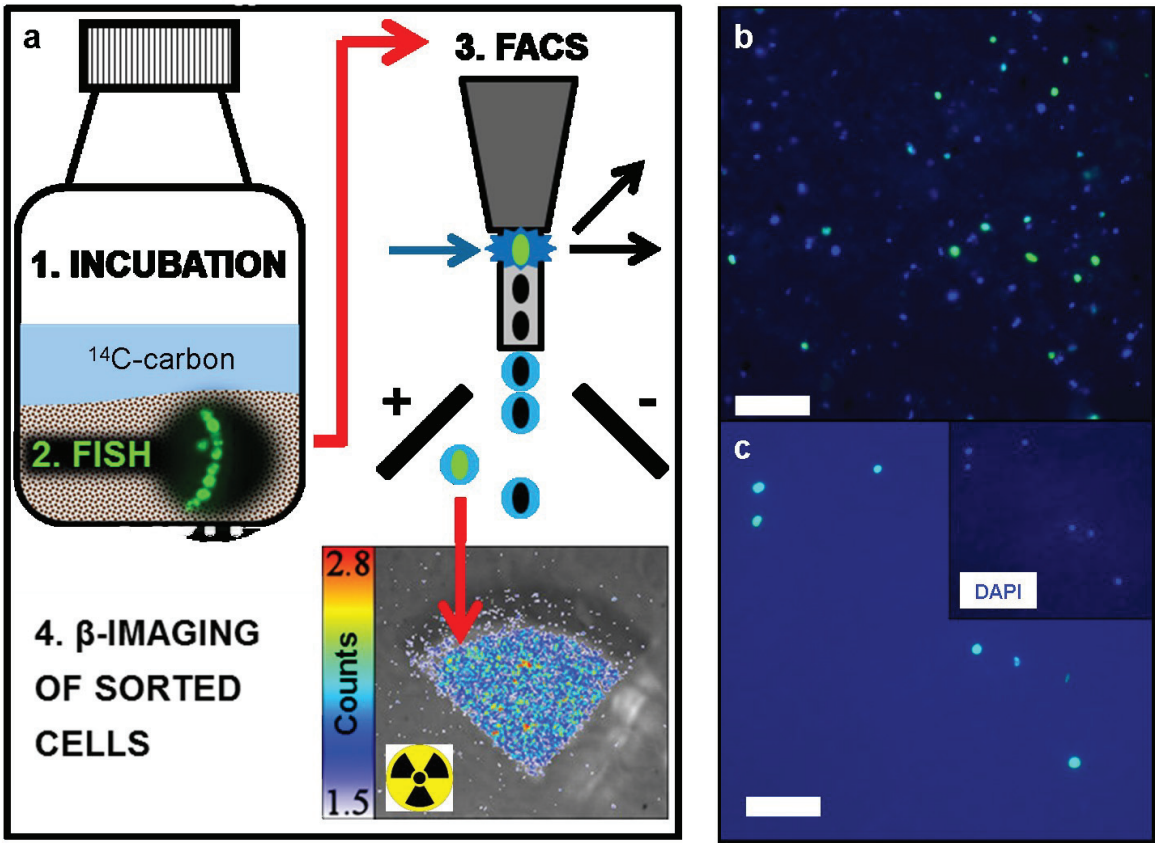


**Figure 11.** A novel approach that combines $^{14}$C carbon-labeling of cells with fluorescence *in situ* hybridization (FISH), fluorescence-activated cell sorting (FACS) and scintillography (*a*). Target cells from sediment incubation experiments were hybridized with specific FISH probes (*b*) and subsequently enriched using FACS (*c*) for quantification of radiotracer uptake. FISH signals are shown in green (*a-c*). In blue: DAPI-stain (*b* and *c*). Scale bars correspond to 10 µm (*b* and *c*).

After incubation of the sediments with radioisotopes cells were fixed using standard protocols and detached from sand grains by ultrasonication as described previously (Lenk *et al.*, 2011). Filtration through an 8 µm filter was used to separate larger particles from the cells prior to flow cytometry. Simple filtration omits elaborate purification steps such as density gradient centrifugation, which may be selective for certain cells and may result in low recovery. After filtration FACS of sediment bacteria and archaea triggered by CARD-FISH probe fluorescence resulted in high purity (always above 93%).

FISH can be too insensitive to comprehensively target organisms with very low ribosome content. Therefore, it would be possible that FACS after CARD-FISH may be biased towards active cells. However, the activity of organisms in organic rich surface sediments is generally high and in our experimental set up cell sorting was not selective. We identified similar abundances of $^{14}$C-assimilating gammaproteobacterial cells using microautoradiography-FISH (MAR-FISH) with a general probe for *Gammaproteobacteria* (GAM42a) on the initial $^{14}$C-incubated sediment sample before cell sorting compared to MAR-identification on flow-sorted *Gammaproteobacteria.* This was repeated for different sediment incubations with $^{14}$C

bicarbonate and $^{14}C$ acetate suggesting that the work flow was not selective although a fraction of the cells were lost during filtration. Moreover, MAR-FISH on sedimentary bacteria and archaea would benefit from flow cytometric enrichment of target population beforehand. Low abundant and little active populations are difficult to identify within a complex microbial community using MAR. Lenk (2011) identified no $^{14}C$ acetate-assimilating sulfate-reducing bacteria of the *Desulfosarcina/Desulfococcus*-clade in incubations with sediment from a tidal flat (Janssand). On the contrary, after flow sorting of *Desulfosarcina/Desulfococcus*-clade bacteria and subsequent MAR we identified $^{14}C$ acetate-assimilating cells in the same sample (Figure 12) and we were able to quantify their uptake (**Manuscript III**).

Commencing with short-term radiotracer incubation, the entire workflow to analyze various phylogenetic clades from multiple samples can be conducted within 1-2 days. Our novel workflow was technically highly reproducible and for the first time it combines high-throughput, phylogenetic identification and an accurate quantification of substrate assimilation. Thereby, our approach outclasses other isotope-labeling methods such as MAR-FISH, HISH-SIMS and stable isotope probing (Boschker *et al.*, 1998; Lee *et al.*, 1999; Radajewski *et al.*, 2000; Manefield *et al.*, 2002; Musat *et al.*, 2008) as it overcomes their limitations in throughput and precision. Furthermore, the radioactive label does not need to be channeled into nucleic acids as for RNA- and DNA-SIP. This allowed us to identify cells that incorporated a substrate, which was directly used to build intracellular storage compounds such as PHAs (**Manuscript III**).

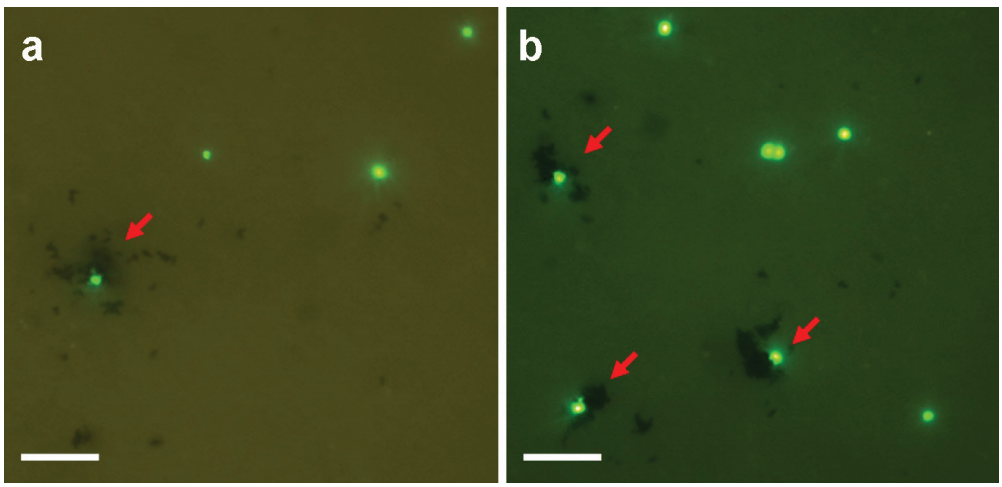


**Figure 12.** Microautoradiography on sorted cells of *Gammaproteobacteria* (*a*, probe GAM42a) and the *Desulfosarcina/Desulfococcus*-clade (*b*, probe DSS658). Precipitation of silver grains around the cell (red arrows) indicate uptake of the radioactive substrate ($^{14}C$ acetate).

## 4.8) Future perspectives of FACS in microbial ecology of sediment bacteria

GeneFISH provides the possibility to visualize the presence of a functional gene within phylogenetically identified microorganisms (Moraru *et al.*, 2010). The current geneFISH protocols (Moraru *et al.*, 2010; Barrero-Canosa *et al*., in prep.) are still limited to samples with

low background. Sediment samples generally have high background that weakens the signal to noise ratio and thereby a clear identification of specific gene signals is not possible. FACS triggered by unspecific DNA-stain would extract all microbial cells from sediment background and allow applying the geneFISH protocols on sediment bacteria.

Another interesting combination is bioorthogonal non-canonical amino acid tagging (BONCAT) on environmental microbes (Hatzenpichler *et al.*, 2014) with FACS. BONCAT is based on incorporation of artificial amino acids carrying clickable alkyne or azide moieties into newly synthesized proteins of active cells (Figure 13). Thus, active microbes can be separated from a complex microbial community by cell sorting based on the BONCAT-signal for a subsequent identification or analysis. Furthermore, BONCAT together with FACS of FISH-identified cells would enable to purify the newly synthesized proteome from a particular phylogenetic clade by azide/alkyne-affinity chromatography. Analysis of the purified proteins would allow identification of newly expressed protein dependent on different environmental parameters such as carbon sources, electron donors and acceptors within a target population.

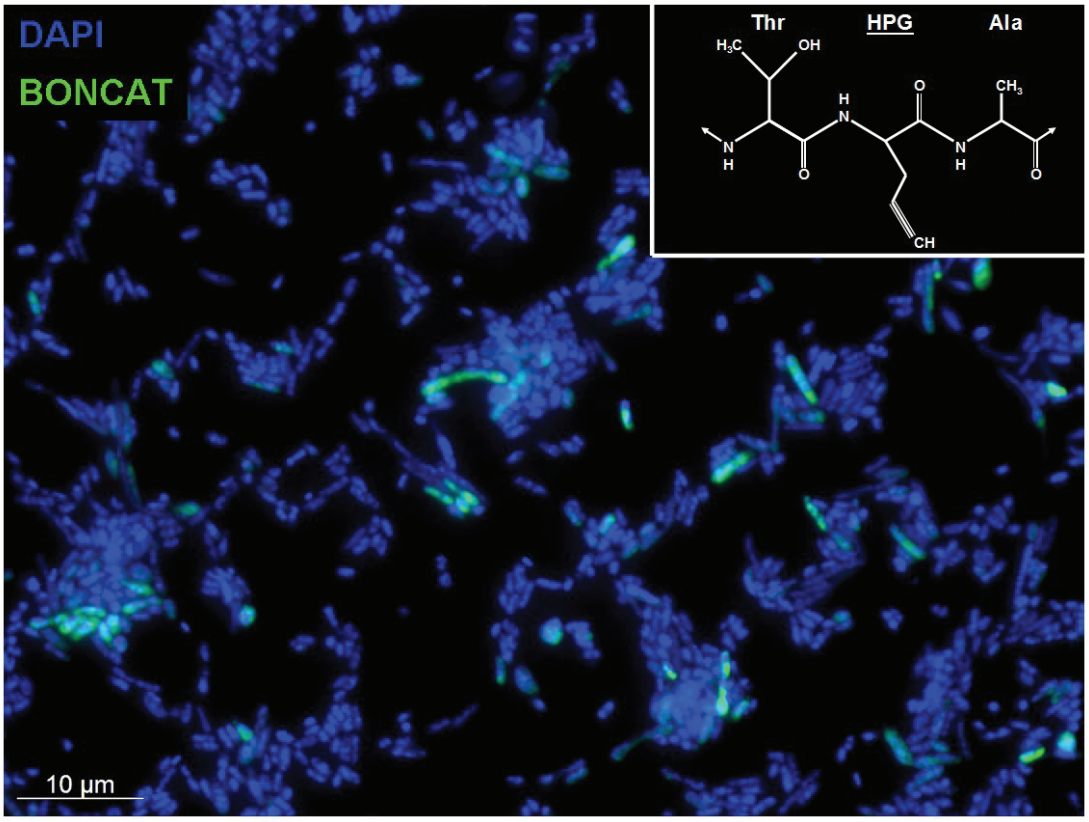


**Figure 13**. Bacterial culture after bioorthogonal non-canonical amino acid tagging (BONCAT). BONCAT-signals of cells that synthesized new proteins during incubation in presence of homoproparagylglycine (HPG) appear in green. The artificial amino acid HPG carries a free alkyne moiety and is built into newly synthesized proteins of active cells analogue to methionine (upper right corner of the figure). The incorporated HPG can be linked to an azide-modified dye in a click reaction. In blue: DAPI-stain.

So far the approach combining radio-labeling of sediment bacteria, FACS after CARD-FISH and scintillography introduced in this study depends on the incorporation of radioisotopes. Commercially available $^{14}C$ carbon compounds are still limited and other elements such as nitrogen have radioisotopes with short half-life that makes them hardly applicable for tracer experiments in microbial ecology. The use of stable isotopes with our novel approach would circumvent these limitations. Nanoscale secondary ion mass spectrometry (nanoSIMS) has been used to trace uptake of stable isotopes into environmental microbes (e.g., Behrens *et al.*, 2008; Musat *et al.*, 2008; Morono *et al.*, 2011; Dekas and Orphan, 2011; Dekas *et al.*, 2014; Vasquez-Cardenas *et al.*, 2015). Single microbial cells can be analyzed at a spatial resolution of 50 nm but measurements of larger cell batches (thousands of cells) are very time-consuming and thereby unfeasible. Here, time-of-flight secondary ion mass spectrometry (TOF-SIMS) may be an alternative for analysis of the sorted cell batches. TOF-SIMS is a surface analytical technique that used a primary ion beam to produce secondary ions from the surface of a sample analyzed by time-of-flight measurement. In a single run an area of several square millimetres can be analyzed by TOF-SIMS. Batches of FISH-identified and flow-sorted cells from incubation experiments may be spotted on a defined area of a wafer or slide for TOF-SIMS analysis thereby allow the quantification of population-specific stable isotope-labeled substrate uptake.

Our novel isotope probing approach using either stable- or radioisotopes is a valuable tool for future experiments that aim at unravelling the ecological role of uncultured microorganisms in carbon turnover within complex communities. It can be easily adapted to various other ecosystems besides sediments such as soil, marine- and freshwater.

# 5.) Outlook

This thesis provided a first glimpse at the metabolism of the enigmatic JTB255-clade as we demonstrated their capability to fix inorganic carbon. However, it is still unresolved what physiological traits make this clade globally successful in benthic marine environments. No isolates or genomes are currently available for members of the gammaproteobacterial JTB255-clade. So far, we were not successful to recover a sequence bin affiliating with the JTB255-clade using metagenomics, although this group is abundant at the site where we conducted our metagenomic approach. Metagenomics as well as single cell genomics targeting the JTB255-clade should be subject of future studies and will be essential to establish concepts of potential energy metabolism and carbon assimilation pathways. In addition, the genomic information may help to enrich and ultimately isolate a representative of the JTB255-clade. Isolation and cultivation will be vital to in-depth study ecophysiological responses to single parameters in a controlled environment also for other ubiquitous and abundant but uncultured groups identified in this study such as the SSr- and the Sva0081-clade.

Acetate turnover in marine sediments has been studied for several decades. But it is surprising that some basic questions regarding the turnover of acetate still remain unresolved: are there key groups of microorganisms that oxidize acetate *in situ* and particularly how much do they contribute to total acetate assimilation? What pathways are important for acetate turnover in the environment? To some extent we were able to shed light on the first question as we quantified acetate assimilation for phylogenetically identified groups in a coastal sediment. *Gammaproteobacteria* accounted for a major fraction of total acetate assimilation at site Janssand but the responsible subgroups within the *Gammaproteobacteria* need to be identified on a higher phylogenetic resolution. Using SIP several gammaproteobacterial groups have been identified in the past that assimilate acetate. Our novel approach can be used to quantify their contribution to total acetate assimilation and also to screen additional sites. The results presented within this study suggest that acetate is used by a phylogenetically and metabolically versatile range of bacteria besides the *Gammaproteobacteria* and thereby pave the way for future studies aiming to further elucidate spatial and temporal patterns of acetate incorporation in marine sediments. Using single cell- and metagenomics combined with metatranscriptomics possible pathways for acetate assimilation, growth on acetate and PHA formation should be further investigated. A change in expression of these pathways with sediment depth and across different electron donor/acceptor regimes will be vital to unravel the role of acetate as substrate for different functional groups such as sulfate reducers and sulfur oxidizers.

# References


Adhikari RR, Glombitza C, Nickel JC, Anderson CH, Dunlea AG, Spivack AJ, *et al.* (2016). hydrogen utilization potential in subsurface sediments. *Microbiol Chem Geomicrobiol* 8.

Alain K, Querellou J. (2009). Cultivating the uncultured: limits, advances and future challenges. *Extremophiles* **13**: 583–594.

Amann RI, Ludwig W, Schleifer KH. (1995). Phylogenetic identification and *in situ* detection of individual microbial cells without cultivation. *Microbiol Rev* **59**: 143–169.

Anantharaman K, Breier JA, Sheik CS, Dick GJ. (2013). Evidence for hydrogen oxidation and metabolic plasticity in widespread deep-sea sulfur-oxidizing bacteria. *Proc Natl Acad Sci* **110**: 330–335.

Andreae MO, Raemdonck H. (1983). Dimethyl sulfide in the surface ocean and the marine atmosphere: a global view. *Science* **221**: 744–747.

Aragno M, Schlegel HG. (1992). The mesophilic hydrogen-oxidizing (knallgas) bacteria. In: *The Prokaryotes*. 2nd edn, pp. 344–384. Edited by Balows A, Trüper HG, Dworkin M, Harder W & Schleifer K-H. New York: Springer Verlag.

Archer D, Maier-Reimer E. (1994). Effect of deep-sea sedimentary calcite preservation on atmospheric $CO_2$ concentration. *Nature* **367**: 260–263.

Arnosti C. (2004). Speed bumps and barricades in the carbon cycle: substrate structural effects on carbon cycling. *Mar Chem* **92**: 263–273.

Azam F, Fenchel T, Field J, Gray J, Meyer-Reil L, Thingstad F. (1983). The ecological role of water-column microbes in the sea. *Mar Ecol Prog Ser* **10**: 257–263.

Azam F, Malfatti F. (2007). Microbial structuring of marine ecosystems. *Nat Rev Microbiol* **5**: 782–791.

Baker BJ, Lazar CS, Teske AP, Dick GJ. (2015). Genomic resolution of linkages in carbon, nitrogen, and sulfur cycling among widespread estuary sediment bacteria. *Microbiome* **3**: 14.

Bassham JA, Calvin M. (1960). The path of carbon in photosynthesis. In: Pirson PDA (ed) Handbuch der Pflanzenphysiologie / Encyclopedia of Plant Physiology. *Die $CO_2$-Assimilation / The Assimilation of Carbon Dioxide*. Springer Berlin Heidelberg, pp 884–922.

Behrens S, Lösekann T, Pett-Ridge J, Weber PK, Ng W-O, Stevenson BS, *et al.* (2008). Linking microbial phylogeny to metabolic activity at the single-cell level by using enhanced element labeling-catalyzed reporter deposition fluorescence *in situ* hybridization (EL-FISH) and nanoSIMS. *Appl Environ Microbiol* **74**: 3143–3150.

Berg IA. (2011). Ecological aspects of the distribution of different autotrophic $CO_2$ fixation pathways. *Appl Environ Microbiol* **77**: 1925–1936.

Berg IA, Kockelkorn D, Buckel W, Fuchs G. (2007). A 3-hydroxypropionate/4-hydroxybutyrate autotrophic carbon dioxide assimilation pathway in archaea. *Science* **318**: 1782–1786.

Berg IA, Kockelkorn D, Ramos-Vera WH, Say RF, Zarzycki J, Hügler M, *et al.* (2010). Autotrophic carbon fixation in archaea. *Nat Rev Microbiol* **8**: 447–460.

Bergstein T, Henis Y, Cavari BZ. (1979). Investigations on the photosynthetic sulfur bacterium *Chlorobium phaeobacteroides* causing seasonal blooms in Lake Kinneret. *Can J Microbiol* **25**: 999–1007.

Bienhold C, Zinger L, Boetius A, Ramette A. (2016). Diversity and biogeography of bathyal and abyssal seafloor bacteria. *PLoS ONE* **11**. Doi: 10.1371/journal.pone.0148016.

Böer SI, Hedtkamp SIC, van Beusekom JEE, Fuhrman JA, Boetius A, Ramette A. (2009). Time- and sediment depth-related variations in bacterial diversity and community structure in subtidal sands. *ISME J* **3**: 780–791.

Bok FAM de, Roze EHA, Stams AJM. (2002). Hydrogenases and formate dehydrogenases of *Syntrophobacter fumaroxidans*. *Antonie Van Leeuwenhoek* **81**: 283–291.

Boschker HTS, Nold SC, Wellsbury P, Bos D, Graaf W de, Pel R, *et al.* (1998). Direct linking of microbial populations to specific biogeochemical processes by $^{13}C$-labeling of biomarkers. *Nature* **392**: 801–805.

Boschker HTS, Vasquez-Cardenas D, Bolhuis H, Moerdijk-Poortvliet TWC, Moodley L. (2014). Chemoautotrophic carbon fixation rates and active bacterial communities in intertidal marine sediments. *PLoS ONE* **9**: e101443.

Bowman JP, McCammon SA, Dann AL. (2005). Biogeographic and quantitative analyses of abundant uncultivated γ-proteobacterial clades from marine sediment. *Microb Ecol* **49**: 451–460.

Bowman JP, McCuaig RD. (2003). Biodiversity, community structural shifts, and biogeography of prokaryotes within Antarctic continental shelf sediment. *Appl Environ Microbiol* **69**: 2463–2483.

Brinkhoff T, Muyzer G, Wirsen CO, Kuever J. (1999). *Thiomicrospira kuenenii* sp. nov. and *Thiomicrospira frisia* sp. nov., two mesophilic obligately chemolithoautotrophic sulfur-oxidizing bacteria isolated from an intertidal mud flat. *Int J Syst Bacteriol* **49**: 385–392.

Brune DC. (1989). Sulfur oxidation by phototrophic bacteria. *Biochim Biophys Acta BBA - Bioenerg* **975**: 189–221.

Brüser T, Lens PNL, Trüper HG. (2000). The biological sulfur cycle. In: *Environmental Technologies to Treat Sulfur Pollution*. Lens P and Hulshoff Pol, l. IWA London. pp 47–85.

Bryantseva I, Gorlenko VM, Kompantseva EI, Imhoff JF, Süling J, Mityushina L. (1999). *Thiorhodospira sibirica* gen. nov., sp. nov., a new alkaliphilic purple sulfur bacterium from a Siberian soda lake. *Int J Syst Evol Microbiol* **49**: 697–703.

Buchan A, González JM, Moran MA. (2005). Overview of the marine *Roseobacter* lineage. *Appl Environ Microbiol* **71**: 5665–5677.

Buchanan BB, Arnon DI. (1990). A reverse KREBS cycle in photosynthesis: consensus at last. *Photosynth Res* **24**: 47–53.

Burdige DJ. (2007). Preservation of organic matter in marine sediments: controls, mechanisms, and an imbalance in sediment organic carbon budgets? *Chem Rev* **107**: 467–485.

Burggraf S, Olsen GJ, Stetter KO, Woese CR. (1992). A phylogenetic analysis of *Aquifex pyrophilus*. *Syst Appl Microbiol* **15**: 352–356.

Caldwell PE, MacLean MR, Norris PR. (2007). Ribulose bisphosphate carboxylase activity and a Calvin cycle gene cluster in *Sulfobacillus* species. *Microbiology* **153**: 2231–2240.

Campbell BJ, Engel AS, Porter ML, Takai K. (2006). The versatile ε-proteobacteria: key players in sulphidic habitats. *Nat Rev Microbiol* **4**: 458–468.

Canfield DE. (1993). Organic matter oxidation in marine sediments. In: Wollast R, Mackenzie FT, Chou L (eds) NATO ASI Series. *Interactions of C, N, P and S biogeochemical cycles and global change*. Springer Berlin Heidelberg, pp 333–363.

Canfield DE, Kristensen E, Thamdrup B. (2005a). Aquatic Geomicrobiology. Gulf Professional Publishing.

Canfield DE, Kristensen E, Thamdrup B. (2005b). Heterotrophic carbon metabolism. In: Donald E. Canfield EK and BT (ed) Aquatic Geomicrobiology Vol. 48. *Advances in Marine Biology*. Academic Press, pp 129–166.

Canfield DE, Stewart FJ, Thamdrup B, Brabandere LD, Dalsgaard T, Delong EF, *et al.* (2010). A cryptic sulfur cycle in oxygen-minimum–zone waters off the Chilean coast. *Science* **330**: 1375–1378.

Canfield DE, Thamdrup B, Hansen JW. (1993). The anaerobic degradation of organic matter in Danish coastal sediments: iron reduction, manganese reduction, and sulfate reduction. *Geochim Cosmochim Acta* **57**: 3867–3883.

Christensen D, Blackburn TH. (1982). Turnover of $^{14}$C-labeled acetate in marine sediments. *Mar Biol* **71**: 113–119.

Christensen D, Blackburn TH. (1980). Turnover of tracer ($^{14}C$, $^{3}H$ labeled) alanine in inshore marine sediments. *Mar Biol* **58**: 97–103.

Curson ARJ, Todd JD, Sullivan MJ, Johnston AWB. (2011). Catabolism of dimethylsulphoniopropionate: microorganisms, enzymes and genes. *Nat Rev Microbiol* **9**: 849–859.

Dahl C, Friedrich C, Kletzin A. (2001). Sulfur oxidation in prokaryotes. In: *eLS*. John Wiley & Sons, Ltd. http://onlinelibrary.wiley.com/doi/10.1002/9780470015902.a0021155/abstract

Dahl DC. (2008). Inorganic sulfur compounds as electron donors in purple sulfur bacteria. In: Hell R, Dahl DC, Knaff D, Leustek T (eds) Advances in Photosynthesis and Respiration. *Sulfur Metabolism in Phototrophic Organisms*. Springer Netherlands, pp 289–317.

Dauwe B, Middelburg JJ, Herman PMJ, Heip CHR. (1999). Linking diagenetic alteration of amino acids and bulk organic matter reactivity. *Limnol Oceanogr* **44**: 1809–1814.

Dekas AE, Chadwick GL, Bowles MW, Joye SB, Orphan VJ. (2014). Spatial distribution of nitrogen fixation in methane seep sediment and the role of the ANME archaea. *Environ Microbiol* **16**: 3012–3029.

Dekas AE, Orphan VJ. (2011). Identification of diazotrophic microorganisms in marine sediment via fluorescence *in situ* hybridization coupled to nanoscale secondary ion mass spectrometry (FISH-NanoSIMS). *Methods Enzymol* **486**: 281–305.

Demaison GJ, Moore GT. (1980). Anoxic environments and oil source bed genesis. *Org Geochem* **2**: 9–31.

Devereux R, Delaney M, Widdel F, Stahl DA. (1989). Natural relationships among sulfate-reducing eubacteria. *J Bacteriol* **171**: 6689–6695.

Dhillon A, Teske A, Dillon J, Stahl DA, Sogin ML. (2003). Molecular characterization of sulfate-reducing bacteria in the Guaymas Basin. *Appl Environ Microbiol* **69**: 2765–2772.

Diekert G, Wohlfarth G. (1994). Metabolism of homoacetogens. *Antonie Van Leeuwenhoek* **66**: 209–221.

Drews G, Imhoff JF. (1991). Phototrophic purple bacteria. *Var Autotroph Life Acad Press Ltd NY* 51–97.

Drobner E, Huber H, Wächtershäuser G, Rose D, Stetter KO. (1990). Pyrite formation linked with hydrogen evolution under anaerobic conditions. *Nature* **346**: 742–744.

Duarte CM, Middelburg JJ, Caraco N. (2005). Major role of marine vegetation on the oceanic carbon cycle. *Biogeosciences* **2**: 1–8.

Dubilier N, Bergin C, Lott C. (2008). Symbiotic diversity in marine animals: the art of harnessing chemosynthesis. *Nat Rev Microbiol* **6**: 725–740.

Dubini A, Pye RL, Jack RL, Palmer T, Sargent F. (2002). How bacteria get energy from hydrogen: a genetic analysis of periplasmic hydrogen oxidation in *Escherichia coli*. *Int J Hydrog Energy* **27**: 1413–1420.

Dumont MG, Murrell JC. (2005). Stable isotope probing - linking microbial identity to function. *Nat Rev Microbiol* **3**: 499–504.

Dunne JP, Sarmiento JL, Gnanadesikan A. (2007). A synthesis of global particle export from the surface ocean and cycling through the ocean interior and on the seafloor. *Glob Biogeochem Cycles* **21**: GB4006.

Emil Ruff S, Probandt D, Zinkann A-C, Iversen MH, Klaas C, Würzberg L, *et al.* (2014). Indications for algae-degrading benthic microbial communities in deep-sea sediments along the Antarctic Polar Front. *Deep Sea Res Part II Top Stud Oceanogr* **108**: 6–16.

Evrard V, Soetaert K, Heip C, Huettel M, Xenopoulos M, Middelburg J. (2010). Carbon and nitrogen flows through the benthic food web of a photic subtidal sandy sediment. *Mar Ecol Prog Ser* **416**: 1–16.

Falkowski P, Scholes RJ, Boyle E, Canadell J, Canfield D, Elser J, *et al.* (2000). The global carbon cycle: a test of our knowledge of earth as a system. *Science* **290**: 291–296.

Falkowski PG, Raven JA. (2013). Aquatic photosynthesis: (Second Edition). Princeton University Press.

Farmer WR, Liao JC. (1997). Reduction of aerobic acetate production by *Escherichia coli*. *Appl Environ Microbiol* **63**: 3205–3210.

Fenchel TM, Jørgensen BB. (1977). Detritus food chains of aquatic ecosystems: the role of bacteria. In: Alexander M (ed) Advances in Microbial Ecology. *Advances in Microbial Ecology*. Springer US, pp 1–58.

Field CB, Behrenfeld MJ, Randerson JT, Falkowski P. (1998). Primary production of the biosphere: integrating terrestrial and oceanic components. *Science* **281**: 237–240.

Finke N, Vandieken V, Jørgensen BB. (2007). Acetate, lactate, propionate, and isobutyrate as electron donors for iron and sulfate reduction in Arctic marine sediments, Svalbard. *FEMS Microbiol Ecol* **59**: 10–22.

Fossing H, Gallardo VA, Jørgensen BB, Hüttel M, Nielsen LP, Schulz H, *et al.* (1995). Concentration and transport of nitrate by the mat-forming sulphur bacterium *Thioploca*. *Nature* **374**: 713–715.

Fourqurean JW, Duarte CM, Kennedy H, Marbà N, Holmer M, Mateo MA, *et al.* (2012). Seagrass ecosystems as a globally significant carbon stock. *Nat Geosci* **5**: 505–509.

Fox JD, He Y, Shelver D, Roberts GP, Ludden PW. (1996a). Characterization of the region encoding the CO-induced hydrogenase of *Rhodospirillum rubrum*. *J Bacteriol* **178**: 6200–6208.

Fox JD, Kerby RL, Roberts GP, Ludden PW. (1996b). Characterization of the CO-induced, CO-tolerant hydrogenase from *Rhodospirillum rubrum* and the gene encoding the large subunit of the enzyme. *J Bacteriol* **178**: 1515–1524.

Friedrich CG, Bardischewsky F, Rother D, Quentmeier A, Fischer J. (2005). Prokaryotic sulfur oxidation. *Curr Opin Microbiol* **8**: 253–259.

Frigaard N-U, Dahl C. (2008). Sulfur metabolism in phototrophic sulfur bacteria. In: Poole RK (ed) Vol. 54. *Advances in Microbial Physiology*. Academic Press, pp 103–200.

Froelich PN, Klinkhammer GP, Bender ML, Luedtke NA, Heath GR, Cullen D, *et al.* (1979). Early oxidation of organic matter in pelagic sediments of the eastern equatorial Atlantic: suboxic diagenesis. *Geochim Cosmochim Acta* **43**: 1075–1090.

Fuchs G. (2011). Alternative pathways of carbon dioxide fixation: insights into the early evolution of life? *Annu Rev Microbiol* **65**: 631–658.

Fuchs G. (1994). Variations of the acetyl-CoA pathway in diversely related microorganisms that are not acetogens. In: Drake HL (ed) Chapman & Hall Microbiology Series. *Acetogenesis*. Springer US, pp 507–520.

Gattuso J-P, Gentili B, Duarte CM, Kleypas JA, Middelburg JJ, Antoine D. (2006). Light availability in the coastal ocean: impact on the distribution of benthic photosynthetic organisms and their contribution to primary production. *Biogeosciences* **3**: 489–513.

Gittel A, Mußmann M, Sass H, Cypionka H, Könneke M. (2008). Identity and abundance of active sulfate-reducing bacteria in deep tidal flat sediments determined by directed cultivation and CARD-FISH analysis. *Environ Microbiol* **10**: 2645–2658.

Glöckner FO, Fuchs BM, Amann R. (1999). Bacterioplankton compositions of lakes and oceans: a first comparison based on fluorescence *in situ* hybridization. *Appl Environ Microbiol* **65**: 3721–3726.

Gobet A, Böer SI, Huse SM, van Beusekom JEE, Quince C, Sogin ML, *et al.* (2012). Diversity and dynamics of rare and of resident bacterial populations in coastal sands. *ISME J* **6**: 542–553.

González JM, Covert JS, Whitman WB, Henriksen JR, Mayer F, Scharf B, *et al.* (2003). *Silicibacter pomeroyi* sp. nov. and *Roseovarius nubinhibens* sp. nov., dimethylsulfoniopropionate-demethylating bacteria from marine environments. *Int J Syst Evol Microbiol* **53**: 1261–1269.

González JM, Kiene RP, Moran MA. (1999). Transformation of sulfur compounds by an abundant lineage of marine bacteria in the alpha-subclass of the class *Proteobacteria*. *Appl Environ Microbiol* **65**: 3810–3819.

González JM, Moran MA. (1997). Numerical dominance of a group of marine bacteria in the alpha-subclass of the class *Proteobacteria* in coastal seawater. *Appl Environ Microbiol* **63**: 4237–4242.

Goodwin S, Conrad R, Zeikus JG. (1988). Influence of pH on microbial hydrogen metabolism in diverse sedimentary ecosystems. *Appl Environ Microbiol* **54**: 590–593.

Graaf W de, Wellsbury P, Parkes RJ, Cappenberg TE. (1996). Comparison of acetate turnover in methanogenic and sulfate-reducing sediments by radiolabeling and stable isotope labeling and by use of specific inhibitors: evidence for isotopic exchange. *Appl Environ Microbiol* **62**: 772–777.

Greening C, Biswas A, Carere CR, Jackson CJ, Taylor MC, Stott MB, *et al.* (2015). Genomic and metagenomic surveys of hydrogenase distribution indicate $H_2$ is a widely utilised energy source for microbial growth and survival. *ISME J*. doi: 10.1038/ismej.2015.153.

Grote J, Labrenz M, Pfeiffer B, Jost G, Jürgens K. (2007). Quantitative distributions of *Epsilonproteobacteria* and a *Sulfurimonas* subgroup in pelagic redoxclines of the Central Baltic Sea. *Appl Environ Microbiol* **73**: 7155–7161.

Grote J, Schott T, Bruckner CG, Glöckner FO, Jost G, Teeling H, *et al.* (2012). Genome and physiology of a model epsilonproteobacterium responsible for sulfide detoxification in marine oxygen depletion zones. *Proc Natl Acad Sci* **109**: 506–510.

Hagen KD, Nelson DC. (1996). Organic carbon utilization by obligately and facultatively autotrophic beggiatoa strains in homogeneous and gradient cultures. *Appl Environ Microbiol* **62**: 947–953.

Hansen M, Perner M. (2015). A novel hydrogen oxidizer amidst the sulfur-oxidizing *Thiomicrospira* lineage. *ISME J* **9**: 696–707.

Hatzenpichler R, Scheller S, Tavormina PL, Babin BM, Tirrell DA, Orphan VJ. (2014). *In situ* visualization of newly synthesized proteins in environmental microbes using amino acid tagging and click chemistry. *Environ Microbiol* **16**: 2568–2590.

Hawley AK, Brewer HM, Norbeck AD, Paša-Tolić L, Hallam SJ. (2014). Metaproteomics reveals differential modes of metabolic coupling among ubiquitous oxygen minimum zone microbes. *Proc Natl Acad Sci* **111**: 11395–11400.

Hedges JI, Keil RG. (1995). Sedimentary organic matter preservation: an assessment and speculative synthesis. *Mar Chem* **49**: 81–115.

Hedges JI, Keil RG, Benner R. (1997). What happens to terrestrial organic matter in the ocean? *Org Geochem* **27**: 195–212.

Heising S, Richter L, Ludwig W, Schink B. (1999). *Chlorobium ferrooxidans* sp. nov., a phototrophic green sulfur bacterium that oxidizes ferrous iron in coculture with a ‘Geospirillum’ sp. strain. *Arch Microbiol* **172**: 116–124.

Higuchi Y, Yagi T, Yasuoka N. (1997). Unusual ligand structure in Ni–Fe active center and an additional Mg site in hydrogenase revealed by high resolution X-ray structure analysis. *Structure* **5**: 1671–1680.

Hoehler TM, Alperin MJ, Albert DB, Martens CS. (1998). Thermodynamic control on hydrogen concentrations in anoxic sediments. *Geochim Cosmochim Acta* **62**: 1745–1756.

Hoehler TM, Bebout BM, Des Marais DJ. (2001). The role of microbial mats in the production of reduced gases on the early Earth. *Nature* **412**: 324–327.

Holo H. (1989). *Chloroflexus aurantiacus* secretes 3-hydroxypropionate, a possible intermediate in the assimilation of $CO_2$ and acetate. *Arch Microbiol* **151**: 252–256.

Hoor AT-T. (1975). A new type of thiosulphate oxidizing, nitrate reducing microorganism: *Thiomicrospira denitrificans* sp. Nov. *Neth J Sea Res* **9**: 344–350.

Howard EC, Henriksen JR, Buchan A, Reisch CR, Bürgmann H, Welsh R, *et al.* (2006). Bacterial taxa that limit sulfur flux from the ocean. *Science* **314**: 649–652.

Howard EC, Sun S, Biers EJ, Moran MA. (2008). Abundant and diverse bacteria involved in DMSP degradation in marine surface waters. *Environ Microbiol* **10**: 2397–2410.

Howarth RW. (1984). The ecological significance of sulfur in the energy dynamics of salt marsh and coastal marine sediments. *Biogeochemistry* **1**: 5–27.

Huber G, Stetter KO. (1991). *Sulfolobus metallicus*, sp. nov., a novel strictly chemolithoautotrophic thermophilic archaeal species of metal-mobilizers. *Syst Appl Microbiol* **14**: 372–378.

Huber H, Gallenberger M, Jahn U, Eylert E, Berg IA, Kockelkorn D, *et al.* (2008). A dicarboxylate/4-hydroxybutyrate autotrophic carbon assimilation cycle in the hyperthermophilic Archaeum *Ignicoccus hospitalis*. *Proc Natl Acad Sci* **105**: 7851–7856.

Huber H, Prangishvili D. (2006). *Sulfolobales*. In: Dr MDP, Falkow S, Rosenberg E, Schleifer K-H, Stackebrandt E (eds). *The Prokaryotes*. Springer New York, pp 23–51.

Huber R, Wilharm T, Huber D, Trincone A, Burggraf S, König H, *et al.* (1992). *Aquifex pyrophilus* gen. nov. sp. nov., represents a novel group of marine hyperthermophilic hydrogen-oxidizing bacteria. *Syst Appl Microbiol* **15**: 340–351.

Hügler M, Huber H, Molyneaux SJ, Vetriani C, Sievert SM. (2007). Autotrophic $CO_2$ fixation via the reductive tricarboxylic acid cycle in different lineages within the phylum *Aquificae*: evidence for two ways of citrate cleavage. *Environ Microbiol* **9**: 81–92.

Hügler M, Sievert SM. (2011). Beyond the Calvin cycle: autotrophic carbon fixation in the ocean. *Annu Rev Mar Sci* **3**: 261–289.

Hügler M, Wirsen CO, Fuchs G, Taylor CD, Sievert SM. (2005). Evidence for autotrophic $CO_2$ fixation via the reductive tricarboxylic acid cycle by members of the ε subdivision of *Proteobacteria*. *J Bacteriol* **187**: 3020–3027.

Hunter EM, Mills HJ, Kostka JE. (2006). Microbial community diversity associated with carbon and nitrogen cycling in permeable shelf sediments. *Appl Environ Microbiol* **72**: 5689–5701.

Ibrahim SF, Engh G van den. (2007). Flow cytometry and cell sorting. In: Kumar A, Galaev IY, Mattiasson B (eds) Advances in Biochemical Engineering/Biotechnology. *Cell Separation*. Springer Berlin Heidelberg, pp 19–39.

Imhoff JF. (2006). The family *Ectothiorhodospiraceae*. In: Dr MDP, Falkow S, Rosenberg E, Schleifer K-H, Stackebrandt E (eds). *The Prokaryotes*. Springer New York, pp 874–886.

Imhoff JF, Trüper HG. (1977). *Ectothiorhodospira halochloris* sp. nov., a new extremely halophilic phototrophic bacterium containing bacteriochlorophyll b. *Arch Microbiol* **114**: 115–121.

Ivanov MV. (1971). Bacterial processes in the oxidation and leaching of sulfide-sulfur ores of volcanic origin. *Chem Geol* **7**: 185–211.

Ivanovsky RN, Fal YI, Berg IA, Ugolkova NV, Krasilnikova EN, Keppen OI, *et al.* (1999). Evidence for the presence of the reductive pentose phosphate cycle in a filamentous anoxygenic photosynthetic bacterium, *Oscillochloris trichoides* strain DG-6. *Microbiology* **145**: 1743–1748.

Jansen K, Thauer RK, Widdel F, Fuchs G. (1984). Carbon assimilation pathways in sulfate reducing bacteria. Formate, carbon dioxide, carbon monoxide, and acetate assimilation by *Desulfovibrio baarsii*. *Arch Microbiol* **138**: 257–262.

Jansen S, Walpersdorf E, Werner U, Billerbeck M, Böttcher ME, Beer D de. (2009). Functioning of intertidal flats inferred from temporal and spatial dynamics of $O_2$, $H_2S$ and pH in their surface sediment. *Ocean Dyn* **59**: 317–332.

Jørgensen BB. (2000). Bacteria and marine biogeochemistry. In: Schulz PDHD, Zabel DM (eds). *Marine Geochemistry*. Springer Berlin Heidelberg, pp 173–207.

Jørgensen BB. (1977a). Bacterial sulfate reduction within reduced microniches of oxidized marine sediments. *Mar Biol* **41**: 7–17.

Jørgensen BB. (2011). Deep subseafloor microbial cells on physiological standby. *Proc Natl Acad Sci* **108**: 18193–18194.

Jørgensen BB. (1977b). Distribution of colorless sulfur bacteria (*Beggiatoa* spp.) in a coastal marine sediment. *Mar Biol* **41**: 19–28.

Jørgensen BB. (1996). Material flux in the sediment. In: Jørgensen BB, Richardson K (eds). *Eutrophication in Coastal Marine Ecosystems*. American Geophysical Union, pp 115–135.

Jørgensen BB. (1982). Mineralization of organic matter in the sea bed - the role of sulphate reduction. *Nature* **296**: 643–645.

Jørgensen BB, Boetius A. (2007). Feast and famine - microbial life in the deep-sea bed. *Nat Rev Microbiol* **5**: 770–781.

Jørgensen BB, Kasten S. (2006). Sulfur cycling and methane oxidation. In: Schulz PDHD, Zabel DM (eds). *Marine Geochemistry*. Springer Berlin Heidelberg, pp 271–309.

Jorgensen SL, Hannisdal B, Lanzén A, Baumberger T, Flesland K, Fonseca R, *et al.* (2012). Correlating microbial community profiles with geochemical data in highly stratified sediments from the Arctic Mid-Ocean Ridge. *Proc Natl Acad Sci* **109**: E2846–E2855.

Jost G, Zubkov MV, Yakushev E, Labrenz M, Jürgens K. (2008). High abundance and dark $CO_2$ fixation of chemolithoautotrophic prokaryotes in anoxic waters of the Baltic Sea. Limnol Oceanogr **53**: 14–22.

Kandler O, Stetter KO. (1981). Evidence for autotrophic $CO_2$ assimilation in *Sulfolobus brierleyi* via a reductive carboxylic acid pathway. *Zentralblatt Für Bakteriol Mikrobiol Hyg Abt Orig C Allg Angew Ökol Mikrobiol* **2**: 111–121.

Kaserer H. (1906). Die Oxydation des Wasserstoffes durch Mikroorganismen. Zentralbl. Bakteriologie II. 16, 681–696.

Kashefi K, Lovley DR. (2000). Reduction of Fe(III), Mn(IV), and Toxic Metals at 100°C by *Pyrobaculum islandicum*. *Appl Environ Microbiol* **66**: 1050–1056.

Kashtan N, Roggensack SE, Rodrigue S, Thompson JW, Biller SJ, Coe A, *et al.* (2014). Single-cell genomics reveals hundreds of coexisting subpopulations in wild *Prochlorococcus*. *Science* **344**: 416–420.

Kennedy H, Beggins J, Duarte CM, Fourqurean JW, Holmer M, Marbà N, *et al.* (2010). Seagrass sediments as a global carbon sink: isotopic constraints. *Glob Biogeochem Cycles* **24**: GB4026.

Kim B-S, Kim BK, Lee J-H, Kim M, Lim YW, Chun J. (2008). Rapid phylogenetic dissection of prokaryotic community structure in tidal flat using pyrosequencing. *J Microbiol* **46**: 357–363.

Kirchman DL, Hanson TE, Cottrell MT, Hamdan LJ. (2014). Metagenomic analysis of organic matter degradation in methane-rich Arctic Ocean sediments. *Limnol Oceanogr* **59**: 548–559.

Kleiner M, Petersen JM, Dubilier N. (2012a). Convergent and divergent evolution of metabolism in sulfur-oxidizing symbionts and the role of horizontal gene transfer. *Curr Opin Microbiol* **15**: 621–631.

Kleiner M, Wentrup C, Holler T, Lavik G, Harder J, Lott C, *et al.* (2015). Use of carbon monoxide and hydrogen by a bacteria–animal symbiosis from seagrass sediments. *Environ Microbiol* n/a–n/a.

Kleiner M, Wentrup C, Lott C, Teeling H, Wetzel S, Young J, *et al.* (2012b). Metaproteomics of a gutless marine worm and its symbiotic microbial community reveal unusual pathways for carbon and energy use. *Proc Natl Acad Sci* **109**: E1173–E1182.

Koch H, Galushko A, Albertsen M, Schintlmeister A, Gruber-Dorninger C, Lücker S, *et al.* (2014). Growth of nitrite-oxidizing bacteria by aerobic hydrogen oxidation. *Science* **345**: 1052–1054.

Könneke M, Schubert DM, Brown PC, Hügler M, Standfest S, Schwander T, *et al.* (2014). Ammonia-oxidizing archaea use the most energy-efficient aerobic pathway for $CO_2$ fixation. *Proc Natl Acad Sci* **111**: 8239–8244.

Kovács ÁT, Rákhely G, Browning DF, Fülöp A, Maróti G, Busby SJW, *et al.* (2005a). An FNR-type regulator controls the anaerobic expression of Hyn hydrogenase in *Thiocapsa roseopersicina*. *J Bacteriol* **187**: 2618–2627.

Kovács KL, Kovács á. T, Maróti G, Mészáros LS, Balogh J, Latinovics D, *et al.* (2005b). The hydrogenases of *Thiocapsa roseopersicina*. *Biochem Soc Trans* **33**: 61–63.

Kuenen JG, Veldkamp H. (1973). Effects of organic compounds on growth of chemostat cultures of *Thiomicrospira pelophila*, *Thiobacillus thioparus* and *Thiobacillus neapolitanus*. *Arch Für Mikrobiol* **94**: 173–190.

Kuenen JG, Veldkamp H. (1972). *Thiomicrospira pelophila*, gen. n., sp. n., a new obligately chemolithotrophic colourless sulfur bacterium. *Antonie Van Leeuwenhoek* **38**: 241–256.

Kuever J. (2014). The Family *Desulfobulbaceae*. In: Rosenberg E, DeLong EF, Lory S, Stackebrandt E, Thompson F (eds). *The Prokaryotes*. Springer Berlin Heidelberg, pp 75–86.

Kuypers MMM, Jørgensen BB. (2007). The future of single-cell environmental microbiology. *Environ Microbiol* **9**: 6–7.

L G Ljungdahl, Wood and HG. (1969). Total synthesis of acetate from $CO_2$ by heterotrophic bacteria. *Annu Rev Microbiol* **23**: 515–538.

Laanbroek HJ, Pfennig N. (1981). Oxidation of short-chain fatty acids by sulfate-reducing bacteria in freshwater and in marine sediments. *Arch Microbiol* **128**: 330–335.

Lasken RS. (2007). Single-cell genomic sequencing using multiple displacement amplification. *Curr Opin Microbiol* **10**: 510–516.

Lavik G, Stührmann T, Brüchert V, Van der Plas A, Mohrholz V, Lam P, *et al.* (2009). Detoxification of sulphidic African shelf waters by blooming chemolithotrophs. *Nature* **457**: 581–584.

Lee N, Nielsen PH, Andreasen KH, Juretschko S, Nielsen JL, Schleifer KH, *et al.* (1999). Combination of fluorescent *in situ* hybridization and microautoradiography - a new

tool for structure-function analyses in microbial ecology. *Appl Environ Microbiol* **65**: 1289–1297.

Leininger S, Urich T, Schloter M, Schwark L, Qi J, Nicol GW, *et al.* (2006). *Archaea* predominate among ammonia-oxidizing prokaryotes in soils. *Nature* **442**: 806–809.

Leloup J, Fossing H, Kohls K, Holmkvist L, Borowski C, Jørgensen BB. (2009). Sulfate-reducing bacteria in marine sediment (Aarhus Bay, Denmark): abundance and diversity related to geochemical zonation. *Environ Microbiol* **11**: 1278–1291.

Lenk S. (2011). Molecular ecology of key organisms in sulfur and carbon cycling in marine sediments.

Lenk S, Arnds J, Zerjatke K, Musat N, Amann R, Mußmann M. (2011). Novel groups of *Gammaproteobacteria* catalyse sulfur oxidation and carbon fixation in a coastal, intertidal sediment. *Environ Microbiol* **13**: 758–774.

Lenk S, Moraru C, Hahnke S, Arnds J, Richter M, Kube M, *et al.* (2012). *Roseobacter* clade bacteria are abundant in coastal sediments and encode a novel combination of sulfur oxidation genes. *ISME J* **6**: 2178–2187.

Liu J, Liu X, Wang M, Qiao Y, Zheng Y, Zhang X-H. (2014). Bacterial and archaeal communities in sediments of the north Chinese marginal seas. *Microb Ecol* 1–13.

LlobetBrossa E, Rabus R, Bttcher ME, Knneke M, Finke N, Schramm A, *et al.* (2002). Community structure and activity of sulfate-reducing bacteria in an intertidal surface sediment: a multi-method approach. *Aquat Microb Ecol* **29**: 211–226.

Llobet-Brossa E, Rosselló-Mora R, Amann R. (1998). Microbial community composition of Wadden Sea sediments as revealed by fluorescence *in situ* hybridization. *Appl Environ Microbiol* **64**: 2691–2696.

Lloyd KG, Schreiber L, Petersen DG, Kjeldsen KU, Lever MA, Steen AD, *et al.* (2013). Predominant archaea in marine sediments degrade detrital proteins. *Nature* **496**: 215–218.

Lovley DR, Dwyer DF, Klug MJ. (1982). Kinetic analysis of competition between sulfate reducers and methanogens for hydrogen in sediments. *Appl Environ Microbiol* **43**: 1373–1379.

Lovley DR, Goodwin S. (1988). Hydrogen concentrations as an indicator of the predominant terminal electron-accepting reactions in aquatic sediments. *Geochim Cosmochim Acta* **52**: 2993–3003.

Lücker S, Wagner M, Maixner F, Pelletier E, Koch H, Vacherie B, *et al.* (2010). A *Nitrospira* metagenome illuminates the physiology and evolution of globally important nitrite-oxidizing bacteria. *Proc Natl Acad Sci* **107**: 13479–13484.

Lukey MJ, Parkin A, Roessler MM, Murphy BJ, Harmer J, Palmer T, *et al.* (2010). How *Escherichia coli* is equipped to oxidize hydrogen under different redox conditions. *J Biol Chem* **285**: 3928–3938.

Luna GM, Manini E, Danovaro R. (2002). Large fraction of dead and inactive bacteria in coastal marine sediments: comparison of protocols for determination and ecological significance. *Appl Environ Microbiol* **68**: 3509–3513.

MacGregor BJ, Boschker HTS, Amann R. (2006). Comparison of rRNA and polar-lipid-derived fatty acid biomarkers for assessment of $^{13}$C-substrate incorporation by microorganisms in marine sediments. *Appl Environ Microbiol* **72**: 5246–5253.

Majewski RA, Domach MM. (1990). Simple constrained-optimization view of acetate overflow in *E. coli*. *Biotechnol Bioeng* **35**: 732–738.

Manefield M, Whiteley AS, Griffiths RI, Bailey MJ. (2002). RNA stable isotope probing, a novel means of linking microbial community function to phylogeny. *Appl Environ Microbiol* **68**: 5367–5373.

Markert S, Arndt C, Felbeck H, Becher D, Sievert SM, Hügler M, *et al.* (2007). Physiological proteomics of the uncultured endosymbiont of *Riftia pachyptila*. *Science* **315**: 247–250.

Maróti J, Farkas A, Nagy IK, Maróti G, Kondorosi É, Rákhely G, *et al.* (2010). A second soluble Hox-type NiFe enzyme completes the hydrogenase set in *Thiocapsa roseopersicina* BBS. *Appl Environ Microbiol* **76**: 5113–5123.

Mattes TE, Nunn BL, Marshall KT, Proskurowski G, Kelley DS, Kawka OE, *et al.* (2013). Sulfur oxidizers dominate carbon fixation at a biogeochemical hot spot in the dark ocean. *ISME J* **7**: 2349–2360.

Mccollom TM, Amend JP. (2005). A thermodynamic assessment of energy requirements for biomass synthesis by chemolithoautotrophic microorganisms in oxic and anoxic environments. *Geobiology* **3**: 135–144.

McDowall JS, Murphy BJ, Haumann M, Palmer T, Armstrong FA, Sargent F. (2014). Bacterial formate hydrogenlyase complex. *Proc Natl Acad Sci* **111**: E3948–E3956.

Meyer B, Kuever J. (2007). Molecular analysis of the diversity of sulfate-reducing and sulfur-oxidizing prokaryotes in the environment, using *aprA* as functional marker gene. *Appl Environ Microbiol* **73**: 7664–7679.

Michener RH, Scranton MI, Novelli P. (1988). Hydrogen ($H_2$) distributions in the carmans river estuary. *Estuar Coast Shelf Sci* **27**: 223–235.

Middelburg JJ. (1989). A simple rate model for organic matter decomposition in marine sediments. *Geochim Cosmochim Acta* **53**: 1577–1581.

Middelburg JJ. (2011). Chemoautotrophy in the ocean. *Geophys Res Lett* **38**: 94-97.

Middelburg JJ, Barranguet C, Boschker HTS, Herman PMJ, Moens T, Heip CHR. (2000). The fate of intertidal microphytobenthos carbon: An *in situ* $^{13}$C-labeling study. *Limnol Oceanogr* **45**: 1224–1234.

Miyatake T, MacGregor BJ, Boschker E. (2009). Stable isotope probing combined with magnetic bead capture hybridization of 16S rRNA: linking microbial community function to phylogeny of sulfate-reducing *Deltaproteobacteria* in marine sediments. *Appl Environ Microbiol*. **75**: 4927–4935.

Miyatake T, MacGregor BJ, Boschker HTS. (2013). Depth-related differences in organic substrate utilization by major microbial groups in intertidal marine sediment. *Appl Environ Microbiol* **79**: 389–392.

Mohapatra BR, Gould WD, Dinardo O, Koren DW. (2008). An overview of the biochemical and molecular aspects of microbial oxidation of inorganic sulfur compounds. *CLEAN – Soil Air Water* **36**: 823–829.

Moraru C, Lam P, Fuchs BM, Kuypers MMM, Amann R. (2010). GeneFISH – an *in situ* technique for linking gene presence and cell identity in environmental microorganisms. *Environ Microbiol* **12**: 3057–3073.

Morono Y, Terada T, Masui N, Inagaki F. (2009). Discriminative detection and enumeration of microbial life in marine subsurface sediments. *ISME J* **3**: 503–511.

Morono Y, Terada T, Nishizawa M, Ito M, Hillion F, Takahata N, *et al.* (2011). Carbon and nitrogen assimilation in deep subseafloor microbial cells. *Proc Natl Acad Sci* **108**: 18295–18300.

Murray JW, Grundmanis V. (1980). Oxygen consumption in pelagic marine sediments. *Science* **209**: 1527–1530.

Musat N, Halm H, Winterholler B, Hoppe P, Peduzzi S, Hillion F, *et al.* (2008). A single-cell view on the ecophysiology of anaerobic phototrophic bacteria. *Proc Natl Acad Sci* **105**: 17861–17866.

Musat N, Werner U, Knittel K, Kolb S, Dodenhof T, van Beusekom JEE, *et al.* (2006). Microbial community structure of sandy intertidal sediments in the North Sea, Sylt-Rømø Basin, Wadden Sea. *Syst Appl Microbiol* **29**: 333–348.

Mußmann M, Ishii K, Rabus R, Amann R. (2005). Diversity and vertical distribution of cultured and uncultured *Deltaproteobacteria* in an intertidal mud flat of the Wadden Sea. *Environ Microbiol* **7**: 405–418.

Muyzer G, Stams AJM. (2008). The ecology and biotechnology of sulphate-reducing bacteria. *Nat Rev Microbiol* **6**: 441–454.

Na H, Lever MA, Kjeldsen KU, Schulz F, Jørgensen BB. (2015). Uncultured *Desulfobacteraceae* and Crenarchaeotal group C3 incorporate $^{13}$C-acetate in coastal marine sediment. *Environ Microbiol Rep* **7**: 614–622.

Nakagawa S, Takai K. (2008). Deep-sea vent chemoautotrophs: diversity, biochemistry and ecological significance. *FEMS Microbiol Ecol* **65**: 1–14.

Nakagawa S, Takai K, Inagaki F, Hirayama H, Nunoura T, Horikoshi K, *et al.* (2005). Distribution, phylogenetic diversity and physiological characteristics of epsilon-*Proteobacteria* in a deep-sea hydrothermal field. *Environ Microbiol* **7**: 1619–1632.

Nielsen JL, Christensen D, Kloppenborg M, Nielsen PH. (2003). Quantification of cell-specific substrate uptake by probe-defined bacteria under *in situ* conditions by microautoradiography and fluorescence *in situ* hybridization. *Environ Microbiol* **5**: 202–211.

Nielsen LP, Risgaard-Petersen N, Fossing H, Christensen PB, Sayama M. (2010). Electric currents couple spatially separated biogeochemical processes in marine sediment. *Nature* **463**: 1071–1074.

Nielsen PH, De Muro MA, Nielsen JL. (2000). Studies on the in situ physiology of *Thiothrix* spp. present in activated sludge. *Environ Microbiol* **2**: 389–398.

Nishihara H, Igarashi Y, Kodama T. (1991). *Hydrogenovibrio marinus* gen. nov., sp. nov., a marine obligately chemolithoautotrophic hydrogen-oxidizing bacterium. *Int J Syst Evol Microbiol* **41**: 130–133.

Novelli P., Michelson A., Scranton M., Banta G., Hobbie J., Howarth R. (1988). Hydrogen and acetate cycling in two sulfate-reducing sediments: Buzzards Bay and Town Cove, Mass. *Geochim Cosmochim Acta* **52**: 2477–2486.

Novelli PC, Scranton MI, Michener RH. (1987). Hydrogen distributions in marine sediments. *Limnol Oceanogr* **32**: 565–576.

Orcutt BN, Sylvan JB, Knab NJ, Edwards KJ. (2011). Microbial ecology of the dark ocean above, at, and below the seafloor. *Microbiol Mol Biol Rev* **75**: 361–422.

Oremland RS, Polcin S. (1982). Methanogenesis and sulfate reduction: competitive and noncompetitive substrates in estuarine sediments. *Appl Environ Microbiol* **44**: 1270–1276.

Oremland RS, Taylor BF. (1978). Sulfate reduction and methanogenesis in marine sediments. *Geochim Cosmochim Acta* **42**: 209–214.

Oren A. (2002). Halophilic microorganisms and their environments. Springer Science & Business Media.

Otte S, Kuenen JG, Nielsen LP, Paerl HW, Zopfi J, Schulz HN, *et al.* (1999). Nitrogen, carbon, and sulfur metabolism in natural *Thioploca* samples. *Appl Environ Microbiol* **65**: 3148–3157.

Overmann J. (2008). Ecology of phototrophic sulfur bacteria. In: Hell R, Dahl DC, Knaff D, Leustek T (eds) Advances in Photosynthesis and Respiration. *Sulfur Metabolism in Phototrophic Organisms*. Springer Netherlands, pp 375–396.

Overmann J. (2006). The family *Chlorobiaceae*. *Prokaryotes Vol 7 Proteobacteria Delta Epsil Subclass* 359–378.

Park S-J, Pham VH, Jung M-Y, Kim S-J, Kim J-G, Roh D-H, *et al.* (2011). *Thioalbus denitrificans* gen. nov., sp. nov., a chemolithoautotrophic sulfur-oxidizing gammaproteobacterium, isolated from marine sediment. *Int J Syst Evol Microbiol* **61**: 2045–2051.

Parkes RJ, Cragg BA, Getliff JM, Harvey SM, Fry JC, Lewis CA, *et al.* (1993). A quantitative study of microbial decomposition of biopolymers in recent sediments from the Peru margin. *Mar Geol* **113**: 55–66.

Petersen JM, Zielinski FU, Pape T, Seifert R, Moraru C, Amann R, *et al.* (2011). Hydrogen is an energy source for hydrothermal vent symbioses. *Nature* **476**: 176–180.

Petri R, Podgorsek L, Imhoff JF. (2001). Phylogeny and distribution of the *soxB* gene among thiosulfate-oxidizing bacteria. *FEMS Microbiol Lett* **197**: 171–178.

Pfeffer C, Larsen S, Song J, Dong M, Besenbacher F, Meyer RL, *et al.* (2012). Filamentous bacteria transport electrons over centimetre distances. *Nature* **491**: 218–221.

Pjevac P. (2014). Co-existence and niche differentiation of sulfur oxidizing bacteria in marine environments.

Pjevac P, Kamyshny A, Dyksma S, Mußmann M. (2014). Microbial consumption of zero-valence sulfur in marine benthic habitats. *Environ Microbiol* **16**: 3416–3430.

Plugge CM, Henstra AM, Worm P, Swarts DC, Paulitsch-Fuchs AH, Scholten JCM, *et al.* (2012). Complete genome sequence of *Syntrophobacter fumaroxidans* strain (MPOBT). *Stand Genomic Sci* **7**: 91–106.

Premuzic ET, Benkovitz CM, Gaffney JS, Walsh JJ. (1982). The nature and distribution of organic matter in the surface sediments of world oceans and seas. *Org Geochem* **4**: 63–77.

Punshon S, Moore RM. (2008). Photochemical production of molecular hydrogen in lake water and coastal seawater. *Mar Chem* **108**: 215–220.

Quayle JR, Fuller RC, Benson AA, Calvin M. (1954). Enzymatic carboxylation of ribulose diphosphate. *J Am Chem Soc* **76**: 3610–3611.

Rabus R, Hansen TA, Widdel F. (2013). Dissimilatory sulfate-and sulfur-reducing prokaryotes. In: *The Prokaryotes*. Springer, pp 309–404.

Rabus R, Venceslau SS, Wöhlbrand L, Voordouw G, Wall JD, Pereira IAC. (2015). A post-genomic view of the ecophysiology, catabolism and biotechnological relevance of sulphate-reducing prokaryotes. In: Poole RK (ed) Vol. 66. *Advances in Microbial Physiology*. Academic Press, pp 55–321.

Radajewski S, Ineson P, Parekh NR, Murrell JC. (2000). Stable-isotope probing as a tool in microbial ecology. *Nature* **403**: 646–649.

Rákhely G, Laurinavichene TV, Tsygankov AA, Kovács KL. (2007). The role of Hox hydrogenase in the $H_2$ metabolism of *Thiocapsa roseopersicina*. *Biochim Biophys Acta BBA - Bioenerg* **1767**: 671–676.

Raven JA. (2009). Contributions of anoxygenic and oxygenic phototrophy and chemolithotrophy to carbon and oxygen fluxes in aquatic environments. *Aquat Microb Ecol* **56**: 177–192.

Ravenschlag K, Sahm K, Knoblauch C, Jørgensen BB, Amann R. (2000). Community structure, cellular rRNA content, and activity of sulfate-reducing bacteria in marine Arctic sediments. *Appl Environ Microbiol* **66**: 3592–3602.

Reinthaler T, van Aken HM, Herndl GJ. (2010). Major contribution of autotrophy to microbial carbon cycling in the deep North Atlantic's interior. *Deep Sea Res Part II Top Stud Oceanogr* **57**: 1572–1580.

Revsbech NP, Jørgensen BB, Blackburn TH. (1980). Oxygen in the sea bottom measured with a microelectrode. *Science* **207**: 1355–1356.

Reysenbach A-L, Cady SL. (2001). Microbiology of ancient and modern hydrothermal systems. *Trends Microbiol* **9**: 79–86.

Riesenfeld CS, Schloss PD, Handelsman J. (2004). Metagenomics: genomic analysis of microbial communities. *Annu Rev Genet* **38**: 525–552.

Roalkvam I, Jørgensen SL, Chen Y, Stokke R, Dahle H, Hocking WP, *et al.* (2011). New insight into stratification of anaerobic methanotrophs in cold seep sediments. *FEMS Microbiol Ecol* **78**: 233–243.

Roelofsen PA. (1934). On the metabolism of the purple sulphur bacteria. In: Vol. 37. *Proc R Acad Sci Amsterdam*. pp 3–12.

Romankevich EA. (2013). Geochemistry of organic matter in the ocean. Springer Science & Business Media.

Røy H, Kallmeyer J, Adhikari RR, Pockalny R, Jørgensen BB, D'Hondt S. (2012). Aerobic microbial respiration in 86-million-year-old deep-sea red clay. *Science* **336**: 922–925.

Røy H, Lee JS, Jansen S, de Beer D. (2008). Tide-driven deep pore-water flow in intertidal sand flats. *Limnol Oceanogr* **53**: 1521–1530.

Ruff SE, Biddle JF, Teske AP, Knittel K, Boetius A, Ramette A. (2015). Global dispersion and local diversification of the methane seep microbiome. *Proc Natl Acad Sci* **112**: 4015–4020.

Rullkötter J. (2006). Organic matter: the driving force for early diagenesis. In: Schulz PDHD, Zabel DM (eds). *Marine Geochemistry*. Springer Berlin Heidelberg, pp 125–168.

Salman V, Bailey JV, Teske A. (2013). Phylogenetic and morphologic complexity of giant sulphur bacteria. *Antonie Van Leeuwenhoek* **104**: 169–186.

Sansone FJ, Martens CS. (1982). Volatile fatty acid cycling in organic-rich marine sediments. *Geochim Cosmochim Acta* **46**: 1575–1589.

Sasikala C, Ramana CV. (1997). Biodegradation and metabolism of unusual carbon compounds by anoxygenic phototrophic bacteria. In: Poole RK (ed) Vol. 39. *Advances in Microbial Physiology*. Academic Press, pp 339–377.

Sass H, Kopke B, Rutters H, Feuerlein T, Droge S, Cypionka H, *et al.* (2010). *Tateyamaria pelophila* sp. nov., a facultatively anaerobic alphaproteobacterium isolated from tidal-flat sediment, and emended descriptions of the genus *Tateyamaria* and of *Tateyamaria omphalii*. *Int J Syst Evol Microbiol* **60**: 1770–1777.

Schauder R, Preuß A, Jetten M, Fuchs G. (1988). Oxidative and reductive acetyl CoA/carbon monoxide dehydrogenase pathway in *Desulfobacterium autotrophicum*. *Arch Microbiol* **151**: 84–89.

Schauer R, Bienhold C, Ramette A, Harder J. (2009). Bacterial diversity and biogeography in deep-sea surface sediments of the South Atlantic Ocean. *ISME J* **4**: 159–170.

Schauer R, Røy H, Augustin N, Gennerich H-H, Peters M, Wenzhoefer F, *et al.* (2011). Bacterial sulfur cycling shapes microbial communities in surface sediments of an ultramafic hydrothermal vent field. *Environ Microbiol* **13**: 2633–2648.

Schimak MP, Kleiner M, Wetzel S, Liebeke M, Dubilier N, Fuchs BM. (2016). MiL-FISH: multilabeled oligonucleotides for fluorescence *in situ* hybridization improve visualization of bacterial cells. *Appl Environ Microbiol* **82**: 62–70.

Schmitz RA, Daniel R, Deppenmeier U, Gottschalk G. (2006). The anaerobic way of life. In: Dr MDP, Falkow S, Rosenberg E, Schleifer K-H, Stackebrandt E (eds). *The Prokaryotes*. Springer New York, pp 86–101.

Scholz-Muramatsu H, Neumann A, Meßmer M, Moore E, Diekert G. (1995). Isolation and characterization of *Dehalospirillum multivorans* gen. nov., sp. nov., a tetrachloroethene-utilizing, strictly anaerobic bacterium. *Arch Microbiol* **163**: 48–56.

Schubert KR, Evans HJ. (1976). Hydrogen evolution: A major factor affecting the efficiency of nitrogen fixation in nodulated symbionts. *Proc Natl Acad Sci* **73**: 1207–1211.

Schulz HN, Beer D de. (2002). Uptake rates of oxygen and sulfide measured with individual *Thiomargarita namibiensis* cells by using microelectrodes. *Appl Environ Microbiol* **68**: 5746–5749.

Schulz HN, Brinkhoff T, Ferdelman TG, Mariné MH, Teske A, Jørgensen BB. (1999). Dense populations of a giant sulfur bacterium in Namibian shelf sediments. *Science* **284**: 493–495.

Schulz HN, Jørgensen and BB. (2001). Big bacteria. *Annu Rev Microbiol* **55**: 105–137.

Schulz HN, Jorgensen BB, Fossing HA, Ramsing NB. (1996). Community structure of filamentous, sheath-building sulfur bacteria, *Thioploca* spp., off the coast of Chile. *Appl Environ Microbiol* **62**: 1855–1862.

Schulz HN, Schulz HD. (2005). Large sulfur bacteria and the formation of phosphorite. *Science* **307**: 416–418.

Schwartz DE, Fritsch J, Friedrich B. (2013). $H_2$-metabolizing prokaryotes. In: Rosenberg E, DeLong EF, Lory S, Stackebrandt E, Thompson F (eds). *The Prokaryotes*. Springer Berlin Heidelberg, pp 119–199.

Segerer A, Stetter KO, Klink F. (1985). Two contrary modes of chemolithotrophy in the same archaebacterium. *Nature* **313**: 787–789.

Seidel M, Graue J, Engelen B, Köster J, Sass H, Rullkötter J. (2012). Advection and diffusion determine vertical distribution of microbial communities in intertidal sediments as revealed by combined biogeochemical and molecular biological analysis. *Org Geochem* **52**: 114–129.

Sekar R, Fuchs BM, Amann R, Pernthaler J. (2004). Flow sorting of marine bacterioplankton after fluorescence *in situ* hybridization. *Appl Environ Microbiol* **70**: 6210–6219.

Seyler LM, McGuinness LM, Kerkhof LJ. (2014). Crenarchaeal heterotrophy in salt marsh sediments. *ISME J* **8**: 1534–1543.

Sievert S, Kiene R, Schulz-Vogt H. (2007). The sulfur cycle. *Oceanography* **20**: 117–123.

Sievert SM, Hügler M, Taylor CD, Wirsen CO. (2008). Sulfur oxidation at deep-sea hydrothermal vents. In: Dahl DC, Friedrich DCG (eds). *Microbial Sulfur Metabolism*. Springer Berlin Heidelberg, pp 238–258.

Sievert SM, Scott KM, Klotz MG, Chain PSG, Hauser LJ, Hemp J, *et al.* (2008b). Genome of the epsilonproteobacterial chemolithoautotroph *Sulfurimonas denitrificans*. *Appl Environ Microbiol* **74**: 1145–1156.

Slepova TV, Sokolova TG, Lysenko AM, Tourova TP, Kolganova TV, Kamzolkina OV, *et al.* (2006). *Carboxydocella sporoproducens* sp. nov., a novel anaerobic CO-utilizing/$H_2$-producing thermophilic bacterium from a Kamchatka hot spring. *Int J Syst Evol Microbiol* **56**: 797–800.

Sokolova TG, González JM, Kostrikina NA, Chernyh NA, Tourova TP, Kato C, *et al.* (2001). *Carboxydobrachium pacificum* gen. nov., sp. nov., a new anaerobic, thermophilic, CO-utilizing marine bacterium from Okinawa Trough. *Int J Syst Evol Microbiol* **51**: 141–149.

Sokolova TG, Jeanthon C, Kostrikina NA, Chernyh NA, Lebedinsky AV, Stackebrandt E, *et al.* (2004). The first evidence of anaerobic CO oxidation coupled with $H_2$ production by a hyperthermophilic archaeon isolated from a deep-sea hydrothermal vent. *Extremophiles* **8**: 317–323.

Sokolova TG, Kostrikina NA, Chernyh NA, Tourova TP, Kolganova TV, Bonch-Osmolovskaya EA. (2002). *Carboxydocella thermautotrophica* gen. nov., sp. nov., a novel anaerobic, CO-utilizing thermophile from a Kamchatkan hot spring. *Int J Syst Evol Microbiol* **52**: 1961–1967.

Sorokin DY. (2008). Diversity of halophilic sulfur-oxidizing bacteria in hypersaline habitats. In: Dahl DC, Friedrich DCG (eds). *Microbial Sulfur Metabolism*. Springer Berlin Heidelberg, pp 225–237.

Sorokin DY. (2003). Oxidation of inorganic sulfur compounds by obligately organotrophic bacteria. *Microbiology* **72**: 641–653.

Sorokin DY. (1995). *Sulfitobacter pontiacus* gen. nov., sp. nov. - A new heterotrophic bacterium from the black sea, specialized on sulfite oxidation. *Microbiology* **64**: 295–305.

Sorokin DY, Tourova TP, Muyzer G. (2005). *Citreicella thiooxidans* gen. nov., sp. nov., a novel lithoheterotrophic sulfur-oxidizing bacterium from the Black Sea. *Syst Appl Microbiol* **28**: 679–687.

Steinmetz MA, Fischer U. (1982). Cytochromes of the green sulfur bacterium *Chlorobium vibrioforme* f. *thiosulfatophilum*. Purification, characterization and sulfur metabolism. *Arch Microbiol* **131**: 19–26.

Steudel R, Holdt G, Visscher PT, Gemerden H van. (1990). Search for polythionates in cultures of *Chromatium vinosum* after sulfide incubation. *Arch Microbiol* **153**: 432–437.

Stewart EJ. (2012). Growing unculturable bacteria. *J Bacteriol* **194**: 4151–4160.

Strous M, Pelletier E, Mangenot S, Rattei T, Lehner A, Taylor MW, *et al.* (2006). Deciphering the evolution and metabolism of an anammox bacterium from a community genome. *Nature* **440**: 790–794.

Suttle CA. (2005). Viruses in the sea. *Nature* **437**: 356–361.

Swan BK, Martinez-Garcia M, Preston CM, Sczyrba A, Woyke T, Lamy D, *et al.* (2011). Potential for chemolithoautotrophy among ubiquitous bacteria lineages in the dark ocean. *Science* **333**: 1296–1300.

Takai K, Suzuki M, Nakagawa S, Miyazaki M, Suzuki Y, Inagaki F, *et al.* (2006). *Sulfurimonas paralvinellae* sp. nov., a novel mesophilic, hydrogen- and sulfur-oxidizing chemolithoautotroph within the *Epsilonproteobacteria* isolated from a deep-sea hydrothermal vent polychaete nest, reclassification of *Thiomicrospira denitrificans* as *Sulfurimonas denitrificans* comb. nov. and emended description of the genus *Sulfurimonas*. *Int J Syst Evol Microbiol* **56**: 1725–1733.

Taylor, Wirsen, Gaill. (1999). Rapid microbial production of filamentous sulfur mats at hydrothermal vents. *Appl Environ Microbiol* **65**: 2253–2255.

Thauer RK, Postgate JR. (1982). Dissimilatory sulphate reduction with acetate as electron donor. *Philos Trans R Soc Lond B Biol Sci* **298**: 467–471.

Thomas F, Giblin AE, Cardon ZG, Sievert SM. (2014). Rhizosphere heterogeneity shapes abundance and activity of sulfur-oxidizing bacteria in vegetated salt marsh sediments. *Front Microbiol* **5**. doi: 10.3389/fmicb.2014.00309.

Tissot B, Welte D. (2012). Petroleum formation and occurrence: a new approach to oil and gas exploration. Springer Science & Business Media.

Treude T, Krause S, Maltby J, Dale AW, Coffin R, Hamdan LJ. (2014). Sulfate reduction and methane oxidation activity below the sulfate-methane transition zone in Alaskan Beaufort Sea continental margin sediments: implications for deep sulfur cycling. *Geochim Cosmochim Acta* **144**: 217–237.

Tsuji K, Yagi T. (1980). Significance of hydrogen burst from growing cultures of *Desulfovibrio vulgaris*, Miyazaki, and the role of hydrogenase and cytochrome c3 in energy production system. *Arch Microbiol* **125**: 35–42.

Vandieken V, Pester M, Finke N, Hyun J-H, Friedrich MW, Loy A, *et al.* (2012). Three manganese oxide-rich marine sediments harbor similar communities of acetate-oxidizing manganese-reducing bacteria. *ISME J* **6**: 2078–2090.

Vandieken V, Thamdrup B. (2013). Identification of acetate-oxidizing bacteria in a coastal marine surface sediment by RNA-stable isotope probing in anoxic slurries and intact cores. *FEMS Microbiol Ecol* **84**: 373–386.

Vargas M, Kashefi K, Blunt-Harris EL, Lovley DR. (1998). Microbiological evidence for Fe(III) reduction on early Earth. *Nature* **395**: 65–67.

Varon-Lopez M, Dias ACF, Fasanella CC, Durrer A, Melo IS, Kuramae EE, *et al.* (2014). Sulphur-oxidizing and sulphate-reducing communities in Brazilian mangrove sediments. *Environ Microbiol* **16**: 845–855.

Vartoukian SR, Palmer RM, Wade WG. (2010). Strategies for culture of 'unculturable' bacteria. *FEMS Microbiol Lett* **309**: 1–7.

Vasquez-Cardenas D, van de Vossenberg J, Polerecky L, Malkin SY, Schauer R, Hidalgo-Martinez S, *et al.* (2015). Microbial carbon metabolism associated with electrogenic sulphur oxidation in coastal sediments. *ISME J*. **9**: 1966–1978.

Vignais PM, Billoud B. (2007). Occurrence, classification, and biological function of hydrogenases: an overview. *Chem Rev* **107**: 4206–4272.

Vignais PM, Billoud B, Meyer J. (2001). Classification and phylogeny of hydrogenases. *FEMS Microbiol Rev* **25**: 455–501.

Vila M, Simó R, Kiene RP, Pinhassi J, González JM, Moran MA, *et al.* (2004). Use of microautoradiography combined with fluorescence *in situ* hybridization to determine

dimethylsulfoniopropionate incorporation by marine bacterioplankton Taxa. *Appl Environ Microbiol* **70**: 4648–4657.

Volbeda A, Charon M-H, Piras C, Hatchikian EC, Frey M, Fontecilla-Camps JC. (1995). Crystal structure of the nickel–iron hydrogenase from *Desulfovibrio gigas*. *Nature* **373**: 580–587.

Vornolt J, Kunow J, Stetter KO, Thauer RK. (1995). Enzymes and coenzymes of the carbon monoxide dehydrogenase pathway for autotrophic $CO_2$ fixation in *Archaeoglobus lithotrophicus* and the lack of carbon monoxide dehydrogenase in the heterotrophic *A. profundus*. *Arch Microbiol* **163**: 112–118.

Wächtershäuser G. (1988). Before enzymes and templates: theory of surface metabolism. *Microbiol Rev* **52**: 452–484.

Wagner M. (2009). Single-cell ecophysiology of microbes as revealed by Raman microspectroscopy or secondary ion mass spectrometry imaging. *Annu Rev Microbiol* **63**: 411–429.

Wahlund TM, Tabita FR. (1997). The reductive tricarboxylic acid cycle of carbon dioxide assimilation: initial studies and purification of ATP-citrate lyase from the green sulfur bacterium *Chlorobium tepidum*. *J Bacteriol* **179**: 4859–4867.

Walsh EA, Kirkpatrick JB, Rutherford SD, Smith DC, Sogin M, D'Hondt S. (2015). Bacterial diversity and community composition from seasurface to subseafloor. *ISME J*. doi: 10.1038/ismej.2015.175.

Walsh GE. (1997). Primary producers. In: FIBiol PCDs, , CBiol (ed). *Handbook of Ecotoxicology*. Blackwell Publishing Ltd., pp 119–144.

Wang L, Liu L, Zheng B, Zhu Y, Wang X. (2013a). Analysis of the bacterial community in the two typical intertidal sediments of Bohai Bay, China by pyrosequencing. *Mar Pollut Bull* **72**: 181–187.

Wang Y, Hammes F, De Roy K, Verstraete W, Boon N. (2010). Past, present and future applications of flow cytometry in aquatic microbiology. *Trends Biotechnol* **28**: 416–424.

Webster G, Rinna J, Roussel EG, Fry JC, Weightman AJ, Parkes RJ. (2010). Prokaryotic functional diversity in different biogeochemical depth zones in tidal sediments of the Severn Estuary, UK, revealed by stable-isotope probing. *FEMS Microbiol Ecol* **72**: 179–197.

Webster G, Watt LC, Rinna J, Fry JC, Evershed RP, Parkes RJ, *et al.* (2006). A comparison of stable-isotope probing of DNA and phospholipid fatty acids to study prokaryotic functional diversity in sulfate-reducing marine sediment enrichment slurries. *Environ Microbiol* **8**: 1575–1589.

Wellsbury P, Parkes RJ. (1995). Acetate bioavailability and turnover in an estuarine sediment. *FEMS Microbiol Ecol* **17**: 85–94.

Wenzhöfer F, Glud RN. (2002). Benthic carbon mineralization in the Atlantic: a synthesis based on in situ data from the last decade. *Deep Sea Res Part Oceanogr Res Pap* **49**: 1255–1279.

Whelan JK, Farrington JW. (2013). Organic matter: productivity, accumulation, and preservation in recent and ancient sediments. Columbia University Press.

Widdel F, Bak F. (1992). Gram-negative mesophilic sulfate-reducing bacteria. In: Balows A, Trüper HG, Dworkin M, Harder W, Schleifer K-H (eds). *The Prokaryotes*. Springer New York, pp 3352–3378.

Widdel F, Pfennig N. (1981). Studies on dissimilatory sulfate-reducing bacteria that decompose fatty acids. *Arch Microbiol* **129**: 395–400.

Wilms R, Köpke B, Sass H, Chang TS, Cypionka H, Engelen B. (2006). Deep biosphere-related bacteria within the subsurface of tidal flat sediments. *Environ Microbiol* **8**: 709–719.

Winfrey MR, Zeikus JG. (1977). Effect of sulfate on carbon and electron flow during microbial methanogenesis in freshwater sediments. *Appl Environ Microbiol* **33**: 275–281.

Wirsen CO, Sievert SM, Cavanaugh CM, Molyneaux SJ, Ahmad A, Taylor LT, *et al.* (2002). Characterization of an autotrophic sulfide-oxidizing marine *Arcobacter* sp. that produces filamentous sulfur. *Appl Environ Microbiol* **68**: 316–325.

Wollast R. (1991). The coastal organic carbon cycle: fluxes, sources and sinks. *Ocean Margin Process Glob Change Rep Dahl Workshop Berl 1990*. doi: 10.1007/978-3-642-76064-8_7.

Woyke T, Teeling H, Ivanova NN, Huntemann M, Richter M, Gloeckner FO, *et al.* (2006). Symbiosis insights through metagenomic analysis of a microbial consortium. *Nature* **443**: 950–955.

Woyke T, Xie G, Copeland A, González JM, Han C, Kiss H, *et al.* (2009). Assembling the marine metagenome, one cell at a time. *PLoS ONE* **4**: e5299.

Yamaguchi T, Fuchs BM, Amann R, Kawakami S, Kubota K, Hatamoto M, *et al.* (2015). Rapid and sensitive identification of marine bacteria by an improved *in situ* DNA hybridization chain reaction (quickHCR-FISH). *Syst Appl Microbiol* **38**: 400–405.

Zarzycki J, Brecht V, Müller M, Fuchs G. (2009). Identifying the missing steps of the autotrophic 3-hydroxypropionate $CO_2$ fixation cycle in *Chloroflexus aurantiacus*. *Proc Natl Acad Sci* **106**: 21317–21322.

Zeikus JG, Kerby R, Krzycki JA. (1985). Single-carbon chemistry of acetogenic and methanogenic bacteria. *Science* **227**: 1167–1173.

Zheng B, Wang L, Liu L. (2014). Bacterial community structure and its regulating factors in the intertidal sediment along the Liaodong Bay of Bohai Sea, China. *Microbiol Res* **169**: 585–592.

Ziehe D. (2009). Aminosäure-D/L-Verhältnisse in biogenen Carbonaten als Schlüssel zur Datierung holozäner Sedimentationsvorgänge im norddeutschen Küstenraum. PhD thesis. University of Oldenburg: Oldenburg, Germany.

Zopfi J, Ferdelman TG, Fossing H. (2004). Distribution and fate of sulfur intermediates - sulfite, tetrathionate, thiosulfate, and elemental sulfur - in marine sediments. *Geol Soc Am Spec Pap* **379**: 97–116.

Zubkov MV, Fuchs BM, Archer SD, Kiene RP, Amann R, Burkill PH. (2002). Rapid turnover of dissolved DMS and DMSP by defined bacterioplankton communities in the stratified euphotic zone of the North Sea. *Deep Sea Res Part II Top Stud Oceanogr* **49**: 3017–3038.

Zubkov MV, Mary I, Woodward EMS, Warwick PE, Fuchs BM, Scanlan DJ, *et al.* (2007). Microbial control of phosphate in the nutrient-depleted North Atlantic subtropical gyre. *Environ Microbiol* **9**: 2079–2089.

Zubkov MV, Tarran GA, Fuchs BM. (2004). Depth related amino acid uptake by Prochlorococcus cyanobacteria in the Southern Atlantic tropical gyre. *FEMS Microbiol Ecol* **50**: 153–161.

# Acknowledgement

Firstly, I would like to thank **Marc Mußmann** for patience during more than four years of great supervision, providing advice and guidance and for many fruitful scientific discussions.

I would like to thank **Rudi Amann** for providing me the opportunity to work in the Molecular Ecology department, for reviewing my thesis and for general support. I also thank **Ulrich Fischer** for reviewing my thesis.

Many thanks to **Michael Friedrich** and **Bernhard Fuchs** for their contributions as members of my thesis committee.

I thank **Jörg Wulf** for excellent technical assistance, in particular for his help with flow cytometry.

Many thanks to **Stefan Sievert**, **Jesse McNichol** and **Petra Pjevac** for the pleasure of nice interaction and collaboration.

Thanks to all people in the **Molecular Ecology department** for a perfect working atmosphere.

Nicht zuletzt möchte ich mich bei meinen Eltern **Elke** und **Kurt** sowie meinem Bruder **Volker** und auch bei **Bastian Brandt** für die großartige Unterstützung bedanken. Ohne Euch wäre das alles nicht möglich gewesen.

# Versicherung an Eides Statt

Ich,
Stefan Dyksma
Matrikel Nr.: 2950966
Dr.-Sasse-Str. 16
28865 Lilienthal

versichere an Eides Statt durch meine Unterschrift, dass ich die vorstehende Arbeit mit dem Titel „Identification and activity of bacteria consuming key intermediates of carbon and sulfur cycling in coastal sands“ selbständig und ohne fremde Hilfe angefertigt und alle Stellen, die ich wörtlich dem Sinne nach aus Veröffentlichungen entnommen habe, als solche kenntlich gemacht habe, mich auch keiner anderen als der angegebenen Literatur oder sonstiger Hilfsmittel bedient habe.
Ich versichere an Eides Statt, dass ich die vorgenannten Angaben nach bestem Wissen und Gewissen gemacht habe und dass die Angaben der Wahrheit entsprechen und ich nichts verschwiegen habe.
Die Strafbarkeit einer falschen eidesstattlichen Versicherung ist mir bekannt, namentlich die Strafandrohung gemäß § 156 StGB bis zu drei Jahren Freiheitsstrafe oder Geldstrafe bei vorsätzlicher Begehung der Tat bzw. gemäß § 161 Abs. 1 StGB bis zu einem Jahr Freiheitsstrafe oder Geldstrafe bei fahrlässiger Begehung.

_____

Ort, Datum Unterschrift